Aix-Marseille Université
Ecole Doctorale 62 - Sciences de la Vie et de la Santé
Institut de Neurobiologie de la Méditerranée - Inmed UMR1249

Thèse présentée pour obtenir le grade universitaire de
Docteur en Neurosciences

Davide Cavalieri

On the developmental origin of CA1 pyramidal neuron diversity in the adult mouse hippocampus

Soutenue le 23/04/2021 devant une commission d'examen composée de:

S. Trouche	Chargée de Recherche, Montpellier	Rapportrice
I. Soltesz	Professeur, Stanford	Rapporteur
F. Francis	Directeur de Recherche, Paris	Examinatrice
J-C. Platel	Chargé de Recherche, Marseille	Examinateur
F. Féron	Professeur, Marseille	Président
R. Cossart	Directeur de Recherche, Marseille	Directrice de thèse

"*Équilibre et harmonie sont atteints, dans la nature, par la différenciation constante, par une diversité toujours croissante. La stabilité [...] n'est pas fonction de la simplicité et de l'homogénéité, mais de la complexité et de la variété. La capacité d'un [éco]système à maintenir son intégrité ne dépend pas de l'uniformité du milieu, mais bien de sa diversité.*"

Murray Bookchin - L'écologie sociale

"*Much of epistemology seems to be parasitic upon religious impulses to discipline and sacrifice [...]. But even if religious overtones are absent or dismissed as so much window dressing, there remains a core of ethical imperative in the literature on how to do science and become a scientist. The mastery of scientific practices is inevitably linked to self-mastery, the assiduous cultivation of a certain kind of self.*"

Lorraine Daston & Peter Galison - Objectivity

Abstract

The hippocampus is associated with several functions including navigation, memory, and emotional processing. It is still unclear how this brain structure parallelly computes relevant information to support this diverse functional repertoire. Several recent studies suggest that separate subsets of principal cells that route information to specific pathways, would provide a circuit basis for the diversity of hippocampal function. This notion of 'division of labor' at the cellular level is in line with the observation that in the CA1 area, the main output region of the hippocampus, pyramidal neurons (PN) are not a homogeneous cell population like previously thought. In fact, experimental evidence demonstrated PN heterogeneity encompassing dendritic morphology, electrophysiological properties, connectivity profiles, gene expression and participation in oscillatory activity. Many of these features correlate with the cell body location along the radial axis of the stratum pyramidale (SP). This adds up to the notion that PNs segregate functionally according to their radial position, forming a deep and a superficial sublayer with distinct characteristics. From embryonic day 11 (E11) to E17, differentiating PNs migrate via an 'inside first-outside last' scheme and position themselves in progressively more superficial positions. However other migratory schemes superpose to the radial one, so that the correspondence between cell birthdate and location is not as clear-cut. Here we asked whether embryonic birthdate, rather than soma location, is a better predictor of CA1 PN identity, and ultimately function. To this aim, we used an inducible genetic fate mapping approach to label PNs according to their birthdate (E12.5, E14.5, E16.5) and studied their morphological and electrophysiological properties in vitro, as well as their connectivity and cFos expression in the adult CA1. We show that the birthdate contributes to defining intrinsic electrophysiological and morphological properties. Likely, a predetermined genetic program acts in synergy with other extrinsic (positional) factors in determining cell identity. In addition, we find that the early-born subpopulation (E12.5) displays remarkable intrinsic features and unique recruitment upon exploration. This study is the first in-depth characterization of CA1 pyramidal cells in the adult hippocampus as a function of the temporal embryonic origin and provides evidence that the embryonic origin of a neuron critically determines its properties, and possibly its function.

Résumé

L'hippocampe est associé à plusieurs fonctions, dont la navigation, la mémoire épisodique ainsi que d'autres processus cognitifs et affectifs. Nous ignorons toujours comment cette structure cérébrale peut intégrer plusieurs types d'information à la fois et ainsi porter ce répertoire fonctionnel diversifié. Plusieurs études récentes indiquent que des sous-populations distinctes de neurones pyramidaux (NP) acheminent les informations vers des voies spécifiques, suggérant ainsi une base cellulaire à la diversité des fonctions de l'hippocampe. Cette notion de 'division de la tâche' au sein du circuit neuronal rejoint l'idée récente que les NP de l'aire CA1, principale sortie de l'hippocampe, ne constitueraient pas une population cellulaire homogène comme supposé auparavant. Ainsi, une hétérogénéité des NP allant de leurs propriétés morpho-physiologiques, connectivité à leur participation aux oscillations neuronales, ou leur activité in vivo a été mise en évidence expérimentalement. Nombre de ces caractéristiques corrèlent avec la position du soma selon l'axe radial de la couche pyramidale de CA1. Ceci renforce l'idée que les NP se séparent fonctionnellement selon leur position radiale selon deux couches, une profonde et une superficielle aux caractéristiques distinctes. A partir du 11e jour embryonnaire (E11) jusqu'à E17, il est établi que les NP migrent selon un schéma 'inside first-outside last', se positionnant progressivement de plus en plus superficiellement. Cependant, d'autres schémas migratoires se superposent au schéma radial, de sorte que la correspondance entre la date de naissance et la localisation des cellules n'est pas aussi stricte. Au cours de cette thèse, nous avons testé l'hypothèse selon laquelle la date précise de naissance embryonnaire, plutôt que la localisation terminale du soma, serait un meilleur indicateur du phenotype cellulaire et de la fonction des NP dans CA1. Dans ce but, nous avons utilisé une approche inductible de « cartographie du devenir génétique » pour marquer les NP en fonction de leur date de naissance (E12.5, E14.5, E16.5) et étudier les propriétés morphologiques et électrophysiologiques in vitro, ainsi que leur connectivité et expression de cFos dans le CA1 adulte. Nous démontrons que la date de naissance embryonnaire des NP contribue à définir les propriétés électrophysiologiques et morphologiques intrinsèques. Il est probable qu'un programme génétique prédéterminé agisse en synergie avec d'autres facteurs extrinsèques (liés à la localisation) pour déterminer l'identité de ces cellules et leur rôle dans le réseau hippocampique. De plus, nous montrons que les NP générés très tôt (E12.5) forment une sous-population aux caractéristiques remarquables et présentant un recrutement unique lors de l'exploration. Cette étude est la première caractérisation en profondeur des cellules pyramidales CA1 dans l'hippocampe adulte en fonction de l'origine embryonnaire temporelle et fournit la preuve que l'origine embryonnaire d'un neurone a un effet sur la détermination de ses propriétés, et éventuellement de sa fonction.

Acknowledgements

The present doctoral project was carried out at the Institut de Neurobiologie de la Méditerranée, Marseille, directed by Dr. Rosa Cossart. I am grateful to Dr. Stéphanie Trouche and Prof. Ivan Soltesz for taking the time to read and evaluate my thesis (as well as for their kindness all along its preparation). I would also like to thank Dr. Fiona Francis, Dr. Jean-Claude Platel for accepting to be part of the jury, as well as Prof. François Féron for chairing the jury.

While being at the head of the lab, Rosa was also my PhD supervisor, so I want to address her my most sincere thanks for her patience, her support and her scientific acumen. La première fois que je suis venu au labo pour discuter de mon stage avec toi, je me souviens que je portais un énorme sac à dos 'trekking' (je sais pas pourquoi... je passais juste trois jours à Marseille), avec lequel j'ai appuyé sur tous les interrupteurs au mur pendant qu'on parlait, en éteignant la lumière et en faisant baisser les rideaux à la fois... Aujourd'hui je ne suis pas moins maladroit mais je sais aussi que je repars avec un plus précieux bagage fait de toutes ces années en thèse dans ton équipe. Je te remercie pour avoir trouvé le temps et l'énergie pour suivre mon projet et de m'avoir appris à toujours mettre "l'humain d'abord".

Of those who were there when I first got to the team, some have left already...

Laura et Yannick, I cherish the many memories of sitting in the back of your car in the midst of cigarette smoke while you two are violently arguing about something nonsensical. "Davide, can you say something?". I wish you two crazy diamonds all the best for your future lifes and careers. Claire et Thomas, je suis très heureux d'avoir fait un bout de chemin avec vous. Claire, malgré ton age t'as été ma grande soeur de thèse, je te souhaite le mieux pour ta passion de fouiller à l'intérieur des vaches. Je dois aussi te remercier de m'avoir appris à suivre une conversation en français à un débit de 20 mots par seconde. Thomas, au début je pensais que tu t'en fichais de tout et de toustes... après j'ai compris que c'est la thèse qui te fait ça. David, dear friend who too soon was summoned back to his fatherland. You are the most sociable self-proclaimed-socially-awkward person I have ever met. Ciao 'grandisimo'. Suzanne, my master project mentor, who used to call me 'master of disaster', if you ever read this you'll have to use the 'Doctor of disaster' formula, please. Thank you Su for giving me the warmest welcome to the team one could hope for. Laurène, merci pour m'avoir trasmis ton expérience en patch (sache que je ne suis plus un 'bourrin'!). Loris, sans toi j'en serais pas à la moitié des manips faites aujourd'hui. T'as vraiment été essentiel dans le projet, même si caché dans les sombres pièces de l'animalerie.

...some others are still warming their chair.

Lexi, you are a great friend and a brilliant team-mate. Thank you for always sharing your enthusiasm and for helping me go through the final rush. Co-Star today: "They will not judge you for writing a memoir, they'll encourage it" (no joke). Agnès, merci infiniment pour ton aide, surtout lors de l'écriture du papier. Souvent il a fallu te rappeler mon projet depuis le début, mais t'as toujours filé un coup de main quand j'étais dans le besoin. Erwanito, merci beaucoup d'avoir adouci nos soirées au bureau grâce à tes talents d' auteur-compositeur-interprète. Je te souhaite le mieux pour la suite (The Voice?). Marco, non solo guru dell'elettrofisiologia ma anche vero e proprio compagno di banco. Grazie di cuore per essere stato disponibile per tutte le mie domande più o meno idiote, di lavoro o pannolini. Catherine, j'ai énormément apprécié te connaitre avant la fin de ma

thèse et travailler avec toi côte à côte alors que le labo était désert. Je te dois toujours une bière, Catheurineu! Michel, tu sais que je ne peux pas l'écrire ici mais tu vois très bien. Artem, keep up the good work! I know you can do it, I believe in you. Richard, thanks for the nice time we spent together in Berlin during FENS. Pepe, s'il te plaît, ne m'en veux pas si finalement je n'ai pas été ton thésard. Je t'apprecie beaucoup, sache que je n'ai pas oublié que t'as été à fond pendant tous les Journal Club, alors que au début tu voulais pas y participer. Merci aussi à Robin, Julien, Hervé, Shrisha, Salomé, Marie, Anas Islah et Lilia.

Inoltre, tengo a citare: Carla, grazie per la tua generosità e la tua capacità di ascolto, però questo me l'hai già raccontato... Sei forte, finisci presto la tesi! Alla, thank god that we stopped trying to be friends so we could finally be friends! I hope when the pandemics is over you can bring GreenMed back to life (by the way, greetings to Françoise and Lucas too). Catia & Caroline, merci d'avoir rendu le tournage du film de Noël un des plus beaux moments que j'ai passé au labo! Anas, que ça soit autour d'un café ou d'une bière, j'ai beaucoup apprécié ton vouloir refaire le monde, et la recherche. On lâche rien. Mostafa, my bright PhD brother, go show the British how we do it in Marseille! Stefania, grazie ancora per aver capito cosa cavolo volevo fare coi miei dati e per avermi saputo aiutare. Pauline & Manal, merci pour avoir toujours amené de la couleur dans les grisatres journées de travail. Romain, le premier Inmedien que j'ai jamais connu, merci pour tes conseils.

Et un grand merci à Laurent, FX, Olivier, Milene, Andrew, Clément, Nail et ceux et celles qui m'ont aidé dans mes galères de manip. Je remercie aussi le personnel de l'INMED pour leur soutien de fond: Bahija, Gwendoline, Aurélie, Christine et Robert.

Infine gli affetti. *J'adresse toute ma reconnaissance à ma compagne, Maud Alessandra, pour son soutien et son aide*... sans blague Maudì, t'as été le bouée dans l'océan de ma thèse et t'es la plage paradisiaque pour mon naufrage de chômeur.. A ton coté la vie "n'est jamais une mauvaise piste". Merci merci merci. Un grazie sincero va ai miei genitori e mia sorella: nonostante la distanza, mi avete sempre sostenuto, dimostrato affetto e spinto a dare il meglio.
A te, Fiamma, dedico la mia tesi. Prendilo come un elogio alla diversità.

9/03/2021
Davide

Contents

List of Figures

List of Abbreviations

ACC	Anterior cingulate cortex
Ach	Acetylcholine
Amy	Amygdala
CA	Cornu Ammonis
dCA1	dorsal CA1
vCA1	ventral CA1
Cb	Calbindin
CB1R	Cannabinoid receptor type 1
CCK	Cholecystokinin
CGE	Caudal ganglionic eminence
CH	Cortical hem
CreER	Tamoxifen-inducible Cre recombinase
DBB	Diagonal band of Broca
DG	Dentate gyrus
Dox	Doxycycline
EC	Entorhinal cortex
LEC	Lateral entorhinal cortex
MEC	Medial entorhinal cortex
GDP	Giant depolarizing potential
GFP	Green fluorescent protein
GRIN	Gradient refractory index
HCN	Hyperpolarization-activated cyclic nucleotide–gated channel
HP	Hippocampal plate
IEG	Immediate early gene
Ih	H-current
IL	Infralimbic cortex
IZ	Intermediate zone
LFP	Local field potential
LHA	Lateral hypothalamic area
LS	Lateral septum
LTP	Long-term potentiation
MAZ	Multipolar cell accumulation zone

MCH	Melanin-concentrating hormone
MGE	Medial ganglionic eminence
mPFC	Medial prefrontal cortex
MS	Medial septum
NAcc	Nucleus accumbens
Ngn2	Neurogenin2
OLM	Oriens/lacunosum-moleculare cell
PaS	Parasubiculum
PN	Pyramidal neuron
dPN	Deep pyramidal neuron
sPN	Superficial pyramidal neuron
PP	Perforant path
PrS	Presubiculum
PV	Parvalbumin
PVBC	PV-expressing basket cell
Re	Nucleus reuniens
REM	Rapid eye-movement sleep
RGC	Radial glial cell
RSC	Retrosplenial cortex
SC	Schaffer collaterals
SGC	Semilunar granule cell
slm	stratum lacunosum-moleculare
so	stratum oriens
sp	stratum pyramidale
sr	stratum radiatum
SPA	Synchronous plateau assembly
SPW-R	Sharp wave-ripple complex
Sub	Subiculum
SWS	Slow-wave sleep
TA	Temporo-ammonic path
VZ	Ventricular zone
WT	Wild-type

A Stitchette

Part I

Introduction

1. The Hippocampal Formation

1.1 Nomenclature and anatomy

Originally identified in the human brain as a bulge in the floor of the lateral ventricle, the hippocampus was named by early anatomists after the sea-horse (hippókampos in Ancient Greek) due to its curved, elongated shape. This region is found bilaterally beneath the temporal lobe of the mammalian cortex and is linked interhemispherically by the hippocampal commissure.

It should be noted that the anatomical nomenclature of the hippocampus has varied across time and is still causing some controversy. Following the classification started by Ramón y Cajal (1893) and his disciple Lorente De Nó (1934), the *hippocampus proper* consists exclusively of the subdivisions of the cornu ammonis (CA1, CA2, CA3)[1]. However, by synecdoche the term 'hippocampus' is employed for the region including the dentate gyrus and the subiculum as well. Many neuroscientists now use the more comprehensive *hippocampal formation*, in which the presubiculum, parasubiculum and entorhinal cortices are considered (Amaral and Lavenex, 2007). In the text, I will follow a slightly different nomenclature (Strange et al., 2014) where the term hippocampus comprises the dentate gyrus and CA1-CA3 domains (without the subiculum). However, the word 'hippocampal' will refer interchangeably to the hippocampus or the hippocampal formation.

Figure 1.1 recapitulates anatomy of the hippocampal region in a rat brain. Anatomically the hippocampus is described by two main axes. First, the *septo-temporal axis*, also called long axis owing to the elongated banana-like shape. This divides it anatomically in two poles: the septal, located anteriorly and dorsally, and the temporal, at the posterior-ventral end. Interestingly the two portions are now considered as two functional regions with distinct implications in mnemonic processes, despite a stunningly constant architecture along the axis (Fanselow and Dong, 2010; Dong et al., 2009)[2]. Second, the *horizontal* or proximo-distal axis. In CA1 for instance, the proximal end is close to CA3 and the distal one to the subiculum, following the same direction as the trisynaptic circuit (see section 1.2). The same applies to the other subregions. A third axis is specific to the layer

[1] Lorente de Nó called CA4 what is now considered the hilar part of CA3 (Lorente De Nó, 1934). This is not in use anymore.

[2] For the sake of consistency with the vast majority of publications, I will use 'dorsal' and 'ventral' as substitutes for 'septal' and 'temporal', respectively. Please note that the use of 'posterior' instead of 'ventral' often leads to confusion, because both the septal and the temporal poles are present posteriorly.

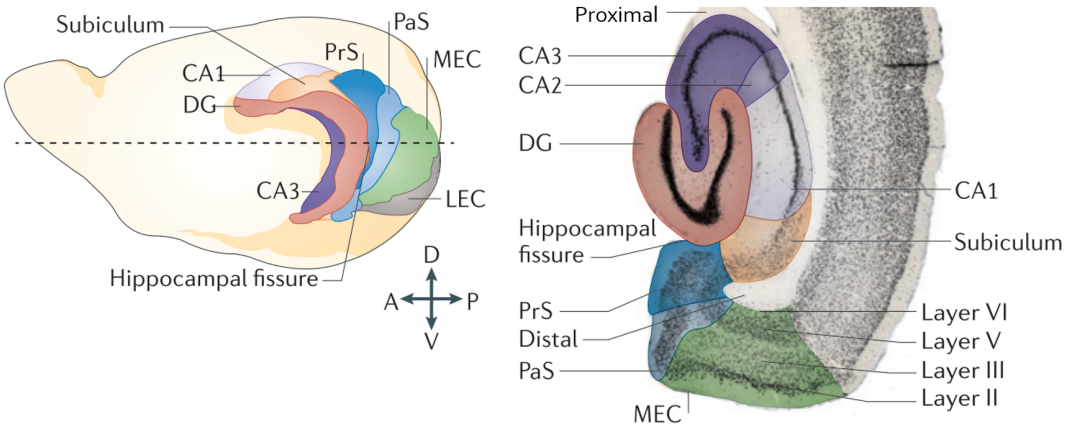

FIGURE 1.1: Anatomy of the hippocampal formation. On the left, a schematized rodent brain, showing the hippocampus with the dentate gyrus (DG), CA3 and CA1; the subicular region including subiculum, presubiculum (PrS) and parasubiculum (PaS) and the entorhinal cortex divided in the medial (MEC) and lateral (LEC) part. The dashed line represents the horizontal section shown in the adjacent panel. On the right, the same regions are depicted with a corresponding color-code. In addition, CA2 and the layers in MEC are shown. Please note that 'proximal' and 'distal' refer to the horizontal axis of CA1. (Adapted from Moser et al. (2014))

formed by pyramidal cells (present in the cornu ammonis and subiculum): the radial or *deep-superficial axis*. Later in the text, I will elaborate on how these three axes are relevant for pyramidal cell diversity (chapter 3) and on how they link to hippocampal development (chapter 4).

The reader can appreciate that, although the hippocampus is located internally and is hidden by the cortical surface, it is not separated anatomically from its partner regions. In fact, despite its subcortical location, the hippocampus is cortical from a developmental and evolutionary standpoint. Embryologically it derives from the pallium that in mammals generates the 6-layered neocortex (dorsal pallium) and the more phylogenetically ancient allocortex (Medina and Abellán, 2009). More precisely, the medial portion of the pallium gives rise to the archicortex including the hippocampus proper, dentate gyrus and subiculum, characterized by 3 layers, whereas the lateral pallium develops into structures with more than 3 layers that are closely related to the hippocampus by their connectivity and function, i.e. the entorhinal cortex (EC) (see figure 1.2). EC is anatomically divided into two parts, lateral entorhinal cortex (LEC) and medial entorhinal cortex (MEC). Despite being adjacent and sharing the same 4-layered architecture of an allocortical–neocortical transition cortex, they process distinct types of information and exhibit different connectivity, including towards the hippocampus (Witter et al., 1989).

The hippocampal formation appears then as a heterogeneous region, composed of subdivisions having different cytoarchitecture and embryology, although unified by the anatomical continuity. The main reason why it can be considered an 'operational unit' is the largely (but not exclusively) unidirectional neuronal circuit formed by its components, with the entorhinal cortex acting as an interface between the hippocampus and the neocortex,

since the latter does not provide any direct input to the former (Amaral and Lavenex, 2007). The hippocampal connectivity will be discussed in more details in the following section.

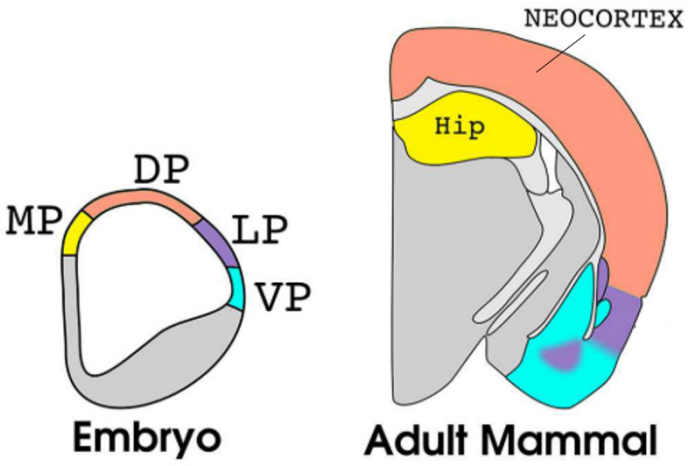

FIGURE 1.2: The hippocampus derives from the medial pallium. On the left, a schematic section of the neural tube at early developmental stages with the pallium subdivided in a medial (MP), dorsal (DP), lateral (LP) and ventral (VP) portions. On the right, in the adult brain the hippocampus is derived from the MP, whereas the DP gives rise to the neocortex. (Adapted from Luzzati (2015))

1.2 The 'revisited' tri-synaptic loop

As mentioned earlier in the text, intrahippocampal connectivity is constituted by a predominantly feed-forward excitatory pathway. The entry is provided by the entorhinal cortex. Both medial (MEC) and lateral entorhinal (LEC) cortex layer II (L2) project to the dentate gyrus via the perforant path. Then dentate granule cells send axonal terminals to CA3 via the mossy fibers, and CA3 projects to CA1 through Schaffer collaterals (SC). This circuit, known for decades under the name of 'trisynaptic circuit' (Andersen et al., 1971), only captures a limited fraction of the connections among hippocampal subdivisions. Despite the functional importance of this pathway, largely responsible for the unidirectionality of the information flow (Buzsáki, 2013), a number of other projections are worth mentioning.

- The EC layer V (L5) receives projections from both CA1 area and subiculum, and CA1-to-subiculum connections are also present (Naber et al., 2001).
- CA1 and subiculum are targeted via the temporoammonic pathway by MEC/LEC axons from layer III (L3) (Naber et al., 2001).
- Two major inputs to CA3 neurons are provided by MEC/LEC L2 (Witter, 1993) and by recurrent collaterals originated in CA3 itself.

- CA2 is also integrated in the synaptic pathway, being contacted by CA3, dentate gyrus and entorhinal L2 input (Kohara et al., 2014). In turn, CA1 is a known target of CA2 (Chevaleyre and Siegelbaum, 2010).
- Backprojections exist between the subiculum and CA1 (Xu et al., 2016b), CA3 and dentate gyrus (Scharfman, 2007).

The ensemble of these connections is schematised in Figure 1.3. As the reader can see, the relations among subdivisions in the hippocampal formation are more complex than the classic trisynaptic model describes. A 'revisited' hippocampal circuit emerges in which multiple loops are integrated in the larger hippocampus-EC network, the EC representing the gate to/from the neocortex (Buzsáki, 2013). Obviously, this model does not take into account the complete extrahippocampal connectivity, neuromodulatory innervation or fine-scale microcircuitry of all areas. These aspects will be treated in further details only for CA1 in chapter 2 of the introduction, since the work presented in this text is related to this area.

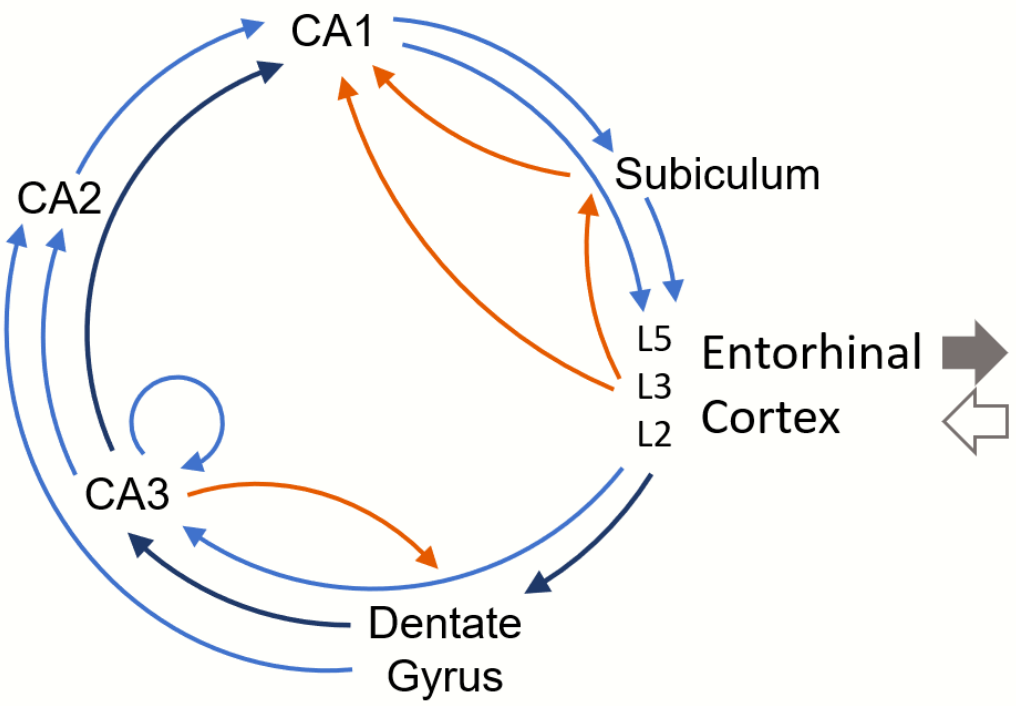

FIGURE 1.3: Schematic representation of the intrahippocampal connectivity. Dark blue arrows depict the trisynaptic circuit, with EC contacting the dentate gyrus via the perforant path, the dentate gyrus sending mossy fibers to CA3, and CA3 contacting CA1 via the Schaffer collaterals. Light blue arrows are connections that were not originally included in the model and that follow the same directionality. On the contrary, back projections, running in the opposite sense, are represented by orange arrows. Large arrows symbolise the flow of (neo)cortical information gated by the EC (Adapted from Xu et al. (2016b))

1.3 Roles of the hippocampal formation

Little was known of the intimate relationship between the hippocampus and memory before Scoville and Milner (1957) reported severe loss of memory in an epileptic patient, patient H.M., after bilateral surgical removal of the hippocampal formation and the surrounding medial temporal lobe areas. "*After operation this young man could no longer recognize the hospital staff nor find his way to the bathroom, and he seemed to recall nothing of the day-to-day events of his hospital life. [...] he did not remember the death of a favourite uncle three years previously, nor anything of the period in hospital [...]. His early memories were apparently vivid and intact.*". They conclude that these observations point to "*the importance of the hippocampal region for normal memory function.*".

Since this seminal paper, H.M.'s memory impairment has been replicated and tested in laboratory animals and a now large body of evidence has confirmed Scoville and Milner's insight. The current understanding is that the hippocampal formation is an associational area[3] of the cerebral cortex intimately linked to mnemonic processes. It contributes to the encoding, association, consolidation and recall of representations of the external and internal world through the coordinated firing of neurons in its subfields. The hippocampus, together with the subiculum, the EC and other regions, is thought to represent specific life events (places, episodes, items...) by the firing of groups of neurons (assemblies) in a temporally organized fashion (sequences) (Somogyi and Klausberger, 2017).

It is noteworthy that the citation above already hints at the multitude of features of the external world that the hippocampus can contribute to encode. The bilateral hippocampal ablation resulted in a severe anterograde amnesia that made it impossible for H.M. to retain notions about WHERE, WHAT and WHEN of specific events. Additionally, he could not recognise people he met (WHO), and was severely impaired regardless of the kind of memory test, regardless of the kind of stimulus material and of the sensory modality through which information was presented (Corkin, 2002).

In the following paragraphs, I will give an overview of these types of memory in rodent and briefly discuss the current understanding of how they can coexist in and be supported by the same brain region. One central idea of the present work is that such a variety of mnemonic processes require specialized systems that are able to treat them simultaneously. Thus, if we accept the notion that the activity of the groups of neurons within the hippocampus is a neurobiological correlate of memory, we can reasonably speculate that diversity of functions corresponds to variety of cell types. In a successive section of the introduction I will emphasise on the description of this variety, focusing on the CA1 area.

1.3.1 Neural correlates of space in the hippocampal formation

In a freely behaving animal, i.e. a mouse, the activity of neurons in the hippocampal formation is modulated by the animal's location in space. *Place cells* were the first class of

[3] An associational area is a part of the cerebral cortex that processes and integrates information coming from various other areas of the brain, thus is often linked to complex functions.

neurons identified by extracellular recording thanks to their property of firing selectively at one (or few) location(s) in space (O'Keefe and Dostrovsky, 1971). Another way to see it is that, in any given point of an environment, a subset of hippocampal cells are recruited, so that different neuronal ensembles map the animal's location in different environments, forming what is called a 'spatial map'. Place cells are predominantly recorded in CA1 and CA3, but can also be found in other regions of the hippocampal formation.

Place cells are memory cells. Two basic observations suggest why this is the case. First, when the mouse is exposed to an arena for the first time and even in absence of any cognitive task, the formation of 'place fields', the receptive fields of place cells, is almost instantaneous. The neurobiological trace of that specific arena can be stable over days, weeks or even months, as the same subset of place cells would reactivate in the same locations (Sheintuch et al., 2017). However, exposing the mouse to another arena causes the activation of another population of neurons (a phenomenon called 'remapping') and these two maps are minimally overlapping ('orthogonal') (Leutgeb et al., 2005). Second, place cells express current as well as past and future locations. This is the most evident when considering how place cells fire in respect to a hippocampal oscillation that is commonly recorded by local field potential (LFP), the *theta rhythm*. The theta rhythm is a slow oscillatory activity that ranges from 5 to 12 Hz and that dominates the LFP signal during locomotion and during periods of active engagement in the environment, such as rearing, exploring an object, as well as during REM sleep. If we observe closely the firing of place cells within a theta cycle (120-150 ms), we will notice that one or few cells fire maximally at the trough, as the animal goes through the center of their place field. In the descending phase (before the trough), place cells whose place field was crossed earlier fire at lower frequency. The earlier the spikes occur in respect to the trough, the longer distance was run from the place field. These spikes represent the past location of the animal. Oppositely, when the animal is approaching a location, the place cells corresponding to it fire more and more intensely, on the ascending phase of the cycle before reaching the trough[4]. These cells code for the future directions.

More recently, the existence of other cell types whose firing is tightly linked to the motion of an animal in its environment was demonstrated (see figure 1.4). *Grid cells* are abundant in the superficial layers of the medial entorhinal cortex and fire at several regularly space locations, forming a grid-like pattern (Hafting et al., 2005). *Head-direction cells* are sensitive to the orientation of the animal's head with respect to the environmental frame (and not of the animal's location) and are found in the pre- and parasubiculum, as well as the entorhinal cortex (Sargolini et al., 2006; Taube, 2007). *Border cells*, found mostly in subiculum and EC, are active specifically along one or several borders of the local environment (i.e. walls of the experimental arena) (Solstad et al., 2008; Lever et al., 2009). Describing in greater details all these classes is beyond the scope of the present text (cf. Grieves and Jeffery (2017) for an extensive review); however, it has become clear that spatially modulated cells (above all place and grid cells) are part of a diverse and entangled

[4]This phenomenon is called 'phase precession' (Skaggs et al., 1996)

network of cell types throughout the hippocampal formation with distinct functions in spatial representation (Moser et al., 2015).

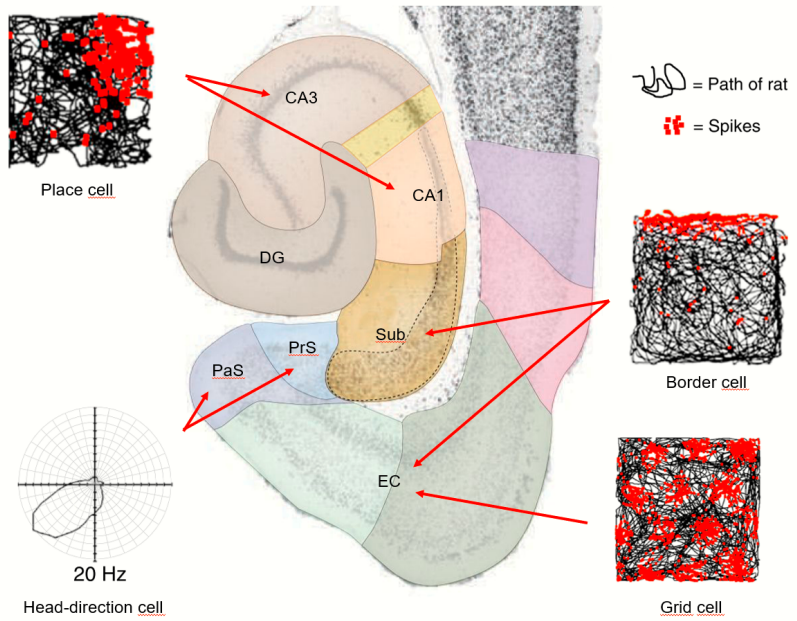

FIGURE 1.4: Space modulated cells in the hippocampal formation. A representative firing plot is illustrated for each space modulated cell, active when a rat is exploring a square arena (except for head-direction cell, spikes are red dots, and the black line is the path taken by the animal). Place cells are mostly found in the hippocampus proper and fire preferentially in a certain location of the environment. Head-direction cells, mostly in presubiculum (PrS) and parasubiculum (PaS), are most active at a certain angle of the animal's head with respect to arena, regardless of the position. Border cells in subiculum (Sub) and entorhinal cortex (EC) signal when the animal is next to the wall (or obstacle) in the environment. Grid cells are mainly found in the medial EC and fire regularly in a grid-like pattern across the whole arena. DG: dentate gyrus. Adapted from Marozzi and Jeffery (2012)

1.3.2 Navigation and episodic memory

Nonetheless, H.M.'s cognitive deficits were not exclusively in his sense of orientation in space, but also extended to episodic memory, which is defined as 'the ability to recall events in a spatiotemporal context' (Sugar and Moser, 2019). Whether navigation is the prominent feature of the hippocampus and directly supports episodic memory (or the opposite), is matter of long-lasting debate. Undoubtedly, the last decades of intense hippocampal research have brought forward the notion that the two might be intimately related. Two basic observations suggest why this is the case.

First, when the mouse is exposed to an arena for the first time and even in absence of any cognitive task, the formation of 'place fields', the receptive fields of place cells, is almost instantaneous. The neurobiological trace of that specific arena can be stable over days, weeks or even months, as the same subset of place cells would reactivate in the same locations (Sheintuch et al., 2017). However, exposing the mouse to another arena causes

the activation of another population of neurons (a phenomenon called 'remapping') and these two maps are minimally overlapping ('orthogonal') (Leutgeb et al., 2005). Second, place cells express current, as well as past and future locations. This is most evident when considering how place cells fire in respect to a hippocampal oscillation that is commonly recorded by local field potential (LFP), the *theta rhythm*. The theta rhythm is a slow oscillatory activity whose frequency ranges from 5 to 12 Hz and that dominates the LFP signal during locomotion and during periods of active engagement in the environment, such as rearing, exploring an object, as well as during (rapid eye movement) REM sleep (Vanderwolf, 1969). If we observe closely the firing of place cells within a full theta cycle (120-150 ms), we will notice that at the trough one or few cells fire maximally, as the animal goes through the center of their place field. In the descending phase (before the trough), place cells whose place field was crossed earlier fire at lower frequency. The earlier the spikes occur in respect to the trough, the longer distance was run from the place field. These represent the past location of the animal. Oppositely, when the animal is approaching a location, the corresponding place cells fire more and more intensely, on the ascending phase of the cycle before reaching the trough . These cells code for the future directions (Buzsáki and Moser, 2013).

It should also be noted that the expression of such rhythmic activity, carrying a precise, population-level organization of neuronal firing is critical for navigation, as well as for memory-guided spatial tasks. A proof of principle is that perturbating theta sequences degrades the consolidation of newly acquired memories and affects behavioral performance (Bolding et al., 2020; Drieu et al., 2018; Robbe and Buzsáki, 2009). Sequences are observed at several time scales: (i) behavioral time scale (several seconds), the progression of place cell firing when a rodent is crossing successive fields; (ii) nested within theta oscillations (hundreds of milliseconds), like mentioned above; (iii) compressed timescale (40-100 ms), during fast oscillations. I will explain more thoroughly in 2 how these oscillations are generated in CA1 and how they relate to one another.

Although this remains partially speculative, sequences of neuronal activation seem to be a common governing principle explaining how the hippocampus provides a flexible structure to store and bind together 'snapshots' of experience. "Although re-experiencing the past appears as a continuous process, we are consciously aware of only short segments of the episodes at any one time" (Buzsáki and Moser, 2013). It should be noted that these segments are associated to one another and can be related to multiple dimensions of the experience (not only space, but also time, emotional state, motivation, . . .). This view has generated interest because it bridges the gap between the hippocampal spatial map (O'Keefe and Nadel, 1978) and the function of the hippocampus in the formation of episodic memory (Scoville and Milner, 1957; Eichenbaum et al., 2007), in which non-spatial information is an essential compontent. In fact, hippocampal cells have also been shown to code other features of an experience in their firing rates, and sometimes through sequences, like time (Eichenbaum, 2014), odors (Allen et al., 2016), task- and context-related variables (Aronov et al., 2017; Wood et al., 2000), social space (Schafer and Schiller, 2018), to

mention just a few. Of course, the hippocampus does not operate on its own, and its interactions with other brain regions are crucial in supporting these many types of information processes. This is particularly evident when looking at the involvement of the hippocampus in behaviors with an emotional component, which I will delineate in the next section. More examples will also be provided by describing behaviorally-relevant pathways from and to CA1 in chapter 2 and 3.

1.3.3 Hippocampus and Emotions

Historically, the hippocampus was considered the entry and exit point of a large brain network thought to control emotion, the Papez circuit (Papez, 1937). Although this terminology is considered outdated nowadays, the link between the hippocampal formation and affect is currently widely accepted and experimentally investigated. Among those emotional states that relate to hippocampal activity are fear and anxiety, which promote adaptive avoidance behaviors to proximal and distal threats, respectively, to safely navigate in an environment. Hippocampal activity is essential to the induction of fear conditioning, mostly in respect to the contextual component of an aversive episode (Corcoran and Maren, 2001; Jimenez et al., 2020; Kim and Fanselow, 1992). In addition, some studies showed that hippocampal inactivation can also block tone-cued fear memory, that is regardless of the context (Hunsaker and Kesner, 2008; Maren and Holt, 2004). For the execution of fear-related behavioral response, such as freezing in rodents, reciprocal connections between the amygdala and the temporal-most aspect of the hippocampus are known to be crucial (Tovote et al., 2015).

Similarly, lesions of the ventral hippocampus reduce avoidance response when rodents are exposed to potential threats, such as cat odor (Pentkowski et al., 2006), or to an elevated plus maze, a test commonly used to probe anxiety-like behavior (Kjelstrup et al., 2002). Manipulation of the hippocampus itself or its inputs and cortical outputs can directly impact these responses (Felix-Ortiz et al., 2013; Padilla-Coreano et al., 2016; Parfitt et al., 2017), suggesting that they form a functional circuit that processes emotional information.

Not surprisingly, owing to its connectivity to cortical, striatal and hypothalamic regions, the hippocampus occupies a key position to control alertness and stress. First, it exerts strong regulatory control of the hypothalamic-pituitary-adrenal axis. It was shown that hippocampal lesions impair modulation of the hormonal stress response (Dedovic et al., 2009; Jacobson and Sapolsky, 1991) and that increase of stress hormones, such as glucocorticoids, can induce hippocampal dysfunction (McEwen and Magarinos, 1997). Second, the temporal pole of the hippocampus can bimodally regulate locomotion (Bast et al., 2001; Zhang et al., 2002), supposedly through the interaction with the nucleus accumbens of the ventral striatum and the dopaminergic system (Peleg-Raibstein and Feldon, 2006; Rosen et al., 2015). These observations are also coherent with the engagement of hippocampal activity in goal-directed behaviors (Schumacher et al., 2018; Yoshida et al., 2019) and the presence of specific neurons that signal the presence (or lack thereof) of a seeked reward (Ciocchi et al., 2015; Gauthier and Tank, 2018).

As an additional proof of the importance of the hippocampal region in mood and affect, some psychological disorders with strong affective components, such as posttraumatic stress disorder, bipolar disorder, and depression, are associated to decreased hippocampal volumes and hippocampal dysfunction in patients (Bonne et al., 2008; Frey et al., 2007). From a behavioral perspective, the feature these conditions share in common is that avoidance responses are exacerbated or occur in absence of a specific threat (Kheirbek et al., 2012).

2. CA1 anatomy and Physiology

2.1 Cytoarchitecture and cell types

CA1 is the area of the hippocampus with the simplest cytoarchitectural organization. It is divided in 4 layers, according to the orderly arrangement of cells and afferent fibers (see figure 2.1). The *stratum pyramidale*, or pyramidal cell layer, comprises the large majority of glutamatergic principal cells (also called pyramidal cells) and form a relatively compact sheet of approximately 5-to-10 somata in mice. These cells extend a prominent apical dendritic tree in one direction, and smaller yet more numerous basal dendrites in the other. The latter is the called stratum oriens and is located between the pyramidal layer and the alveus. It contains excitatory fibers arising from CA3, CA2 and entorhinal cortex to a lesser extent, as well as interneurons. The former is further subdivided in the *stratum radiatum* and the *stratum lacunosum-moleculare*. Both are enriched with a variety of interneuron classes but can be grossly distinguished by the presence of CA3 Schaffer collaterals and temporo-ammonic fibers from EC, respectively. In addition, the pyramidal apical dendrite forms in the stratum radiatum one or more two main branches, as well as oblique dendrites (proximal dendrites), and ramifies more conspicuously in the stratum lacunosum-moleculare in what is called the 'dendritic tuft' (distal dendrites) (Amaral and Lavenex, 2007).

2.1.1 Pyramidal cells in CA1

Pyramidal cells are the most numerous neuron class in CA1, representing almost 90% of the all neurons (Bezaire and Soltesz, 2013). They are glutamatergic projection neurons with their axon contacting regions located several millimeters away from the hippocampus. The fundamental role of pyramidal cells is to integrate excitatory and inhibitory input originating from different sources, and to provide an output to intra- and extrahippocampal targets. Although this is a general principle of neuronal networks, it is even more prominent for pyramidal cells, if we consider their stance within the hippocampal circuitry. Since CA1 is the 'gateway region' between the hippocampus and the EC (as well as many other extrahippocampal regions)[5], the activity of these cells can arguably be seen as the readout of the hippocampus as a whole.

Information processing in the hippocampus is often interpreted in a framework of the dynamic interaction between a large population of principal neurons and a plethora of

[5] According to the nomenclature used, CA1 shares this feature with the subiculum as well.

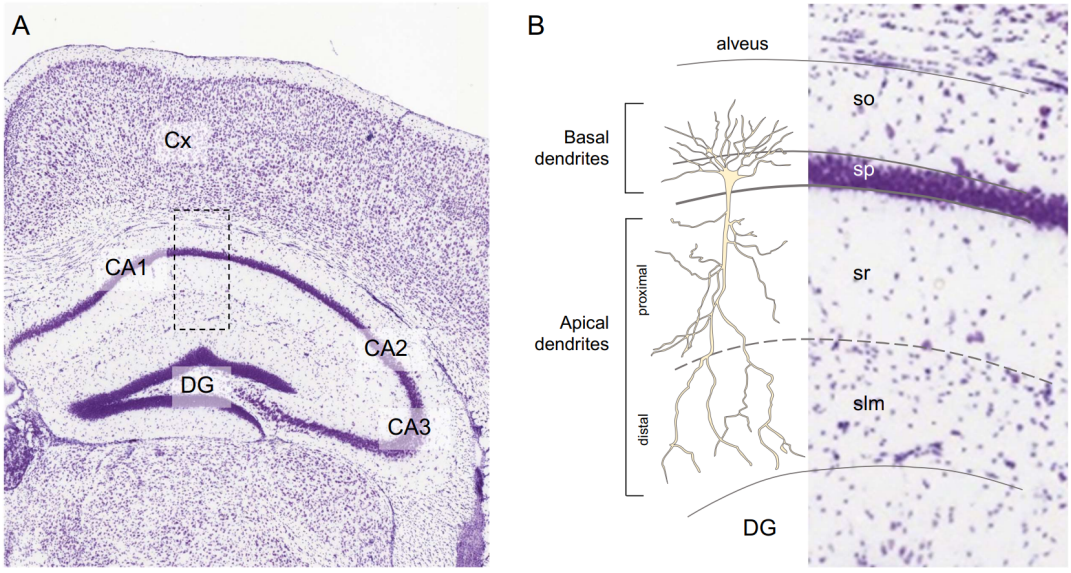

FIGURE 2.1: Laminar composition of CA1 field of the hippocampus. A) Nissl staining of a coronal section including the dorsal pole of the hippocampus, from the publicly available Allen Brain Reference Atlas for mouse. B) Magnification of the dashed rectangle in A, showing the laminar composition of CA1 and the corresponding dendritic compartments of a stylized pyramidal cell. From top to bottom, alveus, below the cortex (Cx) and containing axons from principal cells; stratum oriens (so); stratum pyramidale (sp), where most pyramidal cell somata are found; stratum radiatum (sr) and stratum lacunosum-moleculare (slm), above the dentate gyrus (DG). CA1 pyramidal cells extend their basal dendrites in the so and proximal and distal apical dendrites in the sr and slm, respectively.

highly heterogeneous interneuron classes (Klausberger and Somogyi, 2008). This model emphasizes on the description of these classes and how they organize local inhibition onto pyramidal cells in a spatially and temporally segregated manner.

Although it has been extremely useful in the mechanistic explanation of the neurophysiology of CA1 microcircuitry (see section 2.2), an essential aspect is largely overlooked and has come to gain more attention in the last decade. Pyramidal cells are a not a monolithic cell type, with a constant phenotype, but present an appreciable degree of diversity (Slomianka et al., 2011; Soltesz and Losonczy, 2018; Cembrowski and Spruston, 2019; Mallory and Giocomo, 2018). Importantly, the heterogeneity observed within pyramidal cells, ranging from morphology to connectivity or firing in vivo, is not chaotic or unorganized, but rather follows topographic gradients matching the three axes of the hippocampus. The existence of pyramidal cell diversity raises the intriguing possibility that different subpopulations might differentially subserve specific mnemonic processes. I will treat extensively this topic (chapter 3), and jointly with the experimental results of the present work, I will suggest (chapter 4) that these 'axes of diversity' are developmentally defined.

2.1.2 GABAergic interneurons in CA1

As mentioned above, GABAergic interneurons are characterized by their pronounced diversity (Ascoli et al., 2008). At present, there is only partial consensus on how to subdivide them.

A given classification criterion (such as neuropeptide expression, morphology, physiology...) might capture some level of heterogeneity and neglect others. In fact, in the light of modern technological advances even the existence of defined interneuron classes (as opposed to a continuum of cell phenotypes) appears questionable (Harris et al., 2018). However, in figure 2.1, I synthetically present the main interneuron types in respect to the spatial organization of their synaptic innervation onto pyramidal dendritic compartments, pyramidal cells being the focus of this work (for a more exhaustive description, see Klausberger and Somogyi (2008)).

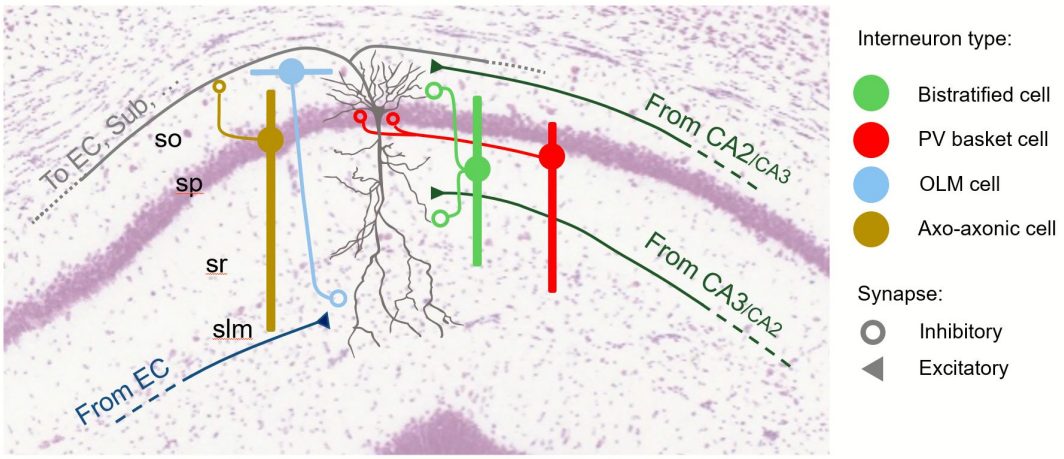

FIGURE 2.2: Schematic representation of the main interneuron classes innervating different compartments of CA1 pyramidal cells. In green, a bistratified cell forms synapses onto basal and proximal distal dendrites, where excitatory input from CA2/CA3 is most represented; in red, parvalbumin (PV)-expressing interneurons innervate the peri-somatic region; in light blue, an oriens/lacunosum-moleculare (OLM) cell targets the distal dendritic compartment, similarly to EC axons; in beige, axo-axonic cells can control pyramidal cell firing via direct innervation of their axons.

- **Peri-somatic innervating interneurons** are named *basket cells* due to their abundant axonal arborization around the pyramidal soma and proximal dendrites. This rich somatic innervation grants them a privileged role in modulating the firing activity of pyramidal cells and in the generation of oscillatory ripples (see section 2.2) (Gan et al., 2016). Basket cells are either parvalbumin (PV) or cholecystokinin (CCK) expressing interneurons. PV+ interneurons have their soma within or in the proximity of the pyramidal layer, dendrites spread across all layers and are mostly fast spiking. CCK+ cells can be located either around the stratum pyramidale or at the radiatum/lacunosum-moleculare border and express endocannabinoid receptor 1 (CB1R) at the presynaptic site.

- **Axon innervating interneurons**, also called axo-axonic or *chandelier cells*. The soma is found within or near the stratum pyramidale, and their dendrites are spread across all layers of CA1. They contact the axon initial segment of pyramidal cells, through which they control the generation and back-propagation of pyramidal action

potentials through fast spiking activation. Unlike PV-basket cells, they are inhibited during sharp wave-ripples (Klausberger and Somogyi, 2008).

- **Dendrite innervating interneurons** include several subfamilies, among which *oriens/lacunosum-moleculare* (OLM) cells, *bistratified* cells, *Schaffer collateral-associated* cells, *perforant path-associated* cells. Beside the differences in their physiology and expression of neuropeptides, a common underlying principle is that they associate their synapses mainly with one of the major glutamatergic input zones, thus supporting a pathway-specific regulation of pyramidal cell activation (Somogyi and Klausberger, 2017). For instance, (i) the axon of OLM interneurons contacts the apical dendritic tuft of pyramidal cells in the same location as the EC input; (ii) bistratified cells innervate principal neurons in the stratum oriens and radiatum, matching the distribution of Schaffer collateral fibers (Müller and Remy, 2014).

- Other classes include **long-range projecting** GABAergic neurons, whose targets are located outside CA1, and **interneuron-specific** interneurons, that do not contact pyramidal cells.

2.2 Microcircuitry and neurophysiology

When recorded extracellularly, the CA1 network exhibits distinct oscillations at various frequencies and these are correlated with certain behaviors or brain states. The common understanding of how they are generated is that, in combination with excitatory input (mainly CA3 and EC), various classes of interneurons cooperatively support the firing of specific ensembles of pyramidal cells (Klausberger and Somogyi, 2008). This is made possible by compartmentalization of their axonal targets on pyramidal dendrites, as well as by the temporal organization of interneuron activation during these events. The following are the main oscillatory activities that can be recorded extracellularly in CA1 (figure 2.3).

As mentioned in section 1.3.2, theta rhythm is a slow frequency oscillation (5-12 Hz), observed in the entire hippocampal region during locomotion, memory tasks and REM sleep (Vanderwolf, 1969). When a CA1 pyramidal cell fires, for example, because the animal entered the cell's place field, it can fire with bursts of action potentials that are modulated by the theta rhythm and are subject to *phase precession* on subsequent theta cycles. This rhythmic activation changing in rate and phase cannot be solely explained by entorhinal input in the stratum lacunosum-moleculare, where the theta signal is robust and highly regular (Buzsáki, 2002). It has become clear that pyramidal cells are periodically inhibited and display the lowest firing probability at the peak of the theta cycle, which is when axo-axonic interneurons are the most active. PV+- and CCK+-basket cells fire at the descending and ascending phase of the cycle, respectively. On the contrary, at the trough place cells receive little inhibition on the somatic region (thus the high firing probability) but are hyperpolarized by GABA release at various dendritic compartments due to OLM and bistratified cells, among others. On average, Pyramidal cells fire action potentials at a time when the soma is most depolarized and after the discharge of PV+ basket and axo-axonic

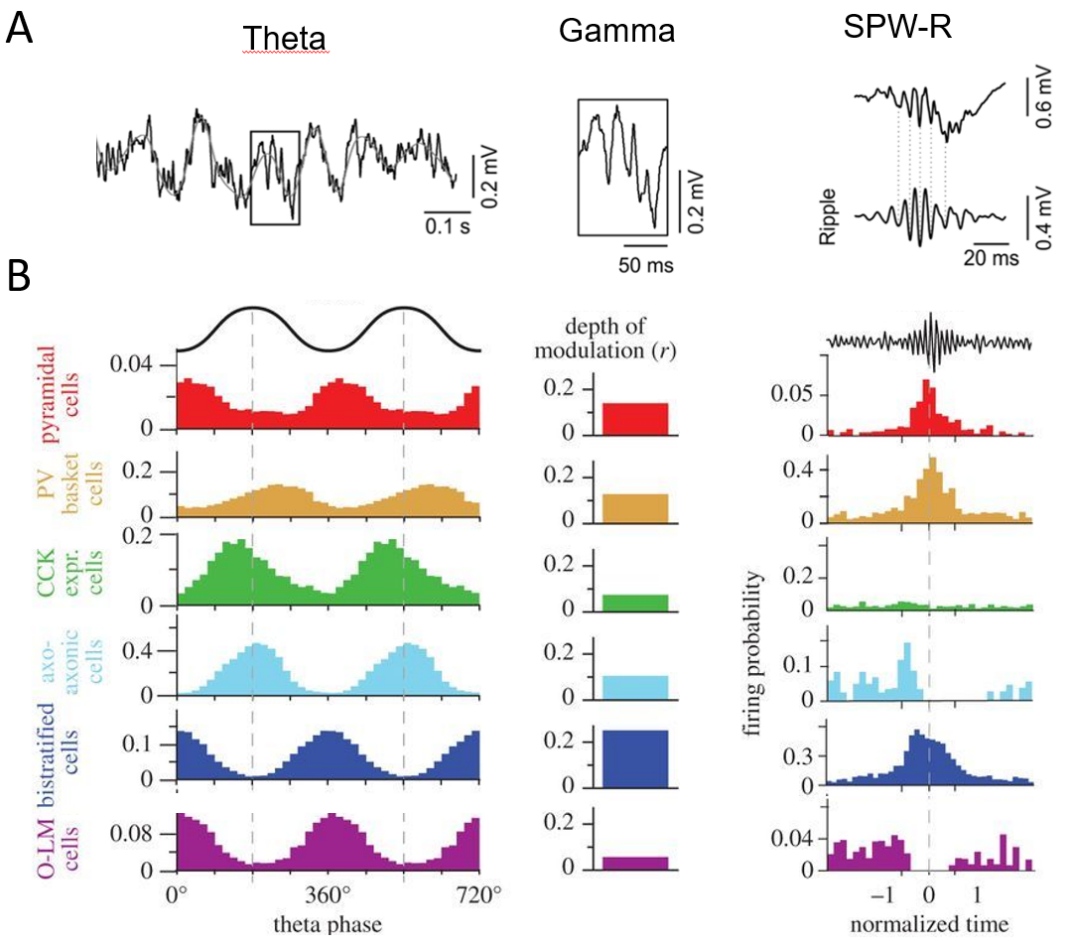

FIGURE 2.3: Distinct local field potential (LFP) patterns in the hippocampal circuit and cell-type specific recruitment. A) Left, LFP trace of theta oscillations from CA1 pyramidal cell layer of rodent hippocampus recorded during REM sleep (filtered theta oscillations (4–10 Hz) in gray tone). Middle, LFP trace of theta-nested gamma oscillations (30–80 Hz) from the previous trace (black rectangle). Right, LFP trace of an individual hippocampal sharp wave-ripple (SPW-R, upper trace) and band-pass filtered ripples (100–300 Hz, lower trace, marked with dashed lines) recorded during slow wave sleep (SWS). Adapted from Çalışkan and Stork (2019). B) Temporal relationships between hippocampal oscillations and 6 cell types, including GABAergic interneurons cited above and pyramidal cells. Left, firing probability histograms during theta oscillations. Note that pyramidal cell firing probability is lowest at the theta peak, when axo-axonic cells fire maximally and the sum of CCK- and PV-expressing basket cell firing probability is also maximal. Middle, depth of firing modulation during gamma waves (r). Here, bistratified cells show the highest gamma coupling, and most of their dendrites are in the input zone from CA3 pyramidal cells which are strongly modulated by (slow) gamma oscillations. Right, firing probability histograms centered on the ripple peak. Axonal inhibition from axo-axonic cells is withdrawn, allowing maximal pyramidal cell discharge synchronized by PV-expressing basket and bistratified cells. Adapted from Somogyi et al. (2014).

cells. In parallel, dendritic hyperpolarization may contribute to 'resetting' pyramidal cell firing, by reactivation of voltage sensitive channels (Somogyi and Klausberger, 2005).

Theta activity often occurs in concert with *gamma oscillations*, at higher frequency (25-100 Hz) but smaller amplitude (Csicsvari et al., 2003). Although not restricted to a

single brain region or behavioral state, gamma rhythms are of particular interest in the hippocampal framework. In the CA1 region, at least two distinct gamma oscillations coexist, with opposite theta phase preferences, distinct spatial distributions in CA1 input-layers, and different frequency ranges (Colgin, 2016). Gamma in the 25 to 55 Hz frequency band (or 'slow gamma') is mostly present in the stratum radiatum, has higher amplitude in the theta peak/descending phase and is driven by CA3. By contrast, EC input entrains 'fast gamma' (60-100 Hz), which is the strongest in the stratum lacunosum-moleculare at the theta trough (Colgin et al., 2009; Schomburg et al., 2014). In a similar fashion to what has been shown for theta oscillations, CA1 interneuron classes are differentially modulated by separate gamma frequencies in behaving or anesthetized rats (Klausberger and Somogyi, 2008; Lasztóczi and Klausberger, 2014).

Sharp wave-ripples (SPW-R) represent brief transitory network state recorded in CA1 during awake immobility and consummatory behaviors (drinking, eating, grooming...), as well as slow-wave sleep (Buzsáki et al., 1983). They consist of a large negative deflection of the field potential recorded in the stratum radiatum, accompanied by a high frequency (140-200 Hz) oscillation in the stratum pyramidale, lasting 50 to 100 ms. Despite being temporally coupled, sharp waves and the ripple events are thought to have different mechanistic origins. Sharp waves are explained by a massive synaptic input in the stratum radiatum, which is in turn largely due to a synchronous discharge of CA3 pyramidal cells (Buzsáki, 1986) (CA2 is also a potential trigger (Oliva et al., 2016b)). By contrast, ripples are generated locally in CA1 by specific interneurons (Somogyi and Klausberger, 2005). While axo-axonic and OLM interneurons are silenced, bistratified and PV+-basket cells increase their firing during the ripple, inducing rapid cycles of hyperpolarization. Thus, in combination with the strong excitation from CA3 area, this might produce pyramidal cell discharges at the ripple frequency.

2.3 Oscillations and memory

The description and mechanistic dissection of hippocampal oscillations illustrate the need for the existence of numerous specific types of interneurons supporting temporally organized pyramidal cell and, ultimately, network activity. As mentioned previously, these are not mere epiphenomena of hippocampus neuronal firing, but are the neurobiological correlates of cognitive states, and more specifically mnemonic processes (Colgin, 2016).

The most parsimonious way to explain how we form new memories is to suppose the existence of two main stages (Buzsáki, 1989). First, the hippocampus rapidly encodes information of an ongoing experience during wakefulness in the form of a memory trace. Then, during 'offline periods', memory traces are reactivated by the hippocampus, thus allowing the long-term storage in cortical networks or strengthening associations between traces in different brain regions (O'Neill et al., 2010). In addition to this, when the behavioral context requires it, memories need to be retrieved. The coupling of theta-gamma rhythms is thought to be critical for the encoding of memory and its successive

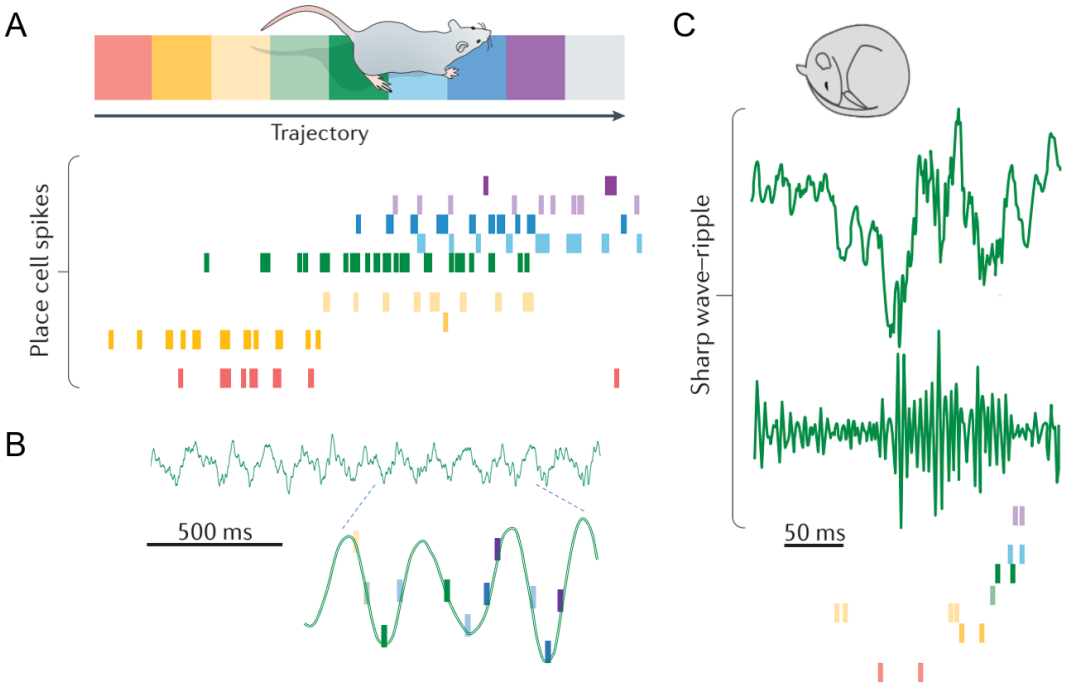

FIGURE 2.4: Neuronal sequences are expressed in CA1 at different time scales. A) Spikes from successively activated place cells (bottom) as a rodent passes through the cells' place fields in a particular trajectory on a linear track (top). B) Schematic drawing illustrating theta oscillations recorded during exploration (top) and place cell sequences within a theta cycle (*theta sequences*). Note how spikes occur at progressively earlier theta phases across successive theta cycles (*phase precession*). C) Example of sharp wave–ripple (SPW-R, top) recorded during rest after exploration of the linear track and a bandpass filtered (150–300 Hz) version of the sharp wave–ripple is shown immediately. Spikes from the same place cells (forming an assembly) reactivate during SPW-R in the same order as in exploration. Note the much faster timescale. Adapted from Colgin (2016)

recall. When a mouse is exploring a novel environment (i.e. a linear track, figure 2.4), a subset of CA1 pyramidal neurons will respond to defined aspects of the experience, e.g. location (as well as context, sensory cues, emotional state...) and will synchronize their firing within a theta cycle. This group of co-active neurons is called a *cell assembly* (Harris et al., 2003). During each single cycle (about 125 ms), they activate one after the other in a coordinated fashion, producing a so-called 'theta sequence' (Skaggs et al., 1996). These orderly discharges, nested within a theta cycle, are modulated by gamma oscillations, whose shorter time window is in the same range of what predicted by spike-dependent synaptic plasticity (Buzsáki and Draguhn, 2004). In other words, gamma would allow the binding of those cells whose activity carries related information (an assembly); theta would coordinate these assemblies into discrete 'chunks' of experience that are linked together at the behavioral scale and collectively form a memory trace (Colgin, 2016). There is increasing evidence that distinct gamma sub-bands are selectively involved in either memory encoding or recall. Fast gamma, driven by the entorhinal cortex and most prominent in CA1 lacunosum-moleculare, is likely to support the transfer of processed sensory information during learning. Oppositely, slow gamma might help CA3-CA1 coordination during retrieval

of a past experience (Tort et al., 2009; Shirvalkar et al., 2010; Siegle and Wilson, 2014). In section 2.5, the importance of neuromodulation by acetylcholine in this transition will be further discussed.

After the mouse has explored the environment, previously active neuronal sequences can be reinstated in a temporally compressed manner, the so-called 'replay' during sharp wave-ripples (Nádasdy et al., 1999) (figure 2.4. As mentioned above, this occurs at times of immobility or slow wave sleep post-experience and has been causally linked to memory consolidation (Girardeau et al., 2009). According to the current theory, long-term storage is supported by the transfer of the memory trace from the hippocampal formation to the neocortex and highly synchronous activity associated to sharp wave-ripple events is a candidate mechanism for hippocampo-cortical coordination (Girardeau and Zugaro, 2011).

2.4 Long-range connectivity

In addition to the intrahippocampal circuitry, CA1 presents a rich structural and functional connectivity with many other brain areas. In this section, I will schematically present the main afferents and efferents, giving account of the behavioral or cognitive processes in which these pathways are involved.

- The **prefrontal cortex** is one of the main targets of the hippocampus, attracting a great deal of scientific interest. The organization of CA1 projections to the neocortex has been the object of extensive tracing studies (Groen and Wyss, 1990; Verwer et al., 1997) that revealed axon terminals innervating a wide portion of the frontal lobe in rat. Specifically, the septal pole of CA1 sends projections mainly to the *retrosplenial* (RSC) and the *anterior cingulate area* (ACC). The *infralimbic* (IL), *prelimbic* (PL) and *perirhinal* (PRC) cortices are favored by the ventral pole. Cenquizca and Swanson (2007) complemented these findings and identified structural connections that were previously neglected. Ventral CA1 neurons appear to also contact olfactory-related regions (orbitofrontal, piriform area and accessory olfactory bulb) and, to a lesser extent, other cortical associational areas.

  CA1 projections to IL/PL have traditionally been associated to spatial memory and goal-directed tasks (Burton et al., 2009; Hok et al., 2005), especially from the dorsal pole. More recently, ventral hippocampal-prefrontal interaction was found to be a key player in anxiety (Ciocchi et al., 2015; Padilla-Coreano et al., 2016; Padilla-Coreano et al., 2019), social recognition (Phillips et al., 2019; Sun et al., 2020a) and modulation of fear memory (Marek et al., 2018; Twining et al., 2020), in concert with the amygdala. It is crucial to mention that the prefrontal cortex does not provide input to the hippocampus, despite this rich innervation originating from CA1 (Cassel et al., 2013).

- The **nucleus reuniens** (Re) is a small portion of the midline thalamus that forms a tripartite network with the prefrontal cortex and the hippocampus and is thought to

serve as a 'relay' between the two regions. Cassel and colleagues (2013) discussed the functional relevance of the circuit, that appears to be crucial in the acquisition and retrieval of memory in goal-directed or spatial tasks requiring "the coordinated activation of prefrontal cortex and the hippocampal system".

From a structural standpoint, this is supported by numerous experimental findings. First, the Re provides excitatory input in the stratum lacunosum-moleculare of CA1 (Witter et al., 1989; Wouterlood et al., 1990) and forms a disynaptic circuit with CA1 through the subiculum (McKenna and Vertes, 2004). Second, the nucleus reuniens is bidirectionally connected to the prefrontal cortex, mainly IL, PL and more weakly to ACC (Vertes, 2006). These findings were confirmed in two studies using retrograde tracers (fluorogold and cholera toxin subunit B), which additionally showed that hippocampal projections are denser from ventral than dorsal CA1 (Hoover and Vertes, 2012; Varela et al., 2014). Importantly, almost 10% of Re projecting neurons present collaterals in both the hippocampus and the prefrontal cortex, supporting the notion of Re as a relay between the two structures.

- **Amygdala**.There is considerable evidence implicating the hippocampus-amygdala circuit in conditioned fear. A pioneering study showed that lesions in either the hippocampus or the amygdala abolished fear conditioning to an electric foot-shock, specifically when it was dependent on the context (conditioning apparatus), and not on auditory cues (Phillips and LeDoux, 1992). Furthermore, recent studies have suggested that inactivation of either dorsal or ventral hippocampal pyramidal neurons can differentially affect specific aspects of contextual fear conditioning. Goshen et al. (2011) found that dorsal CA1 inactivation impaired both fear memory acquisition and retrieval, whereas the same manipulation in the ventral pole resulted in the disruption of memory consolidation only, but not encoding or retrieval (Zhu et al., 2014). Other than fear conditioning, in the past ten years the functional relevance of this pathway was extended to anxiety (Felix-Ortiz et al., 2013; Pi et al., 2020), social (Felix-Ortiz and Tye, 2014) and consumptive behavior (Ewin et al., 2019). How these different aspects coexist and interact is still not clear, however one should not forget that many regions are simultaneously involved in these cognitive operations. In addition, the amygdala is a composite structure, formed by several nuclei, each with its own specific cellular composition, physiology and connectivity (Pitkänen et al., 1997).

  Anatomically, projections to the basal, basomedial and accessory basal nucleus of amygdala originate mostly from the ventral end of CA1 and the subiculum (Canteras and Swanson, 1992; Groen and Wyss, 1990). Pitkänen and colleagues gathered evidence of the bidirectionality of these connections (Pikkarainen and Pitkänen, 2001; Pitkänen et al., 2000). They highlighted how the same basal nuclei send axons back to the ventral hippocampus. Furthermore, they found that the central and medial portion of the amygdala are outputs of the ventral pole of CA1 as well, but only the medial nucleus appears to provide input.

- The **nucleus accumbens** (NAcc) of the ventral striatum is composed of a *core*, surrounded by an external *shell* and plays a key role in reward learning and motivated behavior (Humphries and Prescott, 2010). Most structural and functional studies in relation with the hippocampus have focused on the NAcc shell. Indeed, synaptic tracing initially brought to light the existence of a ventral CA1-NAcc shell connection (Britt et al., 2012; Kelley and Domesick, 1982; Groen and Wyss, 1990) [6]. Later, the manipulation of this pathway was shown to alter spatial reward-seeking behavior (Britt et al., 2012; Ito et al., 2008; LeGates et al., 2018). It should be noted that a direct route from dorsal CA1 was proved essential in recruiting NAcc shell neuronal ensembles in a conditioned place preference assay (Trouche et al., 2019), challenging the notion that these projections originate only from the ventral pole.

  In addition, another functional circuit including hippocampus-NAcc projections was unraveled by the collective effort of several teams (see review by Okuyama (2018)). In a nutshell, hypothalamic supramammillary body contact dorsal CA2, and can drive principal cell firing in response to social novelty (Robert et al., 2020; Chen et al., 2020). CA2 in turns projects to ventral CA1 pyramidal neurons, which are functionally connected to the nucleus accumbens shell. This circuit is modulated by oxytocin (Raam et al., 2017; Tirko et al., 2018) and a large body of evidence proved its crucial implication in the expression of social memory, i.e. recognizing familiar versus unknown conspecifics (Chen et al., 2020; Hitti and Siegelbaum, 2014; Meira et al., 2018; Rao et al., 2019; Okuyama et al., 2016).

- The **septal region** and the hippocampus are reciprocally connected (Raisman, 1966; Nyakas et al., 1987). The medial septum (MS) and diagonal band of Broca (DBB) send cholinergic afferents in CA1 onto all types of neurons, with a bias towards interneurons, whereas GABAergic afferents specifically contact CA1 interneurons (Freund and Antal, 1988). Septo-hippocampal back-projections to MS and DBB arise from long-range GABAergic cells, and not from principal cells (Takács et al., 2008). Collectively, MS and DBB form a complex whose input to the hippocampus is involved in the generation of theta oscillations. Indeed, MS cholinergic afferent stimulation in CA1 increases frequencies in the theta-band, while abolishing SPW-R (Vandecasteele et al., 2014). Conversely, inhibition of the MS-DBB complex abolishes theta oscillations, which in turn leads to learning impairments (Lawson and Bland, 1993; Leutgeb and Mizumori, 1999). In addition, a causal link between memory retrieval and GABAergic input from MS was recently established in a contextual fear paradigm (Sans-Dublanc et al., 2020).

  The lateral part of the septum (LS) is richly innervated by CA1 (Alonso and Köhler, 1982; Arszovszki et al., 2014; Groen and Wyss, 1990) in a topographic manner (see section 3.1 (Risold and Swanson, 1997)). It is noteworthy that almost all neurons

[6] However, synaptic terminals found in the core might control the formation and retrieval of memory in a drug-induced place preference paradigm (Zhou et al., 2019)

send collaterals to the lateral septum and that many of these axons collateralize to multiple extrahippocampal targets (Calderazzo et al., 1996; Swanson et al., 1981). Recently, it was quantitatively demonstrated that bifurcated neuronal trajectories including the LS (i.e. LS + NAcc, LS + mPFC, LS + lateral hypothalamus) are significantly more represented than others (Gergues et al., 2020). Although the importance of each of these motifs is not elucidated yet, a few studies probed the role of CA1-LS projections and pointed at an implication in innate behaviors, such as feeding and foraging-related memory (Sweeney and Yang, 2015; Davis et al., 2020), response to threat (Chee et al., 2015) and anxiety (Parfitt et al., 2017; Anthony et al., 2014).

- Axonal innervations to the **hypothalamus** from ventral CA1 have been related to food intake (Noble et al., 2019), anxiety (Jimenez et al., 2018) and social behavior (Lo et al., 2019). This is not dissimilar from other projectional motifs mentioned previously, like with the prefrontal cortex and the septum. Although we cannot yet clearly discern the single contribution of each pathway, this body of evidence seems to converge on one observation. The hippocampus receives and integrates a multitude of exogenous (spatial, contextual, sensory cues...) and endogenous (endocrine, emotional, motivational...) signals to regulate innate and learned behaviors (Tannenholz et al., 2014). As a proof, the densest projections are found in lateral area of the hypothalamus (LHA, but also in the anterior and the ventromedial nuclei) (Cenquizca and Swanson, 2006; Groen and Wyss, 1990). A subpopulation expressing MCH (melanin-concentrating hormone) in LHA is reciprocally connected to CA1 and the MCHR1 receptor is heavily expressed along the entire hippocampal long axis (Chee et al., 2013; Lembo et al., 1999). Synaptic terminals from MCH+-cells were recently discovered in the dorsal pole and shown to be involved in the process of forgetting associated to REM sleep. Indeed, their chemogenic inactivation increased memory performance in different hippocampus-dependent behavioral tasks (Izawa et al., 2019). Furthermore, MCH signaling onto ventral CA1 appears to modulate impulsivity in feeding, in line with its known role in food intake (Kowalski et al., 2004).

- The **bed nucleus of stria terminalis** receives heavy projections from, among other areas, the hippocampus and basolateral amygdala, and in turn targets hypothalamic and brainstem nuclei that mediate many autonomic and behavioral responses to aversive or threatening stimuli. Recent studies have shown that the bed nucleus of the stria terminalis does participate in certain types of anxiety and stress responses (see reviews by Walker et al. (2003) and Adhikari (2014)).

Finally, other structures exhibit some degree of connectivity with CA1, but their relevance has only been started to be investigated. Two examples are the Edinger-Westphal nucleus (Li et al., 2018) and the nucleus incertus (Szőnyi et al., 2019).

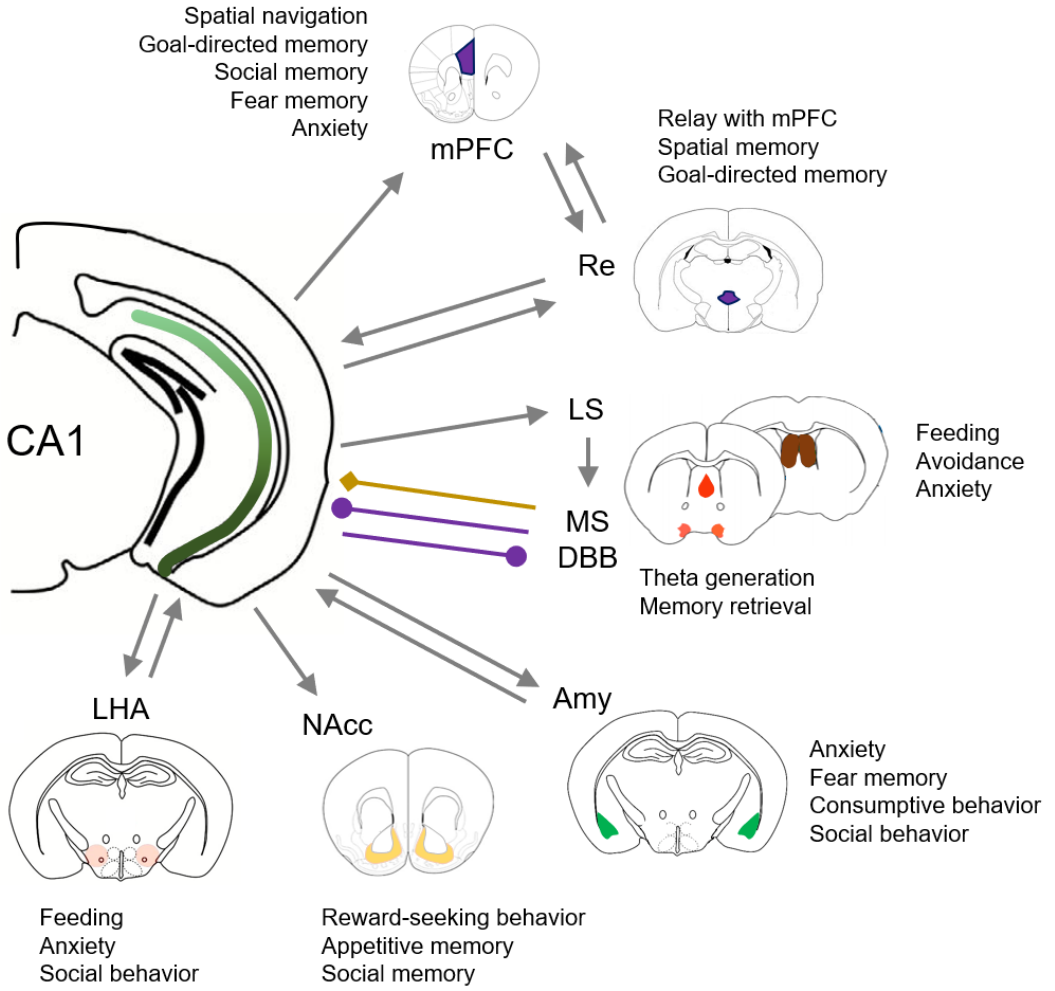

FIGURE 2.5: Main extra-hippocampal inputs and outputs of CA1. Each region is stylized in coronal sections reporting their location in the brain. Connections are color-coded (gray arrow: glutamate, purple dot: GABA, beige square: acetylchole) and behavioral functions associated to each pathway are summarized (see text for specific references). Please note that the arrangements of regions does not correspond to the septo-temporal organisation of these projections. Medial prefrontal cortex (mPFC), nucleus reuniens (Re) of the thalamus, lateral septum (LS), medial septum (MS), diagonal band of Broca (DBB), amygdala (Amy), nucleus accumbens (NAcc), lateral hypothalamic area (LHA).

2.5 Neuromodulation

Intuitively, we know that not all experiences are turned into actual memories. Some sort of filter must operate to select and store only the most salient events for a certain behavioral context. A proposed mechanism by which this happens is through neuromodulation of the hippocampal network. Acetylcholine, serotonin, dopamine, and several neuropeptides are released in association to certain cognitive states (arousal, stress...) or in response to specific stimuli (reward, pain...) and exert a variety of effects on synaptic plasticity. As mentioned above, dynamic changes in the strength of neurotransmission between neurons are thought to underlie the association (or loss thereof) of cell assemblies, making

neuromodulation a well-suited candidate for controlling this process (Palacios-Filardo and Mellor, 2019). The main neuromodulatory systems acting on CA1 are listed here, in an attempt to illustrate how their orchestrated action is linked to memory processes.

Cholinergic system

During exploration and concomitantly with theta-gamma oscillations, *acetylcholine* levels are increased in the hippocampus (Marrosu et al., 1995). This neurotransmitter is released by afferents exclusively originating from the MS-DBB complex, which is involved in the generation of theta rhythms. Indeed, application of scopolamine, a cholinergic receptor antagonist, suppresses electrically-induced hippocampal theta oscillations (Siok et al., 2006). Both pyramidal cells and interneurons of practically all hippocampal fields are sensitive to acetylcholine, which acts on a combination of fast nicotinic (ionotropic) and slow muscarinic (metabotropic) receptors. The wide range of receptor subtypes and their heterogenous expression localization enables this neurotransmitter to modulate cellular and network activity and behavior in a complex manner (Teles-Grilo Ruivo and Mellor, 2013). At synapse level, long-term potentiation (LTP) is enhanced by cholinergic receptor activation (Leung et al., 2003). However, reducing acetylcholine levels seems to cause attentional deficits, rather than direct memory impairment (see review by Micheau and Marighetto (2011)). At cell level, acetylcholine depletion compromises the formation of new place fields, without influencing the basic properties of place cells (Ikonen et al., 2002).

In the attempt to bring these elements together, Hasselmo and colleagues proposed that acetylcholine modulates hippocampal function by favoring the switch between two different network states (Hasselmo et al., 2002; Hasselmo, 2006). At times of attentional demand, high acetylcholine promotes memory encoding by enhancing the influence of entorhinal input carrying new sensory information at the trough of each theta cycle. Consistently with the notion that the cholinergic stimulation induces LTP, this creates a window for updating synaptic weights, and possibly cell assemblies. Oppositely, at theta peak, the CA3 recurrent network is more likely excited and its input onto CA1 is predominant. This is when already established associations are reactivated for memory recall (Hasselmo et al., 2002; Hasselmo, 2006). Recent experimental evidence appears to support this fascinating model (Douchamps et al., 2013; Betterton et al., 2017; Palacios-Filardo et al., 2020; Udakis et al., 2020).

Serotonergic system

Despite the historical importance of *serotonin* in the study of synaptic plasticity as a molecular and cellular correlate of memory (Carew et al., 1971; Kandel, 2004), its contribution to hippocampal function is not clear. The hippocampus receives serotonergic input from the dorsal and medial raphe nuclei located in the brainstem (Vertes, 1991; Vertes et al., 1999). Recent studies have shown that the serotonergic system promotes plasticity in CA3-CA1 (Teixeira et al., 2018) or EC-CA1 (Cai et al., 2013) synapses. In addition, the global effect

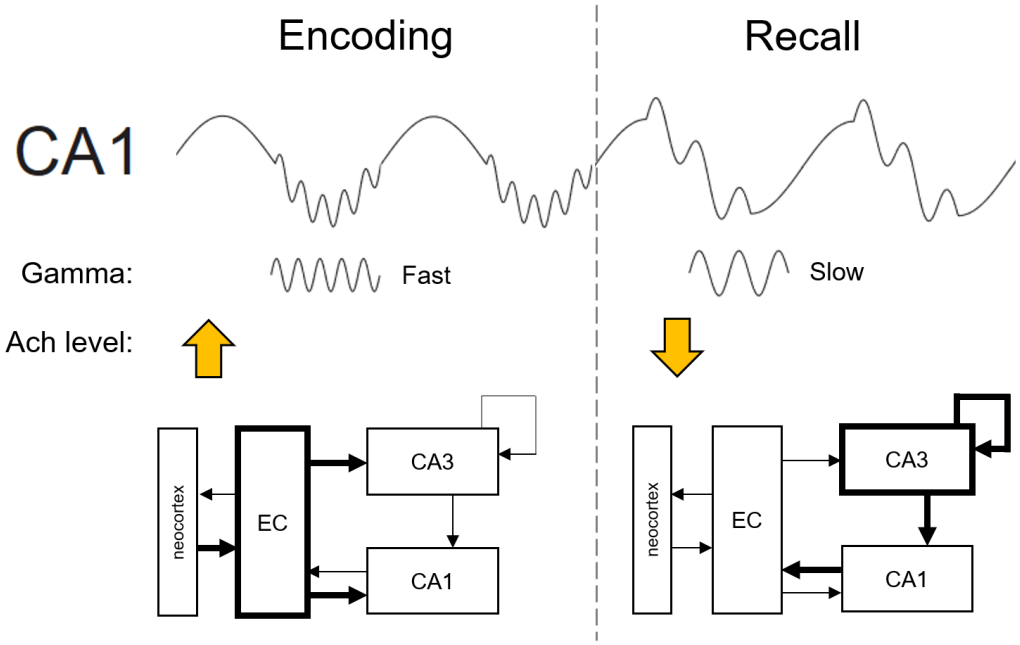

FIGURE 2.6: The cholinergic system and memory. Acetylcholine (Ach) is thought to promote a network switch between memory encoding and memory retrieval. When Ach is high, entorhinal (EC) predominates and drives CA1 activity, as witnessed by the stronger fast gamma in the LFP. When Ach is low, the network is entrained by recurrent connections in CA3, which becomes the main input of CA1. Here, slow gamma is predominant. Adapted from Colgin (2016) and Hasselmo (2006)

of raphe innervation is likely distinct in the dorsal versus ventral poles. Knowing that the latter has a preferential role in emotional and anxiety-related behaviors, it was suggested that serotonin tone encodes the threat- or reward-related salience of signals processed by the hippocampus (Mlinar and Corradetti, 2018; Yoshida et al., 2019). A role in the control of attention in hippocampus-dependent tasks was also recently proposed (Li et al., 2018). A unified role of the neuromodulator can hardly emerge from this variety of phenotypes from the cellular to behavioral level. What is to be kept in mind is that a plethora of receptor types and molecular cascades are expressed by all cell types present in CA1 and these can operate in synergistic or opposing ways (Meneses, 2013).

Dopaminergic system

Two midbrain nuclei send dopaminergic axons to the hippocampal region, the ventral tegmental area (VTA) and the locus coeruleus (LC). While in earlier studies, the contribution of VTA to *dopamine* levels was considered the most prominent (Lisman and Grace, 2005), this is now put into question. More recently, the LC was found to send dense projections and it is now seen as the key source of dopamine release, at least in the dorsal aspect of the hippocampus (Kempadoo et al., 2016). Overall, several studies have linked this neuromodulatory system and the encoding of novelty of an experience (Wagatsuma et al., 2017; Takeuchi et al., 2016). The novel component might be crucial in everyday life to select which memory traces will be turned from labile associations to stable representations.

Indeed, enhancing dopaminergic input can induce hippocampal synaptic strength through metabotropic receptors (Li et al., 2003; Lemon and Manahan-Vaughan, 2012) and ultimately facilitate learning and memory consolidation (Kempadoo et al., 2016; McNamara et al., 2014).

Interestingly, both VTA and LC can co-release dopamine and norepinephrine at their synaptic targets, and the individual effect of either neuromodulator is the object of some controversy (Palacios-Filardo and Mellor, 2019).

Cannabinoid modulation

Endocannabinoids, e.g. *anandamide* and *2-arachidonoylglycerol*, are lipidic signaling molecules acting at the synapse on metabotropic receptors CB1R and CB2R (Castillo et al., 2012). In the CA1 field of the hippocampus, endocannabinoids can be released at the post-synaptic sites by pyramidal cells onto CCK-expressing interneurons, that highly express CB1R receptors, and onto Schaffer collateral terminals. Here, they modulate neurotransmitter release and induce several forms of short- and long-term synaptic plasticity in both glutamatergic and GABAergic neurons (described in details Soltesz et al. (2015)).

Globally, the cannabinoid system exerts a strong modulatory effect on hippocampal function. Indeed, cannabinoid administration in the hippocampus dampens theta oscillations, severely disrupts the temporal coordination of cell assemblies, which is accompanied by memory impairment in hippocampus-dependent spatial tasks (Basavarajappa and Subbanna, 2014; Robbe et al., 2006). Recent work has also shown that CB1R controls synaptic integration in the distal dendrites of pyramidal neurons by acting on the hyperpolarization-activated cyclic nucleotide-gated (HCN) channels and enhancing h-currents (Ih) (Maroso et al., 2016). In addition, the abolishment of Ih currents or of CB1R-mediated signaling induces alterations of LTP and memory performance (Maroso et al., 2016; Nolan et al., 2004).

3. Three Axes of Diversity

Pyramidal cells in CA1 are arranged anatomically following three conventional axes: longitudinal, transverse, and radial. As mentioned in the previous chapters, this spatial organization nests at least as many gradients of cellular diversity, spanning from transcriptomic to physiological, projectional to functional properties. In other words, pyramidal neurons are thought to segregate into several subtypes that are spatially organized. These axes associate in a combinatorial manner (i.e. a neuron located in the deep sublayer of the distal part of dorsal CA1) and are similarly present in CA2, CA3, dentate gyrus and subiculum. It should be noted that principal neuron diversity does not represent a mere singularity of the hippocampus, but is known to be a prominent feature in other cortical areas and is possibly a general principle of brain architecture (Gokce et al., 2016; Ramsden et al., 2015; Tasic et al., 2016).

Why should neuroscientists be interested into the details of fine scale diversity of a single cell type? Heterogeneity at the cell level is thought to promote functional diversification at the circuit level. If a given cell type embodies in fact a set of heterogeneous elements, such cell type could perform a corresponding set of unique operations (Cembrowski and Spruston, 2019). As outlined above, hippocampal cell assemblies are thought to form memory traces by coordinating their firing to code for 'chunks' or aspects of a given experience. According to this view, several kinds of information that compose the memory, ranging from spatial and contextual, to motivational and emotional, could be treated by different assemblies and temporally organized in a sequential manner (Buzsáki and Moser, 2013). Whether pyramidal neurons functionally segregate into distinct assemblies according to their cellular phenotype is still partly a speculation. However, it has become clear that unravelling principal cell diversity is of the utmost relevance in the case of the hippocampus, a relatively simple cortical structure implicated in a plethora of cognitive and affective functions.

I will present the three main axes of diversity in an order that mirrors their discovery, as well as the amount of work dedicated to each. Nonetheless, the section dedicated to the 'radial axis' forms a crucial part of the present manuscript and is highly relevant for the interpretation of my work. I will devote an extensive focus to this section and will discuss it in detail. It will become apparent that multiple axes of variability are intertwined so that the 'final' cellular identity is defined by their combination at several levels, from molecules to network (Cembrowski and Menon, 2018). With the last part of the introduction (chapter 4), I wish to convince the reader that the developmental origin is one on them, overlooked

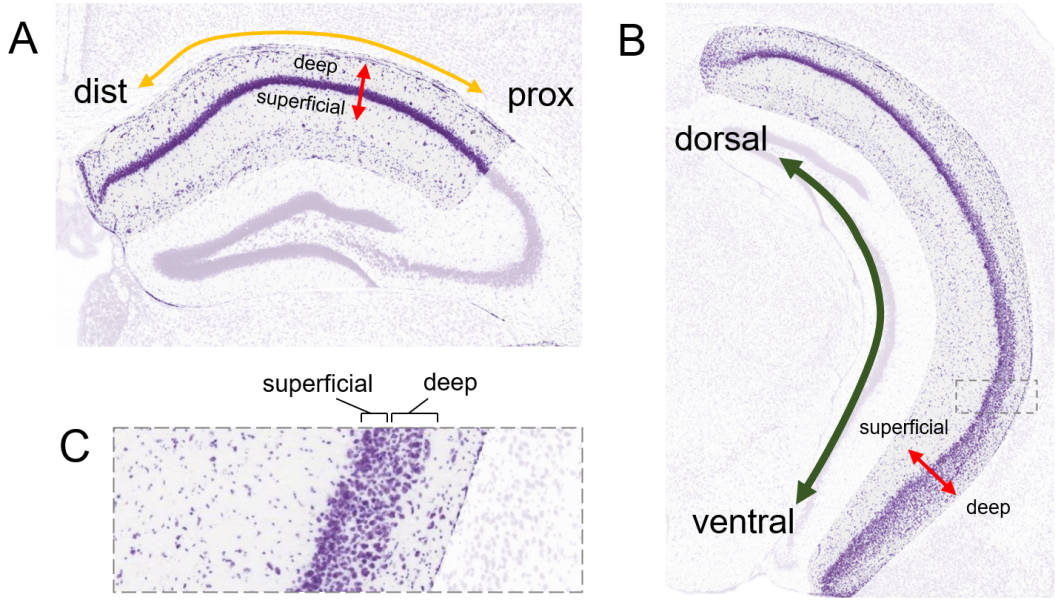

FIGURE 3.1: Schematic illustrations of the three anatomical axes of CA1. A) Coronal view of the rostral (dorsal) hippocampus, where one can distinguish the *transverse axis*, with proximal (towards CA2/CA3) and distal (towards the subiculum) ends of CA1, and the *radial* axis, dividing the pyramidal cell layer in a deep and a superficial portion. B) Coronal view of the caudal hippocampus, where both dorsal and ventral ends of CA1 are represented. The transverse axis here is not identifiable but an even more pronounced segregation of deep and superficial sublayers can be seen. C) Higher magnification of the dashed rectangle in B, further showing the anatomy of the stratum pyramidale across the radial axis. Superficial somata are smaller and tightly arranged; whereas those of deep pyramidal cells are slightly bigger and more loose.

if not ignored in the current understanding of how pyramidal neuron diversity is organized in CA1.

3.1 Dorso-ventral axis

Essentially owing to early lesion studies, the hippocampus, and CA1 by consequence, has been divided into two functionally distinct parts: a 'dorsal' pole (septal or posterior in humans) and a 'ventral' pole (temporal or anterior in humans). This view was later corroborated with more advanced (and less invasive) techniques. The dorsal hippocampus is involved in navigation and related spatial memory, whereas the ventral hippocampus influences stress responses (Henke, 1990), goal-directed (Ciocchi et al., 2015), social (Meira et al., 2018; Okuyama et al., 2016; Rao et al., 2019) and emotional behaviors (Zhu et al., 2014; Xu et al., 2016a).

It is now well-established that hundreds of genes are differentially expressed by pyramidal cells following a dorsal-to-ventral (or septo-temporal) gradient (Cembrowski et al., 2016; Dong et al., 2009) and their spatial distribution correlates with that of other brain regions connected to either pole, even in human (Dong et al., 2009; Vogel et al., 2020). Among

these genes are members of voltage-gated channel or neurotransmitter receptor families, a finding that is in line with the electrophysiological diversity also discovered along the axis. Consistently in mouse and rat, CA1 pyramidal cells were found to differ in their excitability and synaptic transmission, with the ventral ones being more depolarized and able to elicit more action potentials upon stimulation than the dorsal counterpart (Dougherty et al., 2012; Malik et al., 2016; Milior et al., 2016). It was suggested that, despite having a common "default developmental program", the two subpopulations acquire different trajectories during the first postnatal month (Dougherty, 2019).

Furthermore, marked differences on the connectivity level led neuroanatomists to support the dorsal-ventral functional subdivision (see figure 3.2 and Strange et al. (2014) for an exhaustive review).

- **Cortico-hippocampal connectivity**: pyramidal neurons of CA1 are reciprocally connected to the neocortex, by the relay of the entorhinal cortices, following a topographical gradient. For example, the septal-most part of CA1 is preferentially linked to the dorsolateral portion of the MEC and sends dense projections to the retrosplenial and anterior cingulated cortices, involved in visuo-spatial information processing. In contrast, temporal CA1 provides strong connections to the ventromedial part of the MEC and shares intimate bidirectional connectivity with the infralimbic and prelimbic cortices, that are linked to emotional regulation and motivation (Cenquizca and Swanson, 2007; Groen and Wyss, 1990).

- **Subcortico-hippocampal connectivity**: a topographical organization also exists between CA1 and several diencephalic regions, among which the lateral septum. Dorsal CA1 pyramidal neurons send their axons to a very small dorsal portion of the LS, whereas progressively larger regions of the LS are innervated by neurons located more ventrally. It is useful to remind that neurons in ventral CA1 are connected to many other areas including the amygdalar complex, hypothalamus, nucleus accumbens and olfactory regions (Andersen et al., 1971; Cenquizca and Swanson, 2007; Cenquizca and Swanson, 2006; Swanson and Cowan, 1978; Groen and Wyss, 1990), which show little to no dorsal axon terminals.

Despite this variability, Fanselow and Dong (2010) warn not to overlook the "obvious similarities" between the two hippocampal poles: "the intrinsic wiring throughout the longitudinal axis of the hippocampus still revolves around the trisynaptic circuit, whose major characteristics are preserved".

The neuroanatomical data is at least partially in contradiction with the dorsal-ventral dichotomy, which is probably an oversimplified depiction. In fact, a clear-cut spatial/non-spatial subdivision of the two poles was not confirmed by later observations. For instance, the dorsal hippocampus was shown in some experimental paradigms to code for the affective valence of specific stimuli, since strong fear-associated cues can induce increased cell firing (Moita et al., 2003; Wang et al., 2012). Conversely, the ventral pole also plays a role in navigation (Beer et al., 2014; Loureiro et al., 2012) and, although single place cells in

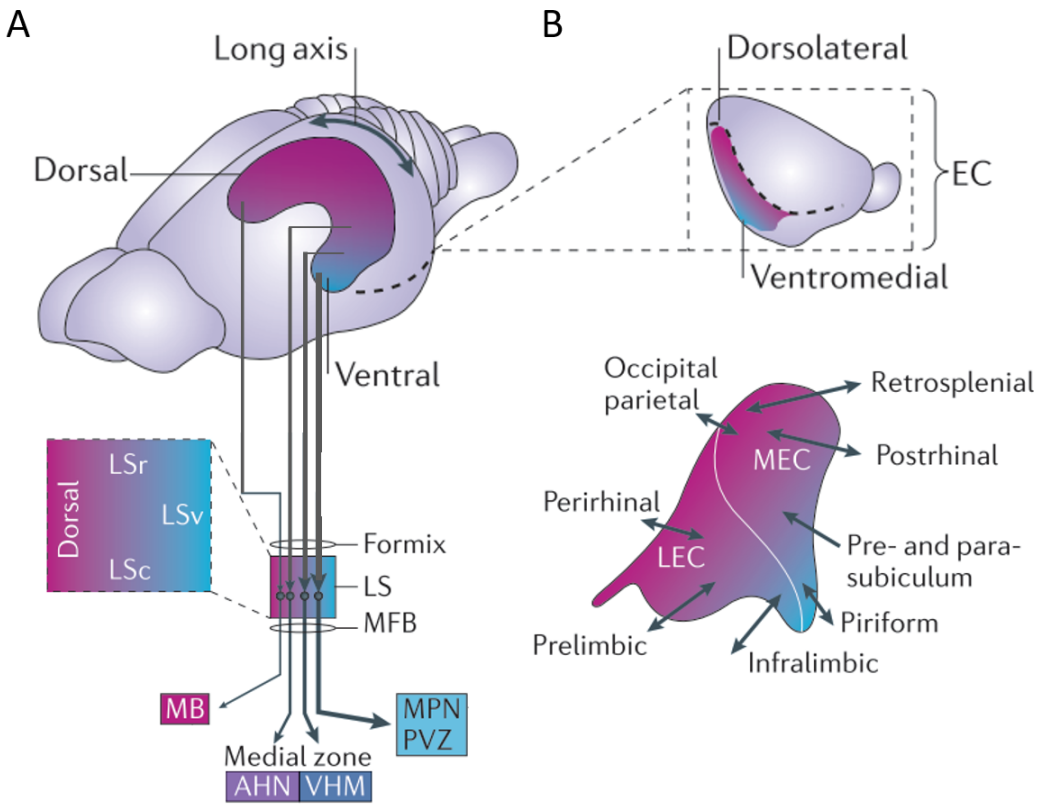

FIGURE 3.2: Extrinsic connectivity gradients along the dorsoventral axis. A) Topographic organisation of projections from the hippocampus (HPC) as a whole to the lateral septum (LS), mirrored by a similar pattern from LS to the hypothalamus, through the medial forebrain bundle (MFB). Three pathways are schematised: 1. dorsal HPC-dorsal LS-mammillary body (MB), linked to spatial memory; 2. intermediate/ventral HPC-rostral LS (LSr)-medial zone nuclei (including the anterior nucleus (AHN) and the ventromedial nucleus (VMH)), linked to social behavior; 3. ventral HPC-ventral LS (LSv)-medial preoptic nucleus (MPN) and hypothalamic periventricular zone (PVZ); involved in endocrine and autonomic responses. B) Topografic organisation of projections from HPC to entorhinal cortices (EC). A dorsolateral portion of EC (magenta) is preferentially connected to the dorsal hippocampus. Increasingly more ventral and medial bands of the EC (purple to blue) are connected to increasingly more ventral levels of the hippocampus. The panel below shows an enlarged EC, indicating the topology of its major cortical connectivity. Note that this connectivity matches projections from the hippocampus to the neocortex. The white line indicates the border between the lateral EC (LEC) and medial EC (MEC). Adapted from Strange et al. (2014)

ventral CA1 (vCA1) are less accurate and have larger place fields (Jung et al., 1994), as a population they convey precise spatial information (Keinath et al., 2014; Royer et al., 2010). Based on the observation that receptive fields of CA1 place cells progressively increase along the long axis (Kjelstrup et al., 2008), it was proposed that the region as a whole provides a flexible multiple-scale representation. In this way, the hippocampal map would have the ability to adapt to complex environments presenting a myriad of navigational cues with varying size and arrangement (Harland et al., 2018).

The present view is that the long axis reveals several genetic, physiological and connectivity profiles (schematized in figure 3.3), defining two main functional domains (dorsal and ventral)[7], reflected by the cellular phenotypes of pyramidal cells. Cembrowski and Spruston (2019) elegantly summarize: "the disparity of [CA1] pyramidal cell identity at the two poles may be an important feature underlying the functional segregation of the dorsal and ventral regions of the hippocampus, allowing to extract and impart foundationally different types of information".

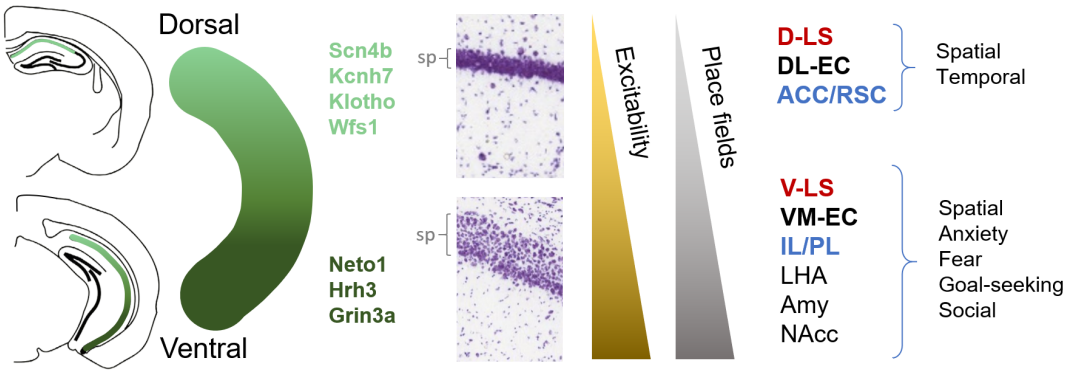

FIGURE 3.3: Heterogeneity of CA1 pyramidal cell properties along the dorso-ventral axis. From left to right, schematic view of the dorsal (dCA1, light green) and ventral CA1 (vCA1, dark green) at two different coronal levels; genetic gradients including genes coding for electrophysiologically relevant proteins, such as sodium channel Scn4b in dorsal and NMDA receptor Grin3a (in ventral); differential anatomy of the pyramidal cell layer, which is wider in ventral than dorsal CA1; excitability and place cell firing (reflected in the size of place fields) increases along the dorso-ventral axis; differential connectivity of dCA1 and vCA1 towards the lateral septum (LS in red, D-LS: dorsal, V-LS: ventral), entorhinal cortices (EC in black, DL-EC:dorsolateral, VM-EC:ventromedial), prefrontal cortex (blue, anterior cingulate (ACC), retrosplenial (RSC), infralimbic (IL), PL (prelimbic)) and other extrahippocampal targets; Functional segregation of dCA1 vs vCA1. Inspired from Masurkar (2018)

3.2 Transverse axis

The transverse or horizontal axis is revealed by sectioning perpendicularly to the septo-temporal length of the hippocampus. Consequently, this axis anatomically divides CA1 in proximal (close to CA2/CA3), middle and distal (bordering with subiculum) and nests an additional gradient of pyramidal cell heterogeneity.

By far, the most striking difference between the proximal and distal part of CA1 is the combination of topographic connectivity gradients, noticed even in pioneering work by Lorente De Nó (1934). Firstly, the proximal end of CA1 is preferentially innervated

[7]Supposedly, intermediate CA1 would form a third domain. It is still matter of debate whether they are discrete regions or a continuum, and if the intermediate portion has distinct or mixed functions, in respect to the dorsal and ventral poles (Cembrowski et al., 2016; Dong et al., 2009). Strange et al. (2014) hypothesize that, depending on the features considered, sharp subdivisions and continuous gradients might be superimposed along the axis.

by distal CA3 (closer to CA2) and projects in turn to the distal subiculum. Parallelly, a proximal CA3 -> distal CA1 -> proximal subiculum circuit is observed (Amaral et al., 1991; Ishizuka et al., 1990). Secondly, the entorhinal cortex projections are biased along the transverse axis, with MEC providing input preferentially to neurons in proximal CA1, and LEC terminals to distal CA1 (Tamamaki and Nojyo, 1995; Witter et al., 1989).

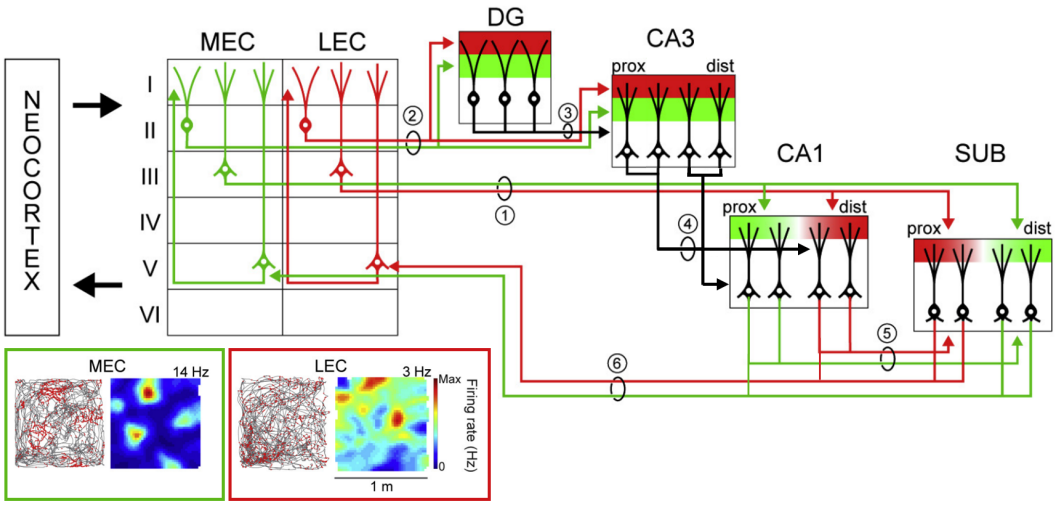

FIGURE 3.4: Schematic diagram of proximo-distal segregation of the two main hippocampal information processing streams. While MEC is mostly involved in the processing of spatial information (green), LEC is the entry point of non-spatial stream (red). Medial (MEC) and lateral (LEC) entorhinal cortices project to CA1 through direct and indirect pathways. In the direct pathway (1) these two streams are segregated: layer III cells in MEC largely project to proximal CA1 (prox), whereas layer III cells in LEC to distal CA1 (dist). By contrast, in the indirect pathway they are supposedly mixed: axons of layer II cells in MEC and LEC (2) converge on the same population of cells in dentate gyrus (DG) and CA3. This mixed information is conveyed to CA1 via mossy fibres (3) and Schaffer collaterals (4). CA1 outputs the entorhinal cortex directly or via subiculum (SUB). Note the inverted connectivity pattern from CA3 to CA1, and from CA1 to SUB. In the insert are an example of grid cell firing in MEC (green) and a representative cell with low spatial information in LEC (red). Rate maps of spikes recorded in 1 m square box are shown. Adapted from Igarashi et al. (2014a).

A consistent portion of MEC neurons are modulated the animal's location or motion relative to the geometry of the environment (grid cells, head direction cells, border cells; see section 1.3.1). By contrast, principal cells in LEC display a less marked spatial modulation but are instead strongly driven by odors or encounters with discrete objects (Deshmukh and Knierim, 2011; Young et al., 1994). These observations are neatly mirrored by data from CA1 neuronal activation in vivo, pointing at a functional subdivision along the transverse axis. A first study by Henriksen et al. (2010) demonstrated that proximal CA1 cells have higher spatial specificity, whereas place cells in distal CA1 have more (up to 7) place fields in the same environment and the fields are wider. In addition distal CA1 firing fields are sensitive to object manipulation (Burke et al., 2011), as well as olfactory cues (Igarashi et al., 2014b), as opposed to proximal ones. In figure 3.4, the reader can see how the proximal and distal ends of CA1 are likely embedded in two separate connectivity streams,

treating spatial and non-spatial information from MEC and LEC, respectively. Moreover, distal CA1 is enriched with bursting neurons (Jarsky et al., 2008), differently from its counterpart, suggesting that proximal-to-distal heterogeneity is not only observed at the circuit-level, but is also present in "intrinsic" physiological properties.

It should be kept in mind that "spatial information is present across the whole transverse axis", meaning that a combined spatial/non-spatial code is likely conveyed by "the activity of a large number of CA1 cells, giving rise to cells with conjunctive firing properties" (Igarashi et al., 2014a). Accordingly, an immediate-early gene (IEG)-based approach (Ito and Schuman, 2012) showed that exposure to novel objects primarily enhanced cFos activation in distal CA1, while exposure to a novel spatial context increased its expression uniformly across proximal and distal CA1.

3.3 Radial axis

Although the radial or deep-superficial axis was already identified by the anatomical distribution and size of cell bodies in the stratum pyramidale (Lorente De Nó, 1934), the lack of high-resolution techniques has long prevented from revealing differences in such small areas. As originally described, deep CA1 pyramidal cells (dPN), closer to stratum oriens, present larger and more loosely distributed somata, whereas superficial ones (sPN), bordering stratum radiatum, are more tightly arranged and relatively smaller in size[8]. This difference, surprisingly conserved across many species (Slomianka et al., 2011), brought forward the idea of the presence of two distinct superficial and deep pyramidal sublayers. Recent technical advances in the recording of neuronal activity in vivo, among which silicone probes and 2-photon calcium imaging, have allowed to further unveil this prominent gradient of pyramidal neuron diversity in CA1[9], despite the close spatial proximity (tens to a hundred microns).

First, I will describe the genetic and morpho-physiological diversity that resides within the layer. Next, I will discuss differences in connectivity between the deep and superficial part and possible circuit-level consequences. Finally, I will address the functional relevance in vivo, highlighted in recent work published by several labs.

Molecular and genetic markers

Since early immunohistological experiments, a few markers have been known to be differentially expressed along the radial gradient, although their physiological implication is still a matter of debate. One of the most studied is calbindin, a calcium chelator linked to

[8] If we consider the surface of the brain, it is counterintuitive that superficial cells are actually located below deep ones. However, I will describe in the next chapter that during embryogenesis the hippocampus is formed from an invagination of pallium, meaning it can be considered upside-down in respect to the neocortex (due to radial migration occurring in the opposite sense). Hence, superficial cells in CA1 are embryologically homologous to neocortical cells in superficial layers (II/III).

[9] Starting from the beginning of the 2010s, this topic has drawn such attention that led to the publication of no less than 6 bibliographic reviews only in the past 3 years.

cellular plasticity (Blatow et al., 2003; Dumas et al., 2004), and another is zinc, a glutamate receptor-binding ion (Paoletti et al., 2009). Both are mainly detected in superficial pyramidal cells (Baimbridge and Miller, 1982; Slomianka, 1992). Later and thanks to the advent of transcriptomics technologies, more subtle genetic differences could be unraveled. In a seminal paper by Cembrowski et al. (2016), CA1 pyramidal neurons were characterized by next-generation RNA sequencing. They validated and extended previous work (Dong et al., 2009) pointing at tens of genes preferentially enriched in either sublayer, i.e. Ndst4 and Col11a1 in dPN, Nov and Htr1a in sPN. In addition, they quantitatively showed that the transcriptional heterogeneity across the radial axis is even more pronounced than that observed proximo-distally.

Dendritic arborization

On the morphological level, a sharp difference was described in anatomical studies (Amaral et al., 1990; Bannister and Larkman, 1995). The main apical dendrite, emerging from the soma and running through the stratum radiatum towards the stratum lacunosum-moleculare, can give rise to a single or twin (bifurcating) trunk. Although initially these two morphological phenotypes were not correlated with the soma location (Bannister and Larkman, 1995; Jarsky et al., 2008), this has now been called into question. Li and colleagues (2017) performed an unbiased morphological analysis on more than 350 reconstructed pyramidal neurons of dorsal CA1 and found the existence of two clusters based on the arborization of apical dendrites (simple and complex), corresponding to the previous classification. In addition, these two clusters were not distributed randomly in the pyramidal layer. The 'complex' (twin-dendrite) group was largely located in the superficial sublayer and was enriched with calbindin-expressing neurons, as opposed to the 'simple' group. Other experimental work highlighted some minor morphological differences in the basal dendritic compartment (in stratum oriens): sPN present a reduced total basal dendritic length (Lee et al., 2014) and a higher proportion of cells with the axon emerging from a basal dendrite, rather than the soma (Thome et al., 2014).

Electrophysiological properties

Although not conclusively, these and other studies attempted to put in relation the morphological and positional data with electrophysiological responses in vitro. In fact, differences in passive membrane properties, such as in the expression of h-currents (Ih), are found across the radial axis. Ih are involved in synaptic integration in the most distal part of pyramidal apical dendrites, where they are mediated by HCN channels (Nolan et al., 2004). They also contribute to the 'sag', a depolarizing response observed when inducing a somatic hyperpolarization. It was shown that sPN present slightly more depolarized membrane potentials and exhibit larger sag responses, whereas dPN have a higher input resistance and smaller sag (Jarsky et al., 2008; Lee et al., 2014; Li et al., 2017). In sPN exclusively, HCN conductances are able to gate long-term potentiation (LTP) through a cannabinoid receptor 1 (CB1R)-dependent pathway (Maroso et al., 2016). Furthermore,

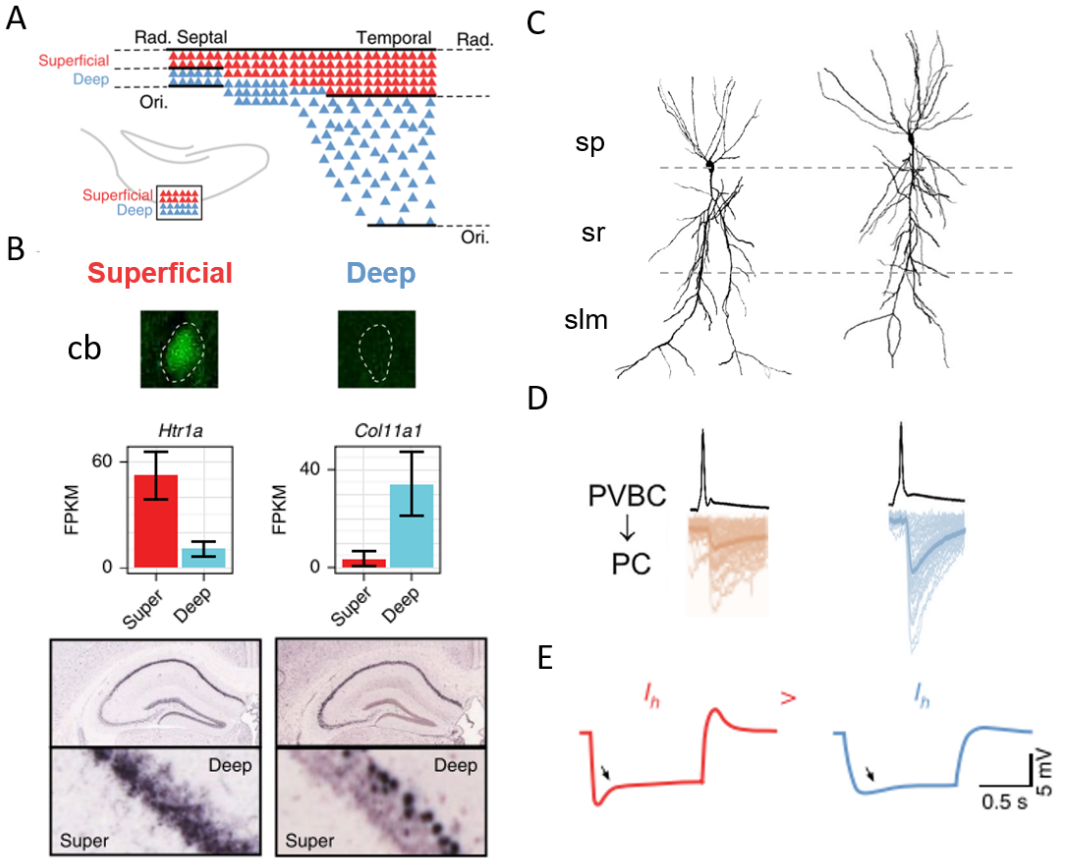

FIGURE 3.5: Genetic, morphological, and electrophysiological differences across the stratum pyramidale. A) Scheme representing the pyramidal cell sublayers (deep and superficial) across different levels of the septo-temporal axis. Globally, this can vary between 50 and 200 µm. B) Genetic and molecular differences between deep (dPN) and superficial (sPN) pyramidal neurons. Among others, sPN express calbindin (cb, top) and high levels of serotonin receptor Htr1a, whereas extracellular matrix gene Col11a1 is greatly expressed in dPN. This was found in both RNA expression (middle) and by in situ hybridization (bottom). C) While sPN mostly display ramified apical dendrites ('complex' morphology), dendritic trees in dPN have a 'simple' arborization. D) PV-expressing basket cells (PVBC) inhibit more strongly dPN than sPN. E) Upon hyperpolarization, sPN exhibit a more pronounced Ih-mediated sag response. Adapted from Soltesz and Losonczy (2018)

the tendency to fire action potentials upon current stimulation was higher in the deep than in the superficial sublayer in acute slices ((Masurkar et al., 2020) but not in Lee et al. (2014) and Li et al. (2017)), as well as in extracellular recordings in vivo, where deep cells were found more 'bursty' than sPN (Mizuseki et al., 2011; Oliva et al., 2016a).

It is important to note that more recently, Masurkar and colleagues (2020) examined the contribution of both the transverse and radial axes to these features and discovered that they interact in a complex manner to define the cellular phenotype[10]. For instance, they found that the disparity in resting and sag potential was only present in proximal CA1,

and that input resistance was higher in dPN vs sPN in middle CA1 exclusively.

Local circuitry

The data described above defines two discrete (or possibly a continuum of) subpopulations in CA1 pyramidal cells spatially segregated along the depth of the stratum pyramidale. Like we saw in the long and transverse axes, this diversity is not limited to intrinsic cell properties but exists at the local circuit level as well (see figure 3.6).

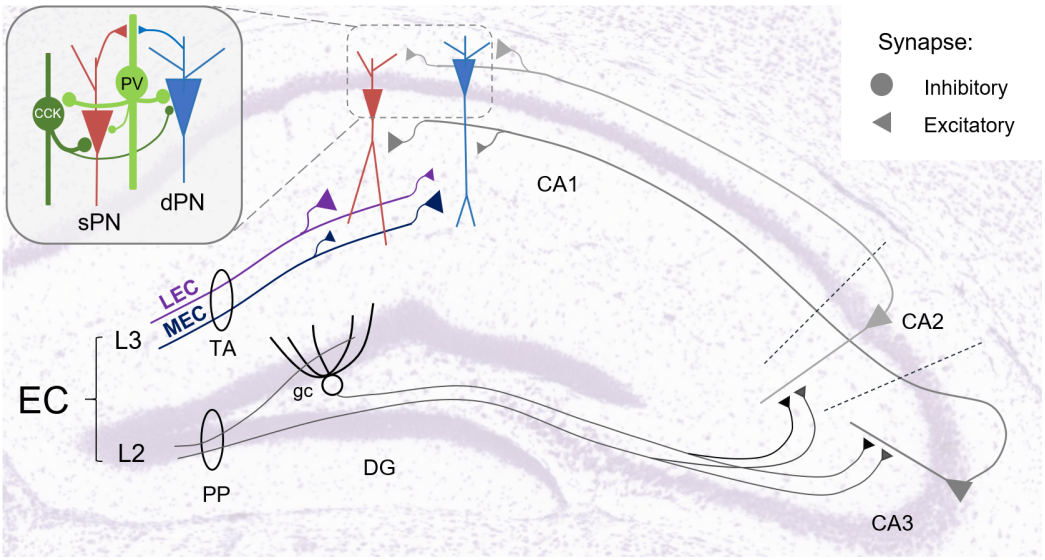

FIGURE 3.6: Intrahippocampal connectivity gradients across the stratum pyramidale. Deep (dPN) and superficial (sPN) pyramidal neurons are differentially innervated from excitatory and inhibitory inputs. CA2 preferentially targets dPNs, while CA3 has a stronger drive on sPN. The medial (MEC) and lateral (LEC) entorhinal cortices display a bias towards the deep and the superficial sublayer, respectively (but see Masurkar et al. (2017)). Note how several parallel streams of connectivity act on either sPN (i.e. through CA3 or LEC via the temporo-ammonic path (TA)) or on dPN (i.e. indirectly by EC/DG driving CA2 or directly via MEC). Finally, cholecystokinin (CCK)-expressing interneurons exert a stronger inhibition on sPN, which in turn are likely to contact parvalbumin (PV)-expressing interneurons. When active, PV cells can effectively silence both dPN and CCK inteneurons and increase sPN firing by disinhibition. gc: granule cell; PP: perforant path, EC: entorhinal cortex.

Two groundbreaking studies addressed the question whether dPN and sPN are equally innervated by GABAergic interneurons. In the first (Lee et al., 2014), authors used a combination of in vitro electrophysiological recordings and optogenetics to show that soma-targeting parvalbumin basket cells (PVBC) preferentially inhibit dPN, in terms of number of synaptic boutons and post-synaptic current amplitude. They additionally proved that PVBC are in turn mainly innervated by sPN, revealing a previously unknown connectivity motif that links the superficial and deep sublayers (sPN $\rightarrow^{(exc)}$ PVBC $\rightarrow^{(inh)}$ dPN). The

[10] To our knowledge, this is one of the few experimental works that thoroughly investigate heterogeneity from a multidimensional perspective, that is considering more than one gradient at the same time. It strongly indicates, like mentioned above, that multiple axes of variability are intertwined and should best be considered jointly.

second study (Valero et al., 2015) confirmed and extended these results, despite some minor differences. Based on their membrane potential responses recorded in anesthetized rats during sharp-wave ripples, they divided dorsal CA1 principal neurons in two groups: depolarized and hyperpolarized cells. They reported that the former were mostly located superficially and expressed calbindin, whereas the deep sublayer was enriched with the latter group. Similarly to Lee and colleagues (2014), hyperpolarized dPN were highly innervated by PVBC. However, they additionally found that CCK-expressing interneurons exhibited the opposite connectivity pattern, with CCK+ boutons being densest on depolarized sPN (unlike Lee et al. (2014))[11]. The interest of this work goes beyond this finding, as authors went further by probing the intrahippocampal circuitry. In a nutshell, they showed that: 1) GABAergic inhibition is stronger on deep cells; 2) thus, Schaffer collateral stimulation induces a global inhibitory and excitatory drive onto dPN and sPN, respectively; 3) participation to SPW-R is higher among sPN; 4) CA2 stimulation causes a stronger glutamatergic activation in the deep portion of the stratum. In the same line, the Tonegawa lab unraveled a new synaptic pathway that can specifically activate dPN in CA1. This circuit originates from the perforant path (EC layer II) and projects to CA2 pyramidal cells directly, or indirectly via the dentate gyrus (Chevaleyre and Siegelbaum, 2010; Kohara et al., 2014). The emerging picture is that parallel streams of information can act in a competing way, depending on the predominant input converging to CA1 (Geiller et al., 2017b). More precisely, CA3 drives superficial and inhibits deep cells, whereas CA2 can induce deep cells to fire[12].

Output projections

As well, several long-range projections likely present a bias according to the soma location in the stratum pyramidale, especially in vCA1 where the variety of outputs is most pronounced. For instance, performing multiple retrograde tracer injections, the Soltesz group showed how mPFC and amygdala are privileged outputs of dPN, while MEC receives homogenous projections from the superficial and deep sublayer (Lee et al., 2014). However, more recent reports point to the presence of a fraction of mPFC-projecting neurons among sPN, possibly depending on their subregional targets (Jimenez et al., 2018; Sánchez-Bellot and MacAskill, 2020). Ventral deep principal cells also provide a preferential input to the nucleus accumbens and to the lateral nucleus of the hypothalamus. These layer-specific pathways seem to be respectively involved in social memory (Okuyama et al., 2016) and anxiety-related behaviors (Jimenez et al., 2018).

It should be noted that up to know only few research groups have probed whether the radial gradient of connections extends to afferents. In a recent study using large scale

[11] It is fascinating to point out that PV+ interneurons and CCK+ are preferentially recruited in distinct behavioral states (Dudok et al., 2021). The former are most active concomitantly with oscillations (theta, SPW-R) and locomotion, while the latter during awake immobility, in absence of ripples. Furthermore, the firing of PV+ inhibits CCK+ neurons, thus forming an additional local circuit motif controlling the transition between hippocampal activity patterns.

[12] It should be kept in mind that, despite the bias towards superficial cells, CA3 input is the main driver of the vast majority of CA1 place cells (Davoudi and Foster, 2019).

viral-genetic tracing, it was suggested that ventral CA1 projection neurons receive similar input from upstream regions (Gergues et al., 2020), although a bias according to the soma location was not probed. Indeed, Pi et al. (2020) found a spatial segregation of the axon terminals coming from basolateral amygdala: the posterior part targeting preferentially sPN, the anterior one targeting dPN. Inputs from other regions should be tested as well.

Functional implications

As for the network-level implications of such diversification, these findings are still elusive, notably in the ventral hippocampus where monitoring neuronal activity in vivo is technically challenging. On the other hand, in the more experimentally accessible dorsal pole, a few recent studies have speculated on the functional role of the radial gradient. In particular, Danielson and colleagues (2016) performed 2-photon calcium imaging to simultaneously monitor tens to hundreds of both superficial and deep sublayers, by rapidly shifting the field of view in the z-plane. Using several behavioral paradigms on imaged head-fixed mice running on a treadmill, they showed that dPN are more prone to remapping (change their preferred firing location in an environment) and their activity was strongly influenced by the presence of a reward. Oppositely, sPN were more stable over time and remapped less when the reward was moved. Interestingly, the Royer group recorded with silicon probes in similar experimental settings and found strikingly comparable results. First, they confirmed that deep cell firing is more tightly linked to tactile and visual cues, constituting external environmental landmarks (Geiller et al., 2017a). Then, by pharmacological inactivation the medial septum, they perturbed MEC grid cell activity, which is thought to underlie self-motion based navigation (or 'path-integration' (McNaughton et al., 2006)). As a result, superficial place fields significantly shifted from cue-poor to cue-rich zones of the treadmill (Fattahi et al., 2018). Altogether, it appears that the two sublayers in dorsal CA1 differently participate to spatial coding, probably contributing to different aspects (external cues vs self-referenced information) of the representation of an environment or episode.

An even more recent study, schematized in figure 3.7, condenses many of these findings (Sharif et al., 2020). In a nutshell, in a linear environment with few landmarks, the majority of active cells was located superficially, and the position of the animal was well predicted by their firing rates. Oppositely, in cue-rich conditions dPN activity was more represented and theta-phase preferences of single spikes could help predict the animal location better than firing rates. According to authors, this implies that when self-motion information is predominant, CA3 input prevails and drives sPN more strongly, as shown by their increased coherence in the slow gamma-band. When many external cues are available, multisensory information might instead converge onto CA1 via the entorhinal cortex and drive dPN.

It is then proposed that coding of space relies on two complementary mechanisms that are spatially segregated and are supported by different physiological mechanisms and connectivity motifs. This 'dual input model' posits that the hippocampus can create an adaptable representation of the external world by shifting from a rate code, more suitable to coarse spatial scales (cue-impoverished), to a phase code, encoding one self's

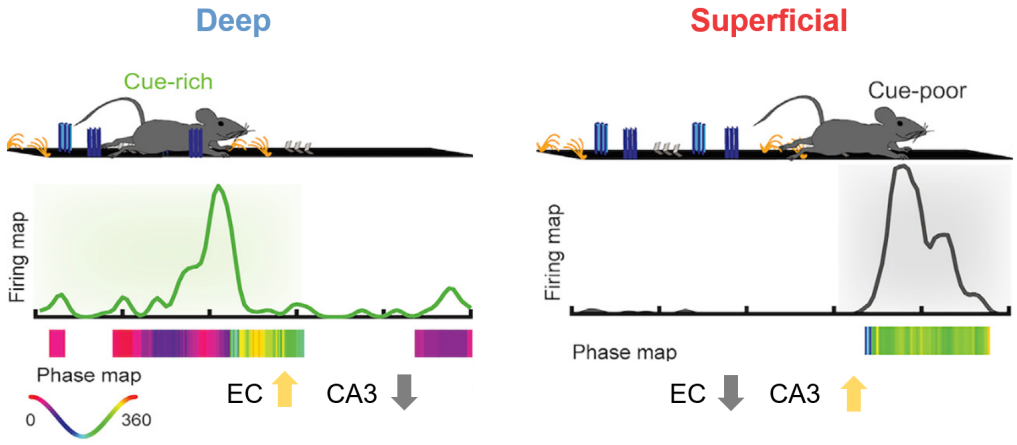

FIGURE 3.7: Differential contribution to spatial coding across the stratum pyramidale. The deep and superficial sublayers of CA1 use different codes for space depending on the availability of cues. Driven by EC input, dPN are more active in cue-rich environments and their firing in respect to theta cycles is predictive of the position of the animal (*phase code*). Oppositely, sPN are preferentially recruited by CA3 input in cue-poor environments and the animal position can be accurately decoded from the firing rates (*rate code*). Adapted from Sharif et al. (2020)

accurate position using fine-scale information from the environment (Fernández-Ruiz et al., 2017). The shifts between the two does not only rely on the predominant excitatory input, like we just mentioned, but is also modulated by different families of interneurons (i.e. PV basket cells). This hypothesis has the strength (and the beauty) of combining data from connectivity, network-level and behavioral studies. However, it does so to explain (dorsal) hippocampal activity only in the prism of the representation of spatial information. If it is true that navigation and episodic memory might share common circuits and mechanisms(Buzsáki and Moser, 2013), it is still unclear how the model can extend to the ventral hippocampus, notably in a larger framework encompassing other functional aspects of memory, such as the affective, social, motivational components of mnemonic processes.

4. An Embryonic Origin for Diversity

In the previous section, I described that the CA1 pyramidal neuron population, which has tacitly been regarded as a homogenous entity, presents in fact a wide range of properties that vary across the three main anatomical axes of the hippocampus. In the superficial-to-deep dimension, most experimental data converge on the definition of seemingly two distinct sublayers. Our driving hypothesis is that this segregation has a developmental origin and that the time of neurogenesis or 'birthdate' is a strong predictor of the observed heterogeneity. Before moving to the experimental part of this work, I will first introduce the main developmental phases of CA1 in the rodent brain, from neurogenesis and cell differentiation to circuit maturation, with a specific focus on pyramidal cells. Next, I will present experimental evidence, notably from our group, supporting the notion that adult hippocampal circuits are sculpted during development, possibly by predetermined genetic programs.

4.1 Development of CA1

4.1.1 Anatomical shaping of the hippocampus

The hippocampal formation derives from the medial portion of the pallium, which as a whole gives rise to all cortical areas. Starting from embryonic day 9 (E9.5), an invagination along the pallial midline causes the medial pallium to progressively fold inwardly in respect to the dorsal part (Monuki et al., 2001). This explains why the hippocampus is ultimately located beneath the neocortex at all septo-temporal levels (and why it is sometimes defined as a 'subcortical' structure, mistakenly). The hippocampal ventricular zone (VZ) is then positioned 'back-to-back' to the neocortical VZ and will coordinate the proliferation and migration of pyramidal cells in the Cornu Ammonis (CA) in a 'inward' fashion (as opposed to the 'outward' neocortical migration)[13].

At this very early stage of embryogenesis (E10.5-E11.5), a major actor in tissue differentiation is the cortical hem, shown in figure 4.1. The cortical hem is contiguous to the medial pallium and is essential to induce the formation of the hippocampal region in

[13] As mentioned in the previous chapter, this explains why in CA1 the so-called deep sublayer is located above and the so-called superficial sublayer is the furthest from the (neo)cortical surface.

the cortical primordium, via the secretion of many different molecular signals, like BMP, Wnt and Lhx2 (reviewed in Subramanian and Tole (2009)).

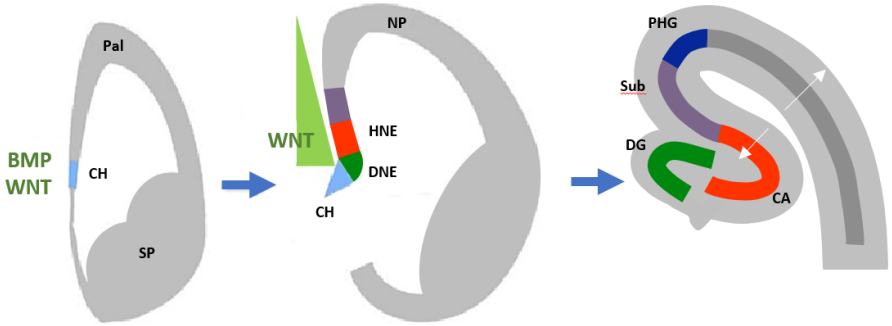

FIGURE 4.1: Anatomical development of the hippocampus. Schematic representation of the pallium at different developmental stages. Right, starting from approximately embryonic day 10 (E10.5), the cortical hem (CH, light blue) is formed at the medial border of the pallium upon signalling of bone morphogenetic protein (BMP) and WNT, among others. Middle, from around E11 on, CH-secreted WNT (light green) forms a gradient that contributes to the formation of hippocampal fields. At this stage, several proliferative (neuroepithelial) zones arise: dentate neuroepithelium (DNE, dark green) and hippocampal neuroepithelium (HNE, red). The neocortical primordium (NP) forms lateral to that. Neuronal migration from each neuroepithelium appears at this stage. Right, the hippocampal formation results from a two-fold invagination of the medial pallium under the neocortex. In the adult brain, it presents an 'S shape' and is patterned (from medial to lateral) into dentate gyrus (DG, green), cornu ammonis (CA, red) and subiculum (Sub, purple). The neocortical parahippocampal gyrus (PHG, blue) lies next to the hippocampal formation. With white arrows are indicated the two opposing directions of pyramidal cell migration of the cornu ammonis (bottom left) and the neocortex (top right). SP: subpallium. Adapted from Pang et al. (2019)

Neurogenesis, and the consequent anatomical expansion, follows this phase and starts from around E11.5 (Angevine, 1965). It should be noted that removal of the cortical hem from E12.5 on does not affect the subsequent definition of hippocampal fields (Tole and Grove, 2001). Within the CA, field-specific markers come in play and mediate the differentiation of pyramidal cells. Tole et al. (1997) identified several genes that are expressed either in CA3 or CA1 during neurogenesis. Notably, KA1 and SCIP begin to be upregulated at E14.5 in CA3 and E15.5 in CA1 respectively from the opposing ends (dentate and subicular poles, respectively) of the CA. They anatomically fuse in CA2 around birth and remain present in either field through adulthood (Grove and Tole, 1999). In other words, mouse hippocampal fields differentiate during the peak of neurogenesis. At this stage, CA1 (and CA3) begin to express characteristic molecular features that continue to define these fields into adulthood.

4.1.2 Pyramidal neurogenesis and migration

Principal neurons in the hippocampus are originated in the hippocampal VZ from *radial glial cells* (RGC). RGC are neural stem cells that display a bipolar morphology with one short apical process anchored to the luminal surface of the VZ, and long basal process extending to the pial surface (Xu et al., 2014). While their somata remain within the VZ, their processes are parallelly organized spanning across the neural tube. During E10.5 to 11.5 in mice, RGC undergo symmetric cell divisions, expanding the proliferative pool (a phase of cortical development which is referred to as 'neural expansion'). Later, RGC undergo asymmetric cell divisions (Mukhtar and Taylor, 2018). More precisely, these specialized embryonic cells give rise to either intermediate progenitors that further divide or to immature glutamatergic neurons that start displacing along radial scaffold, in the so-called *radial migration* to subsequently differentiate into mature neurons (Hatten, 1990).

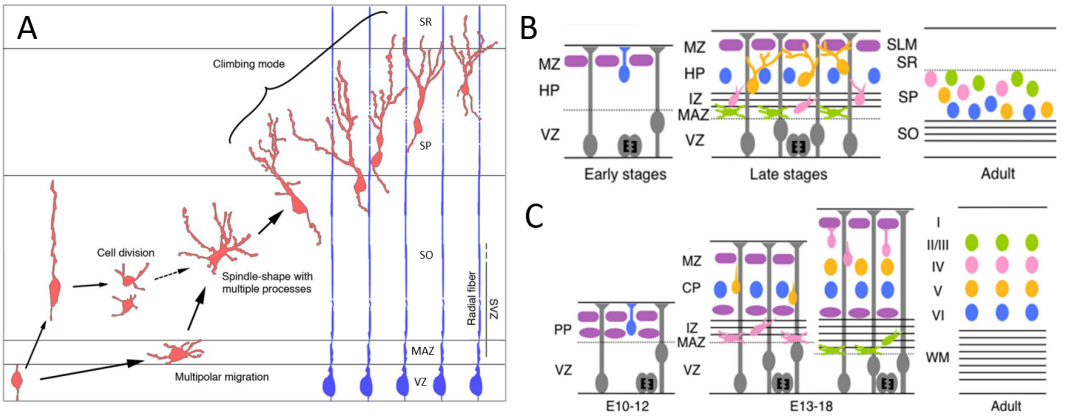

FIGURE 4.2: Migration of pyramidal cells in CA1. A) Schematic representation of the migratory behavior of hippocampal cells. During late development (after 'neural expansion' has occurred) radial glial cell (RGC) division in the ventricular zone (VZ) can generate either basal progenitors, which further divide, or multipolar cells without further cell division. The latter accumulate just above the VZ in the multipolar cell accumulation zone (MAZ). Eventually, all progenitors acquire multipolar morphology, enter the presumptive stratum pyramidale (SP), transform into spindle-shaped bipolar cells and migrate by 'climbing' mode. That is, they translocate several times and change their scaffolds from the original radial fibers to other radial fibers until they reached the top of SP. Towards the end, they also displace by 'radial' migration. SR, stratum radiatum, SO, stratum oriens. Adapted from Kitazawa et al. (2014). B) Scheme representing of the main developmental difference in the organisation of neocortical and hippocampal pyramidal layers. Top, the layer arrangement in the cornu ammonis occurs roughly in a birth-date dependent inside-out manner. This is probabibly due to the 'climbing' migration mode and to radial glia bending at the apical end (not shown, see text). Bottom, Neocortical neurons form neatly-arranged layers in a birthdate-dependent inside-out manner. PP, preplate; VZ, ventricular zone; MZ, marginal zone; CP, cortical plate; IZ, intermediated zone; WM, white matter; HP, hippocampal plate; SLM, stratum lacunosum-moleculare; SR, stratum radiatum; SP, stratum pyramidale; SO, stratum oriens. Adapted from Hayashi et al. (2015).

As mentioned in the previous paragraph, principal cell neurogenesis in CA1 begins as

early as E11 and ends at E19, shortly before birth. However, the majority of pyramidal cells are generated between E14.5 and E16.5, with a peak at E15 (Angevine, 1965; Caviness, 1973; Smart, 1982). Interestingly, the generation of CA3 cells starts approximately 1 day later but peaks earlier than in CA1, at E14 (Bayer, 1980; Stanfield and Cowan, 1979). Newly born post-mitotic cells adopt a *multipolar state* presenting multiple thin processes. Concomitantly, they leave the VZ and stay just above it for a variable lapse of time, before starting to migrate. Early born neurons (E12-E13) sojourn for about 24 hours, whereas later born ones can spend in this transitory state up to 4 days (Kitazawa et al., 2014; Nakahira and Yuasa, 2005). Figure 4.2 (right) illustrates that the pattern of migration is not only radial, like it is observed in the neocortex. Multipolar cells first move obliquely, then gradually migrate along the radial scaffold. After reaching the hippocampal plate (HP, the presumptive pyramidal layer), radially migrating neurons can sequentially contact several radial processes and move in a zigzag manner. This mode was named 'climbing migration' (Kitazawa et al., 2014). Another major difference with the neocortex is that radial glial fibers of hippocampal RGC display a progressive bending at their apical end, towards the HP. This causes cells to displace in an almost perpendicular manner in respect to the previous direction, which causes neurons issued from the same precursor to be aligned along, not across, the stratum pyramidale (Xu et al., 2014).

In spite of differences with between allo- and neocortex, all pyramidal neurons follow an 'inside first-outside last' migration. That is, after the first cells are generated and have migrated to the HP, subsequent waves of newly-born cells will cross this layer and reach more superficial locations. In the end, early born neurons constitute the deep location of the pyramidal layer and late-born neurons take up the superficial part. At the end of this process, the vast majority pyramidal cells will accumulate in a seemingly single stratum of 50 to 200 µm, depending on the septo-temporal level. However, as the reader can see in the left side of figure 4.2, pyramidal cells in the cornu ammonis are not as orderly arranged according to their birthdate as in the neocortex, where the layering is clearly visible. Likely, both the climbing migration mode and the apical bending of the radial glia contribute to this. In addition, it should be noted that ectopic cells are found in the stratum radiatum (Gulyás et al., 1998; Savić and Sciancalepore, 2001) and the boundary with the stratum oriens becomes progressively looser at distal/ventral locations of CA1 (Slomianka et al., 2011). Many genes, including reelin, doublecortin or Lis1, are crucial for correct lamination. As a matter of fact, their suppression induces not only severe brain malformations, but also alterations that are specific to the arrangement of CA1 pyramidal layer, like a two-layered stratum in mice with mutated reelin gene (see Slomianka et al. (2011) for an overview).

4.1.3 Pyramidal neuron differentiation

At the state of an immature post-mitotic neuron, the cell has already committed to its future cell fate. In our population of interest, pyramidal cells in CA1, migrating cells are differentiating and acquiring their glutamatergic, projection neuron phenotype. This process is regulated by a complex chain of gene interactions. While some transcription factors help

maintain cells in a proliferative mode, like Notch (Shimojo et al., 2008), others promote pyramidal neuronal differentiation, such as Emx1, Neurogenin 1/2 and Pax6.

The Role of Neurogenin2

In the present work, the genetic approach we used to fate-map neurons in a temporal manner relies on the selective expression pattern of Neurogenin2 (Ngn2). Ngn2 belongs to the Neurogenin family, which encode basic-helix-loop-helix (bHLH) proneural transcription factors (Schuurmans et al., 2004). In the hippocampus and the neocortex[14], Ngn2 is specifically and transiently expressed in glutamatergic progenitors (Ozen et al., 2007). In general, expression of Ngn2 was shown to temporarily increase in cells exiting the mitotic phase of cell cycle and entering quiescence or G0 (Britz et al., 2006). In addition, Ngn2 has proved to have a key role in the initiation of pyramidal cell fate specification, by enhancing other downstream gene targets (Seo et al., 2007). Oppositely, its suppression induces migration deficits during cortex formation and prevents neurons from acquiring a pyramidal unipolar dendritic morphology (Hand et al., 2005). In accordance with the specificity of a glutamatergic phenotype, it is not surprising that Ngn2 expression is mutually exclusive with that of genes necessary for GABAergic neuron specification, such as Mash1 or Dlx1/2 (Schuurmans et al., 2004).

Given the specific and transient expression of Ngn2 in glutamatergic progenitors, this gene represents a powerful tool to selectively label cohorts of newborn cells (see figure 4.3). To this end, we used a knock-in mouse line in which the expression of tamoxifen-inducible Cre recombinase is under the control of the endogenous Ngn2 promoter (Zirlinger et al., 2002). It should be noted as well that tamoxifen has a half-life of 12 hours in vivo (Danielian et al., 1998), which further restricts the induction system to a relatively narrow time window.

4.1.4 Interneuron neurogenesis and migration

Unlike pyramidal neurons, prospective hippocampal and neocortical interneurons originate in the subpallium. Two transitory regions located in the subpallium are largely responsible for interneuron proliferation, the medial (MGE) and caudal (CGE) ganglionic eminences (Pleasure et al., 2000). The earliest-born inhibitory neurons originate around E9.5 in the MGE, with a peak of neurogenesis occurring three days later (E12.5). CGE-derived neurons are presumably generated later, between E12.5 and E16.5 (Tricoire et al., 2011). It is now well-established that the cell fate acquired by newly-born cortical GABAergic neurons is rooted in their embryonic origin, both in space (MGE vs CGE) and time of neurogenesis (Chittajallu et al., 2013; Ishino et al., 2017; Miyoshi and Fishell, 2011; Tricoire et al., 2010). Indeed, in a very comprehensive investigation, Tricoire and colleages (2011) showed that different chemically-defined interneuron subpopulations are originated in timely organized waves of neurogenesis. First, mostly PV-, SST- and nitric oxide synthase (nNOS)-expressing

[14] Ngn2 expression is also found subcortically (Gouty-Colomer et al., 2018).

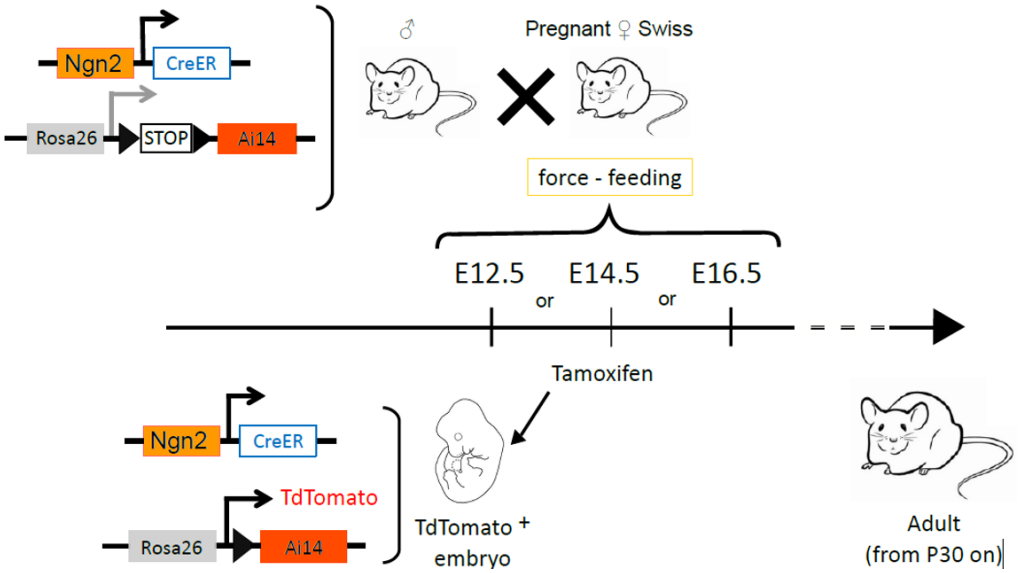

FIGURE 4.3: Inducible genetic fate-mapping based on Ngn2 gene expression. Synthetic scheme of the genetic fate-mapping strategy used in the present work to label pyramidal cells based on their time of birth. A male mouse carrying the Ngn2-CreER^{TM} driver (tamoxifen-inducible Cre recombinase gene under the control of Ngn2 promoter) and the Ai14 reporter cassette (loxP-flanked STOP codon preceding Tdtomato gene) is crossed with a non transgenic (Swiss background) female. In embryos, post-mitotic pyramidal cell precursors transiently express Ngn2, which drives CreER expression. At embryonic days 12.5 (E12.5), E14.5 or E16.5, the pregnant female is force-fed with tamoxifen, which activates CreER. This leads to excision of the STOP codon and expression of red fluorescent Tdtomato protein, specifically in cells expressing Ngn2 at the time of force-feeding. Once induced, fate-mapped are permanently labelled with Tdtomato.

interneurons arise from the MGE, then CGE-derived CCK-, vasoactive intestinal peptide (VIP)-, and later calretinin-expressing neurons take the lead.

Collectively, MGE- and CGE-derived interneurons start being observed within the cornu ammonis from E14/E15 on (Manent et al., 2006). They leave the ganglionic eminences and adopt a tangential migration, that is perpendicular to the RGC scaffold. Once arrived in the hippocampal primordium, interneurons can invade the hippocampal plate (see Danglot et al. (2006) for an extensive review). Here, they recognize specific molecular motifs on target cells to establish appropriate inhibitory connections.

4.1.5 Circuit wiring and maturation

Concurrently with the last phases of neurogenesis, wiring within the hippocampal formation begins to be established and the network reaches completion over the course of the first postnatal month in rodents. In the next paragraphs, I will briefly describe the emergence of such connectivity (figure 4.4), then I will mention early hippocampal dynamics and their link to circuit maturation (summarised in figure 4.5).

Strikingly, extrahippocampal inputs reach CA1 earlier than axons from CA3. First, entorhinal afferents are observed in CA1 from E16 and by E17 they start innervating the

stratum lacunosum-moleculare and increase in density during the first postnatal week. In turn, CA1 cells were shown to send axonal projections to the EC as early as E17 (Deng et al., 2007; Supèr and Soriano, 1994). Second, the septum sends projections to CA1 around the same time, targeting putative GABAergic interneurons and pyramidal cells at E16 and E17, respectively (Supèr and Soriano, 1994). Differently from the EC, the maturation of this pathway is prolonged postnatally until 10 days after birth. Third, axons from the nucleus reuniens of the thalamus reach CA1 around P1, and they are reciprocated only at P5 by CA1 projections (Hartung et al., 2016).

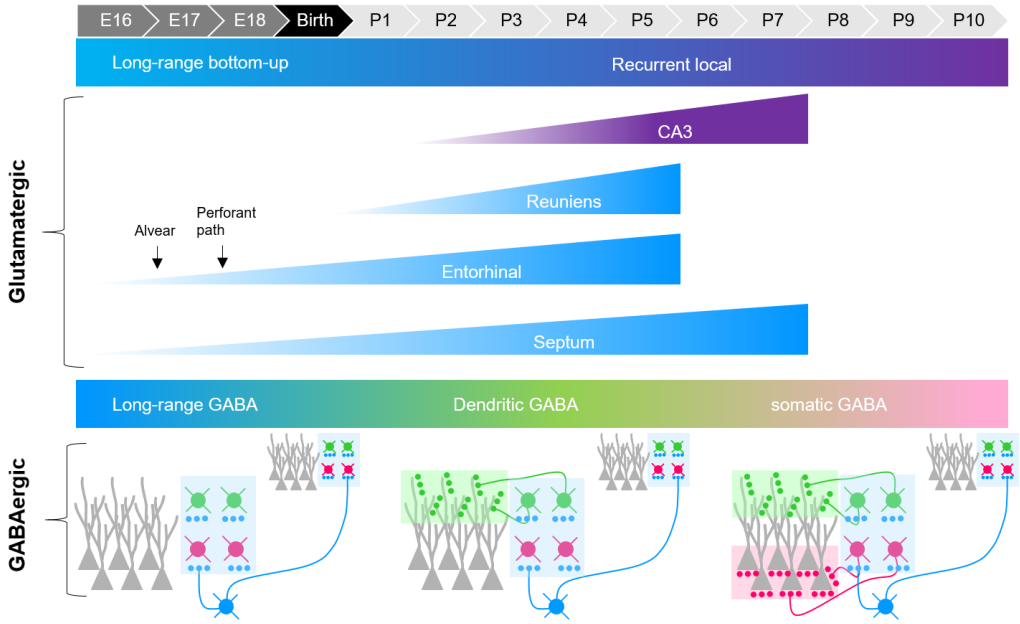

FIGURE 4.4: Developmental timeline of hippocampal synaptogenesis. Long-range glutamatergic inputs from the entorhinal cortex and septum as well as long-range GABAergic inputs reach CA1 first, towards the end of the last embryonic week. Axons originating from nucleus reuniens appear in the first postnatal days, a few days before CA3. In turn, CA1 interneurons with a long-range projection (and putative hubs) mature before dendritic-targeting interneurons, while somatic GABAergic inputs develop last, towards the end of the first postnatal week. Adapted from Cossart and Khazipov (n.d.), under revision.

During the first postnatal week, local connections see the light as well, both from interneurons and from CA3. CA3 Schaffer collaterals form glutamatergic synapses onto CA1 pyramidal neurons from P2 (Durand et al., 1996). Parallelly, GABAergic synapses develop initially on the dendritic and then on the perisomatic compartment as well (Harris and Teyler, 1983; Swann et al., 1989). Possibly however, the very first GABAergic connections originate from MGE-derived early born (E9.5) interneurons, which operate as *hubs* during early postnatal development and become long-range projecting cells (see section 4.2.1) (Bocchio et al., 2020; Villette et al., 2016). Overall, GABAergic synapses are functional before glutamatergic ones, although, unlike in adult, GABA exerts mostly a depolarizing effect as a result of higher intracellular chloride concentrations, until P10 approximately (Ben-Ari et al., 2012; Tyzio et al., 1999).

Different kinds of hippocampal activity have been described in the embryonal or perinatal stages, mostly in ex vivo conditions, represented in figure 4.5. These early dynamics are thought to be essential for proper hippocampal network maturation and, ultimately for the emergence of its many functions, like spatial navigation, which are established by the end of the first postnatal month (Tan et al., 2017). First, in absence of any functional synapses (either electrical or chemical), spontaneous uncorrelated activity is observed in CA1 before birth (Crépel et al., 2007). Concomitantly with the appearance of gap-junction-mediated connectivity, neuronal activity becomes more correlated. This corresponds to the appearance of *synchronous plateau assemblies* (SPA), characterized by sustained firing and large calcium conductances (Crépel et al., 2007), around birth. Both pyramidal cells and interneurons participate, although their recruitment seems to be associated to their stage of maturation (Allene et al., 2012). Indeed, around P4 developing interneurons are still active during SPA, while more mature interneurons begin to engage in *giant depolarizing potentials* (GDP). GDPs are large synchronous events, associated to burst firing and increase of intracellular calcium concentration of both pyramidal and GABAergic cells (Ben-Ari et al., 1989; Garaschuk et al., 1998; Khazipov et al., 2004). Their appearance follows the course of Schaffer collateral connectivity, since many GDP events propagate from CA3 to CA1 (Menendez de la Prida et al., 1996) and GDP frequency is the highest at P7, when collaterals from CA3 notably increase in density (Gómez-Di Cesare et al., 1997). However, the contribution of local GABA release is crucial and GDPs wear off and cease completely by the end of the second postnatal week, when GABA progressively loses its depolarizing effect to become inhibitory (Khazipov et al., 2004; Tyzio et al., 2007).

It should be noted that these activities are recorded in brain slices, in absence of extra-hippocampal and sensory influences. This implies that they are most likely the product of internally generated hippocampal dynamics, emerging from the maturation stage of the neuronal population. Oppositely, *early sharp waves* (eSPW) are preceded by myoclonic movements of the pup. They are observed in vivo from P1 in CA1 and seem to be mainly driven by entorhinal input (Leinekugel et al., 2002; Mohns and Blumberg, 2010). At this stage, perisomatic inhibition is not fully mature yet (Doischer et al., 2008) and eSPWs are not accompanied by ripple oscillations, which co-occurs with adult sharp waves and appear only from around P14 (Buhl and Buzsáki, 2005)

4.2 Evidence for a developmental origin of diversity

In the light of what was exposed above, we can summarize by saying that "successive molecular, cellular, and electrical events operate to carry out progressive neuronal [and circuit] maturation" (Khalaf-Nazzal and Francis, 2013), leading to a fully functional hippocampal network composed of neatly organized cell types and finely-tuned connections. In other words, its development follows a precise sequential program that attributes given elements (regions, neurons, synapses, . . .) to specific roles and that preconfigures the

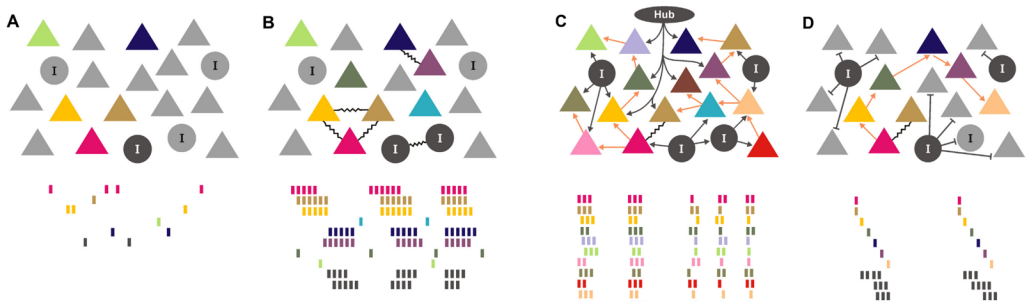

FIGURE 4.5: Developmental stages of hippocampal activity. Triangles are principal cells and circles indicate GABAergic interneurons ('I'). Colored or dark grey symbols represent active neurons. At the bottom of each network sketch, spikes are indicated by bars in corresponding colors. (A) The most immature networks show little to no connectivity and, hence, mostly uncorrelated neuronal activation. (B) Before or around birth, electrical coupling between neurons allows weakly synchronous activity, in the form of synchronous plateau assemblies (SPAs). (C) From around postnatal day 4 (P4), multiple neurons are recruited into strongly synchronous patterns called giant depolarizing potentials (GDPs). These rely mainly on GABAergic signaling and are modulated by hub neurons. (D) Mature hippocampal networks contain highly specific assemblies of neurons with inhibitory or excitatory synaptic coupling. The emerging patterns of activity sustain highly ordered sequences, serving specific functions in information processing. Adapted from **Egorov2013**.

adult hippocampus to sustain certain patterns of activity. The present work is based on the hypothesis that these programs, established during embryogenesis, are also responsible for within-cell type heterogeneity, specifically in the case of CA1 pyramidal cells (described in chapter 4). As I will argue in the following paragraphs, there is increasing evidence in favor of this hypothesis and that the embryonic origin is pivotal for the diversification of many, if not all, hippocampal cell types. First, I will summarize research from our lab that has focused on early born neurons, then I will draw from other groups as well and highlight the convergence of these data.

4.2.1 Findings from our group: cell fate in the hippocampus is developmentally determined

While most of the data supporting the idea that the embryonic origin determines (at least partially) neuronal cell fate in the hippocampus was indirect, the use of inducible genetic fate mapping granted the possibility to identify neurons according to the time of neurogenesis (Joyner and Zervas, 2006). In such way, glutamatergic and GABAergic neurons could be fluorescently labelled by the means of Ngn2 and Dlx1/2, respectively, at specific developmental stages to provide direct evidence.

The first results were obtained in CA3 during the first postnatal week. By combining this genetic approach with calcium imaging, Allene and collaborators (2012) found that earlier born interneurons (E11.5) started participating in GDPs, while their younger counterpart (E18.5) was still involved in SPAs. Also, the morpho-physiological profile of the former

seemed to nicely mirror the overall maturation of the circuit (Villette et al., 2016). Interestingly, even earlier born GABAergic cells (E7.5/E9.5, from now on ebGABA) appear to form a unique functional subpopulation (Picardo et al., 2011). Here, ebGABA were shown to present a highly arborized axon and could single-handedly impact network dynamics when stimulated ex vivo. These and other features, such as their long-range projections, lead our group to conclude that they represented a type of *hub neurons* (Bonifazi et al., 2009), key players in the coordination of neuronal activity within and across networks.

Similarly, ebGABA in the developing CA1 also operate as hubs, as their manipulation synchronizes GDP occurrence, likely thanks to their widespread axon (Bocchio et al., 2020). The unique cell morphology and functional connectivity are maintained in adulthood, in both CA1 and CA3 (Bocchio et al., 2020; Villette et al., 2016). In addition, ebGABA imaged in awake mice displayed a higher recruitment during locomotion and during population bursts, as compared to random interneurons, strongly vouching for their uniqueness, and further confirming the notion of a developmental imprint on the mature hippocampus.

Given the relationship between an early neurogenesis and the fate of interneurons, brought to light by our group, glutamatergic cells were also probed under the developmental prism (Marissal et al., 2012; Save et al., 2019). CA3 pyramidal cells born at E11.5 were found to be located in the deeper portion of the pyramidal layer, mostly in the distal end of CA3, both developing before their superficial / proximal counterpart (Bayer, 1980). Furthermore, differently from later born neurons (E15.5), they participated in the early phase of GDPs and exhibited burst firing and less ramified dendritic trees (Marissal et al., 2012). Interestingly, these findings were more recently corroborated by a study from the Spruston lab, in which two different pyramidal subpopulations were identified in adult CA3 (Hunt et al., 2018). Here, neurons with a stunningly analogous phenotype to those above (deeply-located, bursting and a 'simple' morphology) were shown to be active in the early phase of sharp waves, and to possibly initiate them.

Likewise in the dentate gyrus: *semilunar granule cells* (SGC) are a specific subclass of granule cells, that can be distinguished by their widespread dendritic tree (Williams et al., 2007). In our group, Save et al. (2019) extensively characterized this population in vitro and proved that SGCs are mostly generated in early phases of development (between E12 and E16)[15]and have distinct membrane properties. Once again, an ensuing publication extended on this, showing that fate mapped SGC, born predominantly at E15-16, were preferentially activated in a wide range of behavioral paradigms (Erwin et al., 2020)[16].

[15]The reader should bear in mind that primary neurogenesis in this regions spans from E12 to P7.

[16]Here the fundamental difference between the two studies is that Erwin et al. (2020) highlighted how the suprapyramidal blade of the DG is enriched with this cell subtypes, in respect to the infralaminar blade, while Save et al. (2019) looked at the soma location in the depth of the granule cell layer altogether.

On a personal note, the early- versus late-born dichotomy is possibly an oversimplification. I illustrated above how cellular heterogeneity spans several gradients simultaneously, the most evident ones being observed along the anatomical axes, and one dimension alone does not suffice to explain diversity as a whole. However, taking into account the developmental imprint on molecular, physiological and synaptic features, our group contributed with a significant step forward to understanding hippocampal cell diversity. Therefore, this body of work has the undeniable worth of systematically showing how hippocampal neurons are set to specific differentiation paths in early development and largely by their precise temporal (and spatial) origin. Compared to principal cells CA3 and DG, it is less clear how CA1 pyramidal cells situate within this developmental framework. Yet, no experimental work has addressed this question in depth, and this is precisely the purpose of the present study. To properly lay the ground, in the next couple of paragraphs I will outline several converging data pointing in this direction.

4.2.2 Converging evidence for a developmental imprint onto hippocampal cell fate

As previously described, correct lamination of the CA1 area depends on the expression of several genes involved in migration, mostly encoding cellular cytoskeleton proteins (Caviness, 1973; Deller et al., 1999; Hirotsune et al., 1998; Deuel et al., 2006). Misexpression of these genes causes severe heterotopias, often inverting the inside first-outside last patterning. "In reeler [reelin mutated mice], it is the more superficial cells which are the earliest formed, and the deepest lying the latest formed" (Caviness, 1973). In a recent paper, D'amour and colleagues (2020) provided convincing data that pyramidal neurons maintain a temporally-based subtype identity, despite the inversed layering. In a Lis1-mutated mouse line, which is phenotypically similar to the reeler model, they observe (i) diffuse, but not exclusive, Cb expression in the deep (thus later born) sublayer; (ii) PV+-somata shift to more superficial positions, where earlier born pyramidal neurons are misplaced[17]; (iii) inverted gradient of dendritic morphologies, with 'complex' cells in the deep and 'simple' cells in the superficial sublayer.

In another publication, the transcription factor Zbtb20, involved in CA1 pyramidal neuron specification, was experimentally manipulated (Nielsen et al., 2010). While this gene co-labels with Cb in normal conditions, downregulation of Zbtb20 suppresses Cb expression in the superficial sublayer and affects distal apical dendrite formation in the stratum lacunosum-moleculare. Taken together, these studies suggest that Lis1, Zbtb20 (among others) participate to an intrinsic genetic program that starts in early CA1 maturation and exerts a stronger influence than the soma location alone in the determination of pyramidal cell fate.

The early developmental schedule might not be limited to morpho-physiological properties (that can be seen as 'intrinsic' to the cell type) and local innervation, but could

[17] CB1R+ puncta were also found in more superficial positions, which is opposite to the expected shift of CCK+ cells in the deep sublayer.

also extend to global connectivity. On one hand, the Caroni lab has brought to light the existence of subpopulations of cells that were interconnected according to the temporal schedule of neurogenesis and synaptogenesis. First, principal cells within the trisynaptic pathway appeared to establish connections preferentially with other temporally-matched principal cells (Deguchi et al., 2011), so that neurons maturing simultaneously in DG, CA3 and CA1 were more likely integrated into the same network, and ultimately formed related functional assemblies. Second, early born PV cells were found to target deep CA1 cells while late born PV cells targeted superficial CA1 cells (Donato et al., 2015). On the other hand, extrinsic factors are also likely to play a role. For instance, in the reeler mouse, the disorganization of the entorhinal afferent fibers mirrors the cellular disorganization and axon terminals appear to contact their putative targets despite the mis-lamination (Deller et al., 1999). As if "the laminar organization of the hippocampus [depended] on the correct positioning of postsynaptic target cells" (Deller et al., 1999). In addition, experiments where embryonic tissue was grafted onto the adult hippocampal region revealed that afferents growing out from the transplanted tissue innervated the host hippocampus with proper laminar specificity (Förster et al., 2006; Zhou et al., 1990).

Many reviews and papers cited in 3.3 allude (more or less explicitly) to development as a possible contributing factor to heterogeneity in the superficial-deep axis. A (somewhat paradoxical) example is given by the seminal work of Cembrowski et al. (2016). Authors labelled CA1 neuronal subpopulations by in utero viral injections at E14 and E17, performed a high-throughput analysis of their respective transcriptomes and concluded that the radial axis yields a pronounced genetic variability. However, an alternative interpretation of these results is that the differences in gene expression between E14- and E17-labelled cells are due to the embryonic birthdate, which incidentally also determines the soma location within the stratum pyramidale.

All in all, the hypothesis of an embryonic origin of diversity has been making its way in respect to the radial gradient. The reader should note that it is still matter of speculation whether the developmental framework is applicable to the long and transverse axes. By combining observations of cellular and regional heterogeneity with developmental notions, several pieces of evidence point in this direction. Although no obvious temporal gradient along the dorso-ventral axis was identified in the development of CA1, there likely is one in CA3 and the entorhinal cortex, where the dorsal and lateral portions, respectively, originate before ventral CA3 and the more ventral MEC (Bayer, 1980; Donato et al., 2017; Stanfield and Cowan, 1979). Still, it should be noted that CA1 fibers reach the medial (older) part before the lateral (younger) part of the lateral septum (Bayer, 1980; Swanson and Cowan, 1978). By contrast, a developmental gradient is more evident in the transverse axis, with distal ends of CA1 and CA3 supposedly first to emerge, before the proximal counterpart (Bayer, 1980).

A first remark (or reminder) is that connectivity gradients intermingle in their developmental component as well. Distal CA1 is preferentially targeted by LEC, which is generated slightly earlier than MEC (Angevine, 1965). In turn, MEC (generated later) is biased towards the younger proximal CA1 (Masurkar et al., 2017). Also, CA2 is formed early in development (Angevine, 1965) and innervates more densely the deep sublayer (Kohara et al., 2014).

Second, it is important to point out that across these axes, similar electrophysiological gradients seem to be established. Although the pattern not is always consistent, CA1 pyramidal cells occupying earlier formed subregions (deep, distal, and dorsal, supposedly) globally display smaller Ih-mediated sag responses, lower membrane resistance (Jarsky et al., 2008; Malik et al., 2016; Maroso et al., 2016; Masurkar et al., 2020) and higher bursting propensity ((Jarsky et al., 2008; Mizuseki et al., 2011), altough lower for dorsal CA1 (Malik et al., 2016)).

Third, in functional terms, there is a higher likelihood to engage in spatial processing in the deep and dorsal CA1 due to the strong MEC input (presumably older), as opposed to superficial and ventral CA1 treating non-spatial information as well, carried by LEC (Igarashi et al., 2014b; Masurkar et al., 2017). Although the transverse axis obviously does not follow the same pattern, it also shares common functional features with the radial axis. While superficial/proximal cells present fewer place fields with higher spatial tuning, the older counterpart can fire in multiple place fields with lower spatial coherence (Danielson et al., 2016; Henriksen et al., 2010; Mizuseki et al., 2011; Oliva et al., 2016a).

The emerging picture is that early developmental programs constitute the fundamental backbone for the organization across the whole adult hippocampus and the observations above constitute the footprint of circuit pre-wiring at various levels and anatomical scales (Cossart and Khazipov (n.d.), under revision). In other words, at a time when experience has not come in play yet, a set of predetermined features are established at cell and network level, i.e. determining certain physiological properties or connectivity schemes. Later during early postnatal development, the hippocampus receives (indirect) stimuli from the external world and undergoes plastic changes, modelling its wiring and activity based on their preexisting configuration, as recently seen for place cells in CA1 (McKenzie et al., 2021). It becomes clear that elucidating these predetermined developmental sequences is essential for understanding neuronal dynamics and functions observed within the mature hippocampus, and, as the main output of this structure, pyramidal cells in CA1 ought to be considered under the developmental prism. Specifically, in the present work we focused on ventral CA1 pyramidal neurons and asked whether the temporal embryonic origin is a major determinant of the phenotypic diversity observed among this population. I will present the main experimental findings of my doctoral project in the next part (II) and I will elaborate on their significance in part III.

Part II

Experimental Contribution

5. Preamble

It is still debated how the hippocampus, and particularly the ventral pole, can compute various kinds of information supporting a broad functional repertoire, i.e. navigation, episodic memory, and emotional processing (chapters 1 and 2). Unlike previously thought, pyramidal neurons (PN) in adult hippocampal CA1 exhibit a pronounced heterogeneity, including gene expression, dendritic morphology, physiological properties, connectivity and oscillatory activity. Many features correlate with the soma location across the stratum pyramidale (SP) and the existence of two functionally distinct CA1 sublayers, deep and superficial, was proposed. Altogether, these observations point at a cell-level 'division of labor' and provide a circuit basis for the diversity of hippocampal function (chapter 3). During embryogenesis, differentiating PNs migrate via an 'inside first-outside last' scheme and position themselves in progressively more superficial positions. Since this mirrors the radial segregation in cellular properties, the time of birth could play a role in PN cell fate determination (chapter 4).

Thus, we asked whether the temporal embryonic origin is a major determinant of ventral CA1 PN neuronal heterogeneity observed in adulthood. To this aim, we labelled PNs according to their time of birth during neurogenesis (E12.5, E14.5 and E16.5, see 4.1.3) and described their properties using a combination of *ex vivo* electrophysiology, neuronal tracing, immunohistrochemistry and behavioral assays. Specifically, we probed excitatory and inhibitory input connectivity, dendritic morphology, intrinsic membrane properties, extrahippocampal projections and recruitment upon exploration.

The main experimental findings are illustrated and commented in the next chapter (6), in the form of an article. We show that the embryonic birthdate contributes to defining PN diversity in ventral CA1, from intrinsic morpho-physiological properties, to projection patterns and exploration-induced cFos expression. In addition, we find that pioneer PNs (E12.5) display unique characteristics. Hence, we provide evidence that the developmental origin, likely in synergy with positional factors, critically determines CA1 PN properties, and possibly function. At this moment, the manuscript is available as a preprint and is soon to be submitted to a scientific journal. Note that it contains a detailed 'Materials and Methods' section, not reproduced elsewhere.

Furthermore, the reader will find a summary of two additional experiments that are not mentioned in the article. We tested a novel viral strategy for anterograde tracing (annex A) and calcium imaging combined to microendoscopy in ventral CA1 of the awake mouse (annex B), but neither yielded a successful outcome.

6. Article

CA1 pyramidal cell diversity is rooted in the time of neurogenesis.

Davide Cavalieri, Alexandra Angelova, Anas Islah, Catherine Lopez, Agnes Baude and Rosa Cossart*

Aix Marseille Univ, Inserm, INMED, Turing Center for Living Systems, Marseille France

*corresponding author

Abstract

Cellular diversity supports the computational capacity and flexibility of cortical circuits. Accordingly, principal neurons at the CA1 output node of the hippocampus are increasingly recognized as a heterogeneous population. Their genes, molecular content, intrinsic morpho-physiology, connectivity, and function seem to segregate along the main anatomical axes of the hippocampus. Since these axes reflect the temporal order of principal cell neurogenesis, we directly examined the relationship between birthdate and CA1 pyramidal neuron diversity, focusing on the ventral hippocampus. We used a genetic fate-mapping approach that allowed tagging three groups of age-matched principal neurons: pioneer, early- and late-born. Using a combination of neuroanatomy, slice physiology, connectivity tracing and cFos staining, we show that birthdate is a strong predictor of CA1 principal cell diversity. We unravel a subpopulation of pioneer neurons recruited in familiar environments with remarkable positioning, morpho-physiological features, and connectivity. Therefore, despite the expected plasticity of hippocampal circuits, given their role in learning and memory, the diversity of their main components is significantly predetermined at the earliest steps of development.

Introduction

Hippocampal circuits serve multiple complex cognitive functions including navigation, learning, and episodic memory. For this purpose, they form highly associative networks integrating external inputs conveying multi-sensory, proprioceptive, contextual and emotional information onto internally-generated dynamics. For many years, in contrast to their inhibitory counterparts, principal glutamatergic cells have been treated experimentally and modeled computationally as identical twins. Hence, multiple streams of information serving a variety of functions were considered to be integrated by a uniform group of neurons. This conundrum has been recently clarified by converging results indicating that the hippocampus is in reality comprised of heterogeneous principal cell populations forming at least two distinct, nonuniform parallel circuit modules that are

independently controlled and involved in different behaviors. This diversity would contribute to the computational flexibility and capacity of the hippocampal circuit (Soltesz and Losonczy, 2018; Valero and de la Prida, 2018).

At population level, it is becoming increasingly evident that most features of neuronal diversity within the CA1 output node of the hippocampus distribute in a way that matches the temporal schedules of development across transverse and radial axes. According to early autoradiographic studies, mouse CA1 principal neurons (CA1 PNs) are born between E12 and birth with a peak at E14 (Angevine, 1965; Bayer, 1980). In the radial axis, successive generations of PNs occupying the principal pyramidal layer migrate past the existing earlier born neurons thus creating layers in an ‘‘inside-out’’ fashion. Therefore, superficial neurons (closer to the *stratum radiatum*) are in general born later than *deep neurons* (closer to the stratum radiatum). In the transverse axis, distal CA1 neurons (CA1a and b, closer to the subiculum) are born first, followed by proximal CA1 (closer to CA2). In contrast, there is no apparent developmental gradient along the dorsoventral axis in CA1 as compared to CA3 or entorhinal cortex, where ventral neurons are born significantly later that dorsal ones (Bayer, 1980; Donato et al., 2017). In sum, in CA1, early born neurons are preferentially found throughout the dorsoventral axis, in CA1a,b (distal) and in deep radial positions, whereas later born ones are located in CA1c and closer to the *stratum radiatum*.

Heterogeneity of the morpho-physiology of CA1 PNs distributes in a similar pattern. Hence, adult CA1 PNs located in regions associated with a presumed earlier birth date (i.e. CA1 deep and/or distal) display a smaller HCN-mediated h-current (Ih) (Jarsky et al., 2008; Lee et al., 2014; Maroso et al., 2016; Masurkar et al., 2020), a lower membrane resistance (Rm) (Graves et al., 2012; Masurkar et al., 2020) as well as a higher excitability ((Cembrowski et al., 2016; Mizuseki et al., 2011) and bursting propensity (Jarsky et al., 2008). The same applies to the local and long-range connectivity schemes of CA1 PNs. For example, seminal early studies noted how the order of neurogenesis in the entorhinal cortex, proceeding from lateral to medial, also strictly correlated with the order of its termination on CA1 PNs along transverse and radial axes (Bayer, 1980); a property recently probed at functional level (Masurkar et al., 2017). The temporal order of neurogenesis was directly evidenced at single-cell level to impose the local patterning of glutamatergic connectivity to form isochronic circuits throughout the hippocampal trisynaptic circuit (Deguchi et al., 2011). This also applies for the mesoscopic organization

of adult GABAergic inhibitory circuits. Indeed, both along the radial and transverse axes of development, late born PNs and subregions are more likely to drive CA1 interneurons, while early born regions and PNs receive stronger inhibitory inputs (Donato et al., 2017; Lee et al., 2014; Oliva et al., 2016; Valero et al., 2015).

Finally, functional diversity also appears to correlate with presumed birthdate. When combining the information of many recent reports a picture emerges by which in the dorsal hippocampus putatively early born PNs are comprised of a higher fraction of place-modulated neurons (Danielson et al., 2016; Mizuseki et al., 2011) with a poorer spatial coding specificity (Danielson et al., 2016; Geiller et al., 2017; Hartzell et al., 2013; Henriksen et al., 2010; Oliva et al., 2016). More particularly, in CA1, presumably older PNs are better tuned to receive external sensory inputs as their firing is more anchored to external landmarks while later born ones, may be more likely to convey an internal "memory stream", more likely to participate in SWRs and to convey self-referenced information, with slower if any remapping and more stable place maps (Danielson et al., 2016; Fattahi et al., 2018; Mizuseki et al., 2011; Sharif et al., 2020; Valero et al., 2015). Similarly, function segregates along the radial axis in the ventral hippocampus where deep CA1PNs specifically projecting to the nucleus accumbens shell (NAcc) or to the Lateral hypothalamus (LHA) were reported to contribute to social and anxiety-related behaviors, respectively (Jimenez et al., 2018; Okuyama et al., 2016).

Altogether, mostly based on the tight correlation between their soma position and their morpho-functional attributes, these recent results indirectly support the intriguing possibility that CA1PNs diversity may be partly determined at their time of neurogenesis. Alternatively, diversity may simply reflect final soma position and the influence of local circuits rather than an early predetermination. In order to test directly these two non-mutually exclusive possibilities, we have fate-mapped three groups of age-matched CA1PNs: pioneer (i.e. born around embryonic day 12: E12.5), early (E14.5)- and late (E16.5)-born as described previously (Marissal et al., 2012; Save et al., 2019). We analyzed their morphophysiological properties, connectivity, and activation during the free exploration of differently familiar environments. We focused on the ventral hippocampus as this region displays the wider diversity of CA1PNs in terms of projection patterns (Cembrowski et al., 2016; Jimenez et al., 2018; Jin and Maren, 2015; Kim and Cho, 2017; Lee et al., 2014; Okuyama et al., 2016; Parfitt et al., 2017; Xu et al., 2016).

Whereas the radial position of CA1PNs correlates with some features of synaptic connectivity like the frequency of excitatory synaptic currents they receive, other morphophysiological properties including apical dendritic length *in the stratum radiatum*, parvalbumin somatic coverage, long-range projection, spiking in response to current injections, sag current or input resistance distinguish between cells with different birthdates. In particular, pioneer E12-CA1PNs stand out as a singular subset of cells regarding many parameters, broadly distributed along the radial axis and preferentially activated when mice explore a familiar environment. Therefore, the present study reveals how the heterogeneity of CA1PN diversity extends beyond the mere subdivision into two sequentially generated sublayers along the radial axis. It likely encompasses many, at least three, intermingled subtypes specified at progenitor stage by their temporal origin.

Results

Pioneer CA1 pyramidal cells broadly integrate the pyramidal layer and display remarkable features.

CA1 pyramidal neurons (PNs) were fate-mapped using the inducible transgenic driver line *Ngn2-Cre*^{ER}, expressing Cre^{ER} under the control of the Ngn2 promoter. We crossed *Ngn2Cre*^{ER} mice with the Ai14 reporter line (Madisen et al., 2010), including a Cre-dependent TdTomato allele (see Methods). Like in our previous studies(Marissal et al., 2012; Save et al., 2019), three different groups of pyramidal neurons were labelled by TdTomato expression via tamoxifen administration at separate embryonic time points: embryonic day 12.5 (E12.5), E14.5 and E16.5. We first focused on the main features classically expected to segregate into two CA1 sublayers, the *deep* and *superficial* one.

We first examined the somatic location of CA1PNs in the stratum pyramidale according to their fate-mapped date of birth (Fig. 1A). The location was calculated as the distance between the center of the soma and a line representing the stratum radiatum/pyramidale border. Coherently with an *inside first-outside last* patterning (Angevine, 1965; Bayer, 1980), we found that E16.5 CA1PNs were mostly located in the superficial part of the pyramidal layer, whereas the deep sublayer was enriched in E14.5 CA1PNs. In both dorsal and ventral CA1, E12.5 cells were also positioned in the deeper portion, although significantly shifted towards the *stratum oriens.* Noteworthy, not only did the location in respect to the *radiatum/pyramidale* border change, also the spatial dispersion of cells in the pyramidal layer varied with the birthdate. More specifically, E12.5 were the most spread out (E12.5 interquartile range or $IQR_{E12.5}$ = 63.14 in dorsal and

104.44 in ventral CA1) and later born cells showed drastically reduced values of dispersion ($IQR_{E14.5}$ =22 and 30.71, $IQR_{E16.5}$ = 22 and 12.95 dorsally and ventrally, respectively). The broad distribution of E12.5PNs and its shift towards the *stratum oriens* was particularly obvious in cumulative distribution plots obtained from dorsal and ventral CA1 where a consistent fraction of the labelled E12PNs were located outside from the *stratum pyramidale*, in the *stratum oriens and, fewer, in the stratum radiatum* (Fig. 1B).

These results are globally in line with previous work. However, they indicate how not only the location, but also the dispersion of somata in the pyramidal layer depends on the birth date. In addition, they show how the deep CA1 sublayer is comprised of a mixed population of E12.5 and E14.5 CA1PNs while cells located in the *stratum oriens* are predominantly of E12.5 origin.

We next investigated the diversity among CA1PNs with parvalbumin, a classical immunohistochemical marker used in several previous studies to distinguish the deep and superficial sublayers. Indeed, parvalbumin was demonstrated to preferentially decorate the somata of deep CA1PNs, indicating a stronger innervation by putative PV-basket cells (Lee et al., 2014; Soltesz and Losonczy, 2018; Valero et al., 2015). For this reason, we expected to find a preferential PV innervation of E12.5 and E14.5 PNs, both located in the deep sublayer (Fig. 1C). Surprisingly, this labelling was better segregating according to birthdate than position. Indeed, E12.5CA1PNs displayed significantly less putative PV contacts than E14.5CA1PNs, even though their somata were mainly located in the deep CA1 (see Fig. 1B).

These first observations indicate that, at single-cell level, birthdate may better correlate with the properties of CA1PNs than position along the radial axis. They also point-out at the pioneer subset of CA1PNs as potential outliers in the relationship between cell diversity and birth order. To further analyze the relationship between birthdate, cell position and single-cell morpho-physiological features, we next performed a series of *ex vivo* whole cell patch clamp recordings in acute brain slices from adult *Ngn2-Cre*^{ER}-Tdt mice (n = 72 cells from 34 mice; 22 E12.5 CA1PNs, 27 E14.5 CA1PNs, 23 E16.5 CA1PNs), sampling from intermediate to ventral CA1.

Synaptic input drive onto CA1PNs reflect both radial positioning and birthdate.

Previous studies suggest that cells located in the *deep* or *superficial* portion of the CA1 pyramidal layer, differ in their synaptic inputs (Kohara et al., 2014; Lee et al., 2014;

Masurkar et al., 2017; Valero et al., 2017). In order to investigate whether this pattern would also depend on birthdate we have voltage-clamped the fate-mapped CA1PNs at the reversal potential for GABAergic and glutamatergic currents to record spontaneous excitatory and inhibitory postsynaptic currents (s-EPSCs and s-IPSCs, Fig. 2). The location of the neurobiotin-filled somata of the recorded cells was measured in respect to the depth of the pyramidal layer and expressed as a ratio between 0 and 1, representing the border with the *stratum radiatum* and the *stratum oriens* respectively. Although the amplitude and frequency of neither s-EPSCs (Fig. 2C) nor s-IPSCs (Fig. 2D) differed, the excitatory/inhibitory balance (computed as the E/I amplitude ratio, Fig. 2E) was lower for E14.5 than both E12.5 (P: 0.020) and E16.5 CA1PNs (P: 0.018). This indicates that neurons born at E14.5 are subject to a synaptic drive leaning more towards inhibition that the other two groups, in agreement with their receiving more putative perisomatic PV contacts (see above). In contrast, the frequency of s-EPSCs (Fig. 2C) showed a linear correlation with the cell body location (r= 0.49, p: 0.002). This was also reflected in the E/I frequency ratio (r=0.43, P: 0.0047), indicating a higher excitatory synaptic drive in deep than in superficial neurons, regardless of their birthdate (Fig. 2E).

To acquire further understanding of the different connectivity profiles, we applied brief electric stimulations in the *stratum radiatum*, which contains CA3 Schaffer collaterals innervating CA1, and recorded evoked PSCs in voltage-clamp mode (Fig. 3A). In contrast to (Valero et al., 2015), we could not observe any correlation between the properties of evoked synaptic excitation and the soma location or the birth date (Fig. 3B & 3C). This contrasted with evoked inhibitory responses (Fig. 3B & 3D). Indeed, evoked IPSC amplitude increased linearly towards the *stratum oriens* (r=0.34, P: 0.0128), while IPSC kinetics (half-width and time constant) inversely correlated with the location (respectively, r=-0.36, P: 0.008 and r=-0.36, P: 0.0051, Fig. 3D). This suggests that cells in the deep sublayer receive stronger and faster presumably CA2/CA3-driven GABAergic input (Lee et al., 2014). Finally, we tested paired-pulse (PP) responses as a proxy of the input release probability and found that inhibitory PP ratio was consistently higher in E12.5 CA1PNs as compared to E14.5 (P: 0.0326) and E16.5 (P: 0.0177) CA1PNs (Fig. 3D).

Altogether these results indicate that input connectivity motifs might be expressed as a gradient through the depth of the pyramidal cell layer. However, they also show that some functional features, such as the E/I balance and the SC-associated GABAergic release probability, may rather be established through developmental programs that are revealed uniquely by the temporal origin.

Relationship between birthdate, soma position and synaptic output

We have seen above that the radial position of CA1PNs is partly reflected in their synaptic input drive. Given that these cells were shown to be diverse regarding their projection area, we decided to test whether birthdate could segregate CA1PNs with different projection patterns. The ventral CA1 is known to display multiple projections targeting the EC, the amygdala (Amy), nucleus accumbens (NAcc), the medial prefrontal cortex (mPFC), the lateral septum (LS) and lateral hypothalamus (LHA) (Arszovszki et al., 2014; Cenquizca and Swanson, 2007; Ciocchi et al., 2015; Kim and Cho, 2017; van Groen and Wyss, 1990). Interestingly, an anatomical segregation in a laminar fashion was often reported when comparing cells with different projections.

To this aim, we performed injections of the retrograde tracer cholera toxin subunit B (CTB) CTB-647 into the Amy, NAcc, mPFC, LS and LHA and counted CTB^+-Tdt^+ co-labelled cells in the ventral CA1 (Fig. 4, and S4 in the supplementary material). Co-labelling data from a given animal was translated into a binary vector of length N equal to the total amount of Tdt^+- birthdated cells, with “1” entries reporting the number of those that were also positive for CTB. Vectors representing animals for which the same birth date was labelled were added. Birth dated groups were next compared in a pairwise-fashion using a resampling approach (See Methods).

When comparing the three birthdate groups, excluding the regions where each projected the most densely (LS for E12.5 and E16.5 CA1PNs, NAcc for E14.5 CA1PNs), the fraction of CTB^+-Tdt^+ was significantly higher in E12.5 than E16.5 ($P<0.05$) and presented a trend between E12.5 and E14.5 ($P=0.070$, Fig. 4B). In addition, E12.5 neurons projected homogeneously to all structures analyzed, while marked differences in output innervation were found within E14.5 and E16.5 neurons (Fig. 4C). E14.5 CA1PNs showed a clear bias towards the NAcc, followed by LS and mPFC. Similarly, and despite some variability, LS and NAcc were also preferred outputs of E16.5 CA1PNs, while the remaining three structures (Amy, mPFC, LHA) presented little to no co-labelling.

The overall higher CTB^+-Tdt^+ fraction in E12.5 PNs (Fig. 4B) was found as well when looking within given target structures (Fig. 4D). Indeed, E12.5CA1PNs projected proportionally more than E16.5CA1PNs to Amy, and more than both E14.5 and E16.5CA1PNs to mPFC. In contrast, within NAcc-projecting neurons, CTB^+-Tdt^+ proportion was the greatest among E14.5 neurons, as compared to E12.5 and E16.5. In addition, E14.5 cells projected more to Amy than their later-generated counterparts (Fig.

4D). These results are in line with previous findings that NAcc, Amy and mPFC are preferentially targeted by earlier-generated neurons located in the deep sublayer (Jimenez et al., 2018; Lee et al., 2014; Okuyama et al., 2016). Furthermore, they point at a specific contribution of the embryonic origin in defining output connectivity motifs (e.g. NAcc-projecting neurons mainly identified among E14.5 CA1PNs). In addition, the tendency of E12.5CA1PNs to contact at consistent rates all retro-traced regions is reminiscent of multiple projecting CA1 cells (Ciocchi et al., 2015; Gergues et al., 2020).

Intrinsic electrophysiological properties of CA1PNs reflect birthdate

Together with synaptic input connectivity, intrinsic electrophysiological properties are known to contribute to the specific activation of CA1PNs, for example in the formation of place fields (Bittner et al., 2017; Epsztein et al., 2011). They have been shown to vary across cells (Dougherty et al., 2012; Graves et al., 2012; Maroso et al., 2016; Masurkar et al., 2020; Mizuseki et al., 2011). We have therefore examined their relationship with birthdate by performing current-clamp experiments in adult slices where CA1PNs from the three age groups could be identified (Fig. 5).

We first probed the intrinsic membrane excitability via a series of hyperpolarizing current steps (Fig. 5D) and found that pioneer E12.5CA1PNs exhibited a reduced repolarizing sag response (E12.5 vs E14.5, P: 0.0078), and rebound potential (not shown) in respect to later generated neurons, while their membrane time constant was faster than E16.5 neurons (P: 0.0264, Fig. 5B). On the contrary, pyramidal neurons born at E14.5 had a higher input resistance (Fig. 5C) and, upon depolarizing current injections of increasing amplitude, were globally able to trigger more action potentials than the earlier- and later-born counterparts (Fig. 5E, main effect of birth date $P < 0.0001$, E12.5 vs E14.5: $P < 0.0001$, E14.5 vs E16.5: $P < 0.0001$, E14.5 vs E16.5: $P = 0.645$, ordinary two-way ANOVA), despite no differences in action potential threshold, half-width or rheobase (see supplementary table S1).

Interestingly, none of the intrinsic electrophysiological properties measured here correlated with the location in *the stratum pyramidale*, suggesting that the embryonic birth date is a major determinant of the observed cell heterogeneity, which cannot solely be explained by the radial gradient.

Dendritic morphology of CA1PNs correlates with birthdate

We next asked whether the dendritic morphology of CA1PNs could reflect their birthdate, since pyramidal neurons with different dendritic arborizations were recently shown to distribute radially in the distal part of CA1 (Li et al., 2017). We used a set of neurobiotin-filled cells ($n_{E12.5}$ = 30, $n_{E12.5}$ = 14, $n_{E16.5}$ = 19) and considered the overall dendritic arborization (Fig. 6). We measured the distance between the cell soma and the first bifurcation of the primary apical dendrite (Fig. 6B). Earlier-generated neurons (both E12.5- and E14.5- CA1PNs) had a significantly longer shaft than later generated neurons (Fig. 6C, E12.5 vs E16.5, P: 0.0001; E14.5 vs E16.5, P < 0.0001). In addition, the shaft length increased linearly with the distance of the cell body from the *radiatum/pyramidale* border (r=0.51, CI_{95} [0.32; 0.68], P< 0.0001, Fig. 6C). However, we next reasoned that this correlation could be redundant, owing that a portion of the dendritic shaft includes the distance of the soma from the *radiatum/pyramidale* border, hence its location (Fig. 6B). To avoid this confounding factor, we computed as a substitute the distance between the primary apical dendrite birfucation to the *radiatum/pyramidale* border (Fig. 6C) and observed that indeed the correlation with the soma location could no longer be found (r=0.16, CI_{95} [-0.07; 0.38], P: 0.0865). However, differences related to the birth date remained, and E14.5 CA1PNs cells were found to display a longer dendritic main branch within the *stratum radiatum* than both E12.5- and E16.5CA1PNs (E12.5 vs E14.5, P: 0.0056; E14.5 vs E16.5, P: 0.0004, Fig. 6C). Thus, consistent with our previous findings in CA3 (Marissal et al., 2012), the dendritic morphology appears to be determined by the temporal embryonic origin, at least in its basic features. Again, this correlation with birthdate is not linear since E12.5 CA1PNs were found to be more similar to E16.5PNs than E14.5CA1PNs, their closer peers in age.

cFos labelling following the exploration of familiar or novel environments correlates with birthdate

The dorsal CA1 was recently shown to comprise two functional sublayers with deep CA1PNs supporting the formation of landmark-based spatial maps during a novel experience, while superficial CA1PNs were more active in cue-poor conditions and likely to convey self-referenced information (Danielson et al., 2016; Fattahi et al., 2018; Geiller et al., 2017; Sharif et al., 2020). We asked whether similar differences could be observed in the ventral CA1 and whether they could reflect developmental origin, given the different connectivity schemes and excitability across CA1PNs with different birthdates. To this aim, we tested the activation of birth dated ventral pyramidal neurons during the exploration of an environment, by the means of cFos immunoreactivity, given the poor

accessibility of the ventral hippocampus to imaging and the sparsity of pioneer CA1PNs. cFos is an immediate early gene whose expression does not simply reflect previous activity in labelled neurons but also the induction of activity-related plasticity (West et al., 2002).

Ngn2-Cre^{ER}-Tdt mice (n=25) induced at E12.5, E14.5 and E16.5 were divided into three groups (Fig. 7A): one explored a cue-enriched arena during 20 minutes for 3 consecutive days, the familiar group (FAM), whereas another group was exposed to the same environment during only one session on the third day, the novel group (NOV). A control group was handled by the experimenter but did not explore any arena, the home cage group (HC). As expected, FAM mice decreasingly explored the arena throughout the 3 consecutive sessions (repeated measures one-way ANOVA, test for trend: $P< 0.01$, Fig. 7A). Coherently, the distance run by NOV mice was significantly higher than that of the second and third FAM sessions (one-way ANOVA, NOV vs FAM_2, $P < 0.001$; NOV vs FAM_3, $P < 0.001$), but not of the first session (FAM_1).

As expected, the overall proportion of cFos$^+$/DAPI neurons was significantly higher in NOV (10.76 % ± 3.42) and FAM (9.40 % ± 1.31) than the HC condition (5.44% ± 2.45), further confirming that cFos expression in hippocampal neurons is up-regulated upon exploratory activity (Fig. 7B).

To study how cFos activation may vary according to a neuron's embryonic origin, we first computed the proportion of cFos$^+$/Tdt$^+$ cells by birth date group, regardless of the condition (Fig. 7C). Doing so, we observed that E16.5 mice displayed significantly lower proportions of co-labelled cells than both E12.5 (95% Confidence interval or CI_{95} [0.0097; 0.0483], $P < 0.01$) and E14.5 (CI_{95} [0.0137; 0.0459], $P < 0.001$). Hence, late-born E16.5CA1PNs are less prone to express cFos, as expected from the previously reported global difference in overall recruitment between *deep* and *superficial* CA1 PNs (Mizuseki et al., 2011). Using the same approach as for retrograde tracing analysis, we examined the cFos$^+$/Tdt$^+$ fraction per condition per group. We found that pioneer E12.5CA1PNs were highly likely to express cFos following habituation (E12.5-FAM), as compared across conditions within the same birth date group (E12.5-FAM vs E12.5-HC, $P < 0.001$; E12.5-FAM vs E12.5-NOV, P: 0.066) and across birthdates for the same FAM condition (E12.5-FAM vs E14.5FAM, $P < 0.01$; E12.5-FAM vs E16.5-FAM, $P < 0.05$, Fig. 7C). Although more than twice less than for E12.5CA1PNs, E16.5CA1PNs were also significantly more likely to express cFos in FAM than HC conditions. These cells were overall very unlikely to express cFos, especially in the HC condition where co-labelling was significantly lower

than observed in E14.5 mice (E16.5-HC vs E14.5-HC, $P < 0.01$). Importantly, in the NOV condition, earlier-generated cells showed more cFos+ activation than later born ones, though this only appeared significant for E14.5 CA1PNs (E14.5-NOV vs E16.5-NOV, $P < 0.05$; E14.5-NOV vs E12.5-NOV, P: 0.165). Taken together, these results are in line with previous research, in that deep CA1PNs are more likely to express IEGs than superficial ones upon exposition to a novel environment (Kitanishi et al., 2009). Yet, pioneer E12.5CA1PNs form a distinct subpopulation more specifically expressing cFos after familiarization to the environment. Hence, these last results indicate a different involvement in novelty detection of pyramidal neurons in the ventral CA1 according to their developmental origin.

Discussion

In this study, we have employed a manifold description of CA1PNs with different birthdates in the adult hippocampus to study the origin of diversity at single-cell level. We have found that the now well-established subdivision of the CA1 pyramidal layer into two distinct sublayers, a *deep* and *superficial* one, masks a much greater heterogeneity, which logic can be exposed when considering the temporal origin of individual neurons. This heterogeneity encompasses several morpho-physiological properties and translates in the propensity of cells to be recruited in familiar or novel environments. Furthermore, we find that pioneer CA1PNs generated at the earliest stages of glutamatergic cell neurogenesis are prone to be recruited in familiar environments, forming a subpopulation with distinct anatomical distribution, morphophysiological features and wiring.

Birthdate rather than birth order is a better predictor of diversity

Several studies converge in suggesting that the CA1 pyramidal layer comprises two subtypes of CA1PNs based on their radial positioning. We would like to propose that the diversity of CA1PNs is even better predicted by birthdate than position. More specifically, we found that the following metrics were better reflecting birthdate than radial positioning based on the lack of correlation with soma position and the existence of a significant correlation with birthdate: (1) the length of primary apical dendrite in the *stratum radiatum;* (2) the input resistance, sag current and firing rate in response to

depolarizing current injections; (3) the E/I ratio; (4) the short-term facilitation of evoked synaptic inhibitory currents. The two main metrics that linearly correlate with layering reflect the local microcircuit integration of CA1PNs as they are the frequency of sEPSCs and the evoked IPSC decay. It was previously reported that both ectopic CA1PNs with a soma located in the *stratum oriens* received a higher rate of sEPSCs than cells located within the stratum pyramidale (Cossart et al., 2000). Similarly, we find that CA1PNs located closer to the stratum oriens receive sEPSCs at a higher rate. This could reveal either a slicing artefact or the contribution of glutamatergic inputs from the CA1 axonal collaterals arborizing in that area. The faster kinetics of evoked IPSCs may reflect the increased contribution of parvalbumin basket cell inputs to evoked IPSCs as cells move towards the *oriens*. Indeed, the alpha1-containing postsynaptic GABAA-Rs contributing to PV synapses were shown to display faster kinetics than those formed by CCK basket cells (Thomson et al., 2000). In light with studies indicating specified microcircuitry among deep versus superficial principal cells and PV basket cells, we have found that the PV staining was denser towards the *stratum oriens*. However, within the deep CA1PNs, cells born at E12.5 were exceptionally less decorated with putative PV contacts than deep CA1PNs born 2 days later. Overall, we observed that E12.5 cells were more similar to E16.5 CA1PNs regarding their lower intrinsic excitability, dendritic morphology, lower PV coverage and higher E/I ratio. As E16.5CA1PNs, they can even be found in the superficial layer and even in the *stratum radiatum*. Altogether, one could foresee that the main source of activation for both E12.5 and E16.5 CA1PNs would be through synaptic glutamatergic excitation. However, it is likely that the main glutamatergic inputs onto E16.5 and E12.5 CA1PNs differ. While the main excitatory drive onto E16.5CA1PNs, given their location likely originates in CA3, future studies are needed to determine whether E12.5 cells receive specific inputs. Such studies remain at the moment technically challenging due to the poor accessibility of E12.5 cells to genetic manipulation using our fate-mapping strategy. These cells also differ in their extrahippocampal outputs. Accordingly, these cells could also be discriminated based on their cFos expression following spatial exploration with E12.5, like E14.5 CA1PNs being more likely to express cFos during random exploration than E16.5CA1PNs. Future studies are needed to determine the conditions favoring cFos expression in E16.5CA1PNs. These may require analyzing these cells in conditions of elevated anxiety, social interactions or goal-directed behaviors (Ciocchi et al., 2015; Jimenez et al., 2018; Okuyama et al., 2016). If E12.5CA1PNs and E14.5CA1PNs displayed comparable cFos expression levels, as

expected from previous work (Mizuseki et al., 2011), the former signals familiarity and the latter novelty, suggesting that the mechanisms supporting hippocampal representation of novelty may require cells with a higher intrinsic neuronal excitability (Epsztein et al., 2011).

If our results are mostly in agreement with previous reports, we were not able to observe any significant correlation between laminar position and sag current amplitude, resting membrane potential or input resistance in our dataset. Only E12.5CA1PNs could be distinguished by their lower sag amplitude value and input resistance. This apparent discrepancy may have several explanations. First, our experiments were not performed in the presence of blockers for other postsynaptic membrane currents and of antagonists for all metabotropic and ionotropic GABA and glutamate receptors (Jarsky et al., 2008; Lee et al., 2014; Maroso et al., 2016; Masurkar et al., 2017). Second, we focused on ventral and not dorsal hippocampus (Maroso et al., 2016), and cells were sampled evenly across the transverse axis, while radial correlations could only be revealed at fixed positions along the proximo-distal axis (Masurkar et al., 2017). We were also surprised not to observe any bursting cell (Graves et al., 2012; Jarsky et al., 2008), but again these are mainly present closer to the subiculum and were reported in slices from juvenile (P15-17 (Jarsky et al., 2008), P25-28 (Graves et al., 2012)) rats using a gluconate-containing intracellular solution (Kaczorowski et al., 2007). Last, while we could observe a linear correlation between soma location and dendritic morphology as reported previously (Graves et al., 2012; Jarsky et al., 2008; Lee et al., 2014; Li et al., 2017), this was no longer observed when considering only the dendritic portion within the *stratum radiatum*. When computing this metric, E14.5CA1PNs could be distinguished from E12.5 and E16.5 CA1PNs by their longer primary apical segment. Also, one needs to consider one major limitation of the fate mapping approach employed here when interpreting the results of the present study. Indeed, our labelling is based on the Cre-dependent and tamoxifen-induced expression of a fluorescent reported protein in *Ngn2* expressing progenitors. This is a stochastic process, and a variable and sparse subset of progenitors get labelled. We are only describing small numbers and the most distinctive features are more likely to show up as significantly different whereas other metrics may require denser sampling.

Altogether, our results globally indicate that the order of neurogenesis does not imprint a continuous gradient in the specification of cell laminar positioning and diversity. Instead, these are predetermined by the specific temporal origin of individual cells. Interestingly, the notion that early specification has a stronger importance than final

layering in the determination of CA1PNs intrinsic properties is supported by recently observations with a transgenic mouse model of lissencephaly where CA1 lamination is impaired while cell identity is relatively spared (D'Amour et al., 2020). Therefore, the recently uncovered system of parallel information processing in CA1, with two information streams segregated through distinct inhibitory domains (Soltesz and Losonczy, 2018), may need to consider this additional level of complexity.

The mechanisms by which diversity among CA1PNs may be temporally-regulated during neurogenesis remain to be determined. Increasing evidence indicates that glutamatergic neurons are issued from the same multipotent progenitors and that fate distinctions are mostly temporally controlled (Jabaudon, 2017)(but see (Franco et al., 2012)). Interestingly, progenitor potential was shown to be progressively, temporally restricted, with early cortical progenitors being multipotent in comparison to later ones (Lodato et al., 2015). In combination with genetic predetermination, single-cells display tightly orchestrated sequences of spontaneous activity patterns (Allene et al., 2012), which in turn may contribute to the maturation of physiological specificity. Therefore, cells with similar birthdates will follow similar activity development schedules. Interestingly, both Ih and Rin, two parameters that segregate between CA1PNs with different birthdates, are developmentally regulated, both progressively decreasing as cells mature (Dougherty, 2019). As such, they are ideal proxys of neuronal maturation stage. Given that the earlier born CA1PNs can be distinguished by lower values of Ih and Rin, one could propose that these cells could maintain into adulthood the advance in maturation originating from their early birth date.

Pioneer cells are a different population, possible roles?

This study shows that neurons born at the earliest phases of CA1PNs neurogenesis display distinct somatic distribution, connectivity, morpho-physiological properties as well cfos expression patterns. This distinguishes them from slightly later born neurons, the E14.5CA1PNs that sit mainly in the deep sublayer of the *stratum pyramidale*. We argue that these cells form a distinct subpopulation. The first striking property of E12.5CA1PNs is their scattered distribution. They can be found at ectopic positions in the *stratum oriens* as well as, more rarely, within the *stratum radiatum,* suggesting that these cells may also comprise the previously described radiatum "giant cells", with privileged CA2 input and output to the olfactory bulb (Gulyás et al., 1998; Nasrallah et al., 2019). In fact, cumulative distribution plots indicate that roughly half of the E12CA1PNs in the ventral (and dorsal)

hippocampus are found within less than 100 µm distance from the *stratum radiatum* while the other half distributes closer to *stratum oriens* more than 100 µm away from that border. It is unlikely that such observation results from unspecific labeling from our method. First, the population of E12.5CA1PNs labeled using this method shares many characteristics despite this layer dispersion. Second, this unique arrangement was also recently observed for early born granule cells (Save et al., 2019) and dispersion of early generated glutamatergic cell cohorts was previously suggested using other methods including autoradiographic (Caviness, 1973) and retrovirus labeling (Mathews et al., 2010). Somehow similarly, even if preferentially located in the deep *stratum pyramidale*, early born CA3 pyramidal cells could be found anywhere from *stratum oriens* to *lucidum* (Marissal et al., 2012). It is therefore possible that pioneer cohorts of PNs would display a different migration mode, resulting from the low cellular density when entering the hippocampus in addition to other more specific mechanisms, like an absence of radial glia bending (Xu et al., 2014), that remain to be specifically studied. Regardless, despite this almost even positioning, we observed that E12.5CA1PNs displayed specific input connectivity schemes, including a lower number of putative PV contacts associated with a higher E/I ratio and a facilitation of the evoked IPSC amplitude. We hypothesize that these three measurements may reveal the same feature, namely the lower somatic inhibitory coverage of E12.5CA1PNs. Indeed, facilitating inhibitory responses were found to originate from dendrite-targeting interneurons while perisomatic cells would tend to generate transient inhibitory inputs (Pouille and Scanziani, 2004). This lower PV innervation is comparable with E16.5CA1PNs and contrasts with their early-born peers, the E14.5CA1PNs, which display higher perisomatic PV staining. Whether these CA1PNs are contacted by specific glutamatergic inputs stays an open question that remains an experimental challenge with our fate-mapping strategy. According to the temporal matching rule observed in the hippocampus (Deguchi et al., 2011), and the fact that some of them are found in the *stratum radiatum* and *oriens*, one may expect these cells to receive preferential innervation from CA2, the earliest generated portion of the hippocampal circuit (Caviness, 1973). The significantly higher E/I ratio received by these cells suggests that they may be preferentially recruited by synaptic excitation, since they are otherwise less intrinsically excitable (lower Rm, low firing rate in response to long depolarizing current injections, lower sag). Interestingly, the same lower excitability (across similar metrics), combined with lower levels of PV inputs was observed in early born CA1 GABAergic neurons and DG granule cells (Bocchio et al., 2020; Gupta et al.,

2012; Save et al., 2019), again indicating similar fates in the adult across different subtypes of pioneer neurons.

Ventral E12.5CA1PNs are also remarkable in terms of output since they globally sent more projections to the target regions studied here and did not display any preferred projection pattern in contrast to their later born peers. Of note they were significantly more likely to target the Amy and mPFC than both E14.5 and E16.5 cells. These results would suggest that E12.5CA1PNs may form a sparse population with multiple projections. Triple projection ventral CA1 cells targeting the mPFC, Amy and NAcc were shown to be highly active and in particular during SWRs (Ciocchi et al., 2015). Unfortunately, the sparsity of our labeling method currently prevents opto-tagging E12.5CA1PNs as well as testing the hypothesis that they may be comprised of multiple projection neurons.

Conclusion

We have uncovered a novel population of pioneer cells adding to the diversity of CA1 glutamatergic neurons. Based on their specific properties, we would like to propose a general role for ventral pioneer CA1PNs in the consolidation or retrieval of recent experience. Future work examining their recruitment in SWRs (Ciocchi et al., 2015), their possible CA2 inputs (Kohara et al., 2014; Nasrallah et al., 2019; Valero et al., 2015) and their likely multiple projection targets will certainly inform about this possibility. In any case, the present results indicate that the radial subdivision of the CA1 pyramidal layer into two functional sublayers needs to be revisited by considering the time of neurogenesis. The strongest reliance of CA1 principal neuron diversity on temporal origin or initial genetic blueprint than position may render these cells more resilient to diseases resulting in heterotopias and mislayering, as recently reported (D'Amour et al., 2020).

Materials and Methods

Animals. All protocols were performed under the guidelines of the French National Ethics Committee for Sciences and Health report on “Ethical Principles for Animal Experimentation” in agreement with the European Community Directive 86/609/EEC under agreement # 01 413.03. All efforts were made to minimize pain and suffering and to reduce the number of animals used. Animals were maintained with unrestricted access to food and water on a 12hour light cycle, and experiments were conducted during the light portion of the day. To mark glutamatergic neurons generated during different times of embryogenesis, we use the technique of inducible genetic fate mapping (see ((Marissal et al., 2012; Save et al., 2019)). In brief, double heterozygous *Ngn2-CreER*$^{TM/-}$*/Ai14:LoxP*$^{+/-}$ mice (*Ngn2-Cre*^{ER}*-Ai*14 in the text for simplicity) were obtained by crossing *Ngn2-CreER*$^{TM/-}$/Ai14:LoxP$^{+/+}$ male mice with 7-8-weekold wild-type Swiss females (C.E Janvier, France). To induce Cre activity during embryogenesis, tamoxifen was delivered to pregnant mothers (Sigma, St. Louis, MO; 2 mg per 30 g of body weight of tamoxifen solution, prepared at a concentration of 10 or 20 mg/mL in corn oil) at embryonic days E12.5, 14.5, 16.5.

Slice preparation for *ex vivo* electrophysiology. Ngn2-CreER$^{TM/-}$/Ai14:LoxP$^{+/-}$ mice of either sex aged between post-natal week 4 (W4) and W11 treated with tamoxifen at E12.5, E14.5 or E16.5 were used for experiments. First, they underwent deep anesthesia by intraperitoneal xylazine/ketamine injection (Imalgene 100 mg/kg, Rompun 10 mg/kg) prior to decapitation. 300 µm-thick horizontal slices were cut with a Leica VT1200 Vibratome using the Vibrocheck module in ice-cold oxygenated modified artificial cerebrospinal fluid with the following composition (in mM): 126 CholineCl, 26 $NaHCO_3$, 7 $MgSO_4$, 5 $CaCl_2$, 5 D-glucose, 2.5 KCl, 1.25 NaH_2PO_4). Slices were then transferred for rest at room temperature (at least 1 h) in oxygenated normal aCSF containing (in mM): 126 NaCl, 3.5 KCl, 1.2 NaH_2PO_4, 26 $NaHCO_3$, 1.3 $MgCl_2$, 2.0 $CaCl_2$, and 10 D-glucose, for a total of 300 ± 10 mOsm (pH 7.4). A total of 72 cells were successfully recorded from 34 mice ($n_{E12.5}$ = 22, $n_{E14.5}$ = 27, $n_{E16.5}$ = 23). 63 cells were used for morphological analysis.

Ex vivo patch clamp recordings. Patch clamp recordings in adult slices were performed using a SliceScope Pro 1000 rig (Scientifica) equipped with a CCD camera (Hamamatsu Orca-05G) and with a X-Cite 120Q (Excelitas Technologies Corp.) fluorescence lamp. Recordings were performed from visually identified Tdt+ cells. Patch electrodes (4-7 MΩ resistance) were pulled using a PC-10 puller (Narishige) from borosilicate glass capillaries (GC150F10, Harvard Apparatus). Slices were transferred to a submerged recording chamber and continuously perfused with oxygenated ACSF (3 mL/min) at ~32 °C. Electrophysiological signals were amplified, low-pass filtered at 2.9 kHz and digitized at 10 kHz with an EPC10 amplifier (HEKA Electronik) and acquired using the dedicated software PatchMaster. Neurons were kept at -65 mV throughout the session and recordings started 5-10 minutes after access. For current clamp experiments, the following intracellular solution was used (in mM): 130 K-$MeSO_4$, 5 KCl, 5 NaCl, 10 HEPES, 2.5 Mg- ATP, 0.3 GTP, and 0.5% neurobiotin (~280 mOsm, 7.3 pH). Capacitance compensation and bridge balance were performed before recording and adjusted periodically. Liquid junction potential was not corrected. The resting membrane potential was not measured. For voltage clamp experiments, the solution consisted of (in mM): 130 CsGluconate, 10, HEPES, 5 CsCl, 5 Na_2Phosphocreatine, 2 MgATP, 1 EGTA,

0.3 Na_3GTP, 0.1 $CaCl_2$ and 5% neurobiotin ~290 mOsm, 7.3 pH). Uncompensated series resistance was calculated postacquisition and considered acceptable if below 30 MΩ and if variations were lower than 20%. Liquid junction potential correction (-13 mV) was applied. Excitatory and inhibitory postsynaptic currents were recorded at -86 mV (E_{GABA}) and 0 mV (E_{Glu}) respectively, over 9 sweeps of 20s. A -5 mV step (5 ms duration) was used to monitor series resistance at the beginning of each sweep. For Schaffer collateral stimulation, a bipolar electrode made by two twisted nichrome wires and connected to a DS2A Isolated Voltage Stimulator (Digitimer) was used to deliver 0.2 ms-long stimuli in the *stratum radiatum* of CA1 (between the recorded cell and CA3). Stimulation intensity was set to 2X the minimum intensity capable of eliciting a postsynaptic response (tested between -86 mV and -78 mV). Paired pulse ratio was assessed by two stimulations separated by 50 ms.

Analysis of *ex vivo* patch clamp recordings. Analysis of intrinsic membrane properties was performed using custom-made MATLAB scripts. Traces were filtered using the sgolay MatLab function, unless firing properties were being analysed. The input membrane (R_m) resistance was calculated from the slope of steady-state voltage responses to a series of subthreshold current injections lasting 500 ms (from -100 pA to last sweep with a subthreshold response, 10 or 20 pA step size). The membrane time constant (τ_m) was estimated from a bi-exponential fit of the voltage response to a small (-20 pA) hyperpolarizing pulse. Capacitance was calculated as τ_m/R_m. The sag potential was calculated by injecting a 1 s-long negative current step (-200 pA) as follows: $Sag_{-200pA} = \Delta V_{steady\text{-}state} - \Delta V_{peak}$ (subtraction of the steady-state potential at halfresponse (averaged over 45 ms) to the minimum peak potential at the beginning of the response). The rebound potential was computed by subtracting the depolarization peak after the end of the hyperpolarization to the baseline potential ($Rebound_{-200pA} = \Delta V_{peak} - \Delta V_{baseline}$), in absence of rebound action potentials. Firing curves were determined by applying an increasing range of 1-s long depolarizing current injections (up to 500 pA, +40 pA step). The rheobase (in pA) was defined as the minimum current value necessary to elicit an action potential. The first spike in response to a positive current injection was used to determine: the threshold potential (the peak of the second derivative), the action potential amplitude and fast afterhyperpolarization (both calculated from threshold potential), and the half-width (width at half-amplitude between the threshold potential and the peak of the action potential). Analysis of spontaneous postsynaptic currents (sPSCs) was performed using MiniAnalysis (Synaptosoft). Traces were filtered with a LoPass Butterworth (cutoff frequency 1000 Hz) and PSC amplitude and frequency were calculated over 2 minutes (total of 6 sweeps, 20s). The mean PSC event was analysed with a custom-made MATLAB script to compute rise time (10-90% of the ascending phase); decay time (90-37% of the descending phase); decay τ (from a monoexponential curve adjusted to best fit the trace); half-width (width at half-amplitude between PSC peak and baseline); area (using *trapz* MATLAB function). Mean stimulation-evoked PSC amplitude, area and kinetics were calculated as detailed above. Paired pulse ratio was measured by calculating the amplitude of two 0.2 ms-long stimuli at 50 Hz as follow: $PPR=Peak_2/Peak_1$. The ratio between excitatory and inhibitory PSC (E/I ratio) was calculated by dividing frequency and amplitude values.

Morphological analysis of neurobiotin-filled cells. Slices containing neurobiotin-filled cells were fixed overnight at 4 °C in PFA (4%), rinsed in PBS containing 0.3% Triton X-100 (PBS-T) and incubated overnight at room temperature in streptavidin-AlexaFluor488 (1:1000 in PBS-T). Slices were mounted using Vectashield mount medium containing

DAPI (VectorLabs). Post-hoc analysis was performed using an AxioImager Z2 microscope equipped with Apotome module (Zeiss). The co-localisation of neurobiotin and TdTomato was verified systematically for every recorded cell. Neurobiotin-filled neurons were selected when the apical dendrites were clearly visible and uncut. Stacks of optical sections were collected for these cells. The primary dendrite was identified as the portion of between the soma and a bifurcation generating secondary dendrites of roughly equal size. The length of the primary dendrite was measured by approximating its shape to 1-3 linear segments.

Quantification of cell location in stratum pyramidale. For patch clamp recordings, the cell location was measured from the border between the *stratum pyramidale* (SP) and the *stratum radiatum* (SR) and normalized to the thickness of the SP, meaning that values close to 0 correspond to the proximity of SP/SR border and values close to 1 to *stratum oriens* (SO)/SP border. For the overall quantification of Ngn2 cell location, the cell location was measured from the border between the *stratum pyramidale* (SP) and the *stratum radiatum* (SR) and expressed in micrometers.

Histological processing and immunohistochemistry. After deep anesthesia with a ketamine (250 mg/kg) and xylazine (25 mg/kg) solution (i.p.), animals were transcardially perfused (1 mL/g) with 4% paraformaldehyde in saline phosphate buffer (PBS). Brains were post-fixed overnight, then washed in PBS. For Ctb tracing, a VT1200 Vibratome (Leica) was used to cut coronal slices. Slice thickness was 100 µm for the injection site and 70 µm for the hippocampus. In a subset of experiments, CTB-AlexaFluor647 signal was amplified by immunohistochemistry. Sections were incubated overnight with primary Cholera Toxin beta polyclonal antibody (rabbit; 1:1000, RRID: AB_779810, Invitrogen) diluted in PBS-T and for approximately 1h30 with donkey antirabbit secondary antibody AlexaFluor647 (1:500, Jackson Immunoresearch, 711-606-152) in PBS-T.
For cfos immunostaining, a similar procedure was employed. Coronal slices (50 µm thickness) obtained with a HM450 sliding Microtome (Thermo Scientific, Waltham, MA) were rinsed 3 times in PBS containing 0.3% Triton X (PBS-T) and incubated overnight at 4° C with a solution containing 5% goat serum (GS) and anti-cFos (rabbit; 1:5000, ab190289, Abcam) diluted in PBST. The following day slices were exposed to a goat anti-rabbit AlexaFluor647 secondary antibody (1:500, Jackson Immunoresearch, 111-606-144) in PBS-T. Post-hoc analysis was performed from image stacks (1.5 µm interval, 7 images) obtained using a Zeiss LSM-800 system. Slices were mounted using Vectashield mount medium containing DAPI (VectorLabs). Post-hoc analysis was performed from image stacks obtained using a Zeiss LSM-800 system equipped with emission spectral detection and a tunable laser providing excitation range from 470 to 670 nm.

Quantification of putative PV-expressing synaptic boutons.
For parvalbumin (PV) putative puncta detection, we employed a similar immunostaining procedure as described above. Goat anti-PV primary antibody (1:1000, Swant, pvg-214, AB10000345) and donkey anti-goat AlexaFluor488 secondary antibody (1:500, Jackson Immunoresearch, AB_2336933) were used. Stacks (0.06 x 0.06 x 0.410 µm) centered on the soma of TdTomato+ cells (E12.5: 88 cells; E14.5 : 106 cells; E16.5: 44 cells) were acquired with a Zeiss LSM-800 microscope using a Plan-Apo 40x/1.4 oil objective. Volume overlaps between PV+ boutons and Tdt+ somata were calculated using a custom-made MatLab script. Values were normalized by the number of Z-steps to control for possible differences in soma size or experimental variability.

Stereotaxic injections for retrograde tracing. Ngn2-CreER$^{TM/-}$/Ai14:LoxP$^{+/-}$ adult mice (age > P50) of either sex were anaesthetized using 1-3% isoflurane in oxygen. Analgesia was provided with buprenorphine (Buprecare, 0.1 mg/kg). Lidocaine was applied by cream or subcutaneous injection before the incision for additional local analgesia.
Mice were fixed to a stereotaxic frame with a digital display console (Kopf, Model 940). Under aseptic conditions, an incision was made in the scalp, the skull was exposed, and a small craniotomy was drilled over the target brain region. A 200-400 nl volume of 0.1% AlexaFluor647-conjugate Cholera Toxin subunit b (CTB, Thermofisher Scientific) was delivered using a glass pipette pulled from borosilicate glass (3.5" 3-000-203-G/X, Drummond Scientific) and connected to a Nanoject III system (Drummond Scientific). The tip of the pipette was broken to achieve an opening with an internal diameter of 30-40 µm. Stereotaxic coordinates were based on a mouse brain atlas (Paxinos and Franklin, 3rd edition). All coordinates are indicated in supplementary table S2 in millimeters, and examples of the histological recovery of the injection sites are displayed in supplementary figure S4. Antero-posterior (AP) coordinates are relative to bregma; medio-lateral (ML) coordinates are relative to the sagittal suture; dorso-ventral (DV) coordinates are measured from the brain surface. Mice were perfused 12-15 days later, to allow sufficient CTB uptake and transport from the synaptic terminals.

Analysis of retrograde tracing. To confirm that injections were successful, each injection site was visually inspected and compared to the Paxinos mouse brain atlas. The occurrence of co-labelling with Ctb among Tdt+ cells was verified and the ratio of Ctb+/TdT+ cells calculated manually. This resulted in the generation for each injected animal of a binary vector of length L equal to the total count of Tdt$^+$ cells and as many "1" entries as the number of identified Ctb+/TdT$^+$ cells. Then, vectors corresponding to mice in the same birthdate group and same target region were concatenated. Finally, a bootstrap resampling approach was used to compute the pairwise comparisons (total number of tests = 45). In brief, each of two vectors A and B were randomly resampled with replacement for 10000 times. At each iteration, the difference between the two vector means ($\Delta_\mu = \mu_A - \mu_B$) was calculated and stored. At the end of the resampling, the 99.9% confidence interval (CI) of the distribution of Δ_μ was computed. The difference between vectors A and B was considered significant if the CI did not include the value 0.

cFos expression upon exploration. A total of 25 tamoxifen-treated Ngn2-CreER$^{TM/-}$/Ai14:LoxP$^{+/-}$ mice between 10-12 weeks old of either sex were used. Prior to the experiment, animals were single-housed and divided in 3 groups, named home-cage (HC), familiar (FAM) and novel (NOV), see supplementary table S3. Group HC was carried to the experimental room, handled by the experimenter during 5-10 minutes for three consecutive days (D1, D2, D3) and perfused 1h after handling on D3. Group FAM was exposed to an exploration chamber for 20 minutes from D1 to D3, and returned to their home cage immediately after. Group NOV was handled during D1 and D2 and left in the exploration chamber for one single 20-minute session on D3. FAM and NOV were both perfused 1h after exploration. The chamber consisted of a transparent plastic rat cage sized MISSING containing visual, tactile, and olfactory (butanal) cues. A white noise (20/30 dB) was played in the experimental room for the duration of the exploration and low lighting (~25 lux) was centered over the box. Mice position during each session was

recorded with a Basler Ace camera (Basler AG, Ahrensburg) and tracked with EthoVision XT 11 (Noldus, Leesburg, VA) software.

Analysis of Cfos expression upon exploration. Tdtomato$^+$ somata were segmented with Fiji Trainable WEKA Segmentation plugin. Two custom-made Cellprofiler pipelines were used on DAPI and AlexaFluor647 (cFos) channels (Carpenter et al., 2006). (i) To provide an estimation of DAPI cell density, a single 2D image (from the middle of the stack) was segmented using a Minimum Cross Entropy threshold. (ii) Segmentation of cFos$^+$ nuclei was first achieved by applying the Robust Background thresholding method on each single 2D image composing the stack and converting them into binary masks. Then, these masks were restacked and somas were identified with the 3D Object Counter Fiji plugin across the depth of the stack. To determine TdTomato and cFos colocalization, a custum-made MatLab script was used. In a nutshell, matrices representing TdTomato and cFos binary masks were multiplied, generating a new binary image of areas presenting overlap between the two channels. Finally, each of these areas, which represented putative colocalized cells, was manually inspected for confirmation. At the end of this procedure, we applied the same procedure as described for the analysis of retrograde tracing. We computed for each animal a binary vector of length L equal to the total number of segmented Tdt$^+$ cells and as many "1" entries as the number of identified Cfos$^+$/Tdt$^+$ cells. Then, vectors corresponding to mice in the same birthdate group and same behavioral condition were concatenated. Finally, a bootstrap resampling approach was used to compute the pairwise comparisons (total number of tests = 18). The 95% confidence interval (CI) of the distribution of the bootstrapped differences of means (Δ_μ) was computed. The difference between vectors A and B was considered significant if the CI did not include the value 0.

Statistical Analyses. Statistical analysis was done using Prism (GraphPad) and costum-made MatLab scripts. In patch clamp experiments, outliers were removed (ROUT method, Q = 0.1%). For comparing input-output firing curves, two-way ANOVA was used. When comparing birthdate groups for a given measure, median-based bootstrap resampling was used to compute pairwise comparisons, subsequently corrected with Holm-Bonferroni method to control for family-wise error rate, except for morphological measures where mean and Sidak's correction were used instead. The correlation with cell location was tested using bootstrap resampling. In the analysis of exploratory behavior, repeated-measures and ordinary one-way ANOVA were used to compare distance run in FAM condition and FAM vs NOV, respectively. The volume overlap of putative PV boutons is tested among birthdates with one-way ANOVA with Tukey's correction for multiple comparisons.

References

Allene C, Picardo MA, Becq H, Miyoshi G, Fishell G, Cossart R. 2012. Dynamic changes in interneuron morphophysiological properties mark the maturation of hippocampal network activity. *J Neurosci* **32**:6688–6698. doi:10.1523/JNEUROSCI.0081-12.2012

Angevine JB. 1965. Time of neuron origin in the hippocampal region. *Exp Neurol Suppl* **11**:1–39. doi:10.1016/0014-4886(65)90121-4

Arszovszki A, Borhegyi Z, Klausberger T. 2014. Three axonal projection routes of individual pyramidal cells in the ventral CA1 hippocampus. *Front Neuroanat* **8**:53. doi:10.3389/fnana.2014.00053

Bayer SA. 1980. Development of the hippocampal region in the rat. I. Neurogenesis examined with 3H-thymidine autoradiography. *J Comp Neurol* **190**:87–114. doi:10.1002/cne.901900107

Bittner KC, Milstein AD, Grienberger C, Romani S, Magee JC. 2017. Behavioral time scale synaptic plasticity underlies CA1 place fields. *Science (80-)* **357**.

Bocchio M, Gouny C, Angulo-Garcia D, Toulat T, Tressard T, Quiroli E, Baude A, Cossart R. 2020. Hippocampal hub neurons maintain distinct connectivity throughout their lifetime. *Nat Commun* **11**. doi:10.1038/s41467-020-18432-6

Carpenter AE, Jones TR, Lamprecht MR, Clarke C, Kang IH, Friman O, Guertin DA, Chang JH, Lindquist RA, Moffat J, Golland P, Sabatini DM. 2006. CellProfiler: Image analysis software for identifying and quantifying cell phenotypes. *Genome Biol* **7**:R100. doi:10.1186/gb-2006-7-10-r100

Caviness VS. 1973. Time of neuron origin in the hippocampus and dentate gyrus of normal and reeler mutant mice: an autoradiographic analysis. *J Comp Neurol* **151**:113–20. doi:10.1002/cne.901510203

Cembrowski MS, Bachman JL, Wang L, Sugino K, Shields BC, Spruston N. 2016. Spatial Gene-Expression Gradients Underlie Prominent Heterogeneity of CA1 Pyramidal Neurons. *Neuron* **89**:351–368. doi:10.1016/j.neuron.2015.12.013

Cenquizca LA, Swanson LW. 2007. Spatial organization of direct hippocampal field CA1 axonal projections to the rest of the cerebral cortex. *Brain Res Rev* **56**:1–26. doi:10.1016/j.brainresrev.2007.05.002

Ciocchi S, Passecker J, Malagon-Vina H, Mikus N, Klausberger T. 2015. Selective information routing by ventral hippocampal CA1 projection neurons. *Science (80-)* **348**:560–563. doi:10.1126/science.aaa3245

Cossart R, Hirsch JC, Cannon RC, Dinoncourt C, Wheal H V., Ben-Ari Y, Esclapez M, Bernard C. 2000. Distribution of spontaneous currents along the somato-dendritic axis of rat hippocampal CA1 pyramidal neurons. *Neuroscience*. doi:10.1016/S0306-4522(00)00231-1

D'Amour JA, Ekins TG, Ghanatra S, Yuan X, McBain CJ, Ganatra S, Yuan X, McBain CJ. 2020. Aberrant sorting of hippocampal complex pyramidal cells in Type I Lissencephaly alters topological innervation. *Elife* **9**:1–26. doi:10.1101/2020.02.05.935775

Danielson NB, Zaremba JD, Kaifosh P, Bowler J, Ladow M, Losonczy A. 2016. Sublayer-Specific Coding Dynamics during Spatial Navigation and Learning in Hippocampal Area CA1. *Neuron* **91**:652–665. doi:10.1016/j.neuron.2016.06.020

Deguchi Y, Donato F, Galimberti I, Cabuy E, Caroni P. 2011. Temporally matched subpopulations of selectively interconnected principal neurons in the hippocampus. *Nat Neurosci* **14**:495–504. doi:10.1038/nn.2768

Donato F, Jacobsen RI, Moser M-B, Moser EI. 2017. Stellate cells drive maturation of the entorhinal-hippocampal circuit. *Science (80-)* **355**:eaai8178. doi:10.1126/science.aai8178

Dougherty KA. 2019. Differential developmental refinement of the intrinsic electrophysiological properties of CA1 pyramidal neurons from the rat dorsal and ventral hippocampus. *Hippocampus* hipo.23152. doi:10.1002/hipo.23152

Dougherty KA, Islam T, Johnston D. 2012. Intrinsic excitability of CA1 pyramidal neurones from the rat dorsal and ventral hippocampus. *J Physiol* **590**:5707–5722. doi:10.1113/jphysiol.2012.242693

Epsztein J, Brecht M, Lee AK. 2011. Intracellular Determinants of Hippocampal CA1 Place and Silent Cell Activity in a Novel Environment. *Neuron* **70**:109–120. doi:10.1016/j.neuron.2011.03.006

Fattahi M, Sharif F, Geiller T, Royer S. 2018. Differential representation of landmark and self-motion information along the CA1 radial axis: Self-motion generated place fields shift toward landmarks during septal inactivation. *J Neurosci* **38**:6766–6778. doi:10.1523/JNEUROSCI.3211-17.2018

Franco SJ, Gil-Sanz C, Martinez-Garay I, Espinosa A, Harkins-Perry SR, Ramos C, Müller U. 2012. Fate-restricted neural progenitors in the mammalian cerebral cortex. *Science (80-)*. doi:10.1126/science.1223616

Geiller T, Fattahi M, Choi J-S, Royer S. 2017. Place cells are more strongly tied to landmarks in deep than in superficial CA1. *Nat Commun* **8**:14531. doi:10.1038/ncomms14531

Gergues MM, Han KJ, Choi HS, Brown B, Clausing KJ, Turner VS, Vainchtein ID, Molofsky A V, Kheirbek MA. 2020. Circuit and molecular architecture of a ventral hippocampal network. *Nat Neurosci*. doi:10.1038/s41593-020-0705-8

Graves AR, Moore SJ, Bloss EB, Mensh BD, Kath WL, Spruston N. 2012. Hippocampal pyramidal neurons comprise two distinct cell types that are countermodulated by metabotropic receptors. *Neuron* **76**:776–89. doi:10.1016/j.neuron.2012.09.036

Gulyás AI, Tóth K, McBain CJ, Freund TF. 1998. Stratum radiatum giant cells: A type of principal cell in the rat hippocampus. *Eur J Neurosci* **10**:3813–3822. doi:10.1046/j.1460-9568.1998.00402.x

Gupta A, Elgammal FS, Proddutur A, Shah S, Santhakumar V. 2012. Decrease in tonic inhibition contributes to increase in dentate semilunar granule cell excitability after brain injury. *J Neurosci*. doi:10.1523/JNEUROSCI.4141-11.2012

Hartzell AL, Burke SN, Hoang LT, Lister JP, Rodriguez CN, Barnes CA. 2013. Transcription of the immediate-early gene Arc in CA1 of the hippocampus Reveals activity differences along the proximodistal axis that are Attenuated by advanced age. *J Neurosci* **33**:3424–3433. doi:10.1523/JNEUROSCI.4727-12.2013

Henriksen EJ, Colgin LL, Barnes CA, Witter MP, Moser M-B, Moser EI. 2010. Spatial Representation along the Proximodistal Axis of CA1. *Neuron* **68**:127–137. doi:10.1016/J.NEURON.2010.08.042

Jabaudon D. 2017. Fate and freedom in developing neocortical circuits. *Nat Commun*. doi:10.1038/ncomms16042

Jarsky T, Mady R, Kennedy B, Spruston N. 2008. Distribution of bursting neurons in the CA1 region and the subiculum of the rat hippocampus. *J Comp Neurol* **506**:535–47. doi:10.1002/cne.21564

Jimenez JC, Su K, Goldberg AR, Luna VM, Biane JS, Ordek G, Zhou P, Ong SK, Wright MA, Zweifel L, Paninski L, Hen R, Kheirbek MA. 2018. Anxiety Cells in a Hippocampal-

Hypothalamic Circuit. *Neuron* **97**:670-683.e6. doi:10.1016/j.neuron.2018.01.016

Jin J, Maren S. 2015. Fear renewal preferentially activates ventral hippocampal neurons projecting to both amygdala and prefrontal cortex in rats. *Sci Rep* **5**:8388. doi:10.1038/srep08388

Kaczorowski CC, Disterhoft J, Spruston N. 2007. Stability and plasticity of intrinsic membrane properties in hippocampal CA1 pyramidal neurons: effects of internal anions. *J Physiol* **578**:799–818. doi:10.1113/jphysiol.2006.124586

Kim W Bin, Cho J-H. 2017. Synaptic Targeting of Double-Projecting Ventral CA1 Hippocampal Neurons to the Medial Prefrontal Cortex and Basal Amygdala. *J Neurosci* **37**:4868–4882. doi:10.1523/JNEUROSCI.3579-16.2017

Kitanishi T, Ikegaya Y, Matsuki N, Yamada MK. 2009. Experience-dependent, rapid structural changes in hippocampal pyramidal cell spines. *Cereb Cortex*. doi:10.1093/cercor/bhp012

Kohara K, Pignatelli M, Rivest AJ, Jung H-Y, Kitamura T, Suh J, Frank D, Kajikawa K, Mise N, Obata Y, Wickersham IR, Tonegawa S. 2014. Cell type-specific genetic and optogenetic tools reveal hippocampal CA2 circuits. *Nat Neurosci* **17**:269–79. doi:10.1038/nn.3614

Lee S-H, Marchionni I, Bezaire M, Varga C, Danielson N, Lovett-Barron M, Losonczy A, Soltesz I. 2014. Parvalbumin-positive basket cells differentiate among hippocampal pyramidal cells. *Neuron* **82**:1129–44. doi:10.1016/j.neuron.2014.03.034

Li Y, Xu J, Liu Y, Zhu J, Liu N, Zeng W, Huang N, Rasch MJ, Jiang H, Gu X, Li X, Luo M, Li C, Teng J, Chen J, Zeng S, Lin L, Zhang X. 2017. A distinct entorhinal cortex to hippocampal CA1 direct circuit for olfactory associative learning. *Nat Neurosci* **20**:559–570. doi:10.1038/nn.4517

Lodato S, Shetty AS, Arlotta P. 2015. Cerebral cortex assembly: Generating and reprogramming projection neuron diversity. *Trends Neurosci*. doi:10.1016/j.tins.2014.11.003

Madisen L, Zwingman TA, Sunkin SM, Oh SW, Zariwala HA, Gu H, Ng LL, Palmiter RD, Hawrylycz MJ, Jones AR, Lein ES, Zeng H. 2010. A robust and high-throughput Cre reporting and characterization system for the whole mouse brain. *Nat Neurosci*. doi:10.1038/nn.2467

Marissal T, Bonifazi P, Picardo MA, Nardou R, Petit LF, Baude A, Fishell GJ, Ben-Ari Y, Cossart R. 2012. Pioneer glutamatergic cells develop into a morpho-functionally distinct population in the juvenile CA3 hippocampus. *Nat Commun* **3**:1316. doi:10.1038/ncomms2318

Maroso M, Szabo GG, Kim HK, Alexander A, Bui AD, Lee S-H, Lutz B, Soltesz I. 2016. Cannabinoid Control of Learning and Memory through HCN Channels. *Neuron* **89**:1059–1073. doi:10.1016/j.neuron.2016.01.023

Masurkar A V, Srinivas K V, Brann DH, Warren R, Lowes DC, Siegelbaum SA. 2017. Medial and Lateral Entorhinal Cortex Differentially Excite Deep versus Superficial CA1 Pyramidal Neurons. *CellReports* **18**:148–160. doi:10.1016/j.celrep.2016.12.012

Masurkar A V, Tian C, Warren R, Reyes I, Lowes DC, Brann DH, Siegelbaum SA. 2020. Postsynaptic integrative properties of dorsal CA1 pyramidal neuron subpopulations. *J Neurophysiol*. doi:10.1152/jn.00397.2019

Mathews EA, Morgenstern NA, Piatti VC, Zhao C, Jessberger S, Schinder AF, Gage FH. 2010. A distinctive layering pattern of mouse dentate granule cells is generated by developmental and adult neurogenesis. *J Comp Neurol*. doi:10.1002/cne.22489

Mizuseki K, Diba K, Pastalkova E, Buzsáki G. 2011. Hippocampal CA1 pyramidal cells form functionally distinct sublayers. *Nat Neurosci* **14**:1174-. doi:10.1038/nn.2894.Hippocampal

Nasrallah K, Therreau L, Robert V, Huang AJY, McHugh TJ, Piskorowski RA, Chevaleyre V. 2019. Routing Hippocampal Information Flow through Parvalbumin Interneuron Plasticity in Area CA2. *Cell Rep* **27**:86-98.e3. doi:10.1016/j.celrep.2019.03.014

Okuyama T, Kitamura T, Roy DS, Itohara S, Tonegawa S. 2016. Ventral CA1 neurons store social memory. *Science* **353**:1536–1541. doi:10.1126/science.aaf7003

Oliva A, Fernández-Ruiz A, Buzsáki G, Berényi A. 2016. Spatial coding and physiological properties of hippocampal neurons in the Cornu Ammonis subregions. *Hippocampus* **26**:1593–1607. doi:10.1002/hipo.22659

Parfitt GM, Nguyen R, Bang JY, Aqrabawi AJ, Tran MM, Seo DK, Richards BA, Kim JC. 2017. Bidirectional Control of Anxiety-Related Behaviors in Mice: Role of Inputs Arising from the Ventral Hippocampus to the Lateral Septum and Medial Prefrontal Cortex. *Neuropsychopharmacology*. doi:10.1038/npp.2017.56

Pouille F, Scanziani M. 2004. Routing of spike series by dynamic circuits in the hippocampus. *Nature*. doi:10.1038/nature02615

Save L, Baude A, Cossart R. 2019. Temporal Embryonic Origin Critically Determines Cellular Physiology in the Dentate Gyrus. *Cereb Cortex* **29**:2639–2652. doi:10.1093/cercor/bhy132

Sharif F, Tayebi B, Buzsáki G, Royer S, Fernandez-Ruiz A. 2020. Subcircuits of Deep and Superficial CA1 Place Cells Support Efficient Spatial Coding across Heterogeneous Environments. *Neuron* 1–14. doi:10.1016/j.neuron.2020.10.034

Soltesz I, Losonczy A. 2018. CA1 pyramidal cell diversity enabling parallel information processing in the hippocampus. *Nat Neurosci* **21**:484–493. doi:10.1038/s41593-018-0118-0

Thomson AM, Bannister AP, Hughes DI, Pawelzik H. 2000. Differential sensitivity to Zolpidem of IPSPs activated by morphologically identified CA1 interneurons in slices of rat hippocampus. *Eur J Neurosci*. doi:10.1046/j.1460-9568.2000.00915.x

Valero M, Averkin RG, Fernandez-Lamo I, Aguilar J, Lopez-Pigozzi D, Brotons-Mas JR, Cid E, Tamas G, Menendez de la Prida L. 2017. Mechanisms for Selective Single-Cell Reactivation during Offline Sharp-Wave Ripples and Their Distortion by Fast Ripples. *Neuron* **94**:1234-1247.e7. doi:10.1016/j.neuron.2017.05.032

Valero M, Cid E, Averkin RG, Aguilar J, Sanchez-Aguilera A, Viney TJ, Gomez-Dominguez D, Bellistri E, de la Prida LM. 2015. Determinants of different deep and superficial CA1 pyramidal cell dynamics during sharp-wave ripples. *Nat Neurosci* **18**:1281–90. doi:10.1038/nn.4074

Valero M, de la Prida LM. 2018. The hippocampus in depth: a sublayer-specific perspective of entorhinal–hippocampal function. *Curr Opin Neurobiol* **52**:107–114. doi:10.1016/j.conb.2018.04.013

van Groen T, Wyss JM. 1990. Extrinsic projections from area CA1 of the rat hippocampus: olfactory, cortical, subcortical, and bilateral hippocampal formation projections. *J Comp Neurol* **302**:515–28. doi:10.1002/cne.903020308

West AE, Griffith EC, Greenberg ME. 2002. Regulation of transcription factors by neuronal activity. *Nat Rev Neurosci*. doi:10.1038/nrn987

Xu C, Krabbe S, Gründemann J, Botta P, Fadok JP, Osakada F, Saur D, Grewe BF, Schnitzer MJ, Callaway EM, Lüthi A. 2016. Distinct Hippocampal Pathways Mediate Dissociable Roles of Context in Memory Retrieval. *Cell* **167**:961-972.e16. doi:10.1016/j.cell.2016.09.051

Xu H-T, Han Z, Gao P, He S, Li Z, Shi W, Kodish O, Shao W, Brown KN, Huang K, Shi S-H. 2014. Distinct lineage-dependent structural and functional organization of the hippocampus. *Cell* **157**:1552–64. doi:10.1016/j.cell.2014.03.067

Acknowledgments

This work was supported by the European Research Council under the European Union's Horizon 2020 research and innovation programs (grant agreement no. 646925) as well as by the Agence Nationale pour la Recherche (ANR, Programme Blanc bilatéraux, ANR-13-ISV40002-01 "EbGluNet") and by the Fondation Bettencourt Schueller (Prix des Sciences de la Vie). A.B. and R.C. are supported by the Centre National de la Recherche Scientifique (CNRS). We thank Pr. David Anderson for providing the Ngn2CreERTM mouse. We thank L. Cagnacci for technical support and S. Pellegrino-Corby, M. Kurz and F. Michel from the INMED animal and imaging facilities (InMagic). We are grateful to Dr. S. Reichinnek and Dr. M. Bocchio for valuable scientific input, to Dr. S. Sarno for her help on statistical analysis.

Figure 1

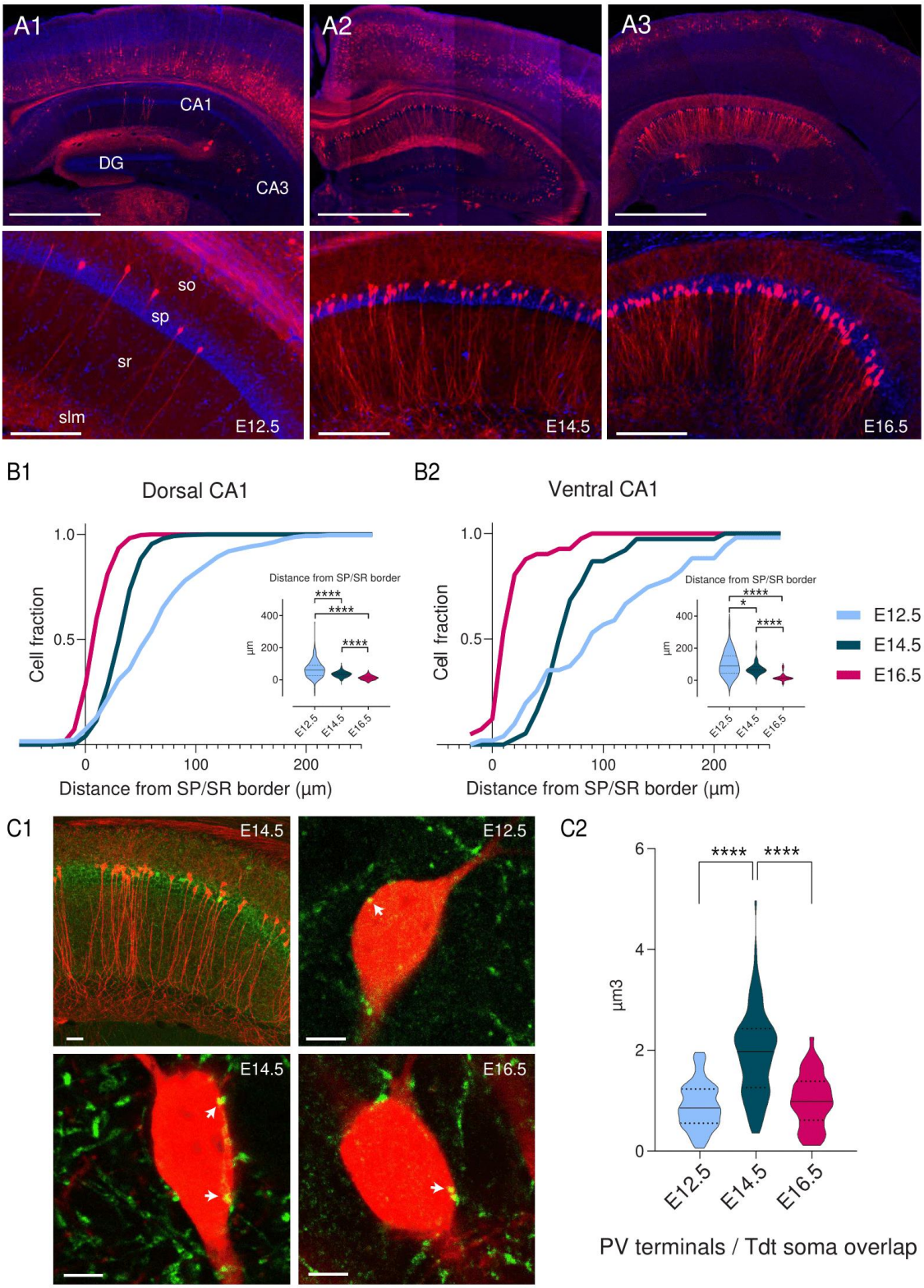
A1
A2
A3
CA1
DG
CA3
so
sp
sr
slm
E12.5
E14.5
E16.5
B1
Dorsal CA1
B2
Ventral CA1
Cell fraction
Distance from SP/SR border (µm)
Distance from SP/SR border
E12.5
E14.5
E16.5
C1
C2
µm3
PV terminals / Tdt soma overlap

Figure 1. Soma location distribution and PV innervation of CA1PNs changes according to birthdate

(A1-3) Top, representative sections of the dorsal hippocampus and cortex, illustrating Tdtomato (Tdt) labelling in CA1 pyramidal neurons (PNs) in Ngn2-CreER-Ai14 mice after tamoxifen induction at embryonic day 12.5 (E12.5), E14.5 and E16.5, from left to right. Bottom, higher magnification on CA1. E12.5 PNs are rare and dispersed, while E14.5 and E16.5 are predominantly found in the deep (upper) and superficial (lower) portion of the pyramidal layer, respectively. Note that in the above cortical areas, E12.5 PNs are restricted to the deepest layers, E14.5 PNs the middle ones (IV-III) and E16.5 PNs are most superficial (layers I-II). Scalebars: top, 1000 µm; bottom, 200 µm. Cx: Cortex; DG: dentate gyrus; so: stratum oriens; sp: stratum pyramidale; sr: stratum radiatum; slm: stratum lacunosum-moleculare. **(B1-2)** Quantification of the soma location distribution of birth-dated CA1 PNs. **(B1)** Cumulative fraction of E12.5, E14.5 and E16.5 PNs in dorsal CA1, calculated as distance in µm from the superficial (lower) border of the *stratum pyramidale*. Insert, E12.5PNs are located further away from the border than E14.5PNs ($P<0.0001$, $CI_{95\%}$ [18.18; 33]) and E16.5 PNs ($P<0.0001$, $CI_{95\%}$ [41; 55.73]). In turn, E14.5PNs also occupy deeper positions than E16.5 PNs ($P<0.0001$, $CI_{95\%}$ [21; 25]). **(B2)** Cumulative fraction of E12.5, E14.5 and E16.5 PNs in ventral CA1. Insert, similarly to dorsal CA1, E12.5PNs are located deeper than E14.5 PNs ($P: 0.0175$, $CI_{95\%}$ [3.13; 57.72]) and E16.5 PNs ($P<0.0001$, $CI_{95\%}$ [53.93; 109.57]), and E14.5 PNs than E16.5PNs ($P<0.0001$, $CI_{95\%}$ [44.47; 59.32]). **(C1-2)** Parvalbumin (PV) innervation onto birth-dated CA1 PNs. **(C1)** Top left, representative view of the CA1 area in a Ngn2-CreER-Ai14 mouse tamoxifen-induced at E14.5, with Tdt+ cells (red) and PV cells (green). Top right, close-up on the soma of E12.5 PNs (red) displaying putative somatic PV boutons (indicated by a white arrow). Bottom left, close-up on E14.5 PNs. Bottom right, close-up on E16.5 PNs. **(C2)** Quantification of the volume overlap (µm) of putative PV terminals with Tdt+ soma depending on the birthdate. E14.5 PNs present more putative boutons than E12.4 ($P<0.0001$, $CI_{95\%}$ [-1.264; -0.81]) and E16.5 ($P<0.0001$, $CI_{95\%}$ [0.66; 1.22]), while the latter two are not significantly different ($P: 0.7038$, $CI_{95\%}$ [-0.389; 0.19]). Scalebars: top left: 50 µm; top right, bottom left and bottom right: 5 µm.

Figure 2

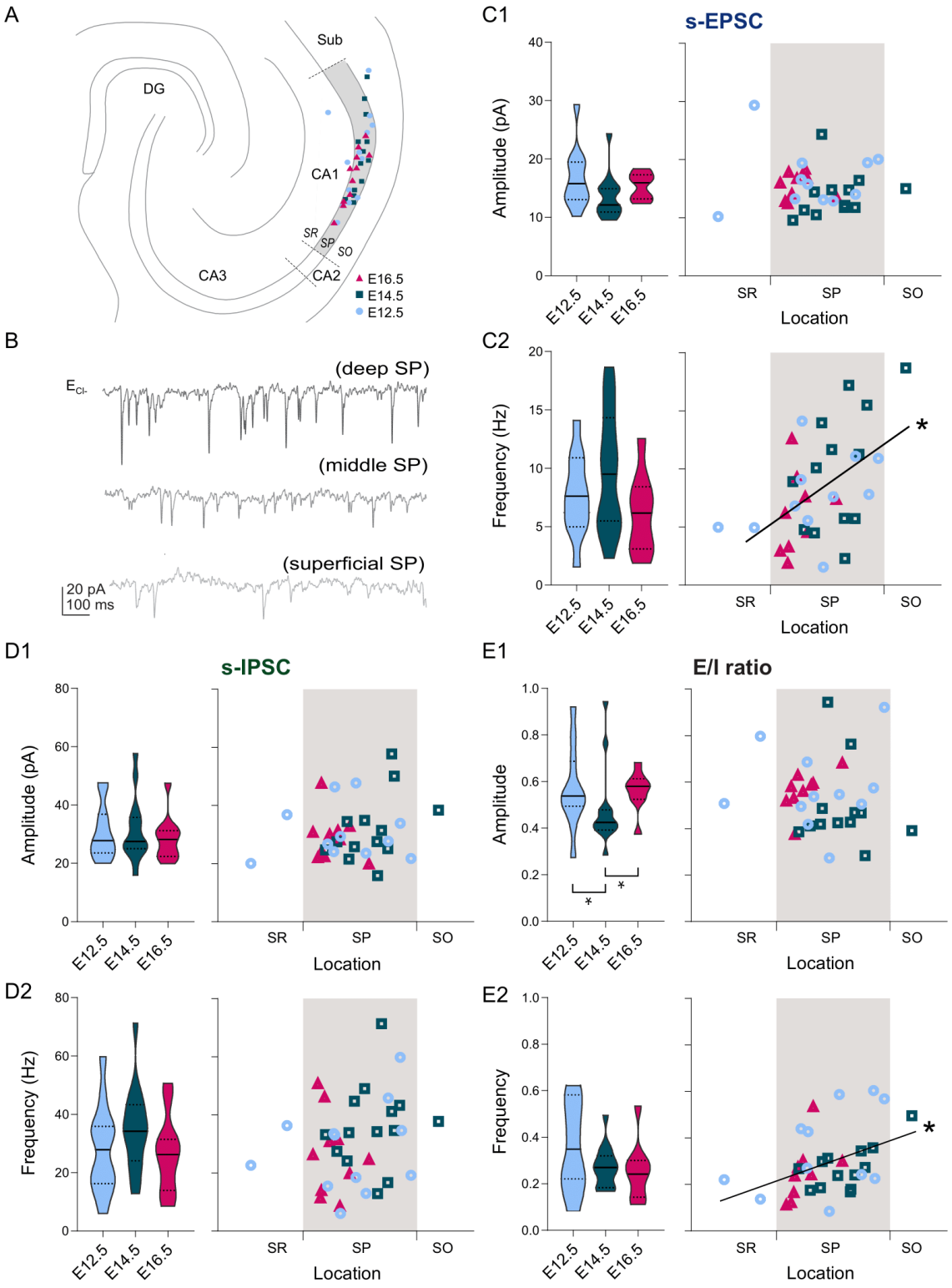
A
Sub
DG
CA1
SR
SP
SO
CA3
CA2
E16.5
E14.5
E12.5
B
(deep SP)
(middle SP)
(superficial SP)
20 pA
100 ms
C1
s-EPSC
Amplitude (pA)
E12.5
E14.5
E16.5
SR
SP
SO
Location
C2
Frequency (Hz)
*
D1
s-IPSC
Amplitude (pA)
D2
Frequency (Hz)
E1
E/I ratio
Amplitude
E2
Frequency

Figure 2. Overall synaptic drive is defined by the time of neurogenesis.
(A) Anatomical location of neurobiotin-filled CA1PNs recorded from acute horizontal slices in voltage-clamp experiments. DG: dentate gyrus, Sub: subiculum, SR: *stratum radiatum*, SP: *stratum pyramidale*, SO: *stratum oriens*. **(B)** Representative traces of spontaneous excitatory synaptic currents (s-EPSCs) recorded cells at chloride ion reversal potential (E_{Cl-}) from three CA1PNs, located respectively in the deep, middle, and superficial portion of the pyramidal layer (SP). Note that the occurrence of synaptic events decreases from top (deep) to bottom (superficial). **(C1)** s-EPSC amplitude recorded in E12.5, E14.5 and E16.5 CA1PNs. On the left panel, violin plot of E12.5, E14.5 and E16.5 PNs s-EPSC amplitude. On the right panel, color-coded scatterplot of the same data plotted against the radial position of each cell. No linear correlation between s-EPSC amplitude and location was found. **(C2)** s-EPSC frequency recorded in E12.5, E14.5 and E16.5 CA1PNs. On the left panel, violin plot of the three birthdate groups. On the right panel, scatterplot of the same data against the radial position. S-EPSC frequency increases linearly with the cell location, the two being positively correlated (P: 0.017; $CI_{95\%}$ [0.186; 0.710]). The deeper, the more frequent spontaneous excitatory events a cell receives. **(D1)** s-IPSC amplitude recorded in E12.5, E14.5 and E16.5 CA1PNs. On the left panel, violin plot of the three birthdate groups. On the right panel, scatterplot of the same data against the radial position. No linear correlation between s-IPSC amplitude and location was found. **(D2)** s-IPSC frequency recorded in E12.5, E14.5 and E16.5 CA1PNs. On the left panel, violin plot of the three birthdate groups. On the right panel, scatterplot of the same data against the radial position. No linear correlation between s-IPSC frequency and location was found. **(E1)** Ratio between EPSC and IPSC (E/I) amplitude recorded in E12.5, E14.5 and E16.5 CA1PNs. On the left panel, violin plot of the three birthdate groups. E14.5 PNs display a lower ratio than E12.5 PNs (P_{adjust}: 0.010; $CI_{95\%}$ [0.031; 0.210]) and E16.5 PNs (P_{adjust}: 0.006; $CI_{95\%}$ [-0.193; -0.057]), suggesting that their overall synaptic drive leans more towards inhibition than the other two groups. On the right panel, scatterplot of the same data against the radial position. No linear correlation between E/I amplitude ratio and location was found. **(E2)** E/I frequency ratio recorded in E12.5, E14.5 and E16.5 CA1PNs. On the left panel, violin plot of the three birthdate groups. On the right panel, scatterplot of the same data against the radial position. E/I ratio linearly correlates with the cell location, similarly to s-EPSC frequency (P: 0.0043; $CI_{95\%}$ [0.126; 0.654]).
Violin present medians (center), interquartile ranges (bounds), minima and maxima. Color-code: E12.5: light blue, E14.5: dark blue, E16.5: magenta. The gray shaded area in scatterplots represents the thickness of the *stratum pyramidale*. *P < 0.05.

Figure 3

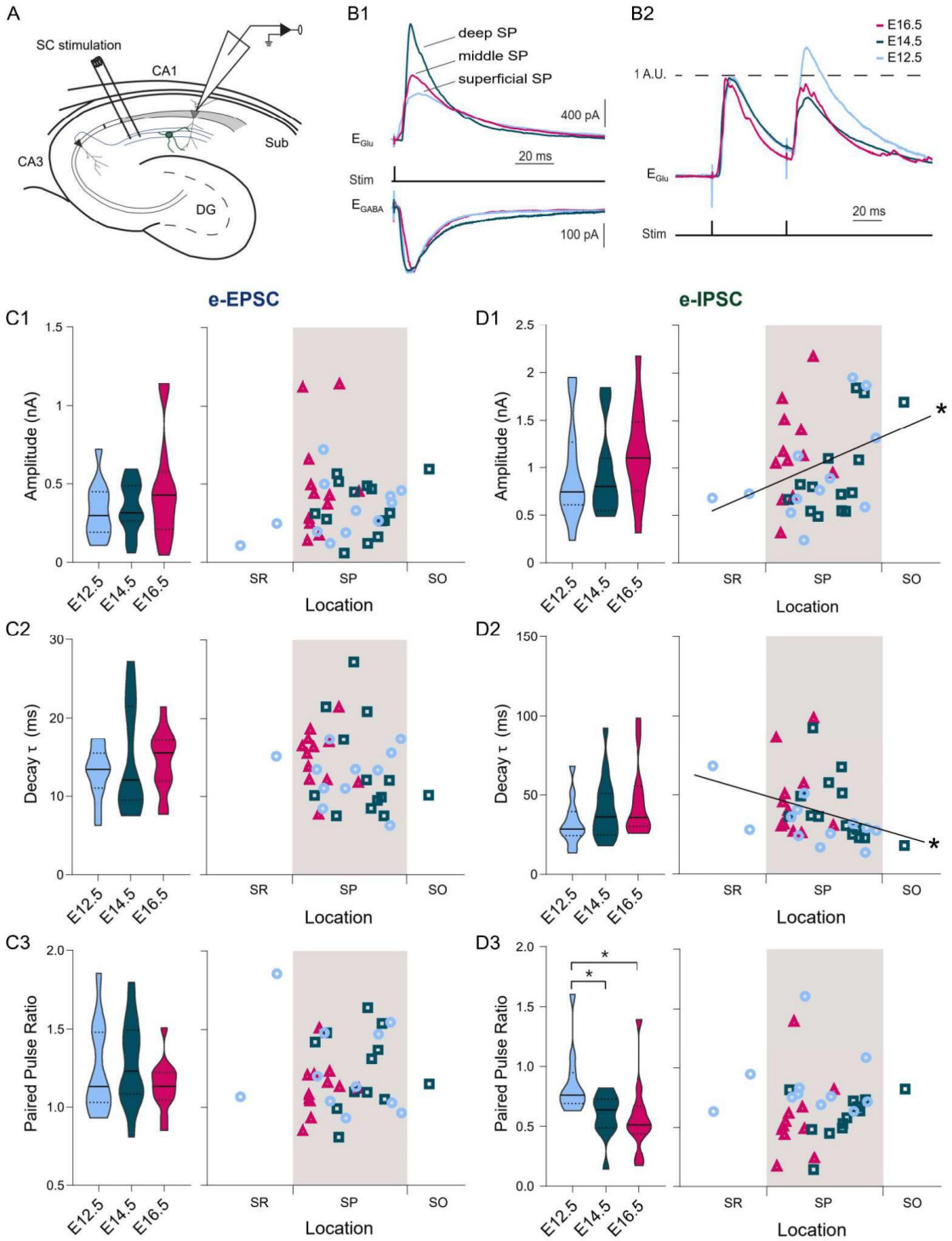
A
SC stimulation
CA1
Sub
CA3
DG
B1
deep SP
middle SP
superficial SP
400 pA
20 ms
Stim
100 pA
B2
E16.5
E14.5
E12.5
1 A.U.
20 ms
Stim
e-EPSC
e-IPSC
C1
D1
Amplitude (nA)
C2
D2
Decay τ (ms)
C3
D3
Paired Pulse Ratio
E12.5
E14.5
E16.5
SR
SP
SO
Location
*

Figure 3. Both developmental and positional factors determine Schaffer collateral-evoked inhibition.

(A) Experimental paradigm in which synaptic responses to Schaffer collaterals (SC) stimulation are recorded from CA1PNs. DG: dentate gyrus, Sub: subiculum**. (B1)** Representative mean traces of evoked inhibitory (top) and excitatory (bottom) synaptic currents (e-IPSCs and e-EPSCs) recorded upon electric stimulation in the *stratum radiatum* from CA1PNs, located respectively in the deep, middle, and superficial portion of the *pyramidal layer* (SP). Note that the amplitude and kinetics of e-IPSCs vary from deep to superficial. **(B2)** Representative mean traces of paired pulse response recorded at glutamatergic receptor reversal potential (E_{Glu}) and normalized on the first pulse amplitude. The current response to the second pulse in the E12.5PNS shown is proportionally larger than in E14.5 and E16.5 CA1PNs. **(C1-3)** e-EPSC amplitude (**C1**), decay (**C2**) and paired pulse ratio (**C3**, PPR) recorded in E12.5, E14.5 and E16.5 CA1PNs. Left, violin plot of the three birthdate groups. Right, scatterplot of the same data against the radial position. No linear correlation between s-IPSC amplitude and location was found in any of the three measures. **(D1-3)** e-IPSC amplitude (**D1**), decay time constant τ (**D2**) and PPR (**D3**) recorded in E12.5, E14.5 and E16.5 CA1PNs. Left, violin plot of the three birthdate groups. Right, scatterplot of the same data against the radial position. e-IPSC amplitude (P: 0.013; $CI_{95\%}$ [0.048; 0.576]) and decay τ (P: 0.0051; $CI_{95\%}$ [-0.599; -0.097]) display a positive and negative correlation with cell location, respectively. Overall, deeper cells are subject to larger and faster SC-associated inhibitory currents than superficial ones. PPR is higher in E12.5 CA1PNs than in E14.5 (P_{adjust}: 0.0326; $CI_{95\%}$ [0.015.; 0.342]) and E16.5 (P_{adjust}: 0.0177; $CI_{95\%}$ [0.083; 0.452]). Violin present medians (center), interquartile ranges (bounds), minima and maxima. Color-code: E12.5PNs: light blue, E14.5: dark blue, E16.5: magenta. The gray shaded area in scatterplots represents the thickness of the *stratum pyramidale*. *P < 0.05

Figure 4

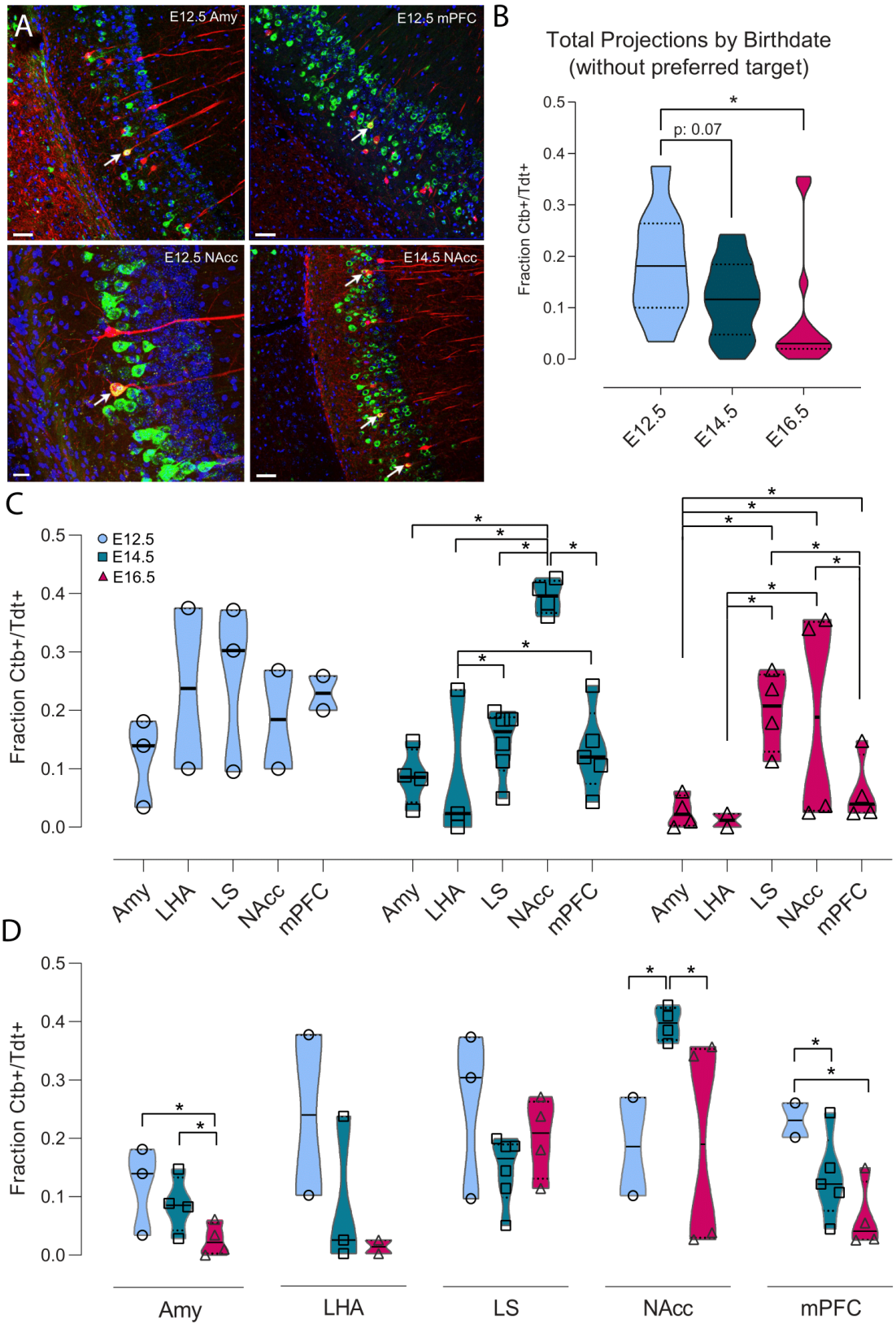
A
E12.5 Amy
E12.5 mPFC
E12.5 NAcc
E14.5 NAcc
B
Total Projections by Birthdate
(without preferred target)
Fraction Ctb+/Tdt+
p: 0.07
E12.5
E14.5
E16.5
C
E12.5
E14.5
E16.5
Fraction Ctb+/Tdt+
Amy
LHA
LS
NAcc
mPFC
D
Fraction Ctb+/Tdt+
Amy
LHA
LS
NAcc
mPFC

Figure 4. Ventral CA1 PNs with different birthdates exhibit distinct output connectivity **(A)** Examples of cholera toxin subunit b (Ctb) retrograde labelling (green) in ventral CA1 after injection in amygdala in Ngn2-CreER-Ai14 mouse induced at E12.5 (top left), medial prefrontal cortex in E12.5 mouse (top right), Nucleus Accumbens (NAcc) in E12.5 mouse (bottom left) and NAcc in E14.5 mouse (bottom right). Colabelled Ctb+/Tdt+ cells are indicated by a white arrow. Scalebars: top left, top right and bottom right, 50 µm; bottom left, 20 µm. **(B)** Quantification of the total Ctb+/Tdt+ cell fraction for the three birthdates, excluding the preferred region for each (E12.5 = lateral septum (LS), E14.5 = NAcc, E16.5 = LS). Overall, significantly more Ctb+/Tdt+ were found in E12.5 PNs than E16.5 (P_{adj}: 0.0129, $CI_{95\%}$ [0.013; 0.19]) and there is also a trend for E12.5 PNs projecting more densely than E14.5 PNs (P_{adj}: 0.07, $CI_{95\%}$ [-0.0050; 0.139]). **(C)** Fraction of Ctb+/Tdt+ cells in E12.5, E14.5 and E16.5 PNs by target region. Note how E12.5 projects more homogeneously to all structures probed, while marked inter-regional differences appear among E14.5 and E16.5 neurons. **(D)** Fraction of Ctb+/Tdt+ cells in amygdala (Amy), lateral hypothalamic area (LHA), lateral septum (LS), nucleus accumbens (NAcc) and medial prefrontal cortex (mPFC) by time of neurogenesis. E12.5 PNs project more prominently than other birthdate groups to Amy and mPFC, while NAcc is preferentially targeted by E14.5.

Figure 5

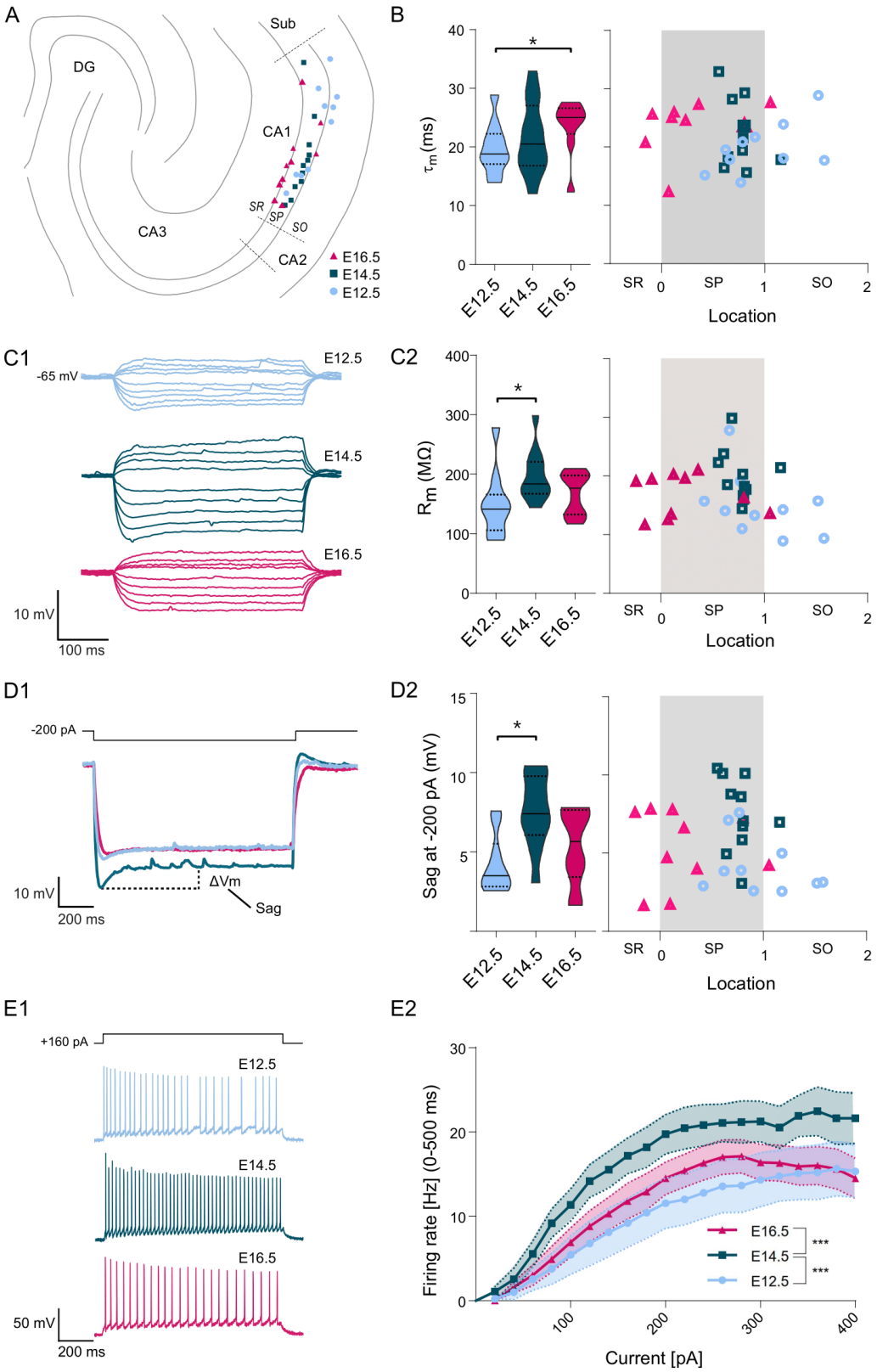
A
Sub
DG
CA1
CA3
CA2
SR
SP
SO
E16.5
E14.5
E12.5
B
τm (ms)
E12.5
E14.5
E16.5
SR
SP
SO
Location
C1
-65 mV
E12.5
E14.5
E16.5
10 mV
100 ms
C2
Rm (MΩ)
D1
-200 pA
10 mV
200 ms
ΔVm
Sag
D2
Sag at -200 pA (mV)
E1
+160 pA
50 mV
200 ms
E2
Firing rate [Hz] (0-500 ms)
Current [pA]
***

Figure 5. Intrinsic excitability varies according to embryonic birthdate.
(A) Anatomical location of neurobiotin-filled CA1PNs recorded from acute horizontal slices in current-clamp experiments. DG: dentate gyrus, Sub: subiculum, SR: stratum radiatum, SP: stratum pyramidale, SO: stratum oriens. **(B)** Membrane time constant (τ_m) of fate mapped CA1PNs. Left, violin plot of the three birthdate groups. Right, scatterplot of the same data against the radial position. E16.5 PNs exhibit a higher τ_m than E12.5 cells (P_{adjust}: 0.0264; $CI_{95\%}$ [-8.82; -1.69]). No linear correlation was found with the cell location. **(C1)** Representative membrane potential responses to a series of hyper- and depolarizing current steps recorded from fate mapped CA1PNs. Note the larger deflection of membrane potential in the E14.5 neuron. **(C2)** Membrane input resistance (R_m) of fate mapped CA1PNs. Left, violin plot of the three birthdate groups. Right, scatterplot of the same data against the radial position. R_m is higher in E14.5 than E12.5 cells (P_{adjust}: 0.0246; $CI_{95\%}$ [-89.71; -11.15]). No linear correlation was found with the cell location. **(D1)** Representative depolarizing sag potentials recorded from fate mapped CA1PNs. In this example, E14.5CA1PNs display a greater sag response than E12.5 and E16.5 PNs. **(D2)** Sag potential response of fate mapped CA1PNs, following -200 pA current injections. Left, violin plot of the three birthdate groups. Right, scatterplot of the same data against the radial position. Sag response is significantly higher in E14.5 than E12.5 cells (P_{adjust}: 0.0026; $CI_{95\%}$ [1.74; 6.05]). No linear correlation was found with the cell location. **(E1)** Examples of firing responses to a depolarizing current step recorded from fate mapped CA1PNs. Note that the number of action potential fired by E16.5 and E12.5PNs is lower than E14.5PNs. **(E2)** Input-output curves of fate mapped CA1PNs. E14.5PNs have a higher firing rate than E12.5PNs (P_{adjust}<0.0001; $CI_{95\%}$ [5.21; 11.14]) and E16 (P_{adjust}<0.0001; $CI_{95\%}$ [-9.91; -4.13]), suggesting that they are more excitable. Effect of current injection $F(2, 540) = 25.65$, $P<0.0001$; effect of birthdate $F(19, 540) = 10.71$, $P<0.0001$; interaction $F(38, 540) = 0.2355$, $P > 0.9999$, ordinary two-way ANOVA with Tukey's post hoc test. Data are represented as means ± standard errors of the means.
Violin present medians (center), interquartile ranges (bounds), minima and maxima. Color-code: E12.5: light blue, E14.5: dark blue, E16.5: magenta. The gray shaded area in scatterplots represents the thickness of the *stratum pyramidale*. *P < 0.05. ***P < 0.001.

Figure 6

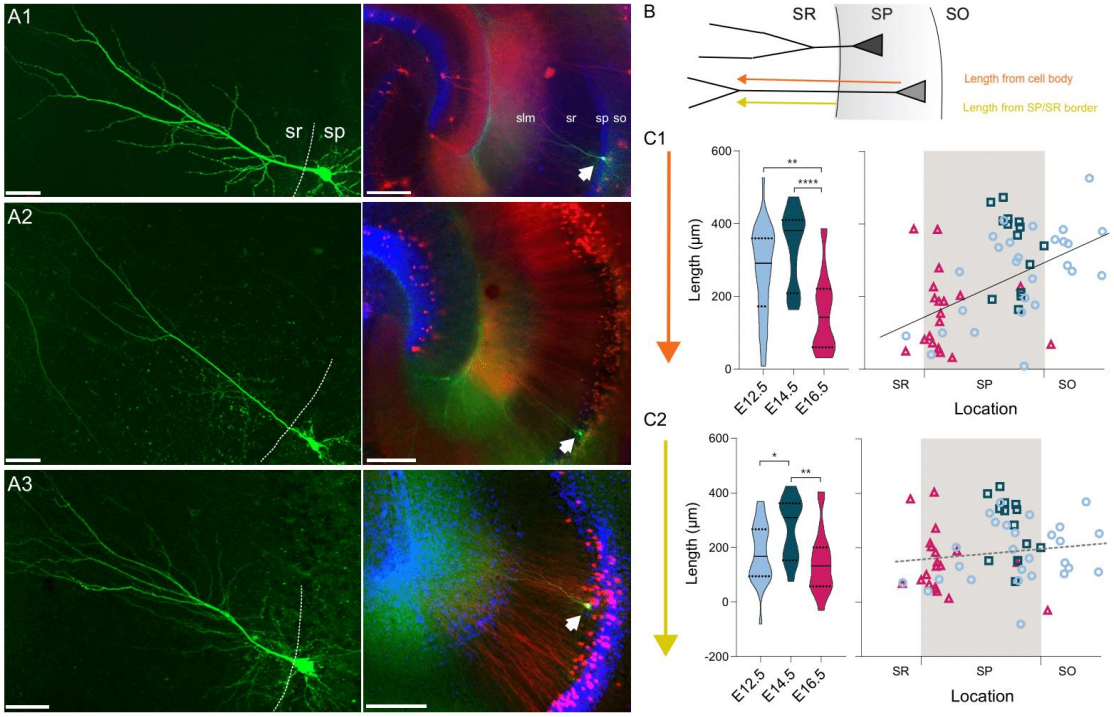

Figure 6. Embryonic origin is a determinant of dendritic morphology
(A1-3) On the left, representative examples of CA1 PNs dendritic arborization in neurobiotin-filled cells**.** The dashed line is drawn at the border between *stratum pyramidale* (SP) and *stratum radiatum* (SR). On the right, the same cell as on the left is shown at lower magnification and indicated by a white arrow. Red and blue channels represent Tdtomato and DAPI, respectively. **(A1)** E12.5 PN, **(A2)** E14.5 PN, **(A3)** E16.5 PN. Note that the main dendritic branch bifurcates more distally in E14.5 cells. Scalebars: left, 50 µm; right, 200 µm. so: stratum oriens; sp: stratum pyramidale; sr: stratum radiatum; slm: stratum lacunosum-moleculare. **(B)** Scheme illustrating the primary dendrite length measured from soma or from the border between SP and SR to the first major dendritic bifurcation. SO: *stratum oriens*. **(C1)** Primary dendrite length from soma to bifurcation in fate mapped CA1PNs. Left, violin plot of the three birthdate groups. Right, scatterplot of the same data against the radial position. E16.5PNs display a reduced dendrite length, in respect to E12.5 (P: 0.0001; $CI_{95\%}$ [37.74; 190.36]) and E14.5 PNs (P< 0.0001; $CI_{95\%}$ [92.07; 262.82]). The dendrite length from soma is markedly correlated with the soma location (P<0.0001; $CI_{95\%}$[0.318; 0.683]), likely due to the contribution of the dendritic segment within the SP. **(C2)** Primary dendrite length measured between the SP/SR border and the dendrite bifurcation in fate mapped CA1PNs. Left, violin plot of the three birthdate groups. Right, scatterplot of the same data against the radial position. The dendritic length is larger in E14.5 than E12.5 PNs (P: 0.0056; $CI_{95\%}$ [-172.99; -6.14]) and E16 cells ((P: 0.0004; $CI_{95\%}$ [36.48; 217.12]). No linear correlation was found with the cell location.
Violin present medians (center), interquartile ranges (bounds), minima and maxima. Color-code: E12.5: light blue, E14.5: dark blue, E16.5: magenta. The gray shaded area in scatterplots represents the thickness of the *stratum pyramidale*. *P < 0.05. **P < 0.01. ****P < 0.0001.

Figure 7

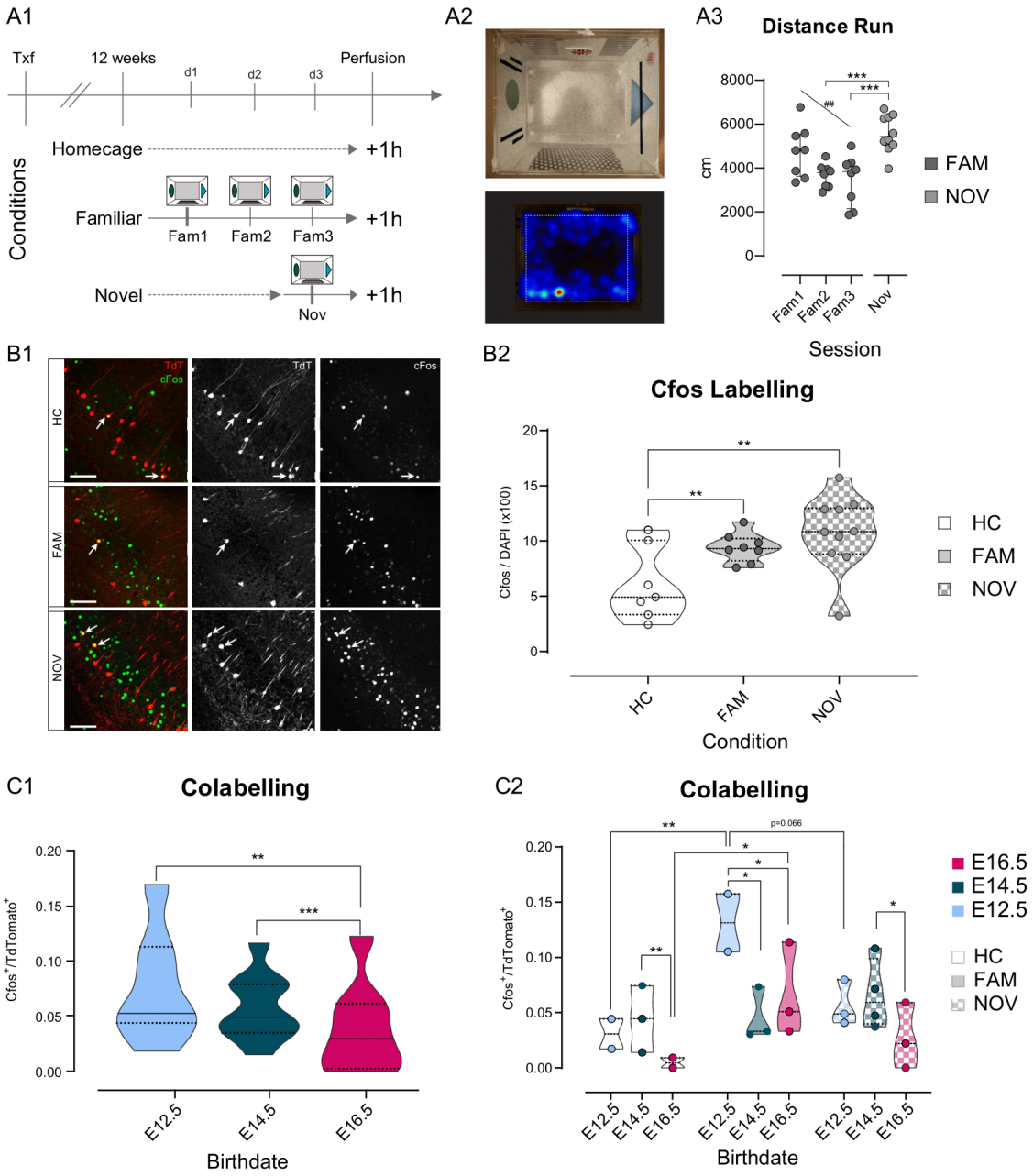

Figure 7. Fate mapped CA1PNs differ in cFos expression following exploratory behavior

(A1-3) Experimental paradigm and validation for detecting cFos expression upon exploration of an arena. **A1** Schematic representation of the behavioral conditions, with 3 cohorts of tamoxifen-induced Ngn2-CreER-Ai14 mice: homecage (HC), no exploration, familiar (FAM), repeated exploration (20') on three consecutive days, and novel (NOV), only one exploration (20'). **A2** Top, view from above of the exploration box containing visual, tactile, and olfactory (butanal) cues. In addition, a white noise was played in the experimental room. Bottom, representative occupancy heat map. **A3** Quantification of the distance run by

animals during exploration of the arena. Upon repeated exposure (Fam1-3), mice explored progressively less the arena (P: 0.0044, $CI_{95\%}$ of slope [-242.95;-1077.2]), suggesting that novelty decreases over sessions. Also, NOV did not differ significantly from Fam1 (P_{adj}: 0.26), where mice explored for the first time, and was higher than Fam3 (P_{adj}: 0.0006, $CI_{95\%}$ [973.4; 3264.8]), corresponding to the last exploration. **(B1-2)** The expression of cFos in ventral CA1 is higher upon exploration of a novel environment, than after repeated exposures. **B1** Immunohistochemistry anti-cFos, performed on three tamoxifen-induced mice (E14). Top, HC; middle, FAM; bottom, NOV condition. Each shows the merged Tdt, cFos and DAPI image (left), Tdt (center), cFos (right). Note the increase in cFos signal from HC to FAM and NOV. Insert: magnification on two cells, one strongly $cFos^+$, the other co-expressing Tdt and cFos. Scalebar: 100 µm. **B2** Fraction of $cFos^+$ cells per animal. In both FAM (P_{adjust}: 0.0006, $CI_{95\%}$ [-5.78; -1.99]) and NOV (P_{adjust}: 0.0006; $CI_{95\%}$ [-7.86; -2.54]) animals, cFos immunoreactivity is increased compared to HC. **(C1-2)** Quantification of the co-expression of cFos and Tdt in fate-mapped CA1PNs. **C1** Fraction of cFos+/Tdt+ cells by birth date group, regardless of the condition. E16 cells display fewer co-labelled cells than E12 (P_{adjust}: 0.0022, $CI_{95\%}$ [0.0097; 0.0483]) and E14 (P_{adjust}: 0.0009, $CI_{95\%}$ [0.0137; 0.0459]). **C2** Fraction of cFos+/Tdt+ cells by birth date and per condition. Note that within the FAM condition, cFos+/Tdt+ cells are more abundant in E12-FAM than E14-FAM (P_{adjust}: 0.008, $CI_{95\%}$ [0.0284; 0.135]) and E16-FAM (P_{adjust}: 0.0325, $CI_{95\%}$ [0.0236;0.136]). Within E12 birth date group as well, E12-FAM fraction of co-labelled cells is higher than E12-HC (P_{adjust}< 0.0001, $CI_{95\%}$ [-0.151; -0.049]), and roughly higher than E12-NOV (P_{adjust}< 0.066, $CI_{95\%}$ [0.0149; 0.123]). In addition, E14-NOV is greater than E16-NOV (P_{adjust}< 0.015, $CI_{95\%}$ [0.0179; 0.0797]).
Violin present medians (center), interquartile ranges (bounds), minima and maxima. Color-code: E12: light blue, E14: dark blue, E16: magenta. *P < 0.05. ##, **P < 0.01. ***P < 0.001.

Supplementary Material

Table S1. Summary of electrophysiological and morphometric properties of fate-mapped CA1PNs.
SD: standard deviation, Rm: membrane resistance, τm: membrane time constant, Cm: membrane capacitance, AP: action potential, EPSC: excitatory postsynaptic current, HW: full-width at half-maximum, IPSC: inhibitory postsynaptic current, F: frequency, E/I ratio: excitation/inhibition ratio,(s): spontaneous, (e): evoked, SP: stratum pyramidale. MΩ: megaohm, ms: millisecond, mV: millivolt, pA: picoampere, Hz: hertz.

			E12.5		E14.5		E16.5	
			Mean	**± SD**	**Mean**	**± SD**	**Mean**	**± SD**
Intrinsic membrane properties	Location	0-1	0.962	0.39	0.769	0.16	0.237	0.44
	Rm	MΩ	145.77	53.32	192.8	42.97	167.866	34.22
	τm	ms	19.335	4.37	23.596	9.4	22.81	5.15
	Cm	pF	148.05	59.38	128.747	68.16	141.234	37.66
	AP threshold	mV	-46.65	5.82	-48.185	4.16	-45.613	2.69
	AP amplitude	mV	95.889	13.45	102.378	8.4	98.382	9.91
	AP duration	ms	0.827	0.16	0.846	0.15	0.94	0.16
	AP fAHP	mV	11.103	3.35	10.88	4.01	13.541	3.73
	Sag Potential	mV	4.315	1.8	7.227	2.42	-5.413	2.31
	Rebound	mV	1.931	0.92	3.973	1.61	3.191	1.4
	Rheobase (x2)	pA	196.36	137.9	98.462	47.93	134.55	76.47
Spontaneous EPSCs	Location	0-1	0.41	0.41	0.62	0.25	0.24	0.14
	Frequency	Hz	10.05	8.48	9.75	4.97	6.17	3.23
	Amplitude	pA	22.77	20.58	15.65	8.20	15.38	2.09
	Area	pA*ms	174.57	153.26	113.87	68.71	128.41	46.35
	Rise	ms	0.87	0.27	1.07	0.43	1.16	0.50
	HW	ms	5.48	0.86	5.91	1.15	7.54	2.84
	Decay	ms	5.31	1.04	5.39	1.03	6.04	2.15
	Tau	ms	5.94	1.20	6.00	1.20	7.19	3.01
	F*Area	pA*ms*Hz	2042.49	2703.34	1264.54	1291.86	872.87	745.29
Spontaneous IPSCs	Frequency	Hz	28.16	14.60	35.12	13.89	26.62	12.73
	Amplitude	pA	41.00	35.10	34.28	14.80	28.56	7.28
	Area	pA*ms	777.14	1028.92	546.49	375.74	439.42	175.68
	Rise	ms	0.93	0.34	0.69	0.21	0.93	0.37
	HW	ms	11.00	2.25	10.23	2.77	13.97	5.05
	Decay	ms	12.40	2.47	12.86	6.25	14.17	3.95
	Tau	ms	13.04	2.25	12.59	3.26	16.26	4.71
	F*Area	pA*ms*Hz	25645.71	37915.35	21225.58	18347.79	11246.98	5878.53
(s) E/I Ratio	Frequency	Hz	0.39	0.23	0.27	0.09	0.25	0.12
	Amplitude	pA	0.57	0.17	0.48	0.17	0.56	0.08
	Area	pA*ms	0.29	0.10	0.26	0.11	0.31	0.10
	F*Area	pA*ms*Hz	0.13	0.10	0.07	0.04	0.08	0.06

Evoked EPSCs	Amplitude	pA	328.78	171.22	348.58	157.54	460.98	326.58
	Area	pA*ms	5811.21	2830.88	6891.26	5110.02	9054.38	7780.20
	Rise	ms	2.63	0.57	2.82	0.78	3.10	0.96
	Decay	ms	15.00	11.28	11.85	5.22	11.50	3.07
	HW	ms	15.92	8.36	13.74	5.09	12.70	3.37
	Tau	ms	16.73	12.89	16.08	9.60	14.46	3.81
	Paired Pulse Ratio		1.25	0.28	1.24	0.23	1.14	0.16
Evoked IPSCs	Amplitude	pA	945.89	505.83	958.36	449.36	1154.54	481.52
	Area	pA*ms	31976.27	18871.5	39160.52	17925.43	61722.07	51361.26
	Rise	ms	4.04	1.81	4.88	2.59	3.70	1.40
	Decay	ms	26.68	11.08	35.94	19.37	39.85	21.79
	HW	ms	25.18	9.05	35.50	19.95	38.53	20.97
	Tau	ms	32.69	14.37	41.38	19.35	46.27	22.84
	Paired Pulse Ratio		0.86	0.27	0.60	0.18	0.58	0.31
(e) E/I	Amplitude	pA	0.41	0.25	0.42	0.17	0.43	0.15
	Area	pA*ms	0.22	0.09	0.26	0.08	0.21	0.05
Primary dendrite	Location	0-1	0.881	0.4631	0.7487	0.1201	0.1783	0.2783
	Length to soma	µm	272	124.2	337.5	105.6	155.9	107.8
	Length to SP border	µm	180.4	107.5	271.4	111.1	142.5	113.4

Table S2. Summary of adult Ngn2-CreER-AI14 mice that used in the exploration experiment for cFos analysis.

N° animals	HC	FAM	NOV	Total
E12.5	2	2	3	7
E14.5	3	3	4	10
E16.5	2	3	3	8
Total	7	8	10	25

Table S3: Stereotaxic coordinates of CA1PNs target regions.

Target Region	AP	ML	DV
Nucleus Accumbens (shell)	+1.8/+2	-0.6/-0.45	-4.0
Basal Amygdala	-1.4	-3.3	-4.3
Medial Prefrontal Cortex	+2.0	-0.35	-1.8
Lateral Hypothalamic Area	-1.34/-1.45	-0.65/-1	-4.8/-4.9
Lateral Septum	+0.6/0.7	-0.4/-0.35	-2.6/2.55

Figure S4. Representative sections including the injection site of Cholera toxin subunit B retrograde tracer, coupled to Alexa647 (here shown in green, DAPI: blue). A: Amygdala; (B) Lateral Hypothalamic Area (LHA); C: Lateral Septum (LS), D: Nucleus Accumbens shell (NAcc); E: medial prefrontal cortex (mPFC). Scalebar: 500 µm.

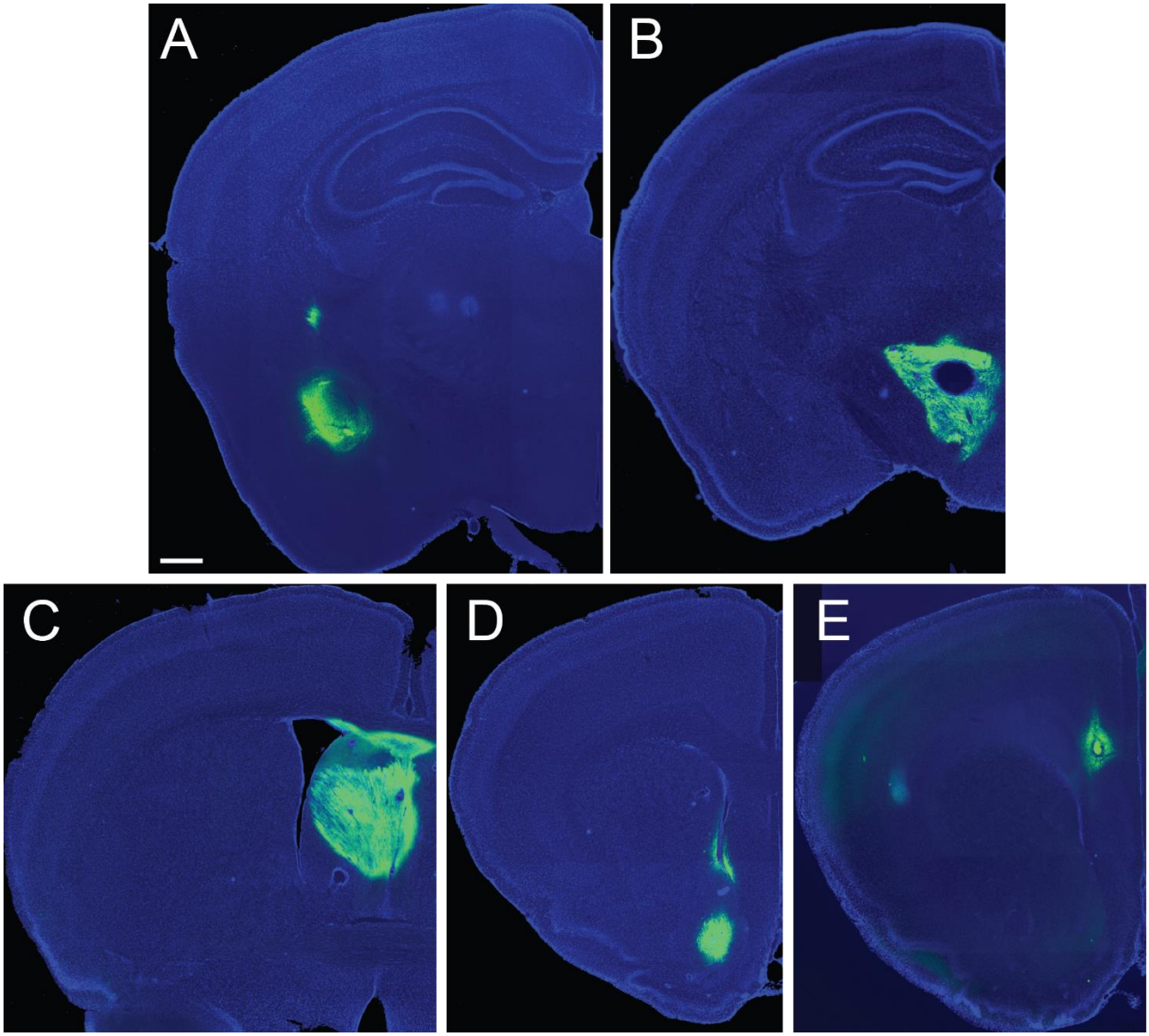

7. Annex A

A genetic strategy for anterograde tracing of fate-mapped CA1 pyramidal neurons

Context & Aim

One major interest of studying CA1 pyramidal neurons (CA1 PNs) is that they are projection cells that are widely connected to numerous cortical and subcortical brain areas. This is particularly true for the ventral pole of the hippocampus, which was the focus of the present experimental work. Recent evidence has shown that subpopulations of pyramidal cells are biased towards different target regions based on their soma location in the stratum pyramidale, and that such pathways are associated to specific behavioral processes (Lee et al., 2014; Okuyama et al., 2016; Jimenez et al., 2018; Ciocchi et al., 2015).

Hence, we hypothesized that the heterogeneity in output connectivity would be determined by the embryonic origin of CA1 PNs. Classically, two approaches are available for addressing this question from a structural standpoint: anterograde and retrograde tracing (Zeng, 2018). Since the latter has the disadvantage of having to aprioristically select certain putative targets to probe, we opted for the former. A major caveat needed to be circumvented. As discussed in section 4.1.3, induction of CreER by tamoxifen administration is temporally specific but not spatially restricted and Ngn2 is a proneural factor expressed by all cortical pyramidal cells, as well as subcortical glutamatergic cells (Ozen et al., 2007; Gouty-Colomer et al., 2018; Hand et al., 2005). This means that it is virtually impossible to discern the origin of Tdtomato-expressing axonal fibers in a given area. In summary, it is necessary to also attain spatial selectivity in our mouse model to reliably identify axon terminals originating from fate-mapped CA1 PNs in putative synaptic targets.

Working in collaboration with my colleague Marco Bocchio, we chose to test the novel Cre recombinase dependent on GFP, hereby CRE-DOG (Tang et al., 2015). It is a chimeric version of Cre enzyme split into two complementary subunits that dimerize upon binding to GFP protein. In the framework of anterograde tracing, local injection of CRE-DOG of tamoxifen-induced Ngn2-CreER-RCE-GFP mice (adult) would lead to the expression Cre-dependent viral constructs specifically in fate-mapped CA1 pyramidal cells. Then, presynaptic sites could be labelled by combining CRE-DOG to a Cre-dependent virus

expressing mRuby under control of synaptophysin promoter (Beier et al., 2015).

Our goal (see figure A1) is to confirm that:

1. CRE-DOG injection in CA1 of induces expression of a floxed viral construct in GFP+ neurons, and not in absence of GFP protein.

2. unspecific CRE-DOG activation does NOT induce GFP expression by acting on the floxed RCE-GFP reporter allele carried by the mouse line Ngn2-CreER-GFP.

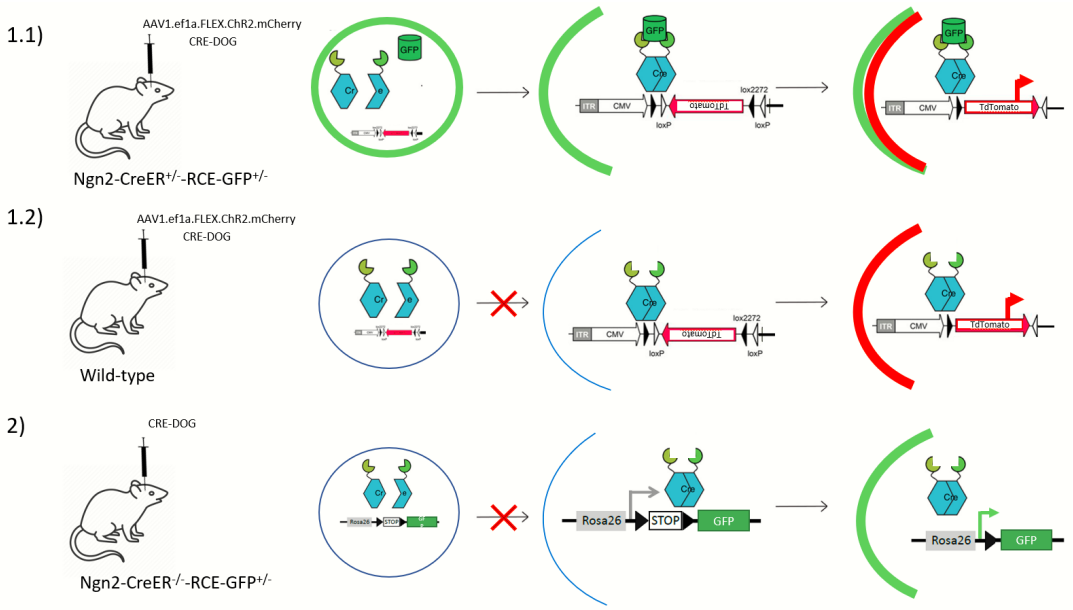

FIGURE A1: Schematic representation of the CRE-DOG experimental goals and procedures. 1.1) Confirmation that CRE-DOG can reliably induce recombination of a viral construct in GFP+ cells. 1.2) Confirmation that CRE-DOG alone cannot induce recombination. 2) Confirmation that CRE-DOG does not act on RCE-GFP allele in absence of GFP.

Methodology & Results

1. **CA1 injections of CRE-DOG in transgenic mice expressing GFP in neuronal subpopulations.** To verify whether using DRE-DOG is suitable for our anterograde tracing experiments, we performed stereotaxical injections of CRE-DOG dimers and AAV1.Syn.Flex.jRGECO1a (300 nl; dilution [1/3: 1/3:1/3]) in dorsal CA1 of a Thy-GFP mouse, expressing GFP constitutively. Then, we injected CRE-DOG and AAV1.ef1a.FLEX.ChR2.mCherry in dorsal and ventral CA1 (300nl x 2; [1/4:1/4:1/2]) of tamoxifen-induced Ngn2-CreER-GFP and Dlx1/2-CreER-GFP, expressing GFP in early born pyramidal cells (E12.5) and interneurons (E8.5) respectively. After 2-3 weeks, animals were sacrified and the expression of the Cre-dependent reporter gene was checked in hippocampal slices. In figure A2, two examples from the Ngn2-CreER-RCE-GFP mouse, injected with CRE-DOG and AAV1.ef1a.FLEX.ChR2.mCherry. Cells epressing both GFP and mCherry were found in the hippocampus, close to the

injection site. However, a number of mCherry+/GFP- neurons were also identified. We quantified the specificity as the ratio of mCherry+/GFP+ and total GFP+ number in all three mice and calculated an estimate of 76.17% $\pm$ 6.47. In other words, 1/4 cell out of four could be inappropriately labelled.

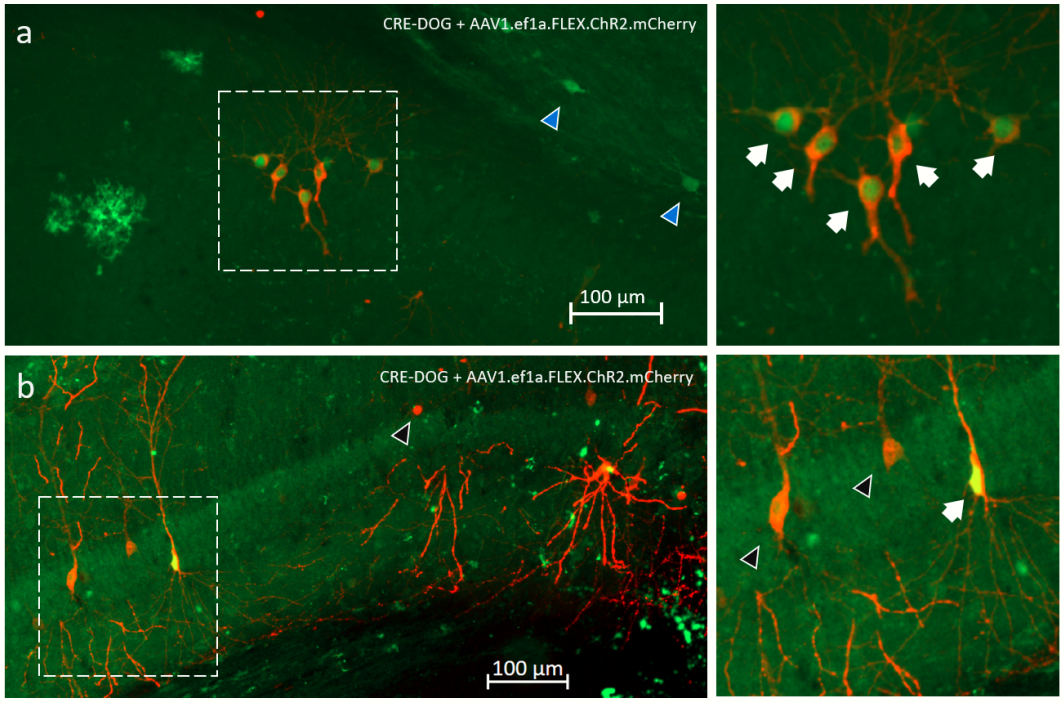

FIGURE A2: CRE-DOG injection in Ngn2-CreER-RCE-GFP mice. Hippocampal sections of a Ngn2-CreER-RCE-GFP mouse injected in the dorsal CA1 with CRE-DOG and a reporter virus (carrying Cre-dependent mCherry gene). Expression of mCherry appears in CA3 (a) and CA1 (b) in the proximity of the injection site. The white arrows indicate cells with clear GFP+ and mCherry+ double labeling; black arrows indicate cells that only exhibit mCherry labelling; blue arrows indicate GFP+ neurons, lacking mCherry expression. Scalebar: 100 µm

We were not satisfied with this value and went on further asking whether this would be due to unspecific activation of either the Cre-dependent reporter viral construst or CRE-DOG. To investigate this, we injected the CRE-DOG and the same reporter (dilution [1:4/1/4:1/2]) in either dorsal (2x 150 nl) or ventral (2x 70 nl) CA1 of two non-transgenic (WT) adult mice and let them express for 15 days. In both cases, we found mCherry+ neurons in the proximity of the injection site (figure A3). Given that FLEX consists of two pairs of heterotypic LoxP-variant recombination sites and is highly stable (Schnütgen et al., 2003), this likely suggests that CRE-DOG could "leak", namely show recombinase activity even in absence of GFP.

2. **CA1 injections of CRE-DOG in mice carrying the RCE-GFP reporter allele.** Although the experiment above is not conclusive to discard this novel viral strategy, we started asking if unspecific activity of CRE-DOG could recombine floxed alleles in our transgenic mouse line. Even in absence of GFP protein, the excision of the stop

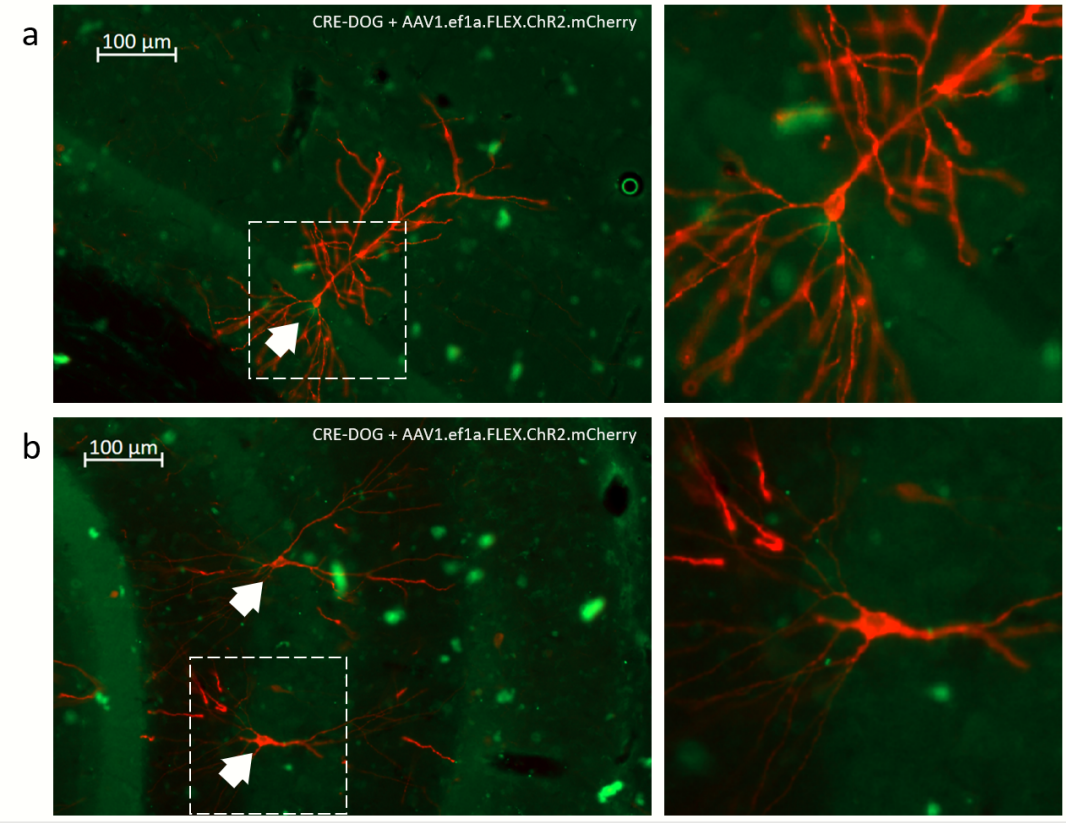

FIGURE A3: CRE-DOG injection in wild-type mice. Hippocampal sections of wild-type mouse injected in the dorsal (a) and ventral (b) CA1 with CRE-DOG and a reporter virus (carrying Cre-dependent mCherry gene). Expression of mCherry appears in few cells close to the injection site, indicated by a white arrow. Scalebar: 100 µm

codon could occur and itself induce GFP expression, which could in turn amplify CRE-DOG activity. As a consequence, this would generate a number of GFP+ cells (false positive) that cannot be distinguished from fate-mapped neurons, biasing heavily the interpretation of experimental results.

Thus, we set out injections of CRE-DOG alone in the dorsal CA1 of Ngn2-CreER-/– RCE-GFP-/+ mice, that lack Ngn2-CreER transgene but carry a floxed-GFP allele. In these animals, GFP cannot be expressed due to the absence of CreER. Two mice were injected with 100 nl of CRE-DOG dimers diluted in 100 nl PBS. Additionally, two mice received an injection at either half volume or half concentration (figure A4). In all four animals, cells expressing GFP were found in the ipsilateral hemisphere, close to the injection site. An average of 1.6 GFP+ cells/slice $\pm$ 0.66 was computed on 20 slices. This seems to indicate that CRE-DOG can act without binding GFP, likely by dimerizing in an unspecific manner. In addition, the fact that on the contralateral side no GFP labelling was found (not shown) does not point to a leakage in the transgenic mouse line.

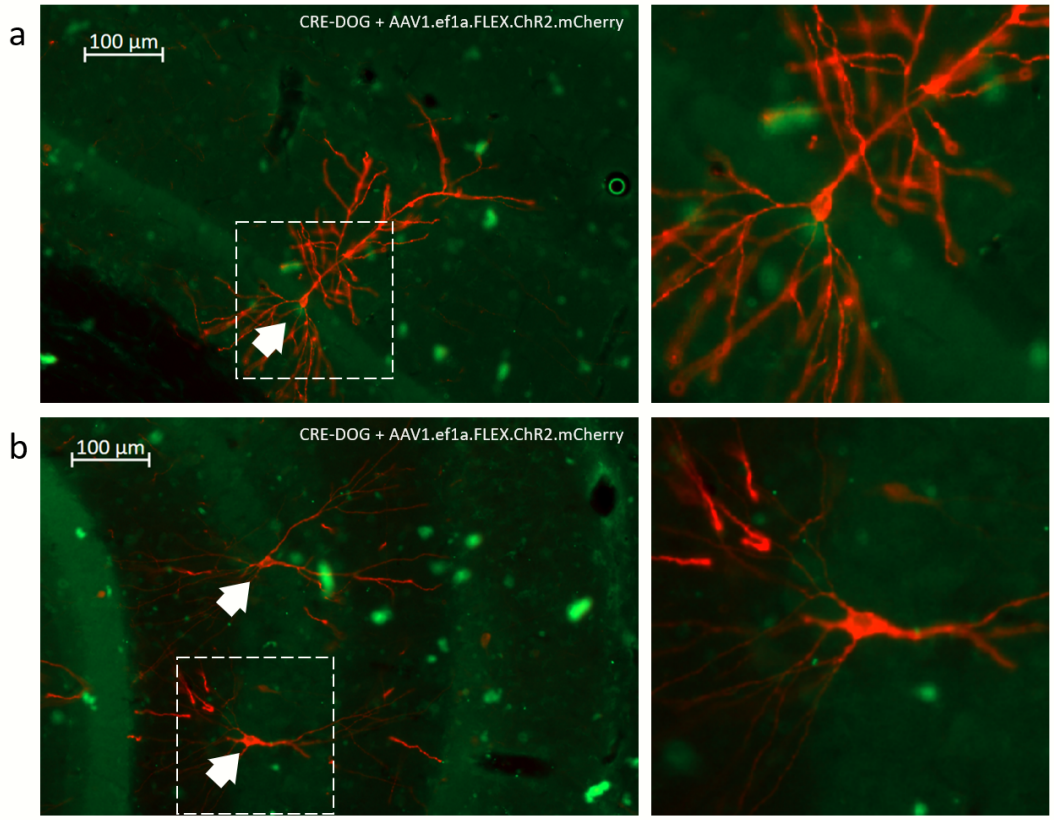

FIGURE A4: CRE-DOG injection in RCE-GFP reporter line. Hippocampal sections of Ngn2-CreER-/-RCE-GFP+/- mice injected with CRE-DOG in the dorsal hippocampus. (a-b) 100 nl in 1:1 PBS, (c) 50 nl in 1:1 PBS, (d) 100 nl in 1:2 PBS. Several GFP+ neurons were observed in all injected animals, suggesting unspecific CRE-DOG activation. Scale bars: (a,c,d) 200 µm, (b) 100 µm.

Conclusion

We tested the novel chimeric CRE-DOG, a dimerized Cre recombinase that activates upon binding of GFP protein. Ideally, this tool would have been combined to temporal genetic fate mapping to add spatial selectivity to the labelling of fate-mapped CA1 PNs and would have allowed precise anterograde tracing. Although CRE-DOG effectively induces the expression of floxed viral constructs of interest in GFP+ cells, it also exhibits unspecific activation. Since our approach already relies on Cre-dependent expression of GFP during the developmental stages, CRE-DOG can lead to major confounds (generating false positives). To our eyes, we gathered sufficient evidence to consider CRE-DOG unreliable for our experimental needs.

8. Annex B

Imaging fate-mapped pyramidal neurons in ventral CA1

Context & Aim

In the present work, we show that the temporal embryonic origin is a major determinant of CA1 PN heterogeneity. The findings supporting this notion mostly originated from the in vitro characterization of electrophysiological, synaptic, and morphometric features of groups of pyramidal cells with distinct birthdates (from E12.5 to E16.5). Although neuronal diversity is thought to underlie functional differences, our description under the developmental prism does not necessarily reflect a 'division of labor' in cognitive and emotional processes. In fact, recent experimental evidence from other groups indicates that distinct PN subpopulations in ventral CA1 are differentially recruited in vivo, and can be anatomically segregated (Okuyama et al., 2016; Ciocchi et al., 2015; Jimenez et al., 2018; Jimenez et al., 2020). To mention only one example, PNs in the deep sublayer with specific projections to the nucleus accumbens were shown to increase their activity when the mouse was interacting with a known conspecific, and were causally linked to the formation of social memory (Okuyama et al., 2016).

From our perspective, it remains to be established if the developmental origin plays a role in this functional diversification. To tackle this question, the activity of birthdated neurons has to be monitored when mice engage in specific behavioral tasks associated to the hippocampus. Two main approaches are available: (i) extracellular recording and (ii) calcium imaging. (i) In our case, we would need to express an excitatory opsin in CA1 birthdated PNs (instead of Tdtomato only) to electrophysiologically identify them upon light stimulation, a technique called *optotagging* (Lima et al., 2009). Given the overall difficulty of stably recording neurons in the ventral hippocampus and the sparsity of E12.5 cells, we discarded this option. (ii) Epifluorescence microscopy of deep brain structures can be achieved by combining miniature endoscopes with gradient refractory index (GRIN) lenses (Ziv and Ghosh, 2015). We reasoned that using a transgenic mouse line carrying the Ai96 allele (Cre-dependent RCL-GCaMP6s), we could express the calcium indicator GCaMP6s with our Ngn2-CreER driver line in developmentally-defined subpopulations of PNs. Ultimately, our goal (figure B1) is to stably record calcium activity on the same fate-mapped cells over consecutive days, while exposing mice to several behavioral tasks.

This part of my doctoral project was conceived with Dr Andrew Scheyer and Dr Olivier Manzoni, with the kind help of Dr Milene Borsoi.

I will first describe a few preliminary (but promising) trials with endoscopy on wild-type (WT) mice and then show how I failed to reproduce the same outcome in Ngn2-CreER-Ai96 mice.

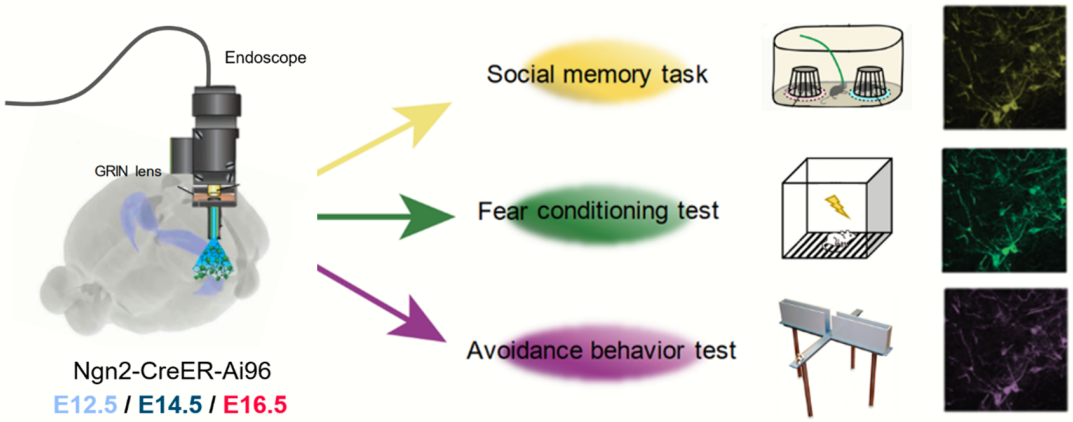

FIGURE B1: Probing fate-mapped CA1 pyramidal cells in vivo. Schematic illustration of the experimental paradigm to study the involvement of fate-mapped PNs in given behavioral tasks. In brief, tamoxifen-induced Ngn2-CreER-Ai96 mice are implanted with a GRIN lens in ventral CA1 and calcium activity is monitored when they undergo different tests (social memory, fear memory, avoidance) in a sequential manner.

Methodology & Results

To achieve GCaMP6s expression in the ventral hippocampus of adult WT mice (non-transgenic), I injected 200 nl of AAV1.Syn.GCaMP6s.WPRE.SV40 virus at coordinates AP: 3.16, ML: 3.25, DV: -3.5 / -3.7 / -3.9 prior to implanting a GRIN lens over the injection site. In Ngn2-CreER-Ai96, tamoxifen-induction was performed at embryonic day 14.5 as described above for Ngn2-CreER-Ai14 and caused E14.5 PNs to express the calcium indicator GCaMP6s. In both cases, the protocol for lens implantation and baseplate installation is identical (see Resendez et al. (2016) for a thorough description). In brief, mice were deeply anesthetized with isoflurane and shaved on the head. The surface of the skull was exposed. 3 evenly spaced skull screws were inserted in the skull around the implantation site to increase dental cement stability. If not already present following viral injection, a small craniotomy was performed at AP: 3.16, ML: 3.25 and the dura removed from the cortical surface. Before lowering the lens in the brain tissue, a 25G needle was used to make a 'pre-track' for 2/3 of the final depth (~2.5 mm). A GRIN lens (0.5 mm diameter, 6.1 mm length) was slowly inserted 4.6 mm deep, while monitoring fluorescence with a miniaturized microscope connected to nVista2 Data Acquisition Box (Inscopix, Palo Alto, CA). The implant was then fixed to the skull using dental cement. After about 10 days, a magnetic baseplate for the endoscope was fixed to the headcap with additional dental cement. At this stage, fluorescence should already be identifiable at low LED intensity values. Recordings could start 3/4 days after baseplate installation.

The data was acquired during isoflurane anesthesia and then analysed with Inscopix Data Processing software (Inscopix, Palo Alto, CA).

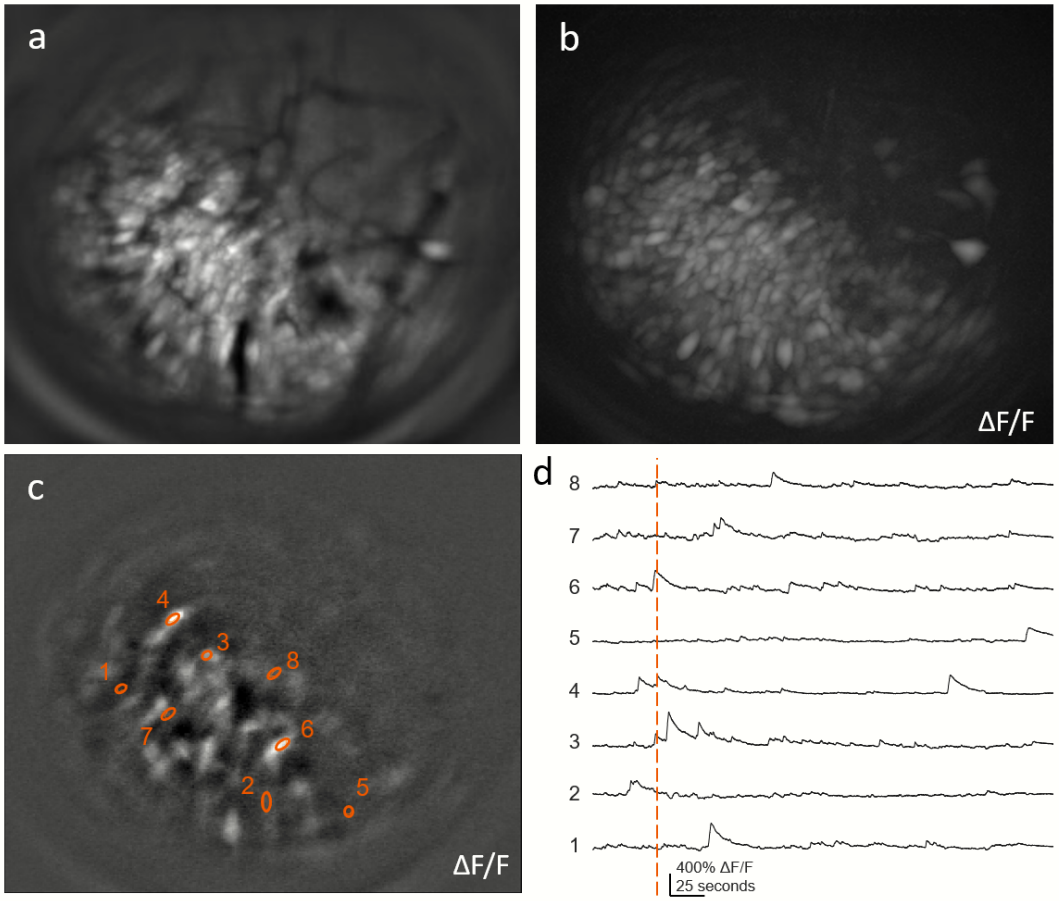

FIGURE B2: Calcium imaging in ventral CA1 with miniature microscope in WT mouse. (a) Maximum intensity projection of the filtered and motion-corrected movie (∼6 minute recording). Notice cells as bright roundish shapes, and blood vessels as darker elongated lines. (b) Maximum intensity projection of the relative fluorescence change (ΔF/F). (c) Single frame from the ΔF/F movie, with 8 ROIs of identified and validated cells. (d) Calcium traces of the 8 cells shown in panel c. The dashed orange line indicates the frame shown in panel c.

In figure B2, the field of view of GCaMP6s-expressing neurons in ventral CA1, after successful surgery in a WT mouse, is illustrated. For this experiment, LED intensity was set to 12% and frame rate to 20 Hz. After spatial/temporal downsampling, the video was filtered and motion-corrected (panel a). At this stage, cells are already recognizable as densely packed round or elongated shapes. Then, the relative change in fluorescence (ΔF/F) was computed (panel b). Finally, a total of 119 putative cells were identified as regions of interest (ROI) using a PCA-ICA algorithm and needed to be visually inspected for validation. In panel (c) is a single frame of the total recording with ROIs of 8 neurons. The change in fluorescence for these neurons is represented on panel (d), where neuronal activation (calcium transients) can be clearly seen in the traces. Similar results were obtained in 2 additional mice (not shown).

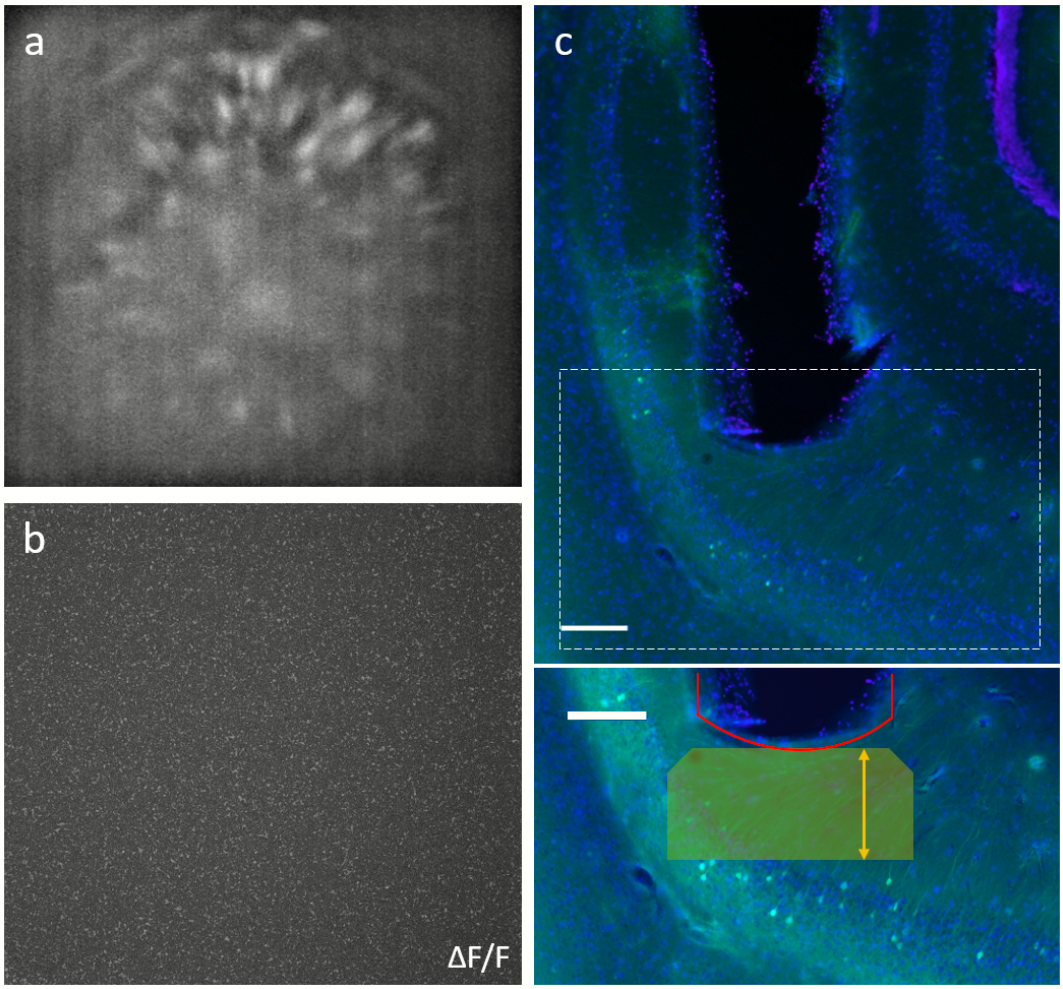

FIGURE B3: Calcium imaging in ventral CA1 with miniature microscope in Ngn2-CreER-Ai96 mouse (E14.5). (a) Maximum intensity projection of the filtered and motion-corrrected movie (∼2 minute recording). A few bright areas resemble cells seen in figure A7 but are less neat. (b) Maximum intensity projection of the relative fluorescence change (ΔF/F). No activity can be detected (c) Top, hippocampal section displaying the location of the GRIN lens in ventral CA1. Blue: DAPI, Green: GFP. Bottom, higher magnification of the image above showing the end of the implant site, indicated by the red line. The yellow arrow represents the ideal distance for the imaging plane (∼290 µm). Scale bar: 200 µm.

Oppositely, imaging from three Ngn2-CreER-Ai96 mice did not yield satisfying results. In figure B3 is an example of a field of view in ventral CA1, similarly to what described above. It is important to point out that this recording was obtained at very high LED values (>50%), while it is normally advised not to exceed 20% (Resendez et al., 2016). Panel (a) shows an image from the filtered and motion-corrected video, where few neuronal shapes can be recognized. However, when computing the ΔF/F no clear ROI could be detected and variation in fluorescence seemed to be completely absent (panel b). This was the case for all imaged mice. When we checked the lens location in coronal slices of the PFA-fixed brain, we found that lens was correctly placed and at an appropriate distance from the stratum pyramidale (panel c). Possibly, tissue cicatrisation below the

tip of the lens could affect the optical quality of the imaging. Thus, we probed this by performing an immunohistochemistry against glial fibrillary acidic protein (GFAP), a marker for glial scar formation, but could not find any substantial difference between implanted and contralateral hemisphere (not shown). Owing to the high LED power and the absence of any fluctuations in fluorescence, these preliminary results seem to indicate that genetically-encoded GCaMP6s is too weakly expressed for proper monitoring of neuronal activity.

Conclusion

We tested whether we could monitor the activity of temporally-fate mapped PNs in ventral CA1 by calcium imaging using epifluorescence endoscopy. Although some preliminary data obtained with virally-expressed GCaMP6s were promising, we could not reproduce them with the Ngn2-CreER-Ai96 mouse line, probably due to weak expression of the genetically-encoded calcium indicator.

Part III

Discussion

9. Discussion

In this thesis work, we focused on pyramidal neurons (PNs) in the ventral CA1 subregion of the murine hippocampus. The main driving hypothesis was that the temporal embryonic origin is a major determinant of neuronal diversity observed among these cells in adulthood. To address this, PNs were labelled according to their date of birth and described in their morpho-physiological profiles and connectivity. Thereby, we confirm this view by illustrating that neurons born at different points of embryogenesis display specific characteristics and that this heterogeneity goes beyond their location within the stratum pyramidale. In particular, we suggest that pioneer neurons (E12.5) are a previously overlooked subpopulation of PNs with distinct anatomical distribution, connectivity and recruitment during exploration.

These findings are compatible and complement our current understanding of pyramidal cell diversity in the hippocampus. In the following paragraphs, I will discuss the limitations of the present study and comment on how it relates to the existing body of literature on the topic. Furthermore, the elements of novelty will be discussed more thoroughly. All along this section, I will attempt to propose insights on future directions by suggesting additional experiments.

9.1 Main limitations

In my opinion, the main limitation of the study is that, although firmly advocating for an embryonic origin of CA1 PN diversity, it does not provide any causal observation and all evidence might be considered merely correlational. In the light of this, it would be advantageous to manipulate the spatio-temporal organization of CA1 circuit development by cell-type specific neuronal ablation (Spampanato and Dudek, 2017). For instance, one could address the question whether suppressing neurons born at E12.5 during the perinatal period alters the phenotype of later (E14.5) PNs. Hypothetically, E14.5 could acquire similar morpho-physiological features as the abolished pioneer neurons, such as scattered distribution, dense output projections and low PV innervation, suggesting that the sequence of integration in the circuit (extrinsically) determines PN identify. Oppositely, PNs maintaining a 'wildtype' phenotype would point at the fundamental role of (intrinsic) genetic programs expressed in neural progenitors and post-mitotic cells. The examination of the hippocampus in cortical malformations, such as the reeler mouse or Lis mutants, corroborate the latter hypothesis. Indeed, these genetic conditions cause a developmental mislamination

of CA1 pyramidal cells so that early and late generated cells locate superficially and deeply, respectively. Many of their morphophysiological properties, however, are unchanged (D'Amour et al., 2020; Deller et al., 1999; Ishida et al., 1994).

A second major technical constraint was due to our genetic mouse model. Using conditional fate mapping with the double transgenic Ngn2-CreER-Ai14 line, we provided temporal specificity to PN labelling, although precluding us from further manipulations. As for example, we could not exploit widely used Cre-dependent viral vectors in our population of interest. Indeed, the expression of light-sensitive opsins would have been extremely valuable to probe their functional role in behaving mice, especially considering the variety of cognitive processes that ventral CA1 is associated to (Ciocchi et al., 2015; Jimenez et al., 2018; Jimenez et al., 2020; Okuyama et al., 2016). As well, based on our analysis of cFos expression following exploration, we speculate that E14.5 cells are particularly recruited in a new environment and perhaps signal novelty. This should be further investigated by optogenetically silencing this subgroup during the first exploration of the arena and verifying whether mice spend an equal amount of time during the next exposure. To circumvent this, reporter lines Ai27 and Ai32, both carrying channelrhodopsin ChR2(H134R) gene, are available in our lab but have not been tested in this framework. In addition, our team has been developing a transgenic mouse line using RCE:LoxP-FLPo-TVA as a reporter (figure 9.1). In this model, tamoxifen-dependent induction of Cre (under Ngn2 promoter) causes the expression of FLPo recombinase and TVA receptor protein. Thus, it can be combined to either viral constructs containing FRT sequences, or EnvA-ΔG rabies virus. The former exploits the library of FLPo-dependent expression of opsins, DREADDs, and other genetic tools (Lo et al., 2019), and can spatially restrict their spread in ventral CA1 by local injection (see annex A). The latter allows for monosynaptic circuit tracing to dissect the afferent connectome of temporally fate-mapped hippocampal neurons (Callaway and Luo, 2015). Unfortunately, this powerful genetic tool was not fully implemented before the end of my doctoral project.

Lastly, we could not show a direct link between the temporal embryonic origin of CA1 PN and their function in vivo. One of the objectives of my PhD was to monitor neural activity of fate-mapped PNs while mice engage in different behaviors. Theoretically, this would have permitted to show that the time of birth does not only shape morpho-physiological properties, but predisposes given subpopulations to processing certain types of information, thus biasing their recruitment to specific cognitive processes. This omission is in part due to technical challenges. Located deep within the temporal cortex, the ventral tip of CA1 is difficult to access experimentally. Although, more and more labs have successfully performed calcium imaging in this region with endoscopes and GRIN (gradient refractive index) lenses, the expression of GCaMP6s in our transgenic line was not sufficient to record neuronal activity (see annex B). In the best-case scenario, this approach would have granted us to track the same neuronal population over days and in different contexts or memory

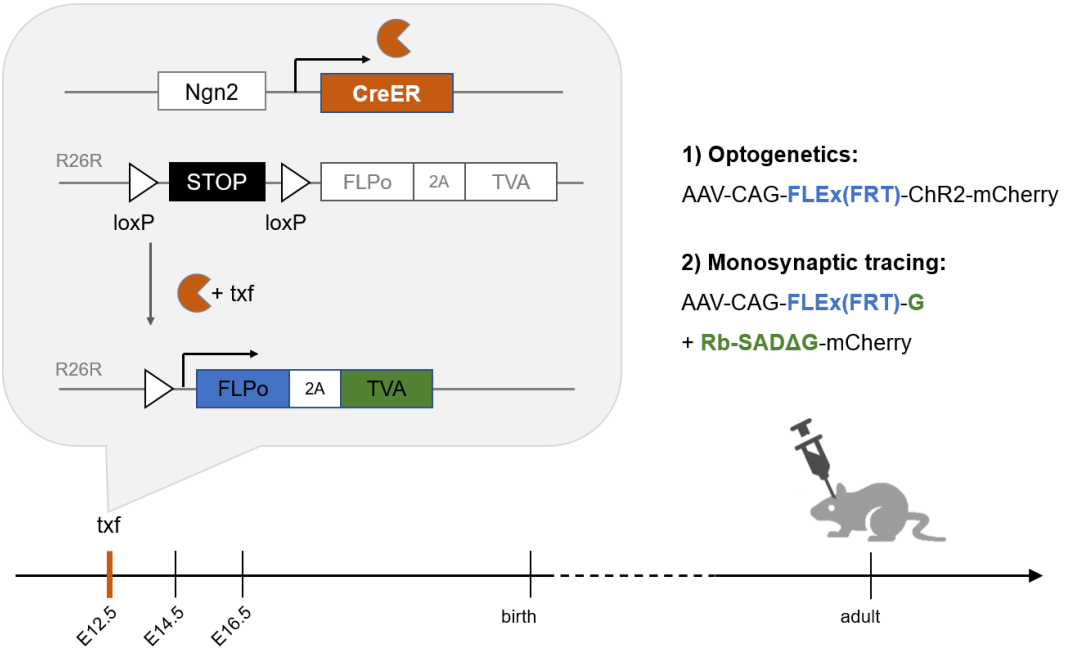

FIGURE 9.1: Fate-mapping CA1 pyramidal cells with temporal and spatial selectivity. Scheme representing the transgenic mouse model that is being implemented in our team to fate-map pyramidal neurons in CA1 with temporal (tamoxifen) and spatial (injection) selectivity. Like Ngn2-CreER-Ai14, it is based on the inducible Cre recombinase that, once activated, leads to the expression of flippase FLPo and rabies virus receptor TVA. These two can then be employed by local viral injections in CA1 for optogenetics or tracing experiments in the adult mouse.

tasks. As an alternative, we opted for an immediate early gene (IEG)-based strategy, looking at cFos as a proxy for neural activity. Its expression is increased upon recent sustained firing of action potentials (i.e. bursts), but is also related to the induction of activity-dependent synaptic plasticity (Mahringer et al., 2019; West et al., 2002). The choice of this technique was particularly motivated by a study in which cFos labelling was used in combination to extracellular recordings, to identify a subpopulation of CA1 neurons that formed a stable representation of a novel context, despite displaying poorer spatial accuracy and stability than other place cells (Tanaka et al., 2018). In our case, a major drawback was that cFos expression needed to be verified post-hoc (after sacrificing the mice), which limited our test to the exposure to one single behavioral paradigm (here, spatial exploration). In other words, it exclusively permitted a posteriori analysis of the recruitment of fate-mapped PNs. In absence of optical access to ventral CA1, a way to complement our experimental approach would be combining it to a 'TetOff' viral strategy (see figure 9.2). Initially, two viral constructs are injected in the hippocampus: (i) the tetracycline transactivator (tTA) gene under the cFos promoter (Zhang et al., 2015), (ii) a reporter gene (ex. fluorescent protein) under the tetracycline response element (TRE) (Chan et al., 2017). Then, the antibiotic doxycycline (Dox, analog of tetracycline) is administered with food and suppresses tTA activity. When Dox is temporarily retrieved, unbound tTA acts on the TRE sequence and enables the tagging of cFos+ neurons during an experience. Finally, TetOff strategy

and classic cFos immunostaining can be used sequentially. Mice are first exposed and familiarized to a given environment, say arena A, and Dox is removed from their diet on their last exploration. Then, the same mice are exposed to a new environment, arena B, and sacrificed after 1 hour to reveal cFos expression. In such way, we could corroborate the hypothesis that E12.5 PNs are specifically recruited in familiar arena A, and not in novel arena B. Alternatively, a similar paradigm could apply to different kinds of behavioral contexts, such as social exploration and fear or anxiety (Jimenez et al., 2018; Jimenez et al., 2020; Okuyama et al., 2016), and investigate if any of these emotionally rich tasks can lead to a differential recruitment of E16.5 neurons (figure 9.2).

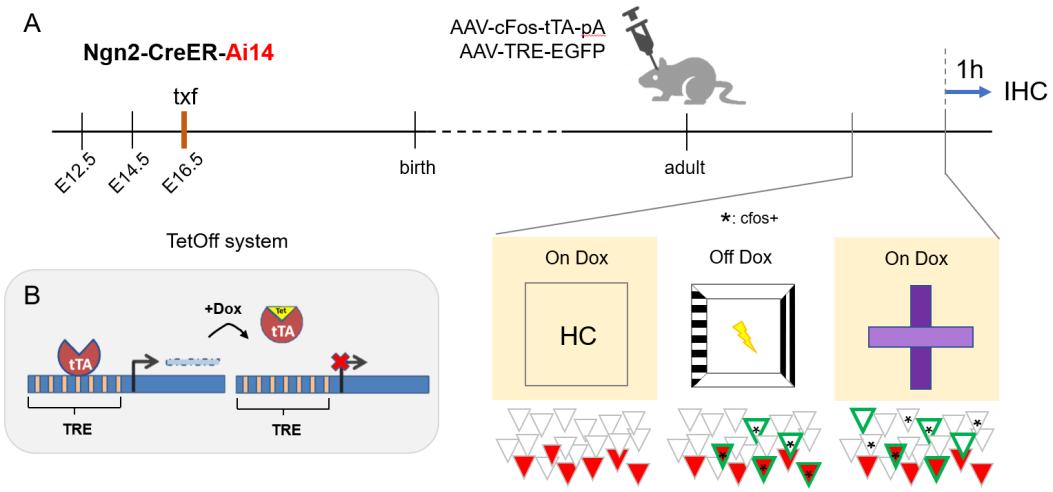

FIGURE 9.2: A TetOff strategy for investigating fate-mapped CA1 pyramidal cell recruitment. A) Schematic representation of an experimental protocol to probe the recruitment of fate-mapped CA1 pyramidal cells, here E16.5, in emotionally-rich behavioral contexts. After tamoxifen-induction in Ngn2-CreER-Ai14 animals, two viral constructs are locally injected into ventral CA1 : tetracycline transcriptional activator (tTA) under control of cFos, EGFP under control of tetracycline response element (TRE). TRE-dependent genes can only be expressed in absence of tetracycline/doxycycline (Dox, panel B). When Dox is removed from their diet, mice undergo a contextual fear conditioning paradigm. cFos activation (shown with '*') will drive the expression of EGFP, thus labeling neurons forming the memory trace. Next, when Dox is reintroduced, mice will be exposed to another context, here the anxiety-related elevated plus maze. One hour after the experiment, when cfos expression is maximal, mice can be sacrificed and cFos-labelling can be verified by immunohistochemistry (IHC) for the recent (anxiety), and by EGFP fluorescence for the first experience (fear).

9.2 Comparison with previous studies

It is now acknowledged that the stratum pyramidale in dorsal CA1 is composed of two functionally distinct sublayers, owing to the combined effort of several research teams (see reviews by Soltesz and Losonczy (2018) and Valero and Prida (2018)). Although the dissection of such diversity has proved crucial in widening the knowledge on how CA1 circuitry is built and how it organizes its activity, it has often disregarded the underlying

principles and ontogeny. Oppositely, this study strongly indicates that we cannot grasp the full complexity of the structure-function dyad only without including the developmental component.

In many aspects, the present work is in line with previous experimental evidence. First, we confirmed the finding of early autoradiographic studies that the distribution of PNs in the stratum pyramidale closely mirrors the embryonic origin, with neurons born later during CA1 neurogenesis positioning progressively more superficially than their earlier generated counterpart (Caviness, 1973; Angevine, 1965; Bayer, 1980). Interestingly, it was already noticed that "cells which are to become scattered [...] are virtually all formed through E13 and they are only a small proportion of the total number" (Caviness, 1973). Those described are likely pioneer PNs born between E11 and E13, which we characterized in depth and found to present distinct features from their other deep but later generated counterpart (E14.5).

In turn, E14.5 PNs, independently of their soma location, display a synaptic drive leaning more towards inhibition and a specific bias of their output connectivity towards the nucleus accumbens (NAcc) of the ventral striatum. Both findings are reminiscent of previous studies showing that deep PNs are characterized by a low E/I ratio and are highly innervated by PV+ basket cells (Lee et al., 2014; Masurkar et al., 2017), and underlie a behaviorally-specific pathway to NAcc (Okuyama et al., 2016).

Moreover, our anatomical analysis of recorded cells, consisting of simply measuring the length of the main dendrite shaft, bore out conclusions similar to those of more sophisticated morphological reconstructions (D'Amour et al., 2020; Li et al., 2017; Masurkar et al., 2020). Extending the notion that distinct subpopulations segregate according to their dendritic morphology, with deep ('simple') cells having a longer primary dendrite than superficial ('complex') cells, the current results suggest that E12.5 are an exception to this 'rule'.

Finally, neurons generated at E16.5, located in the most superficial part of the stratum pyramidale, were less excitable, owing to their globally slower membrane time constant and firing propensity reduced in respect to E14.5 PNs (Cembrowski et al., 2016; Mizuseki et al., 2011). However, despite in our experimental conditions superficial received less frequent excitatory input than deep cells, E16.5 displayed higher E/I amplitude ratio, mirrored by lower PV innervation (Lee et al., 2014; Valero et al., 2015). Our results from the analysis of output projections and cFos recruitment also revealed that E16.5 showed the smallest Ctb+/Tdt+ fraction of all birthdate groups, suggesting that they are less likely to innervate the regions we tested. This is coherent with previous investigations, in which NAcc, amygdala and medial prefrontal cortex (mPFC) were all preferentially targeted by deep cells (Jimenez et al., 2018; Lee et al., 2014; Okuyama et al., 2016). The only exception was the medial entorhinal cortex, showing equal innervation from both sublayers (Lee et al., 2014). Thus, it would be tempting to test whether E16.5 PNs exhibit a bias within the hippocampal region. Projections to the lateral entorhinal cortex and the subiculum should be further looked into.

At any rate, the experimental evidence gathered and presented here does not systematically parallel the aforementioned studies. First, we could not replicate the discovery of a radial gradient in depolarizing sag responses (Jarsky et al., 2008; Lee et al., 2014; Maroso et al., 2016), rather deeper-located E14.5 neurons displayed a larger sag than their superficial counterpart. This is all the more puzzling considering that this difference is likely only present in proximal CA1 (Masurkar et al., 2020), which is where most cells were sampled from, although not exclusively. One possible explanation is that, owing to variability in Ih currents along the dorso-ventral axis (Cembrowski et al., 2016; Dougherty et al., 2012; Malik et al., 2016), the expression of sag and rebound potentials might not follow the same pattern in ventral CA1. In fact, to my knowledge all experimental evidence cited above comes from acute slices of the septal-most part. Furthermore, as discussed in the article (chapter 6), our recordings were performed in the absence of specific pharmacological blockers for other postsynaptic membrane currents, as well as of antagonists for metabotropic and ionotropic GABA and glutamate receptors (Jarsky et al., 2008; Lee et al., 2014; Maroso et al., 2016; Masurkar et al., 2017).

Second, we could not observe any burst firing pattern in recorded cells in acute slice (Cembrowski et al., 2016; Graves et al., 2012; Jarsky et al., 2008; Mizuseki et al., 2011). One possible explanation is that in our study, recordings were performed on adult mice, and not juvenile rats, using a methylsulfate-based intracellular solution, and not a gluconate-based one, differently from Graves et al. (2012) and Jarsky et al. (2008). Indeed, the choice of intracellular solution can have an effect on electrophysiological properties, such as the post-firing hyperpolarization (Kaczorowski et al., 2007). It should be reminded that one of the main references is a study where bursting was evaluated from extracellular recordings in vivo (Mizuseki et al., 2011) and in other ex vivo work there was no clear sign of intracellularly-defined 'burstiness' in CA1 PNs (Dougherty et al., 2012; Li et al., 2017).

Lastly, differently from Li et al. (2017), no variation along the radial axis was seen in the magnitude CA3-driven excitation, quantified upon electrical stimulation of Schaffer Collateral (SC) fibers in CA1 stratum radiatum. However, this finding was not or only partially reproduced in other two studies (Masurkar et al., 2017; Valero et al., 2015). In this case, the discrepancies might be explained by the different technical approaches used (optogenetics in the first publication, CA3 and radiatum electrical stimulation, respectively, in the other two). Oppositely, we found that EPSC frequency was higher in deep cells and this gradient, which was already reported for PNs located in the stratum oriens (here called 'ectopic') compared to PNs located in the stratum pyramidale (Cossart et al., 2000).

9.3 Recruitment of birthdated neurons upon exploration

Investigating cFos activation after mice explored a familiar or novel arena revealed that E16.5 PNs displayed globally low levels of recruitment, including the control home-cage condition. It should be noted that neurons in the superficial sublayer are more active in cue-poor environments, with stable firing within a same environment and likely driven by a

strong CA3 input (Danielson et al., 2016; Fattahi et al., 2018; Valero et al., 2015; Geiller et al., 2017a). The enrichment of the arena with proximal (colored shapes and patterns) and distal (odor, sound) cues might have hindered sustained firing, and ultimately cFos activation, in these cells, which are supposedly critical for self-referenced navigation (Sharif et al., 2020). Furthermore, cFos expression is likely induced by intense burst firing and that its absence in a cell population "does not preclude the involvement of that population in a functional circuit" (Labiner et al., 1993). Indeed, late generated superficial cells are less 'bursty' in vivo (Mizuseki et al., 2011) and might exhibit lower basal levels or other immediate early genes (IEGs). Importantly, it was recently described that distinct granule cell population in the dentate gyrus can be separated by the expression of two IEGs and differently contribute to information coding in a contextual fear paradigm (Sun et al., 2020b). A similar scenario could apply to CA1 (Tronson et al., 2009; Tyssowski et al., 2018).

Compared to their younger counterpart, E14.5 PNs were slightly but significantly more recruited in the novel condition, and E12.5 displayed a pronounced cFos activation after exploration of a known environment. Both groups are predominantly found in the deep sublayer, the activity of which is biased towards cue-rich environments and predicts goal-oriented behavioral performance (Danielson et al., 2016; Geiller et al., 2017a; Sharif et al., 2020). On the one hand, this is consistent with the finding that E14.5 PNs send axons primarily to NAcc, of all regions probed. CA1 projections to this striatal nucleus are known to be involved in reward seeking and learning (LeGates et al., 2018; Trouche et al., 2019). It was also proposed that NAcc, along with the dopaminergic system, "is important for signaling the occurrence of novel and potentially salient events" (Baudonnat et al., 2013). As such, E14.5 recruitment in the novel environment could be interpreted as an 'update' of information regarding a new situation with uncertain outcome. On the other hand, a specific pathway of deep neurons projecting to NAcc increased their firing in presence of known conspecific (Okuyama et al., 2016), suggesting that they rather store the memory of a previous (social) experience (Okuyama, 2018). Opposetely, in our experiment, it was the E12.5 subpopulation, lacking preferential innervation to NAcc, that was biased towards the familiar condition. Is E12.5 cFos expression related to the encoding of spatial information? Do E14.5 PNs provide an instantaneous map of a novel environment? Is either birthdate group highly involved in social discrimination? Or do they signal novelty in other behavioral paradigms? These questions merit further investigation.

9.4 A new insight into CA1 pyramidal cell diversity

Prior knowledge on migratory patterns in developing CA1 indicated that PN positioning in the stratum pyramidale and functional segregation of PN subpopulations could not be separated. Not surprisingly, even in the first experimental papers dealing with CA1 PN diversity (Deguchi et al., 2011; Lee et al., 2014; Mizuseki et al., 2011), the developmental factor was either mentioned or explicitly proposed as a fundamental determinant of this

heterogeneity. As a result, one could expect that those experimental measures that distinguished fate-mapped PN in CA1 follow a linear trend from early to late born neurons, mirroring the inside first-outside last migration scheme, or else, that pioneer neurons share a mixed phenotype (given their spread from deep to superficial stratum pyramidale). Neither of these speculations is supported by the current data. Rather, we illustrate for the first time that birthdate groups have each specific morpho-physiological and synaptic features. In some cases, i.e. membrane resistance, PV innervation, dendritic morphology, E12.5 PNs are more similar to E16.5 than to the embryonically and spatially closer E14.5. In other cases, E12.5 and E16.5 display clearly separate properties, like output connectivity and cFos recruitment.

Thus, a significant novel finding is that the relationship between neuronal gradients of diversity and sequential neurogenesis is neither linear nor it can be accurately predicted by the soma position. Nonetheless, in our voltage-clamp experiments we also confirm that input connectivity varies according to gradients that are not always matched by the embryonic origin. In other words, the positional factor is not to be neglected but integrated in a view where CA1 diversity at cell level emerges from the interaction of developmental (intrinsic) and purely anatomical mechanisms (extrinsic).

9.5 CA1 pioneer neurons display unique features

To our knowledge, this is the first in depth description of pioneer E12.5 PNs in CA1, which are shown to form a unique pyramidal subtype with peculiar characteristics. First is their scattered distribution, with somata found as deep as the stratum oriens and, although more rarely, also in the stratum radiatum. The stratum oriens is enriched with axons originating from CA2 pyramidal cells, which mainly contact deep cells as well as giant radiatum cells or GRCs (Kohara et al., 2014; Nasrallah et al., 2019). GRCs are a rare population of ectopic pyramidal cells displaying two thick apical dendrites and projecting directly to the olfactory bulb from ventral CA1 (Megías et al., 2001; Groen and Wyss, 1990). It would be relevant to look more closely into the possibility that GRC are embryologically defined, perhaps belonging to pioneer subpopulation. First, out of all cell recorded in slice, one E12.5 neuron was found to have these positional and morphological features, while none in the later generated birthdates (data not shown). Second, pioneer cells display a prominent spread that extends to the stratum radiatum for a non negligeable fraction (see article in chapter 6). Further experiments are required to test if E12.5 PNs are preferentially targeted by CA2 and if they innervate olfactory areas.

If this additional pathway were to be confirmed, more evidence would point to the notion that pioneer neurons display a remarkable range of output targets, which resulted from retrograde tracing with Cholera toxin B. Unfortunately, this technique does not allow to discriminate connectivity motifs at single-cell level. It is then still unclear whether all E12.5 cells innervate many structures at once, or if this is an average effect within the E12.5 population and single neurons diverge in their targets. A recent study (Gergues

et al., 2020) demonstrated that, although for the most part single PNs innervate only one extrahippocampal region, ventral CA1 is enriched with multiple-projecting neurons. Likely, among these neurons is the population described with optogenetic tagging by Ciocchi and colleagues (2015). They were functionally connected to three structures (amygdala, medial prefrontal cortex and nucleus accumbens) and exhibited higher firing rates in several behavioral tasks, as well as greater propensity to participate in sharp-wave ripples (SWR) than other neurons. Needless to say, despite the technical limitations mentioned above and in annex B, studying the activity of pioneer neurons in vivo is of crucial interest. The probability of E12.5 PNs to be active during ripples could be measured by comparing field potential recorded in the ventral hippocampus and calcium traces obtained by endoscopy.

Finally, when evoking inhibitory currents by SC stimulation, E12.5 showed a higher paired pulse ratio than the other two birthdate groups, suggesting that GABA release probability of CA3-driven interneurons contacting CA1 E12.5 is lower. This might stem from differential pre/postsynaptic plasticity or from GABAergic input diversity, a tempting hypothesis given the variability of PV+ contact number among birthdate groups and considering that different paired pulse responses can arise depending on the interneuron subtype (Sarihi et al., 2012).

9.6 Pioneer neurons across the hippocampus

As discussed before, the present study gathers additional evidence directly linking the development origin to the determination of adult neuronal diversity. It is therefore proposed that the temporal order of neurogenesis sequentially defines subpopulations of pyramidal neurons in CA1. Moreover, E12.5 PNs exhibit specific properties that corroborate our group's hypothesis that pioneer neurons, either glutamatergic or GABAergic, form distinct classes with unique roles in the hippocampal circuitry.

Precedingly, we demonstrated that early-born GABAergic cells in CA1 and CA3 are long-range 'hub' cells. They display remarkable connectivity schemes, gate synchronous network events during post-natal development and signal a variety of network states in vivo (Bocchio et al., 2020; Picardo et al., 2011; Villette et al., 2016). The discovery that early born neurons could operate as functional hubs was inspired by graph theory. In a pivotal paper, Barabasi and Albert (1999) postulated that the development of certain networks is achieved by adding new elements (nodes) forming connections to those nodes that already have a large of number of connections (hubs). This principle, known as preferential attachment, appears to match the existence of hubs in the hippocampus. I ought to remind that the translation of graph theory to biological systems is to be taken with caution, especially because the definition of a network can be established with more precision in silico than in the brain.

That said, studying pioneer glutamatergic cells in CA3 and DG also lead our team to similar conclusions. Stimulation of early generated CA3 PNs can affect network dynamics in the developing hippocampus (Marissal et al., 2012). It should be tested whether these

neurons are more densely connected by recurrent connectivity, like a recent network model appears to suggest (Hunt et al., 2018). In the DG, semilunar granule cells are generated in early phases of development, form a distinct morpho-physiological subtype and are active across a wide range of disparate behavioral paradigms (Erwin et al., 2020; Save et al., 2019; Williams et al., 2007).

Two properties characterizing pioneer neurons emerge from this large body of research: high connectivity and broad recruitment in different cognitive states. Could these cells coordinate local dynamics among structures? Thanks to their wide range output connectivity, E12.5 would be suitable candidates for signaling the relevant cognitive state (arousal, anxiety, reward-seeking, socialization) to other structures involved in the encoding or retrieval of a mnemonic episode. Obviously, more evidence is needed in support of this hypothesis.

9.7 Two or more sublayers?

Based on histological and publicly accessible gene expression data, Dong (2009) observed that "in addition to superficial and deep pyramidal layers, a middle sublayer containing smaller pyramids appears to be sandwiched between the other layers" (Dong et al., 2009). The existence of a third sublayers is also supported or hinted at by data in other studies, in which molecular markers are used to label distinct groups of PNs in ventral CA1 (Li et al., 2018; Okuyama et al., 2016). Even if the precise number of sublayers is not of primary importance, it is worth drawing two considerations.

First, most research on pyramidal neuron diversity has focused on the dorsal pole of CA1, presumably because of its experimental accessibility and its well-known implication in spatial learning and navigation. Nonetheless, a large body of evidence shows that ventral CA1 encompasses an even more pronounced heterogeneity of principal cells and how this relates to network computation and cognitive processes requires more investigation.

Second, the description of PN diversity should be revised. Not only our findings challenge the current deep-superficial dichotomy, but even experimental evidence used to support this (perhaps simplistic) view is not as clear-cut. An example is that, despite the claim that "deep pyramidal cells shifted their preferred phase of firing to the peak of theta during rapid eye movement (REM) sleep", only about one half of deep PNs exhibit this behavior (Mizuseki et al., 2011). Likewise, a sharp subdivision between superficial calbindin (Cb)-positive neurons with ramified dendritic tree and deep Cb-negative neurons with simple morphology is proposed (Li et al., 2017), although the boundaries of Cb expression and morphological features are both rather blurry, notably in the ventral pole. Finally, recent data (Masurkar et al., 2020) prompts us to reconsider the commonly accepted notion that superficial cells display larger Ih currents than deep ones (Lee et al., 2014; Maroso et al., 2016). On one hand, such generalizations are helpful in bringing forward a new understanding of CA1 circuitry. On the other, we should abstain from an explanation that is too reductionist, unless strongly supported by experimental findings. Thus, it is still matter of debate what defines a neuronal PN subpopulation, whether the anatomical

division in sublayers is descriptive enough and what picture would emerge if we combined developmental, genetic, behavioral and connectivity data.

9.8 CA1 diversity and human hippocampus

Variability in the width of the stratum pyramidale of CA1 along the septo-temporal axis is well characterized in many mammalian species (Dong et al., 2009; Slomianka et al., 2011). Interestingly, the review by Slomianka and colleagues (2011) report that the level of cellular compactness seems to relate to phylogeny, with more complex animals (dolphin, fox, marmoset,...) displaying a progressive 'invasion' of the stratum oriens by pyramidal cells. A subdivision in sublayers in the human hippocampus seems to exist as well (Braak, 1974; Shepherd et al., 2007), although it remains unclear whether this anatomical feature underlies a functional segregation resembling that observed in rodent CA1. Owing that antero-posterior gradients (in anatomy, connectivity, and gene-expression) have been linked to a regional diversification of function in the human hippocampus (Poppenk et al., 2013; Vogel et al., 2020), it seems appropriate to seek for empirical validation whether this applies to the radial axis as well.

Furthermore, the anterior pole of the hippocampus (corresponding to ventral in rodents) is involved in emotional processes, as well as the regulation of mood and stress (Poppenk et al., 2013). It is an open question whether the developmental origin influences neuronal susceptibility in the framework of psychiatric disorders, and more generally to pathologies associated to the hippocampus. That said, a few considerations can be made based on positional data. First, genetic markers of the ventral hippocampus that are distributed homogeneously across the stratum pyramidale, such as Grp and Htr2c, have been implicated in psychiatric conditions (Drago and Serretti, 2009; Roesler et al., 2006). Second, alterations in PV-expressing interneurons levels are detected in patients with schizophrenia (Lewis et al., 2012) and silencing PV cells in ventral CA1 reduces social recognition (Deng et al., 2019), which mirrors the mnemonic impairment observed in models of schizophrenia and Alzheimer's disease (AD) (Deacon et al., 2009; Piskorowski and Chevaleyre, 2012). Since we show that E14.5 neurons are preferentially innervated by PV interneurons, it would be tempting to speculate that they are key players in the ontogeny of these conditions. Third, fragile X syndrome is a neurodevelopmental disorder associated with intellectual disability caused by the lack of FMRP (fragile mental retardation protein). Fmr1-KO mice, the murine model of this pathology, are characterized by altered plasticity and network coordination (Jawaid et al., 2018; Talbot et al., 2018), matched by deficits in space coding and contextual fear memory (Li et al., 2020). Interestingly, a strong reduction of Cb expression among CA1 PNs is observed in these mice (Real et al., 2011), which might indicate that superficial late generated cells are more affected by the mutation. Oppositely, deep earlier generated cells might be more susceptible to epilepsy, as they are more likely than superficial cells to degenerate as a consequence of pilocarpine-induced seizures (Towfighi et al., 2004). Nonetheless, preliminary data from our lab seem to indicate

that pioneer GABAergic cells are more likely to survive neurodegeneration in this model of epilepsy. Whether this holds as well for pioneer glutamate neurons should be experimentally verified. In the article included in this manuscript (see chapter 6), we hypothesize that E12.5 neurons are subject to a stronger imprinting by the temporal embryonic origin, as they display distinct characteristics and do not follow a clear positional patterning. As a result, this could render these cells more resilient to neurodegenerative diseases and those associated to cortical heterotopias and mislayering.

9.9 Conclusion

To summarise, we characterized fate-mapped CA1 PNs in depth, exploring ex vivo multiple cellular features, including electrophysiological properties, morphology and connectivity. The present work provides compelling evidence that the temporal embryonic origin of CA1 PNs has a central role of in the determination of cell identity, thereby directly contributing to the emergence of neuronal diversity in the CA1 field of the ventral hippocampus. As a result, we propose that the radial subdivision of the CA1 pyramidal layer into two functional units should be revised by including the time of neurogenesis as a fundamental component. Furthermore, we focused on pioneer neurons and highlighted that they display unique properties. Based on their wide-range connectivity and recruitment upon exploration, we would like to propose they play a key role in the consolidation or retrieval of recent experience by coordinating multiple regions. More generally, how the developmental origin shapes in vivo function in subpopulations of fate-mapped PNs in CA1 is still to be determined. Further investigation will clarify whether they differentially contribute to network dynamics, and ultimately to cognitive processes.

Colophon

This manuscript was realised on a LaTeX template (Version 2.5 as of 27/8/2017) made by **Vel**.
The thesis style was originally created by Steve R. Gunn[18] and modified by Sunil Patel[19].

[18] http://users.ecs.soton.ac.uk/srg/softwaretools/document/templates/
[19] http://www.sunilpatel.co.uk/thesis-template/

Bibliography

Adhikari, Avishek (2014). "Distributed circuits underlying anxiety". *Frontiers in Behavioral Neuroscience* 8.APR, pp. 1–6. DOI: 10.3389/fnbeh.2014.00112.

Allen, T. A., D. M. Salz, S. McKenzie, and N. J. Fortin (2016). "Nonspatial Sequence Coding in CA1 Neurons". *Journal of Neuroscience* 36.5, pp. 1547–1563. DOI: 10.1523/JNEUROSCI.2874-15.2016.

Allene, Camille, Michel A. Picardo, Hélène Becq, Goichi Miyoshi, Gord Fishell, and Rosa Cossart (2012). "Dynamic changes in interneuron morphophysiological properties mark the maturation of hippocampal network activity". *Journal of Neuroscience* 32.19, pp. 6688–6698. DOI: 10.1523/JNEUROSCI.0081-12.2012.

Alonso, Angel and Christer Köhler (1982). "Evidence for separate projections of hippocampal pyramidal and non-pyramidal neurons to different parts of the septum in the rat brain". *Neuroscience Letters* 31.3, pp. 209–214. DOI: 10.1016/0304-3940(82)90021-0.

Amaral, David G., Cynthia Dolorfo, and Pablo Alvarez-Royo (1991). "Organization of CA1 projections to the subiculum: A PHA-L analysis in the rat". *Hippocampus*. DOI: 10.1002/hipo.450010410.

Amaral, David G., N Ishizuka, and B Claiborne (1990). "Neurons, numbers and hippocampal network". *Progress in Brain Research*.

Amaral, David and Pierre Lavenex (2007). "Hippocampal Neuroanatomy". In: *The Hippocampus Book*. DOI: 10.1017/CBO9781107415324.004.

Andersen, P., T.V.P. Bliss, and K.K. Skrede (1971). "Lamellar organization of hippocampal excitatory pathways". *Experimental Brain Research* 13.2. DOI: 10.1007/BF00234087.

Angevine, J B (1965). "Time of neuron origin in the hippocampal region". *Experimental neurology. Supplement* 11, pp. 1–39. DOI: 10.1016/0014-4886(65)90121-4.

Anthony, Todd E, Nick Dee, Amy Bernard, Walter Lerchner, Nathaniel Heintz, and David J Anderson (2014). "Control of stress-induced persistent anxiety by an extra-amygdala septohypothalamic circuit." *Cell* 156.3, pp. 522–36. DOI: 10.1016/j.cell.2013.12.040.

Aronov, Dmitriy, Rhino Nevers, and David W. Tank (2017). "Mapping of a non-spatial dimension by the hippocampal-entorhinal circuit". *Nature* 543.7647, pp. 719–722. DOI: 10.1038/nature21692.

Arszovszki, Antónia, Zsolt Borhegyi, and Thomas Klausberger (2014). "Three axonal projection routes of individual pyramidal cells in the ventral CA1 hippocampus." English. *Frontiers in neuroanatomy* 8, p. 53. DOI: 10.3389/fnana.2014.00053.

Ascoli, Giorgio A., Lidia Alonso-Nanclares, Stewart A. Anderson, German Barrionuevo, Ruth Benavides-Piccione, Andreas Burkhalter, György Buzsáki, Bruno Cauli, Javier DeFelipe, Alfonso Fairén, Dirk Feldmeyer, Gord Fishell, Yves Fregnac, Tamas F. Freund, Daniel Gardner, Esther P. Gardner, Jesse H. Goldberg, Moritz Helmstaedter, Shaul Hestrin, Fuyuki Karube, Zoltán F. Kisvárday, Bertrand Lambolez, David A. Lewis, Oscar Marin, Henry Markram, Alberto Mũoz,

Adam Packer, Carl C.H. Petersen, Kathleen S. Rockland, Jean Rossier, Bernardo Rudy, Peter Somogyi, Jochen F. Staiger, Gabor Tamas, Alex M. Thomson, Maria Toledo-Rodriguez, Yun Wang, David C. West, and Rafael Yuste (2008). *Petilla terminology: Nomenclature of features of GABAergic interneurons of the cerebral cortex*. DOI: 10.1038/nrn2402.

Baimbridge, K.G. and J.J. Miller (1982). "Immunohistochemical localization of calcium-binding protein in the cerebellum, hippocampal formation and olfactory bulb of the rat". *Brain Research* 245.2, pp. 223–229. DOI: 10.1016/0006-8993(82)90804-6.

Bannister, N. J. and A. U. Larkman (1995). "Dendritic morphology of CA1 pyramidal neurones from the rat hippocampus: I. Branching patterns". en. *The Journal of Comparative Neurology* 360.1, pp. 150–160. DOI: 10.1002/cne.903600111.

Barabasi, Albert-Laszlo and Reka Albert (1999). "Emergence of scaling in random networks". *Science* 286.5439, pp. 509–512. DOI: 10.1126/science.286.5439.509.

Basavarajappa, Balapal S. and Shivakumar Subbanna (2014). "CB1 receptor-mediated signaling underlies the hippocampal synaptic, learning, and memory deficits following treatment with JWH-081, a new component of spice/K2 preparations". *Hippocampus* 24.2, pp. 178–188. DOI: 10.1002/hipo.22213.

Bast, T., W. N. Zhang, and J. Feldon (2001). "The ventral hippocampus and fear conditioning in rats: Different anterograde amnesias of fear after tetrodotoxin inactivation and infusion of the GABAA agonist muscimol". *Experimental Brain Research*. DOI: 10.1007/s002210100746.

Baudonnat, Mathieu, Anna Huber, Vincent David, and Mark E. Walton (2013). *Heads for learning, tails for memory: Reward, reinforcement and a role of dopamine in determining behavioral relevance across multiple timescales*. DOI: 10.3389/fnins.2013.00175.

Bayer, S A (1980). "Development of the hippocampal region in the rat. I. Neurogenesis examined with 3H-thymidine autoradiography." *The Journal of comparative neurology* 190.1, pp. 87–114. DOI: 10.1002/cne.901900107.

Beer, Zachery, Caroline Chwiesko, and Magdalena M. Sauvage (2014). "Processing of spatial and non-spatial information reveals functional homogeneity along the dorso-ventral axis of CA3, but not CA1". *Neurobiology of Learning and Memory* 111, pp. 56–64. DOI: 10.1016/j.nlm.2014.03.001.

Beier, Kevin T., Elizabeth E. Steinberg, Katherine E. Deloach, Stanley Xie, Kazunari Miyamichi, Lindsay Schwarz, Xiaojing J. Gao, Eric J. Kremer, Robert C. Malenka, and Liqun Luo (2015). "Circuit Architecture of VTA Dopamine Neurons Revealed by Systematic Input-Output Mapping". *Cell* 162.3, pp. 622–634. DOI: 10.1016/j.cell.2015.07.015.

Ben-Ari, Yehezkel, Ilgam Khalilov, Kristopher T. Kahle, and Enrico Cherubini (2012). "The GABA excitatory/inhibitory shift in brain maturation and neurological disorders". *Neuroscientist* 18.5, pp. 467–486. DOI: 10.1177/1073858412438697.

Ben-Ari, Y., E. Cherubini, R. Corradetti, and J. L. Gaiarsa (1989). "Giant synaptic potentials in immature rat CA3 hippocampal neurones." *The Journal of Physiology*. DOI: 10.1113/jphysiol.1989.sp017762.

Betterton, Ruth T., Lisa M. Broad, Krasimira Tsaneva-Atanasova, and Jack R. Mellor (2017). "Acetylcholine modulates gamma frequency oscillations in the hippocampus by activation of muscarinic M1 receptors". *European Journal of Neuroscience*. DOI: 10.1111/ejn.13582.

Bezaire, Marianne J and Ivan Soltesz (2013). "Quantitative assessment of CA1 local circuits: knowledge base for interneuron-pyramidal cell connectivity." *Hippocampus* 23.9, pp. 751–85. DOI: 10.1002/hipo.22141.

Blatow, Maria, Antonio Caputi, Nail Burnashev, Hannah Monyer, and Andrei Rozov (2003). "Ca2+ buffer saturation underlies paired pulse facilitation in calbindin-D28k-containing terminals". *Neuron* 38.1, pp. 79–88. DOI: 10.1016/S0896-6273(03)00196-X.

Bocchio, Marco, Claire Gouny, David Angulo-Garcia, Tom Toulat, Thomas Tressard, Eleonora Quiroli, Agnès Baude, and Rosa Cossart (2020). "Hippocampal hub neurons maintain distinct connectivity throughout their lifetime". *Nature Communications* 11.1. DOI: 10.1038/s41467-020-18432-6.

Bolding, Kevin A., Janina Ferbinteanu, Steven E. Fox, and Robert U. Muller (2020). "Place cell firing cannot support navigation without intact septal circuits". *Hippocampus* 30.3, pp. 175–191. DOI: 10.1002/hipo.23136.

Bonifazi, P, M Goldin, M A Picardo, I Jorquera, A Cattani, G Bianconi, A Represa, Y Ben-Ari, and R Cossart (2009). "GABAergic hub neurons orchestrate synchrony in developing hippocampal networks." en. *Science (New York, N.Y.)* 326.5958, pp. 1419–24. DOI: 10.1126/science.1175509.

Bonne, Omer, Meena Vythilingam, Masatoshi Inagaki, Suzanne Wood, Alexander Neumeister, Allison C. Nugent, Joseph Snow, David A. Luckenbaugh, Earle E. Bain, Wayne C. Drevets, and Dennis S. Charney (2008). "Reduced posterior hippocampal volume in posttraumatic stress disorder". *Journal of Clinical Psychiatry*. DOI: 10.4088/JCP.v69n0707.

Braak, H. (1974). "On the structure of the human archicortex". *Cell and Tissue Research* 152.3. DOI: 10.1007/BF00223955.

Britt, Jonathan P., Faiza Benaliouad, Ross A. McDevitt, Garret D. Stuber, Roy A. Wise, and Antonello Bonci (2012). "Synaptic and Behavioral Profile of Multiple Glutamatergic Inputs to the Nucleus Accumbens". *Neuron* 76.4, pp. 790–803. DOI: 10.1016/j.neuron.2012.09.040.

Britz, Olivier, Pierre Mattar, Laurent Nguyen, Lisa-Marie Langevin, Céline Zimmer, Sharmila Alam, François Guillemot, and Carol Schuurmans (2006). "A role for proneural genes in the maturation of cortical progenitor cells." *Cerebral cortex* 16 Suppl 1, pp. 138–51. DOI: 10.1093/cercor/bhj168.

Buhl, D. L. and G. Buzsáki (2005). "Developmental emergence of hippocampal fast-field "ripple" oscillations in the behaving rat pups". *Neuroscience*. DOI: 10.1016/j.neuroscience.2005.05.030.

Burke, Sara N., Andrew P. Maurer, Saman Nematollahi, Ajay R. Uprety, Jenelle L. Wallace, and Carol A. Barnes (2011). "The influence of objects on place field expression and size in distal hippocampal CA1". *Hippocampus*. DOI: 10.1002/hipo.20929.

Burton, Brian G., Vincent Hok, Etienne Save, and Bruno Poucet (2009). "Lesion of the ventral and intermediate hippocampus abolishes anticipatory activity in the medial prefrontal cortex of the rat". *Behavioural Brain Research*. DOI: 10.1016/j.bbr.2008.11.045.

Buzsáki, G. (1989). "Two-stage model of memory trace formation: A role for "noisy" brain states". *Neuroscience* 31.3, pp. 551–570. DOI: 10.1016/0306-4522(89)90423-5.

Buzsáki, György (1986). "Hippocampal sharp waves: Their origin and significance". *Brain Research* 398.2, pp. 242–252. DOI: 10.1016/0006-8993(86)91483-6.

— (2002). "Theta oscillations in the hippocampus". *Neuron* 33.3, pp. 325–340.

— (2013). "Hippocampus: Network Physiology". In: *Handbook of Brain Microcircuits*. DOI: 10.1093/med/9780195389883.003.0016.

Buzsáki, György and Andreas Draguhn (2004). "Neuronal oscillations in cortical networks." en. *Science (New York, N.Y.)* 304.5679, pp. 1926–9. DOI: 10.1126/science.1099745.

Buzsáki, György, Leung Lai-Wo S., and Cornelius H. Vanderwolf (1983). *Cellular bases of hippocampal EEG in the behaving rat*. DOI: 10.1016/0165-0173(83)90037-1.

Buzsáki, György and Edvard I. Moser (2013). "Memory, navigation and theta rhythm in the hippocampal-entorhinal system". *Nature Neuroscience* 16.2, pp. 130–138. DOI: 10.1038/nn.3304.

Cai, Xiang, Angy J. Kallarackal, Mark D. Kvarta, Sasha Goluskin, Kaitlin Gaylor, Aileen M. Bailey, Hey Kyoung Lee, Richard L. Huganir, and Scott M. Thompson (2013). "Local potentiation of excitatory synapses by serotonin and its alteration in rodent models of depression". *Nature Neuroscience* 16.4, pp. 464–472. DOI: 10.1038/nn.3355.

Calderazzo, L., E. A. Cavalheiro, G. Macchi, M. Molinari, and M. Bentivoglio (1996). "Branched connections to the septum and to the entorhinal cortex from the hippocampus, amygdala, and diencephalon in the rat". *Brain Research Bulletin*. DOI: 10.1016/0361-9230(96)00033-0.

Çalışkan, Gürsel and Oliver Stork (2019). "Hippocampal network oscillations at the interplay between innate anxiety and learned fear". *Psychopharmacology* 236.1, pp. 321–338. DOI: 10.1007/s00213-018-5109-z.

Callaway, E. M. and L. Luo (2015). "Monosynaptic Circuit Tracing with Glycoprotein-Deleted Rabies Viruses". *Journal of Neuroscience* 35.24, pp. 8979–8985. DOI: 10.1523/JNEUROSCI.0409-15.2015.

Canteras, N. S. and L. W. Swanson (1992). "Projections of the ventral subiculum to the amygdala, septum, and hypothalamus: A PHAL anterograde tract-tracing study in the rat". *Journal of Comparative Neurology*. DOI: 10.1002/cne.903240204.

Carew, Thomas J., Vincent F. Castellucci, and Eric R. Kandel (1971). "An analysis of dishabituation and sensitization of the gill-withdrawal reflex in aplysia". *International Journal of Neuroscience*. DOI: 10.3109/00207457109146995.

Cassel, Jean-christophe, Anne Pereira De Vasconcelos, John C Dalrymple-alford, Robert P Vertes, New Zealand, Brain Sciences, and Boca Raton (2013). "The reuniens and rhomboid nuclei: Neuroanatomy, electrophysiological characteristics and behavioral implications". 111, pp. 34–52. DOI: 10.1016/j.pneurobio.2013.08.006.The.

Castillo, Pablo E., Thomas J. Younts, Andrés E. Chávez, and Yuki Hashimotodani (2012). "Endocannabinoid Signaling and Synaptic Function". *Neuron* 76.1, pp. 70–81. DOI: 10.1016/j.neuron.2012.09.020.

Caviness, V S (1973). "Time of neuron origin in the hippocampus and dentate gyrus of normal and reeler mutant mice: an autoradiographic analysis." *The Journal of comparative neurology* 151.2, pp. 113–20. DOI: 10.1002/cne.901510203.

Cembrowski, Mark S., Julia L. Bachman, Lihua Wang, Ken Sugino, Brenda C. Shields, and Nelson Spruston (2016). "Spatial Gene-Expression Gradients Underlie Prominent Heterogeneity of CA1 Pyramidal Neurons". *Neuron* 89.2, pp. 351–368. DOI: 10.1016/j.neuron.2015.12.013.

Cembrowski, Mark S. and Vilas Menon (2018). "Continuous Variation within Cell Types of the Nervous System". *Trends in Neurosciences* 41.6, pp. 337–348. DOI: 10.1016/J.TINS.2018.02.010.

Cembrowski, Mark S. and Nelson Spruston (2019). "Heterogeneity within classical cell types is the rule: lessons from hippocampal pyramidal neurons". *Nature Reviews Neuroscience* 20.4, pp. 193–204. DOI: 10.1038/s41583-019-0125-5.

Cenquizca, Lee A. and Larry W. Swanson (2006). "Analysis of direct hippocampal cortical field CA1 axonal projections to diencephalon in the rat". *Journal of Comparative Neurology* 497.1, pp. 101–114. DOI: 10.1002/cne.20985.

— (2007). "Spatial organization of direct hippocampal field CA1 axonal projections to the rest of the cerebral cortex". *Brain Research Reviews* 56.1, pp. 1–26. DOI: 10.1016/j.brainresrev.2007.05.002.

Chan, Ken Y., Min J. Jang, Bryan B. Yoo, Alon Greenbaum, Namita Ravi, Wei Li Wu, Luis Sánchez-Guardado, Carlos Lois, Sarkis K. Mazmanian, Benjamin E. Deverman, and Viviana Gradinaru (2017). "Engineered AAVs for efficient noninvasive gene delivery to the central and peripheral nervous systems". *Nature Neuroscience* 20.8, pp. 1172–1179. DOI: 10.1038/nn.4593.

Chee, Melissa J.S., Pavlos Pissios, and Eleftheria Maratos-Flier (2013). "Neurochemical characterization of neurons expressing melanin-concentrating hormone receptor 1 in the mouse hypothalamus". *Journal of Comparative Neurology* 521.10, pp. 2208–2234. DOI: 10.1002/cne.23273.

Chee, San-San A., Janet L. Menard, and Hans C. Dringenberg (2015). "The lateral septum as a regulator of hippocampal theta oscillations and defensive behavior in rats". *Journal of Neurophysiology* 113.6, pp. 1831–1841. DOI: 10.1152/jn.00806.2014.

Chen, Shuo, Linmeng He, Arthur J.Y. Huang, Roman Boehringer, Vincent Robert, Marie E. Wintzer, Denis Polygalov, Adam Z. Weitemier, Yanqiu Tao, Mingxiao Gu, Steven J. Middleton, Kana Namiki, Hiroshi Hama, Ludivine Therreau, Vivien Chevaleyre, Hiroyuki Hioki, Atsushi Miyawaki, Rebecca A. Piskorowski, and Thomas J. McHugh (2020). "A hypothalamic novelty signal modulates hippocampal memory". *Nature* 586.7828, pp. 270–274. DOI: 10.1038/s41586-020-2771-1.

Chevaleyre, Vivien and Steven A. Siegelbaum (2010). "Strong CA2 pyramidal neuron synapses define a powerful disynaptic cortico-hippocampal loop". *Neuron* 66.4, pp. 560–572. DOI: 10.1016/j.neuron.2010.04.013.

Chittajallu, Ramesh, Michael T. Craig, Ashley Mcfarland, Xiaoqing Yuan, Scott Gerfen, Ludovic Tricoire, Brian Erkkila, Sean C. Barron, Carla M. Lopez, Barry J. Liang, Brian W. Jeffries, Kenneth A. Pelkey, and Chris J. McBain (2013). "Dual origins of functionally distinct O-LM interneurons revealed by differential 5-HT3AR expression". *Nature Neuroscience*. DOI: 10.1038/nn.3538.

Ciocchi, S., J. Passecker, H. Malagon-Vina, N. Mikus, and T. Klausberger (2015). "Selective information routing by ventral hippocampal CA1 projection neurons". en. *Science* 348.6234, pp. 560–563. DOI: 10.1126/science.aaa3245.

Colgin, Laura Lee (2016). "Rhythms of the hippocampal network". *Nature Reviews Neuroscience* 17.4, pp. 239–249. DOI: 10.1038/nrn.2016.21.

Colgin, Laura Lee, Tobias Denninger, Marianne Fyhn, Torkel Hafting, Tora Bonnevie, Ole Jensen, May Britt Moser, and Edvard I. Moser (2009). "Frequency of gamma oscillations routes flow of information in the hippocampus". *Nature* 462.7271, pp. 353–357. DOI: 10.1038/nature08573.

Corcoran, Kevin A. and Stephen Maren (2001). "Hippocampal inactivation disrupts contextual retrieval of fear memory after extinction". *Journal of Neuroscience*. DOI: 10.1523/jneurosci.21-05-01720.2001.

Corkin, Suzanne (2002). "What's new with the amnesic patient H.M.?" *Nature Reviews Neuroscience* 2.February, pp. 246–252.

Cossart, R., J. C. Hirsch, R. C. Cannon, C. Dinoncourt, H. V. Wheal, Y. Ben-Ari, M. Esclapez, and C. Bernard (2000). "Distribution of spontaneous currents along the somato-dendritic axis of rat hippocampal CA1 pyramidal neurons". *Neuroscience*. DOI: 10.1016/S0306-4522(00)00231-1.

Cossart, Rosa and Rustem Khazipov (n.d.). "How development sculpts hippocampal memory circuits" (), pp. 1–52.

Crépel, Valérie, Dmitriy Aronov, Isabel Jorquera, Alfonso Represa, Yehezkel Ben-Ari, and Rosa Cossart (2007). "A Parturition-Associated Nonsynaptic Coherent Activity Pattern in the Developing Hippocampus". *Neuron*. DOI: 10.1016/j.neuron.2007.03.007.

Csicsvari, Jozsef, Brian Jamieson, Kensall D. Wise, and György Buzsáki (2003). "Mechanisms of gamma oscillations in the hippocampus of the behaving rat". *Neuron*. DOI: 10.1016/S0896-6273(02)01169-8.

D'Amour, James A., Tyler G. Ekins, Stuti Ghanatra, Xiaoqing Yuan, Chris J. McBain, Stuti Ganatra, Xiaoqing Yuan, and Chris J. McBain (2020). "Aberrant sorting of hippocampal complex pyramidal cells in Type I Lissencephaly alters topological innervation". *eLife* 9, pp. 1–26. DOI: 10.1101/2020.02.05.935775.

Danglot, Lydia, Antoine Triller, and Serge Marty (2006). "The development of hippocampal interneurons in rodents". *Hippocampus* 16.12, pp. 1032–1060. DOI: 10.1002/hipo.20225.

Danielian, Paul S., David Muccino, David H. Rowitch, Simon K. Michael, and Andrew P. McMahon (1998). "Modification of gene activity in mouse embryos in utero by a tamoxifen-inducible form of Cre recombinase". *Current Biology* 8.24, pp. 1323–1326. DOI: 10.1016/s0960-9822(07)00562-3.

Danielson, Nathan B., Jeffrey D. Zaremba, Patrick Kaifosh, John Bowler, Max Ladow, and Attila Losonczy (2016). "Sublayer-Specific Coding Dynamics during Spatial Navigation and Learning in Hippocampal Area CA1". *Neuron* 91.3, pp. 652–665. DOI: 10.1016/j.neuron.2016.06.020.

Davis, Elizabeth A., Clarissa M. Liu, Isabella H. Gianatiempo, Andrea N. Suarez, Alyssa M. Cortella, Joel D. Hahn, and Scott E. Kanoski (2020). "Hippocampus-lateral septum circuitry mediates foraging-related spatial memory in rats".

Davoudi, Heydar and David J. Foster (2019). "Acute silencing of hippocampal CA3 reveals a dominant role in place field responses". *Nature Neuroscience* 22.3, pp. 337–342. DOI: 10.1038/s41593-018-0321-z.

Deacon, R. M.J., E. Koros, K. D. Bornemann, and J. N.P. Rawlins (2009). "Aged Tg2576 mice are impaired on social memory and open field habituation tests". *Behavioural Brain Research* 197.2, pp. 466–468. DOI: 10.1016/j.bbr.2008.09.042.

Dedovic, Katarina, Annie Duchesne, Julie Andrews, Veronika Engert, and Jens C. Pruessner (2009). "The brain and the stress axis: The neural correlates of cortisol regulation in response to stress". *NeuroImage*. DOI: 10.1016/j.neuroimage.2009.05.074.

Deguchi, Yuichi, Flavio Donato, Ivan Galimberti, Erik Cabuy, and Pico Caroni (2011). "Temporally matched subpopulations of selectively interconnected principal neurons in the hippocampus." en. *Nature neuroscience* 14.4, pp. 495–504. DOI: 10.1038/nn.2768.

Deller, Thomas, Alexander Drakew, Bernd Heimrich, Eckart Förster, Albrecht Tielsch, and Michael Frotscher (1999). "The hippocampus of the reeler mutant mouse: Fiber segregation in area CA1 depends on the position of the postsynaptic target cells". *Experimental Neurology* 156.2, pp. 254–267. DOI: 10.1006/exnr.1999.7021.

Deng, Jin Bo, Dong Ming Yu, Ping Wu, and Ming Shan Li (2007). "The tracing study of developing entorhino-hippocampal pathway". *International Journal of Developmental Neuroscience*. DOI: 10.1016/j.ijdevneu.2007.03.002.

Deng, Xiaofei, Lijia Gu, Nan Sui, Jianyou Guo, and Jing Liang (2019). "Parvalbumin interneuron in the ventral hippocampus functions as a discriminator in social memory". *Proceedings of the National Academy of Sciences* 116.33, p. 201819133. DOI: 10.1073/pnas.1819133116.

Deshmukh, Sachin S. and James J. Knierim (2011). "Representation of non-spatial and spatial information in the lateral entorhinal cortex". *Frontiers in Behavioral Neuroscience*. DOI: 10.3389/fnbeh.2011.00069.

Deuel, Thomas A.S., Judy S. Liu, Joseph C. Corbo, Seung Yun Yoo, Lucy B. Rorke-Adams, and Christopher A. Walsh (2006). "Genetic interactions between doublecortin and doublecortin-like

kinase in neuronal migration and axon outgrowth". *Neuron* 49.1, pp. 41–53. DOI: 10.1016/j.neuron.2005.10.038.

Doischer, Daniel, Jonas Aurel Hosp, Yuchio Yanagawa, Kunihiko Obata, Peter Jonas, Imre Vida, and Marlene Bartos (2008). "Postnatal differentiation of basket cells from slow to fast signaling devices". *Journal of Neuroscience* 28.48, pp. 12956–12968. DOI: 10.1523/JNEUROSCI.2890-08.2008.

Donato, Flavio, Ananya Chowdhury, Maria Lahr, and Pico Caroni (2015). "Early- and Late-Born Parvalbumin Basket Cell Subpopulations Exhibiting Distinct Regulation and Roles in Learning". *Neuron* 85.4, pp. 770–786. DOI: 10.1016/J.NEURON.2015.01.011.

Donato, Flavio, R. Irene Jacobsen, May-Britt Moser, and Edvard I. Moser (2017). "Stellate cells drive maturation of the entorhinal-hippocampal circuit". *Science* 355.6330, eaai8178. DOI: 10.1126/science.aai8178.

Dong, Hong-Wei, Larry W Swanson, Lin Chen, Michael S Fanselow, and Arthur W Toga (2009). "Genomic-anatomic evidence for distinct functional domains in hippocampal field CA1." en. *Proceedings of the National Academy of Sciences of the United States of America* 106.28, pp. 11794–9. DOI: 10.1073/pnas.0812608106.

Douchamps, Vincent, Ali Jeewajee, Pam Blundell, Neil Burgess, and Colin Lever (2013). "Evidence for encoding versus retrieval scheduling in the hippocampus by theta phase and acetylcholine". *Journal of Neuroscience* 33.20, pp. 8689–8704. DOI: 10.1523/JNEUROSCI.4483-12.2013.

Dougherty, Kelly A. (2019). "Differential developmental refinement of the intrinsic electrophysiological properties of CA1 pyramidal neurons from the rat dorsal and ventral hippocampus". *Hippocampus*, hipo.23152. DOI: 10.1002/hipo.23152.

Dougherty, Kelly A., Tasnim Islam, and Daniel Johnston (2012). "Intrinsic excitability of CA1 pyramidal neurones from the rat dorsal and ventral hippocampus". *The Journal of Physiology* 590.22, pp. 5707–5722. DOI: 10.1113/jphysiol.2012.242693.

Drago, Antonio and Alessandro Serretti (2009). *Focus on HTR2C: A possible suggestion for genetic studies of complex disorders*. DOI: 10.1002/ajmg.b.30864.

Drieu, Céline, Ralitsa Todorova, and Michaël Zugaro (2018). "Nested sequences of hippocampal assemblies during behavior support subsequent sleep replay". *Science* 362.6415, pp. 675–679. DOI: 10.1126/science.aat2952.

Dudok, Barna, Peter M. Klein, Ernie Hwaun, Brian R. Lee, Zizhen Yao, Olivia Fong, John C. Bowler, Satoshi Terada, Fraser T. Sparks, Gergely G. Szabo, Jordan S. Farrell, Jim Berg, Tanya L. Daigle, Bosiljka Tasic, Jordane Dimidschstein, Gord Fishell, Attila Losonczy, Hongkui Zeng, and Ivan Soltesz (2021). "Alternating sources of perisomatic inhibition during behavior". *Neuron*, pp. 1–16. DOI: 10.1016/j.neuron.2021.01.003.

Dumas, T.C., E.C. Powers, P.E. Tarapore, and R.M. Sapolsky (2004). "Overexpression of calbindin D28k in dentate gyrus granule cells alters mossy fiber presynaptic function and impairs hippocampal-dependent memory". *Hippocampus* 14.6, pp. 701–709. DOI: 10.1002/hipo.10210.

Durand, Guylaine M., Yury Kovalchuk, and Arthur Konnerth (1996). "Long-term potentiation and functional synapse induction in developing hippocampus". *Nature*. DOI: 10.1038/381071a0.

Eichenbaum, H., A. P. Yonelinas, and C. Ranganath (2007). "The medial temporal lobe and recognition memory". *Annual Review of Neuroscience* 30, pp. 123–152. DOI: 10.1146/annurev.neuro.30.051606.094328.

Eichenbaum, Howard (2014). "Time cells in the hippocampus: a new dimension for mapping memories". *Nature Reviews Neuroscience* 15.11, pp. 732–744. DOI: 10.1038/nrn3827.Time.

Erwin, Sarah R., Weinan Sun, Monique Copeland, Sarah Lindo, Nelson Spruston, and Mark S. Cembrowski (2020). "A Sparse, Spatially Biased Subtype of Mature Granule Cell Dominates Recruitment in Hippocampal-Associated Behaviors". *Cell Reports* 31.4, p. 107551. DOI: 10.1016/j.celrep.2020.107551.

Ewin, Sarah E, Antoine G Almonte, Eva Claudia Bach, Chelcie F Heaney, Ann M Chappell, Kimberly F Raab-Graham, and Jeffrey L Weiner (2019). "Chemogenetic inhibition of a monosynaptic projection from the basolateral amygdala to the ventral hippocampus reduces appetitive and consummatory alcohol drinking behaviors". *bioRxiv*, p. 529719. DOI: 10.1101/529719.

Fanselow, Michael S. and Hong-Wei Dong (2010). "Are the Dorsal and Ventral Hippocampus Functionally Distinct Structures?" *Neuron* 65.1, pp. 7–19. DOI: 10.1016/J.NEURON.2009.11.031.

Fattahi, Mohammad, Farnaz Sharif, Tristan Geiller, and Sébastien Royer (2018). "Differential representation of landmark and self-motion information along the CA1 radial axis: Self-motion generated place fields shift toward landmarks during septal inactivation". *Journal of Neuroscience* 38.30, pp. 6766–6778. DOI: 10.1523/JNEUROSCI.3211-17.2018.

Felix-Ortiz, Ada C., Anna Beyeler, Changwoo Seo, Christopher A. Leppla, Craig P. Wildes, and Kay M. Tye (2013). "BLA to vHPC inputs modulate anxiety-related behaviors". *Neuron* 79.4, pp. 658–664. DOI: 10.1016/j.neuron.2013.06.016.

Felix-Ortiz, Ada C. and Kay M. Tye (2014). "Amygdala inputs to the ventral hippocampus bidirectionally modulate social behavior". *Journal of Neuroscience* 34.2, pp. 586–595. DOI: 10.1523/JNEUROSCI.4257-13.2014.

Fernández-Ruiz, Antonio, Azahara Oliva, Gergő A. Nagy, Andrew P. Maurer, Antal Berényi, and György Buzsáki (2017). "Entorhinal-CA3 Dual-Input Control of Spike Timing in the Hippocampus by Theta-Gamma Coupling". *Neuron* 93.5, pp. 1213–1226. DOI: 10.1016/J.NEURON.2017.02.017.

Förster, Eckart, Shanting Zhao, and Michael Frotscher (2006). "Laminating the hippocampus". *Nature Reviews Neuroscience* 7.4, pp. 259–267. DOI: 10.1038/nrn1882.

Freund, Tamás F. and Miklós Antal (1988). "GABA-containing neurons in the septum control inhibitory interneurons in the hippocampus". *Nature*. DOI: 10.1038/336170a0.

Frey, Benicio N., Ana C. Andreazza, Fabiano G. Nery, Marcio R. Martins, João Quevedo, Jair C. Soares, and Flávio Kapczinski (2007). *The role of hippocampus in the pathophysiology of bipolar disorder*. DOI: 10.1097/FBP.0b013e3282df3cde.

Gan, Jian et al. (2016). "Phase-Locked Inhibition, but Not Excitation, Underlies Hippocampal Ripple Oscillations in Awake Mice In Vivo". *Neuron* 0.0, pp. 369–373. DOI: 10.1016/j.neuron.2016.12.018.

Garaschuk, Olga, Eric Hanse, and Arthur Konnerth (1998). "Developmental profile and synaptic origin of early network oscillations in the CA1 region of rat neonatal hippocampus". *Journal of Physiology*. DOI: 10.1111/j.1469-7793.1998.219bu.x.

Gauthier, Jeffrey L and David W Tank (2018). "A Dedicated Population for Reward Coding in the Hippocampus." *Neuron* 99.1, pp. 179–193. DOI: 10.1016/j.neuron.2018.06.008.

Geiller, Tristan, Mohammad Fattahi, June-Seek Choi, and Sébastien Royer (2017a). "Place cells are more strongly tied to landmarks in deep than in superficial CA1". *Nature Communications* 8, p. 14531. DOI: 10.1038/ncomms14531.

Geiller, Tristan, Sebastien Royer, June-Seek Choi, L Davachi, DJ Foster, S Leutgeb, C Ranganath, EI Moser, LM de la Prida, Y Obata, IR Wickersham, and S Tonegawa (2017b). "Segregated Cell Populations Enable Distinct Parallel Encoding within the Radial Axis of the CA1 Pyramidal Layer". *Experimental Neurobiology* 26.1, p. 1. DOI: 10.5607/en.2017.26.1.1.

Gergues, Mark M, Kasey J Han, Hye Sun Choi, Brandon Brown, Kelsey J Clausing, Victoria S Turner, Ilia D Vainchtein, Anna V Molofsky, and Mazen A Kheirbek (2020). "Circuit and molecular architecture of a ventral hippocampal network". *Nature Neuroscience*. DOI: 10.1038/s41593-020-0705-8.

Girardeau, Gabrielle, Karim Benchenane, Sidney I. Wiener, György Buzsáki, and Michaël B. Zugaro (2009). "Selective suppression of hippocampal ripples impairs spatial memory". *Nature Neuroscience* 12.10, pp. 1222–1223. DOI: 10.1038/nn.2384.

Girardeau, Gabrielle and Michaël Zugaro (2011). "Hippocampal ripples and memory consolidation". *Current Opinion in Neurobiology* 21.3, pp. 452–459. DOI: 10.1016/j.conb.2011.02.005.

Gokce, O., G.M. Stanley, B. Treutlein, N.F. Neff, J.G. Camp, R.C. Malenka, P.E. Rothwell, M.V. Fuccillo, T.C. Südhof, and S.R. Quake (2016). "Cellular Taxonomy of the Mouse Striatum as Revealed by Single-Cell RNA-Seq1. Gokce, O. et al. Cellular Taxonomy of the Mouse Striatum as Revealed by Single-Cell RNA-Seq. Cell Rep. 16, (2016)." *Cell Reports*. DOI: 10.1016/j.celrep.2016.06.059.

Gómez-Di Cesare, Caroline M., Karen L. Smith, Frank L. Rice, and John W. Swann (1997). "Axonal remodeling during postnatal maturation of CA3 hippocampal pyramidal neurons". *Journal of Comparative Neurology*. DOI: 10.1002/(sici)1096-9861(19970728)384:2<165::aid-cne1>3.0.co;2-{\%}23.

Goshen, Inbal, Matthew Brodsky, Rohit Prakash, Jenelle Wallace, Viviana Gradinaru, Charu Ramakrishnan, and Karl Deisseroth (2011). "Dynamics of retrieval strategies for remote memories". *Cell*. DOI: 10.1016/j.cell.2011.09.033.

Gouty-Colomer, Laurie-Anne, François J Michel, Agnès Baude, Catherine Lopez-Pauchet, Amandine Dufour, Rosa Cossart, and Constance Hammond (2018). "Mouse subthalamic nucleus neurons with local axon collaterals". *Journal of Comparative Neurology* 526.2, pp. 275–284. DOI: 10.1002/cne.24334.

Graves, Austin R, Shannon J Moore, Erik B Bloss, Brett D Mensh, William L Kath, and Nelson Spruston (2012). "Hippocampal pyramidal neurons comprise two distinct cell types that are countermodulated by metabotropic receptors." English. *Neuron* 76.4, pp. 776–89. DOI: 10.1016/j.neuron.2012.09.036.

Grieves, Roddy M. and Kate J. Jeffery (2017). "The representation of space in the brain". *Behavioural Processes* 135.December, pp. 113–131. DOI: 10.1016/j.beproc.2016.12.012.

Groen, T van and J M Wyss (1990). "Extrinsic projections from area CA1 of the rat hippocampus: olfactory, cortical, subcortical, and bilateral hippocampal formation projections." *The Journal of comparative neurology* 302.3, pp. 515–28. DOI: 10.1002/cne.903020308.

Grove, Elizabeth A. and Shubha Tole (1999). "Patterning events and specification signals in the developing hippocampus". *Cerebral Cortex* 9.6, pp. 551–561. DOI: 10.1093/cercor/9.6.551.

Gulyás, A. I., K. Tóth, C. J. McBain, and T. F. Freund (1998). "Stratum radiatum giant cells: A type of principal cell in the rat hippocampus". *European Journal of Neuroscience* 10.12, pp. 3813–3822. DOI: 10.1046/j.1460-9568.1998.00402.x.

Hafting, Torkel, Marianne Fyhn, Sturla Molden, May Britt Moser, and Edvard I. Moser (2005). "Microstructure of a spatial map in the entorhinal cortex". *Nature* 436.7052, pp. 801–806. DOI: 10.1038/nature03721.

Hand, Randal, Dante Bortone, Pierre Mattar, Laurent Nguyen, Julian Ik-Tsen Heng, Sabrice Guerrier, Elizabeth Boutt, Eldon Peters, Anthony P Barnes, Carlos Parras, Carol Schuurmans, François Guillemot, and Franck Polleux (2005). "Phosphorylation of Neurogenin2 specifies the migration properties and the dendritic morphology of pyramidal neurons in the neocortex." *Neuron* 48.1, pp. 45–62. DOI: 10.1016/j.neuron.2005.08.032.

Harland, Bruce, Marcos Contreras, and Jean-Marc Fellous (2018). "A Role for the Longitudinal Axis of the Hippocampus in Multiscale Representations of Large and Complex Spatial Environments and Mnemonic Hierarchies". In: *The Hippocampus - Plasticity and Functions*. InTech. DOI: 10.5772/intechopen.71165.

Harris, Kenneth D., Jozsef Csicsvari, Hajime Hirase, George Dragoi, and György Buzsáki (2003). "Organization of cell assemblies in the hippocampus". *Nature* 424.6948, pp. 552–556. DOI: 10.1038/nature01834.

Harris, Kenneth D., Hannah Hochgerner, Nathan G. Skene, Lorenza Magno, Linda Katona, Carolina Bengtsson Gonzales, Peter Somogyi, Nicoletta Kessaris, Sten Linnarsson, and Jens Hjerling-Leffler (2018). "Classes and continua of hippocampal CA1 inhibitory neurons revealed by single-cell transcriptomics". *PLoS Biology* 16.6, e2006387. DOI: 10.1371/journal.pbio.2006387.

Harris, Kristen M. and Timothy J. Teyler (1983). "Evidence for late development of inhibition in area CA1 of the rat hippocampus". *Brain Research*. DOI: 10.1016/0006-8993(83)90500-0.

Hartung, Henrike, Marco D. Brockmann, Beatrice Pöschel, Vito De Feo, and Ileana L. Hanganu-Opatz (2016). "Thalamic and entorhinal network activity differently modulates the functional development of prefrontal–hippocampal interactions". *Journal of Neuroscience* 36.13, pp. 3676–3690. DOI: 10.1523/JNEUROSCI.3232-15.2016.

Hasselmo, Michael E. (2006). "The role of acetylcholine in learning and memory". *Current Opinion in Neurobiology* 16.6, pp. 710–715. DOI: 10.1016/j.conb.2006.09.002.

Hasselmo, Michael E., Clara Bodelón, and Bradley P. Wyble (2002). "A proposed function for hippocampal theta rhythm: Separate phases of encoding and retrieval enhance reversal of prior learning". *Neural Computation*. DOI: 10.1162/089976602317318965.

Hatten, Mary E. (1990). *Riding the glial monorail: A common mechanism for glialguided neuronal migration in different regions of the developing mammalian brain*. DOI: 10.1016/0166-2236(90)90044-B.

Hayashi, Kanehiro, Ken-Ichiro Kubo, Ayako Kitazawa, and Kazunori Nakajima (2015). "Cellular dynamics of neuronal migration in the hippocampus." English. *Frontiers in neuroscience* 9, p. 135. DOI: 10.3389/fnins.2015.00135.

Henke, Peter G. (1990). "Hippocampal pathway to the amygdala and stress ulcer development". *Brain Research Bulletin* 25.5, pp. 691–695. DOI: 10.1016/0361-9230(90)90044-Z.

Henriksen, Espen J., Laura L. Colgin, Carol A. Barnes, Menno P. Witter, May-Britt Moser, and Edvard I. Moser (2010). "Spatial Representation along the Proximodistal Axis of CA1". *Neuron* 68.1, pp. 127–137. DOI: 10.1016/J.NEURON.2010.08.042.

Hirotsune, Shinji, Mark W. Fleck, Michael J. Gambello, Gregory J. Bix, Amy Chen, Gary D. Clark, David H. Ledbetter, Chris J. McBain, and Anthony Wynshaw-Boris (1998). "Graded reduction of Pafah1b1 (Lis1) activity results in neuronal migration defects and early embryonic lethality". *Nature Genetics*. DOI: 10.1038/1221.

Hitti, Frederick L. and Steven A. Siegelbaum (2014). "The hippocampal CA2 region is essential for social memory". *Nature* 508.7494, pp. 88–92. DOI: 10.1038/nature13028.

Hok, V, E Save, and B Poucet (2005). "Coding for Spatial Goals in the Prelimbic-Infralimbic". *Proceedings of the National Academy of Sciences (PNAS)*.

Hoover, Walter B. and Robert P. Vertes (2012). "Collateral projections from nucleus reuniens of thalamus to hippocampus and medial prefrontal cortex in the rat: A single and double retrograde fluorescent labeling study". *Brain Structure and Function* 217.2, pp. 191–209. DOI: 10.1007/s00429-011-0345-6.

Humphries, Mark D. and Tony J. Prescott (2010). *The ventral basal ganglia, a selection mechanism at the crossroads of space, strategy, and reward*. DOI: 10.1016/j.pneurobio.2009.11.003.

Hunsaker, Michael R. and Raymond P. Kesner (2008). "Dissociations across the dorsal-ventral axis of CA3 and CA1 for encoding and retrieval of contextual and auditory-cued fear". *Neurobiology of Learning and Memory*. DOI: 10.1016/j.nlm.2007.08.016.

Hunt, David L., Daniele Linaro, Bailu Si, Sandro Romani, and Nelson Spruston (2018). "A novel pyramidal cell type promotes sharp-wave synchronization in the hippocampus". *Nature Neuroscience* 21.7, pp. 1–11. DOI: 10.1038/s41593-018-0172-7.

Igarashi, Kei M., Hiroshi T. Ito, Edvard I. Moser, and May-Britt Moser (2014a). "Functional diversity along the transverse axis of hippocampal area CA1". *FEBS Letters* 588.15, pp. 2470–2476.

Igarashi, Kei M., Li Lu, Laura L. Colgin, May Britt Moser, and Edvard I. Moser (2014b). "Coordination of entorhinal-hippocampal ensemble activity during associative learning". *Nature* 510.7503, pp. 143–147. DOI: 10.1038/nature13162.

Ikonen, Sami, Robert McMahan, Michela Gallagher, Howard Eichenbaum, and Heikki Tanila (2002). *Cholinergic system regulation of spatial representation by the hippocampus*. DOI: 10.1002/hipo.1109.

Ishida, Akihiro, Kuniko Shimazaki, Toshio Terashima, and Nobufumi Kawai (1994). "An electrophysiological and immunohistochemical study of the hippocampus of the reeler mutant mouse". *Brain Research* 662.1-2, pp. 60–68. DOI: 10.1016/0006-8993(94)90795-1.

Ishino, Yugo, Michael J. Yetman, Serena M. Sossi, André Steinecke, Yasufumi Hayano, and Hiroki Taniguchi (2017). "Regional cellular environment shapes phenotypic variations of hippocampal and neocortical chandelier cells". *Journal of Neuroscience* 37.41, pp. 9901–9916. DOI: 10.1523/JNEUROSCI.0047-17.2017.

Ishizuka, N, J Weber, and D G Amaral (1990). "Organization of intrahippocampal projections originating from CA3 pyramidal cells in the rat." *The Journal of comparative neurology* 295.4, pp. 580–623. DOI: 10.1002/cne.902950407.

Ito, Hiroshi T. and Erin M. Schuman (2012). "Functional division of hippocampal area CA1 via modulatory gating of entorhinal cortical inputs". *Hippocampus* 22.2, pp. 372–387. DOI: 10.1002/hipo.20909.

Ito, Rutsuko, Trevor W. Robbins, Cyriel M. Pennartz, and Barry J. Everitt (2008). "Functional interaction between the hippocampus and nucleus accumbens shell is necessary for the acquisition of appetitive spatial context conditioning". *Journal of Neuroscience* 28.27, pp. 6950–6959. DOI: 10.1523/JNEUROSCI.1615-08.2008.

Izawa, Shuntaro, Srikanta Chowdhury, Toh Miyazaki, Yasutaka Mukai, Daisuke Ono, Ryo Inoue, Yu Ohmura, Hiroyuki Mizoguchi, Kazuhiro Kimura, Mitsuhiro Yoshioka, Akira Terao, Thomas S. Kilduff, and Akihiro Yamanaka (2019). "REM sleep–active MCH neurons are involved in forgetting hippocampus-dependent memories". *Science* 365.6459, pp. 1308–1313. DOI: 10.1126/science.aax9238.

Jacobson, Lauren and Robert Sapolsky (1991). "The role of the hippocampus in feedback regulation of the hypothalamic-pituitary-adrenocortical axis". *Endocrine Reviews*. DOI: 10.1210/edrv-12-2-118.

Jarsky, Tim, Rina Mady, Benjamin Kennedy, and Nelson Spruston (2008). "Distribution of bursting neurons in the CA1 region and the subiculum of the rat hippocampus." *The Journal of comparative neurology* 506.4, pp. 535–47. DOI: 10.1002/cne.21564.

Jawaid, Safdar, Grahame J. Kidd, Jing Wang, Carrie Swetlik, Ranjan Dutta, and Bruce D. Trapp (2018). "Alterations in CA1 hippocampal synapses in a mouse model of fragile X syndrome". *Glia* 66.4, pp. 789–800. DOI: 10.1002/glia.23284.

Jimenez, Jessica C, Jack E. Berry, Sean C. Lim, Samantha K. Ong, Mazen A. Kheirbek, and Rene Hen (2020). "Contextual fear memory retrieval by correlated ensembles of ventral CA1 neurons". *Nature Communications* 11.1, p. 3492. DOI: 10.1038/s41467-020-17270-w.

Jimenez, Jessica C, Katy Su, Alexander R Goldberg, Victor M Luna, Jeremy S Biane, Gokhan Ordek, Pengcheng Zhou, Samantha K Ong, Matthew A Wright, Larry Zweifel, Liam Paninski, René Hen, and Mazen A Kheirbek (2018). "Anxiety Cells in a Hippocampal-Hypothalamic Circuit". *Neuron* 97.3, pp. 670–683. DOI: 10.1016/j.neuron.2018.01.016.

Joyner, Alexandra L. and Mark Zervas (2006). "Genetic inducible fate mapping in mouse: Establishing genetic lineages and defining genetic neuroanatomy in the nervous system". *Developmental Dynamics* 235.9, pp. 2376–2385. DOI: 10.1002/dvdy.20884.

Jung, Min W., Sidney I. Wiener, and Bruce L. McNaughton (1994). "Comparison of spatial firing characteristics of units in dorsal and ventral hippocampus of the rat". *Journal of Neuroscience* 14.12, pp. 7347–7356. DOI: 10.1523/jneurosci.14-12-07347.1994.

Kaczorowski, Catherine Cook, John Disterhoft, and Nelson Spruston (2007). "Stability and plasticity of intrinsic membrane properties in hippocampal CA1 pyramidal neurons: Effects of internal anions". *The Journal of Physiology* 578.3, pp. 799–818. DOI: 10.1113/jphysiol.2006.124586.

Kandel, Eric R. (2004). "The molecular biology of memory storage: A dialog between genes and synapses". In: *Bioscience Reports*. DOI: 10.1007/s10540-005-2742-7.

Keinath, Alexander T., Melissa E. Wang, Ellen G. Wann, Robin K. Yuan, Joshua T. Dudman, and Isabel A. Muzzio (2014). "Precise spatial coding is preserved along the longitudinal hippocampal axis". *Hippocampus* 24.12, pp. 1533–1548. DOI: 10.1002/hipo.22333.

Kelley, A.E. and V.B. Domesick (1982). "The distribution of the projection from the hippocampal formation to the nucleus accumbens in the rat: An anterograde and retrograde-horseradish peroxidase study". *Neuroscience* 7.10, pp. 2321–2335. DOI: 10.1016/0306-4522(82)90198-1.

Kempadoo, Kimberly A., Eugene V. Mosharov, Se Joon Choi, David Sulzer, and Eric R. Kandel (2016). "Dopamine release from the locus coeruleus to the dorsal hippocampus promotes spatial learning and memory". *Proceedings of the National Academy of Sciences of the United States of America* 113.51, pp. 14835–14840. DOI: 10.1073/pnas.1616515114.

Khalaf-Nazzal, R. and F. Francis (2013). "Hippocampal development - old and new findings." *Neuroscience* 248, pp. 225–42. DOI: 10.1016/j.neuroscience.2013.05.061.

Khazipov, Roustem, Ilgam Khalilov, Roman Tyzio, Elena Morozova, Yezekiel Ben-Ari, and Gregory L. Holmes (2004). "Developmental changes in GABAergic actions and seizure susceptibility in the rat hippocampus". *European Journal of Neuroscience*. DOI: 10.1111/j.0953-816X.2003.03152.x.

Kheirbek, Mazen A., Kristen C. Klemenhagen, Amar Sahay, and René Hen (2012). *Neurogenesis and generalization: A new approach to stratify and treat anxiety disorders*. DOI: 10.1038/nn.3262.

Kim, Jeansok J. and Michael S. Fanselow (1992). "Modality-specific retrograde amnesia of fear". *Science* 256.5057, pp. 675–677. DOI: 10.1126/science.1585183.

Kitazawa, Ayako, Ken-ichiro Kubo, Kanehiro Hayashi, Yuki Matsunaga, Kazuhiro Ishii, and Kazunori Nakajima (2014). "Hippocampal pyramidal neurons switch from a multipolar migration mode to a novel "climbing" migration mode during development." *The Journal of neuroscience : the official journal of the Society for Neuroscience* 34.4, pp. 1115–26. DOI: 10.1523/JNEUROSCI.2254-13.2014.

Kjelstrup, Kirsten Brun, Trygve Solstad, Vegard Heimly Brun, Torkel Hafting, Stefan Leutgeb, Menno P. Witter, Edvard I. Moser, and May Britt Moser (2008). "Finite scale of spatial representation in the hippocampus". *Science*. DOI: 10.1126/science.1157086.

Kjelstrup, Kirsten G., Frode A. Tuvnes, Hill Aina Steffenach, Robert Murison, Edvard I. Moser, and May Britt Moser (2002). "Reduced fear expression after lesions of the ventral hippocampus". *Proceedings of the National Academy of Sciences of the United States of America* 99.16, pp. 10825–10830. DOI: 10.1073/pnas.152112399.

Klausberger, Thomas and Peter Somogyi (2008). "Neuronal diversity and temporal dynamics: the unity of hippocampal circuit operations." en. *Science (New York, N.Y.)* 321.5885, pp. 53–7. DOI: 10.1126/science.1149381.

Kohara, Keigo, Michele Pignatelli, Alexander J Rivest, Hae-Yoon Jung, Takashi Kitamura, Junghyup Suh, Dominic Frank, Koichiro Kajikawa, Nathan Mise, Yuichi Obata, Ian R Wickersham, and Susumu Tonegawa (2014). "Cell type-specific genetic and optogenetic tools reveal hippocampal CA2 circuits." en. *Nature neuroscience* 17.2, pp. 269–79. DOI: 10.1038/nn.3614.

Kowalski, Timothy J., Constance Farley, Mary E. Cohen-Williams, Geoffrey Varty, and Brian D. Spar (2004). "Melanin-concentrating hormone-1 receptor antagonism decreases feeding by reducing meal size". *European Journal of Pharmacology*. DOI: 10.1016/j.ejphar.2004.06.027.

Labiner, D. M., L. S. Butler, Z. Cao, D. A. Hosford, C. Shin, and J. O. McNamara (1993). "Induction of c-fos mRNA by kindled seizures: Complex relationship with neuronal burst firing". *Journal of Neuroscience* 13.2, pp. 744–751. DOI: 10.1523/jneurosci.13-02-00744.1993.

Lasztóczi, Bálint and Thomas Klausberger (2014). "Layer-specific GABAergic control of distinct gamma oscillations in the CA1 hippocampus". *Neuron* 81.5, pp. 1126–1139. DOI: 10.1016/j.neuron.2014.01.021.

Lawson, Victoria H. and Brian H. Bland (1993). "The Role of the Septohippocampal Pathway in the Regulation of Hippocampal Field Activity and Behavior: Analysis by the Intraseptal Microinfusion of Carbachol, Atropine, and Procaine". *Experimental Neurology*. DOI: 10.1006/exnr.1993.1047.

Lee, Sang-Hun, Ivan Marchionni, Marianne Bezaire, Csaba Varga, Nathan Danielson, Matthew Lovett-Barron, Attila Losonczy, and Ivan Soltesz (2014). "Parvalbumin-positive basket cells differentiate among hippocampal pyramidal cells." *Neuron* 82.5, pp. 1129–44. DOI: 10.1016/j.neuron.2014.03.034.

LeGates, Tara A., Mark D. Kvarta, Jessica R. Tooley, T. Chase Francis, Mary Kay Lobo, Meaghan C. Creed, and Scott M. Thompson (2018). "Reward behaviour is regulated by the strength of hippocampus–nucleus accumbens synapses". *Nature* 564.7735, pp. 258–262. DOI: 10.1038/s41586-018-0740-8.

Leinekugel, Xavier, Rustem Khazipov, Robert Cannon, Hajime Hirase, Yehezkel Ben-Ari, and György Buzsáki (2002). "Correlated bursts of activity in the neonatal hippocampus in vivo". *Science*. DOI: 10.1126/science.1071111.

Lembo, Paola M.C., Eric Grazzini, Jack Cao, Douglas A. Hubatsch, Manon Pelletier, Cyrla Hoffert, Stephane St-Onge, Chantevy Pou, Jean Labrecque, Thierry Groblewski, Dajan O'Donnell, Kemal Payza, Sultan Ahmad, and Philippe Walker (1999). "The receptor for the orexigenic peptide melanin-concentrating hormone is a G-protein-coupled receptor". *Nature Cell Biology* 1.5, pp. 267–271. DOI: 10.1038/12978.

Lemon, Neal and Denise Manahan-Vaughan (2012). "Dopamine D1/D5 receptors contribute to de novo hippocampal LTD mediated by novel spatial exploration or locus coeruleus activity". *Cerebral Cortex*. DOI: 10.1093/cercor/bhr297.

Leung, L. Stan, Bixia Shen, Nagalingam Rajakumar, and Jingyi Ma (2003). "Cholinergic Activity Enhances Hippocampal Long-Term Potentiation in CA1 during Walking in Rats". *Journal of Neuroscience*. DOI: 10.1523/jneurosci.23-28-09297.2003.

Leutgeb, Stefan, Jill K. Leutgeb, Carol A. Barnes, Edvard I. Moser, Bruce L. McNaughton, and May Britt Moser (2005). "Neuroscience: Independent codes for spatial and episodic memory in hippocampal neuronal ensembles". *Science* 309.5734, pp. 619–623. DOI: 10.1126/science.1114037.

Leutgeb, Stefan and Sheri J.Y. Mizumori (1999). "Excitotoxic septal lesions result in spatial memory deficits and altered flexibility of hippocampal single-unit representations". *Journal of Neuroscience*. DOI: 10.1523/jneurosci.19-15-06661.1999.

Lever, Colin, Stephen Burton, Ali Jeewajee, John O'Keefe, and Neil Burgess (2009). "Boundary Vector Cells in the Subiculum of the Hippocampal Formation". *Journal of Neuroscience* 29.31.

Lewis, David A., Allison A. Curley, Jill R. Glausier, and David W. Volk (2012). *Cortical parvalbumin interneurons and cognitive dysfunction in schizophrenia*. DOI: 10.1016/j.tins.2011.10.004.

Li, Jie, Rena Y Jiang, Kristin L Arendt, Yu-tien Hsu, Sophia R Zhai, and Lu Chen (2020). "Defective memory engram reactivation underlies impaired fear memory recall in Fragile X syndrome", pp. 1–20.

Li, Shaomin, William K. Cullen, Roger Anwyl, and Michael J. Rowan (2003). "Dopamine-dependent facilitation of LTP induction in hippocampal CA1 by exposure to spatial novelty". *Nature Neuroscience*. DOI: 10.1038/nn1049.

Li, Xinyan, Wenting Chen, Kai Pan, Hao Li, Pei Pang, Yu Guo, Shu Shu, You Cai, Lei Pei, Dan Liu, Henok Kessete Afewerky, Qing Tian, Ling-Qiang Zhu, and Youming Lu (2018). "Serotonin receptor 2c-expressing cells in the ventral CA1 control attention via innervation of the Edinger–Westphal nucleus". *Nature Neuroscience* 21.9, pp. 1239–1250. DOI: 10.1038/s41593-018-0207-0.

Li, Yiding, Jiamin Xu, Yafeng Liu, Jia Zhu, Nan Liu, Wenbo Zeng, Ning Huang, Malte J Rasch, Haifei Jiang, Xiang Gu, Xiang Li, Minhua Luo, Chengyu Li, Junlin Teng, Jianguo Chen, Shaoqun Zeng, Longnian Lin, and Xiaohui Zhang (2017). "A distinct entorhinal cortex to hippocampal CA1 direct circuit for olfactory associative learning". *Nature Neuroscience* 20.4, pp. 559–570. DOI: 10.1038/nn.4517.

Lima, Susana Q. SQ et al. (2009). "PINP: A New Method of Tagging Neuronal Populations for Identification during In Vivo Electrophysiological Recording". *PLoS ONE* 4.7. Ed. by Michael N. Nitabach, e6099. DOI: 10.1371/journal.pone.0006099.

Lisman, John E. and Anthony A. Grace (2005). *The hippocampal-VTA loop: Controlling the entry of information into long-term memory*. DOI: 10.1016/j.neuron.2005.05.002.

Lo, Liching, Shenqin Yao, Dong Wook Kim, Ali Cetin, Julie Harris, Hongkui Zeng, David J. Anderson, and Brandon Weissbourd (2019). "Connectional architecture of a mouse hypothalamic circuit node controlling social behavior". *Proceedings of the National Academy of Sciences of the United States of America* 116.15, pp. 7503–7512. DOI: 10.1073/pnas.1817503116.

Lorente De Nó, R. (1934). "Studies on the structure of the cerebral cortex. II. Continuation of the study of the ammonic system." *J Psychol Neurol* 46, pp. 113–17.

Loureiro, Michael, Lucas Lecourtier, Michel Engeln, Joëlle Lopez, Brigitte Cosquer, Karin Geiger, Christian Kelche, Jean Christophe Cassel, and Anne Pereira De Vasconcelos (2012). "The ventral hippocampus is necessary for expressing a spatial memory". *Brain Structure and Function* 217.1, pp. 93–106. DOI: 10.1007/s00429-011-0332-y.

Luzzati, Federico (2015). "A hypothesis for the evolution of the upper layers of the neocortex through co-option of the olfactory cortex developmental program". *Frontiers in Neuroscience* 9.APR, pp. 1–12. DOI: 10.3389/fnins.2015.00162.

Mahringer, David, Anders V. Petersen, Aris Fiser, Hiroyuki Okuno, Haruhiko Bito, Jean-François Perrier, and Georg B. Keller (2019). "Expression of c-Fos and Arc in hippocampal region CA1 marks neurons that exhibit learning-related activity changes". *bioRxiv*, p. 644526. DOI: 10.1101/644526.

Malik, Ruchi, Kelly Ann Dougherty, Komal Parikh, Connor Byrne, and Daniel Johnston (2016). "Mapping the electrophysiological and morphological properties of CA1 pyramidal neurons along the longitudinal hippocampal axis". *Hippocampus* 26.3, pp. 341–361. DOI: 10.1002/hipo.22526.

Mallory, Caitlin S and Lisa M Giocomo (2018). "Heterogeneity in hippocampal place coding". *Current Opinion in Neurobiology* 49, pp. 158–167. DOI: 10.1016/j.conb.2018.02.014.

Manent, Jean Bernard, Isabel Jorquera, Yehezkel Ben-Ari, Laurent Aniksztejn, and Alfonso Represa (2006). "Glutamate acting on AMPA but not NMDA receptors modulates the migration of hippocampal interneurons". *Journal of Neuroscience* 26.22, pp. 5901–5909. DOI: 10.1523/JNEUROSCI.1033-06.2006.

Marek, Roger, Jingji Jin, Travis D. Goode, Thomas F. Giustino, Qian Wang, Gillian M. Acca, Roopashri Holehonnur, Jonathan E. Ploski, Paul J. Fitzgerald, Timothy Lynagh, Joseph W. Lynch, Stephen Maren, and Pankaj Sah (2018). "Hippocampus-driven feed-forward inhibition of the prefrontal cortex mediates relapse of extinguished fear". *Nature Neuroscience* 21.3, p. 384. DOI: 10.1038/s41593-018-0073-9.

Maren, Stephen and William G. Holt (2004). "Hippocampus and Pavlovian Fear Conditioning in Rats: Muscimol Infusions into the Ventral, but Not Dorsal, Hippocampus Impair the Acquisition of Conditional Freezing to an Auditory Conditional Stimulus". *Behavioral Neuroscience*. DOI: 10.1037/0735-7044.118.1.97.

Marissal, Thomas, Paolo Bonifazi, Michel Aimé Picardo, Romain Nardou, Ludovic Franck Petit, Agnès Baude, Gordon James Fishell, Yehezkel Ben-Ari, and Rosa Cossart (2012). "Pioneer glutamatergic cells develop into a morpho-functionally distinct population in the juvenile CA3 hippocampus." *Nature communications* 3, p. 1316. DOI: 10.1038/ncomms2318.

Maroso, Mattia, Gergely G. Szabo, Hannah K. Kim, Allyson Alexander, Anh D. Bui, Sang-Hun Lee, Beat Lutz, and Ivan Soltesz (2016). "Cannabinoid Control of Learning and Memory through HCN Channels". *Neuron* 89.5, pp. 1059–1073. DOI: 10.1016/j.neuron.2016.01.023.

Marozzi, Elizabeth and Kathryn J. Jeffery (2012). "Place, space and memory cells". *Current Biology* 22.22, R939–R942. DOI: 10.1016/j.cub.2012.10.022.

Marrosu, Francesco, Chiara Portas, Maria Stefania Mascia, Maria Antonietta Casu, Mauro Fà, Marcello Giagheddu, Assunta Imperato, and Gian Luigi Gessa (1995). "Microdialysis measurement of cortical and hippocampal acetylcholine release during sleep-wake cycle in freely moving cats". *Brain Research*. DOI: 10.1016/0006-8993(94)01399-3.

Masurkar, Arjun V (2018). "Towards a Circuit-Level Understanding of Hippocampal CA1 Dysfunction in Alzheimer's Disease Across Anatomical Axes". *Journal of Alzheimer's Disease & Parkinsonism* 08.01, pp. 1–6. DOI: 10.4172/2161-0460.1000412.

Masurkar, Arjun V, Kalyan V Srinivas, David H Brann, Richard Warren, Daniel C Lowes, and Steven A Siegelbaum (2017). "Medial and Lateral Entorhinal Cortex Differentially Excite Deep versus Superficial CA1 Pyramidal Neurons". *CellReports* 18, pp. 148–160. DOI: 10.1016/j.celrep.2016.12.012.

Masurkar, Arjun V, Chengju Tian, Richard Warren, Isabel Reyes, Daniel C Lowes, David H Brann, and Steven A. Siegelbaum (2020). "Postsynaptic integrative properties of dorsal CA1 pyramidal neuron subpopulations". *Journal of Neurophysiology*. DOI: 10.1152/jn.00397.2019.

McEwen, Bruce S. and Ana Maria Magarinos (1997). "Stress Effects on Morphology and Function of the Hippocampus". *Annals of the New York Academy of Sciences* 821.1 Psychobiology, pp. 271–284. DOI: 10.1111/j.1749-6632.1997.tb48286.x.

McKenna, James Timothy and Robert P. Vertes (2004). "Afferent projections to nucleus reuniens of the thalamus". *Journal of Comparative Neurology*. DOI: 10.1002/cne.20342.

McKenzie, Sam, Roman Huszár, Daniel F. English, Kanghwan Kim, Fletcher Christensen, Euisik Yoon, and György Buzsáki (2021). "Preexisting hippocampal network dynamics constrain optogenetically induced place fields". *Neuron*. DOI: 10.1016/j.neuron.2021.01.011.

McNamara, Colin G., Álvaro Tejero-Cantero, Stéphanie Trouche, Natalia Campo-Urriza, and David Dupret (2014). "Dopaminergic neurons promote hippocampal reactivation and spatial memory persistence". *Nature Neuroscience* 17.12, pp. 1658–1660. DOI: 10.1038/nn.3843.

McNaughton, Bruce L., Francesco P. Battaglia, Ole Jensen, Edvard I. Moser, and May Britt Moser (2006). "Path integration and the neural basis of the 'cognitive map'". *Nature Reviews Neuroscience* 7.8, pp. 663–678. DOI: 10.1038/nrn1932.

Medina, Loreta and Antonio Abellán (2009). "Development and evolution of the pallium". *Seminars in Cell and Developmental Biology* 20.6, pp. 698–711. DOI: 10.1016/j.semcdb.2009.04.008.

Megías, M., Zs Emri, T. F. Freund, and A. I. Gulyás (2001). "Total number and distribution of inhibitory and excitatory synapses on hippocampal CA1 pyramidal cells". *Neuroscience* 102.3, pp. 527–540. DOI: 10.1016/S0306-4522(00)00496-6.

Meira, Torcato, Félix Leroy, Eric W. Buss, Azahara Oliva, Jung Park, and Steven A. Siegelbaum (2018). "A hippocampal circuit linking dorsal CA2 to ventral CA1 critical for social memory dynamics". *Nature Communications* 2018, pp. 1–14. DOI: 10.1038/s41467-018-06501-w.

Menendez de la Prida, L, S Bolea, and J V Sanchez-Andres (1996). "Analytical characterization of spontaneous activity evolution during hippocampal development in the rabbit." *Neuroscience letters* 218.3, pp. 185–7.

Meneses, Alfredo (2013). "5-HT systems: Emergent targets for memory formation and memory alterations". *Reviews in the Neurosciences* 24.6, pp. 629–664. DOI: 10.1515/revneuro-2013-0026.

Micheau, Jacques and Aline Marighetto (2011). "Acetylcholine and memory: A long, complex and chaotic but still living relationship". *Behavioural Brain Research* 221.2, pp. 424–429. DOI: 10.1016/j.bbr.2010.11.052.

Milior, Giampaolo, Maria Amalia Di Castro, Livio Pepe' Sciarria, Stefano Garofalo, Igor Branchi, Davide Ragozzino, Cristina Limatola, and Laura Maggi (2016). "Electrophysiological Properties of CA1 Pyramidal Neurons along the Longitudinal Axis of the Mouse Hippocampus". *Scientific Reports* 6.1, p. 38242. DOI: 10.1038/srep38242.

Miyoshi, Goichi and Gord Fishell (2011). "GABAergic interneuron lineages selectively sort into specific cortical layers during early postnatal development". *Cerebral Cortex*. DOI: 10.1093/cercor/bhq155.

Mizuseki, K, K Diba, E Pastalkova, and G Buzsáki (2011). "Hippocampal CA1 pyramidal cells form functionally distinct sublayers". en. *Nature neuroscience* 14.9, pp. 1174–. DOI: 10.1038/nn.2894.Hippocampal.

Mlinar, Boris and Renato Corradetti (2018). "Differential modulation of CA1 impulse flow by endogenous serotonin along the hippocampal longitudinal axis". *Hippocampus* 28.3, pp. 217–225. DOI: 10.1002/hipo.22825.

Mohns, Ethan J. and Mark S. Blumberg (2010). "Neocortical activation of the hippocampus during sleep in infant rats". *Journal of Neuroscience*. DOI: 10.1523/JNEUROSCI.4832-09.2010.

Moita, Marta A.P., Svetlana Rosis, Yu Zhou, Joseph E. LeDoux, and Hugh T. Blair (2003). "Hippocampal place cells acquire location-specific responses to the conditioned stimulus during auditory fear conditioning". *Neuron*. DOI: 10.1016/S0896-6273(03)00033-3.

Monuki, Edwin S., Forbes D. Porter, and Christopher A. Walsh (2001). "Patterning of the dorsal telencephalon and cerebral cortex by a roof plate-lhx2 pathway". *Neuron* 32.4, pp. 591–604. DOI: 10.1016/S0896-6273(01)00504-9.

Moser, Edvard I., Yasser Roudi, Menno P. Witter, Clifford Kentros, Tobias Bonhoeffer, and May Britt Moser (2014). *Grid cells and cortical representation*. DOI: 10.1038/nrn3766.

Moser, May-Britt, David C Rowland, and Edvard I Moser (2015). "Place Cells, Grid Cells, and Memory". *Cold Spring Harbor perspectives in biology*, pp. 1–16.

Mukhtar, Tanzila and Verdon Taylor (2018). "Untangling Cortical Complexity During Development". *Journal of Experimental Neuroscience* 12, p. 117906951875933. DOI: 10.1177/1179069518759332.

Müller, Christina and Stefan Remy (2014). "Dendritic inhibition mediated by O-LM and bistratified interneurons in the hippocampus". *Frontiers in Synaptic Neuroscience* 6.SEP, p. 23. DOI: 10.3389/fnsyn.2014.00023.

Naber, Pieterke A., Fernando H. Lopes Da Silva, and Menno P. Witter (2001). "Reciprocal connections between the entorhinal cortex and hippocampal fields CA1 and the subiculum are in register with the projections from CA1 to the subiculum". *Hippocampus* 11.2, pp. 99–104. DOI: 10.1002/hipo.1028.

Nádasdy, Zoltán, Hajime Hirase, András Czurko, Jozsef Csicsvari, and György Buzsáki (1999). "Replay and Time Compression of Recurring Spike Sequences inthe Hippocampus". *The Journal of Neuroscience* 19.21, pp. 9497–9507.

Nakahira, Eiko and Shigeki Yuasa (2005). "Neuronal generation, migration, and differentiation in the mouse hippocampal primoridium as revealed by enhanced green fluorescent protein gene transfer by means of in utero electroporation". *Journal of Comparative Neurology* 483.3, pp. 329–340. DOI: 10.1002/cne.20441.

Nasrallah, Kaoutsar, Ludivine Therreau, Vincent Robert, Arthur J.Y. Huang, Thomas J. McHugh, Rebecca A. Piskorowski, and Vivien Chevaleyre (2019). "Routing Hippocampal Information Flow through Parvalbumin Interneuron Plasticity in Area CA2". *Cell Reports* 27.1, pp. 86–98. DOI: 10.1016/j.celrep.2019.03.014.

Nielsen, Jakob V., Jonas B. Blom, Jens Noraberg, and Niels A. Jensen (2010). "Zbtb20-Induced CA1 pyramidal neuron development and area enlargement in the cerebral midline cortex of mice". *Cerebral Cortex* 20.8, pp. 1904–1914. DOI: 10.1093/cercor/bhp261.

Noble, Emily E., Zhuo Wang, Clarissa M. Liu, Elizabeth A. Davis, Andrea N. Suarez, Lauren M. Stein, Linda Tsan, Sarah J. Terrill, Ted M. Hsu, A-Hyun Jung, Lauren M. Raycraft, Joel D. Hahn, Martin Darvas, Alyssa M. Cortella, Lindsey A. Schier, Alexander W. Johnson, Matthew R. Hayes, Daniel P. Holschneider, and Scott E. Kanoski (2019). "Hypothalamus-hippocampus circuitry regulates impulsivity via melanin-concentrating hormone". *Nature Communications* 10.1, p. 4923. DOI: 10.1038/s41467-019-12895-y.

Nolan, Matthew F., Gaël L Malleret, Josh T. Dudman, Derek L. Buhl, Bina Santoro, Emma Gibbs, Svetlana Vronskaya, Gyö Rgy, Buzsá Ki, Steven A. Siegelbaum, Eric R. Kandel, Alexei Morozov, György Buzsáki, Steven A. Siegelbaum, Eric R. Kandel, and Alexei Morozov (2004). "A Behavioral Role for Dendritic Integration: HCN1 Channels Constrain Spatial Memory and

Plasticity at Inputs to Distal Dendrites of CA1 Pyramidal Neurons". *Cell* 119.5, pp. 719–732. DOI: 10.1016/j.cell.2004.11.020.

Nyakas, C., P. G.M. Luiten, D. G. Spencer, and J. Traber (1987). "Detailed projection patterns of septal and diagonal band efferents to the hippocampus in the rat with emphasis on innervation of CA1 and dentate gyrus". *Brain Research Bulletin* 18.4, pp. 533–545. DOI: 10.1016/0361-9230(87)90117-1.

O'Keefe, J. and J. Dostrovsky (1971). "The hippocampus as a spatial map . Preliminary evidence from unit activity in the freely-moving rat". *Brain Research* 34.1, pp. 171–175.

O'Keefe, J. and L. Nadel (1978). *The Hippocampus as a Cognitive Map*. Vol. 27. DOI: 10.5840/philstudies19802725.

O'Neill, Joseph, Barty Pleydell-Bouverie, David Dupret, and Jozsef Csicsvari (2010). *Play it again: reactivation of waking experience and memory*. DOI: 10.1016/j.tins.2010.01.006.

Okuyama, Teruhiro (2018). "Social memory engram in the hippocampus". *Neuroscience Research* 129, pp. 17–23. DOI: 10.1016/J.NEURES.2017.05.007.

Okuyama, Teruhiro, Takashi Kitamura, Dheeraj S Roy, Shigeyoshi Itohara, and Susumu Tonegawa (2016). "Ventral CA1 neurons store social memory." *Science (New York, N.Y.)* 353.6307, pp. 1536–1541. DOI: 10.1126/science.aaf7003.

Oliva, Azahara, Antonio Fernández-Ruiz, György Buzsáki, and Antal Berényi (2016a). "Spatial coding and physiological properties of hippocampal neurons in the Cornu Ammonis subregions". *Hippocampus* 26.12, pp. 1593–1607. DOI: 10.1002/hipo.22659.

Oliva, Azahara et al. (2016b). "Role of Hippocampal CA2 Region in Triggering Sharp-Wave Ripples". *Neuron* 91.6, pp. 1342–1355. DOI: 10.1016/j.neuron.2016.08.008.

Ozen, Ilknur, Christophe Galichet, Colin Watts, Carlos Parras, François Guillemot, and Olivier Raineteau (2007). "Proliferating neuronal progenitors in the postnatal hippocampus transiently express the proneural gene Ngn2." *The European journal of neuroscience* 25.9, pp. 2591–603. DOI: 10.1111/j.1460-9568.2007.05541.x.

Padilla-Coreano, Nancy, Scott S Bolkan, Georgia M Pierce, Dakota R Blackman, William D Hardin, Alvaro L Garcia-Garcia, Timothy J Spellman, and Joshua A Gordon (2016). "Direct Ventral Hippocampal-Prefrontal Input Is Required for Anxiety-Related Neural Activity and Behavior." *Neuron* 89.4, pp. 857–66. DOI: 10.1016/j.neuron.2016.01.011.

Padilla-Coreano, Nancy, Sarah Canetta, Rachel M. Mikofsky, Emily Alway, Johannes Passecker, Maxym V. Myroshnychenko, Alvaro L. Garcia-Garcia, Richard Warren, Eric Teboul, Dakota R. Blackman, Mitchell P. Morton, Sofiya Hupalo, Kay M. Tye, Christoph Kellendonk, David A. Kupferschmidt, and Joshua A. Gordon (2019). "Hippocampal-Prefrontal Theta Transmission Regulates Avoidance Behavior". *Neuron*, pp. 1–10. DOI: 10.1016/j.neuron.2019.08.006.

Palacios-Filardo, Jon and Jack R. Mellor (2019). "Neuromodulation of hippocampal long-term synaptic plasticity". *Current Opinion in Neurobiology* 54, pp. 37–43. DOI: 10.1016/j.conb.2018.08.009.

Palacios-Filardo, Jon, Matt Udakis, Giles A Brown, Benjamin G Tehan, Miles S Congreve, Pradeep J Nathan, Alastair J H Brown, and Jack Mellor (2020). "Acetylcholine prioritises direct synaptic inputs from entorhinal cortex to 1 CA1 by differential modulation of feedforward inhibitory circuits". *bioRxiv*, p. 2020.01.20.912873. DOI: 10.1101/2020.01.20.912873.

Pang, Cindy Chi Ching, Clemens Kiecker, John T. O'Brien, Wendy Noble, and Raymond Chuen Chung Chang (2019). *Ammon's Horn 2 (CA2) of the Hippocampus: A Long-Known Region with a New Potential Role in Neurodegeneration*. DOI: 10.1177/1073858418778747.

Paoletti, P., A. M. Vergnano, B. Barbour, and M. Casado (2009). *Zinc at glutamatergic synapses*. DOI: 10.1016/j.neuroscience.2008.01.061.

Papez, James W. (1937). "A proposed mechanism of emotion". *Archives of Neurology And Psychiatry* 38.4, pp. 725–743. DOI: 10.1001/archneurpsyc.1937.02260220069003.

Parfitt, Gustavo Morrone, Robin Nguyen, Jee Yoon Bang, Afif J. Aqrabawi, Matthew M. Tran, D. Kanghoon Seo, Blake A. Richards, and Jun Chul Kim (2017). "Bidirectional Control of Anxiety-Related Behaviors in Mice: Role of Inputs Arising from the Ventral Hippocampus to the Lateral Septum and Medial Prefrontal Cortex". *Neuropsychopharmacology*. DOI: 10.1038/npp.2017.56.

Peleg-Raibstein, Daria and Joram Feldon (2006). "Effects of dorsal and ventral hippocampal NMDA stimulation on nucleus accumbens core and shell dopamine release". *Neuropharmacology*. DOI: 10.1016/j.neuropharm.2006.06.002.

Pentkowski, Nathan S., D. Caroline Blanchard, Colin Lever, Yoav Litvin, and Robert J. Blanchard (2006). "Effects of lesions to the dorsal and ventral hippocampus on defensive behaviors in rats". *European Journal of Neuroscience*. DOI: 10.1111/j.1460-9568.2006.04754.x.

Phillips, Mary L, Holly Anne Robinson, and Lucas Pozzo-Miller (2019). "Ventral hippocampal projections to the medial prefrontal cortex regulate social memory". *eLife* 8. DOI: 10.7554/eLife.44182.

Phillips, R. G. and J. E. LeDoux (1992). "Differential Contribution of Amygdala and Hippocampus to Cued and Contextual Fear Conditioning". *Behavioral Neuroscience*. DOI: 10.1037/0735-7044.106.2.274.

Pi, Guilin, Di Gao, Dongqin Wu, Yali Wang, Huiyang Lei, Wenbo Zeng, Yang Gao, Huiling Yu, Rui Xiong, Tao Jiang, Shihong Li, Xin Wang, Jing Guo, Si Zhang, Taoyuan Yin, Ting He, Dan Ke, Ruining Li, Honglian Li, Gongping Liu, Xifei Yang, Min–Hua –H Luo, Xiaohui Zhang, Ying Yang, and Jian–Zhi –Z Wang (2020). "Posterior basolateral amygdala to ventral hippocampal CA1 drives approach behaviour to exert an anxiolytic effect". *Nature Communications* 11.1, pp. 1–15. DOI: 10.1038/s41467-019-13919-3.

Picardo, Michel Aimé, Philippe Guigue, Paolo Bonifazi, Renata Batista-Brito, Camille Allene, Alain Ribas, Gord Fishell, Agnès Baude, and Rosa Cossart (2011). "Pioneer GABA cells comprise a subpopulation of hub neurons in the developing hippocampus." *Neuron* 71.4, pp. 695–709. DOI: 10.1016/j.neuron.2011.06.018.

Pikkarainen, Maria and Asla Pitkänen (2001). "Projections from the Lateral, Basal and Accessory Basal Nuclei of the Amygdala to the Perirhinal and Postrhinal Cortices in Rat". *Cerebral Cortex* 11, pp. 1064–1082.

Piskorowski, Rebecca A and Vivien Chevaleyre (2012). "Synaptic integration by different dendritic compartments of hippocampal CA1 and CA2 pyramidal neurons." *Cellular and molecular life sciences* 69.1, pp. 75–88. DOI: 10.1007/s00018-011-0769-4.

Pitkänen, Asia, Vesa Savander, and Joseph E. LeDoux (1997). *Organization of intra-amygdaloid circuitries in the rat: An emerging framework for understanding functions of the amygdala*. DOI: 10.1016/S0166-2236(97)01125-9.

Pitkänen, Asla, Maria Pikkarainen, Nina Nurminen, and Aarne Ylinen (2000). "Reciprocal connections between the amygdala and the hippocampal formation, perirhinal cortex, and postrhinal cortex in rat". *Annals of the New York Academy of Sciences* 911, pp. 369–391. DOI: 10.1111/j.1749-6632.2000.tb06738.x.

Pleasure, Samuel J., Stewart Anderson, Robert Hevner, Anil Bagri, Oscar Marin, Daniel H. Lowenstein, and John L.R. Rubenstein (2000). "Cell Migration from the Ganglionic Eminences Is Required for the Development of Hippocampal GABAergic Interneurons". *Neuron* 28.3, pp. 727–740. DOI: 10.1016/S0896-6273(00)00149-5.

Poppenk, Jordan, Hallvard R. Evensmoen, Morris Moscovitch, and Lynn Nadel (2013). "Long-axis specialization of the human hippocampus". *Trends in Cognitive Sciences* 17.5, pp. 230–240. DOI: 10.1016/j.tics.2013.03.005.

Raam, Tara, Kathleen M. McAvoy, Antoine Besnard, Alexa Veenema, and Amar Sahay (2017). "Hippocampal oxytocin receptors are necessary for discrimination of social stimuli". *Nature Communications* 8.1, p. 2001. DOI: 10.1038/s41467-017-02173-0.

Raisman, G. (1966). "The connexions of the septum". *Brain*. DOI: 10.1093/brain/89.2.317.

Ramón y Cajal, Santiago (1893). "Estructura del asta de Ammon y fascia dentata". *An. Soc. Esp. Hist. Nat.*

Ramsden, Helen L., Gülşen Sürmeli, Steven G. McDonagh, and Matthew F. Nolan (2015). "Laminar and Dorsoventral Molecular Organization of the Medial Entorhinal Cortex Revealed by Large-scale Anatomical Analysis of Gene Expression". *PLoS Computational Biology*. DOI: 10.1371/journal.pcbi.1004032.

Rao, Rajnish P., Moritz von Heimendahl, Viktor Bahr, and Michael Brecht (2019). "Neuronal Responses to Conspecifics in the Ventral CA1". *Cell Reports* 27.12, pp. 3460–3472. DOI: 10.1016/j.celrep.2019.05.081.

Real, M. Angeles, M. Pilar Simón, Raúl Heredia, Yolanda de Diego, and Salvador Guirado (2011). "Phenotypic changes in calbindin D28K immunoreactivity in the hippocampus of Fmr1 knockout mice". *The Journal of Comparative Neurology* 519.13, pp. 2622–2636. DOI: 10.1002/cne.22643.

Resendez, Shanna L., Josh H. Jennings, Randall L. Ung, Vijay Mohan K. Namboodiri, Zhe Charles Zhou, James M. Otis, Hiroshi Nomura, Jenna A. Mchenry, Oksana Kosyk, and Garret D. Stuber (2016). "Visualization of cortical, subcortical and deep brain neural circuit dynamics during naturalistic mammalian behavior with head-mounted microscopes and chronically implanted lenses". *Nature Protocols* 11.3, pp. 566–597. DOI: 10.1038/nprot.2016.021.

Risold, P. Y. and L. W. Swanson (1997). "Connections of the rat lateral septal complex". *Brain Research Reviews* 24.2-3, pp. 115–195. DOI: 10.1016/S0165-0173(97)00009-X.

Robbe, David and György Buzsáki (2009). "Alteration of theta timescale dynamics of hippocampal place cells by a cannabinoid is associated with memory impairment". *Journal of Neuroscience* 29.40, pp. 12597–12605. DOI: 10.1523/JNEUROSCI.2407-09.2009.

Robbe, David, Sean M. Montgomery, Alexander Thome, Pavel E. Rueda-Orozco, Bruce L. McNaughton, and György Buzsaki (2006). "Cannabinoids reveal importance of spike timing coordination in hippocampal function". *Nature Neuroscience*. DOI: 10.1038/nn1801.

Robert, Vincent, Ludivine Therreau, Arthur J Y Huang, Roman Boehringer, Denis Polygalov, Thomas McHugh, Vivien Chevaleyre, and Rebecca A. Piskorowski (2020). "Local circuit allowing hypothalamic control of hippocampal area CA2 activity and consequences for CA1".

Roesler, R, J A Henriques, and G Schwartsmann (2006). "Gastrin-releasing peptide receptor as a molecular target for psychiatric and neurological disorders". *CNS Neurol Disord Drug Targets*.

Rosen, Zev B., Stephanie Cheung, and Steven A. Siegelbaum (2015). "Midbrain dopamine neurons bidirectionally regulate CA3-CA1 synaptic drive". *Nature Neuroscience*. DOI: 10.1038/nn.4152.

Royer, S., A. Sirota, J. Patel, and G. Buzsaki (2010). "Distinct Representations and Theta Dynamics in Dorsal and Ventral Hippocampus". *Journal of Neuroscience* 30.5, pp. 1777–1787. DOI: 10.1523/jneurosci.4681-09.2010.

Sánchez-Bellot, Candela and Andrew F. MacAskill (2020). "Two opposing hippocampus to prefrontal cortex pathways for the control of approach and avoidance behavior". *bioRxiv*, pp. 1–40.

Sans-Dublanc, Arnau, Adrià Razzauti, Srinidhi Desikan, Marta Pascual, Hannah Monyer, and Carlos Sindreu (2020). "Septal GABAergic inputs to CA1 govern contextual memory retrieval". *Science Advances* 6.44, eaba5003. DOI: 10.1126/sciadv.aba5003.

Sargolini, Francesca, Marianne Fyhn, Torkel Hafting, Bruce L. McNaughton, Menno P. Witter, May Britt Moser, and Edvard I. Moser (2006). "Conjunctive representation of position, direction, and velocity in entorhinal cortex". *Science* 312.5774, pp. 758–762. DOI: 10.1126/science.1125572.

Sarihi, Abdolrahman, Javad Mirnajafi-Zadeh, Bin Jiang, Kazuhiro Sohya, Mir Shahram Safari, Masoumeh Kourosh Arami, Yuchio Yanagawa, and Tadaharu Tsumoto (2012). "Cell type-specific, presynaptic LTP of inhibitory synapses on fast-spiking GABAergic neurons in the mouse visual cortex". *Journal of Neuroscience* 32.38, pp. 13189–13199. DOI: 10.1523/JNEUROSCI.1386-12.2012.

Save, Laurène, Agnès Baude, and Rosa Cossart (2019). "Temporal Embryonic Origin Critically Determines Cellular Physiology in the Dentate Gyrus". *Cerebral Cortex* 29.6, pp. 2639–2652. DOI: 10.1093/cercor/bhy132.

Savić, Nataša and Marina Sciancalepore (2001). "Electrophysiological characterization of "giant" cells in stratum radiatum of the CA3 hippocampal region". *Journal of Neurophysiology* 85.5, pp. 1998–2007. DOI: 10.1152/jn.2001.85.5.1998.

Schafer, Matthew and Daniela Schiller (2018). "Navigating Social Space". *Neuron* 100.2, pp. 476–489. DOI: 10.1016/j.neuron.2018.10.006.

Scharfman, Helen E. (2007). *The CA3 "backprojection" to the dentate gyrus*. DOI: 10.1016/S0079-6123(07)63034-9.

Schnütgen, Frank, Nathalie Doerflinger, Cécile Calléja, Olivia Wendling, Pierre Chambon, and Norbert B. Ghyselinck (2003). "A directional strategy for monitoring Cre-mediated recombination at the cellular level in the mouse". *Nature Biotechnology* 21.5, pp. 562–565. DOI: 10.1038/nbt811.

Schomburg, Erik W., Antonio Fernández-Ruiz, Kenji Mizuseki, Antal Berényi, Costas A. Anastassiou, Christof Koch, and György Buzsáki (2014). "Theta Phase Segregation of Input-Specific Gamma Patterns in Entorhinal-Hippocampal Networks". *Neuron* 84.2, pp. 470–485. DOI: 10.1016/j.neuron.2014.08.051.

Schumacher, Anett, Franz R. Villaruel, Alicia Ussling, Sadia Riaz, Andy C.H. Lee, and Rutsuko Ito (2018). "Ventral Hippocampal CA1 and CA3 Differentially Mediate Learned Approach-Avoidance Conflict Processing". *Current Biology* 28.8, pp. 1318–1324. DOI: 10.1016/j.cub.2018.03.012.

Schuurmans, Carol, Olivier Armant, Marta Nieto, Jan M Stenman, Olivier Britz, Natalia Klenin, Craig Brown, Lisa-Marie Langevin, Julie Seibt, Hua Tang, James M Cunningham, Richard Dyck, Christopher Walsh, Kenny Campbell, Franck Polleux, and François Guillemot (2004). "Sequential phases of cortical specification involve Neurogenin-dependent and -independent pathways." *The EMBO journal* 23.14, pp. 2892–902. DOI: 10.1038/sj.emboj.7600278.

Scoville, W. B. and B. Milner (1957). "Loss of recent memory after bilateral hippocampal lesions." *Journal of neurology, neurosurgery, and psychiatry* 20.1, pp. 11–21. DOI: 10.1136/jnnp.20.1.11.

Seo, Seongjin, Jong-Won Lim, Dhananjay Yellajoshyula, Li-Wei Chang, and Kristen L Kroll (2007). "Neurogenin and NeuroD direct transcriptional targets and their regulatory enhancers." *The EMBO journal* 26.24, pp. 5093–108. DOI: 10.1038/sj.emboj.7601923.

Sharif, Farnaz, Behnam Tayebi, György Buzsáki, Sébastien Royer, and Antonio Fernandez-Ruiz (2020). "Subcircuits of Deep and Superficial CA1 Place Cells Support Efficient Spatial Coding

across Heterogeneous Environments". *Neuron*, pp. 1–14. DOI: 10.1016/j.neuron.2020.10.034.

Sheintuch, Liron, Alon Rubin, Noa Brande-Eilat, Nitzan Geva, Noa Sadeh, Or Pinchasof, and Yaniv Ziv (2017). "Tracking the Same Neurons across Multiple Days in Ca2+Imaging Data". *Cell Reports* 21.4, pp. 1102–1115. DOI: 10.1016/j.celrep.2017.10.013.

Shepherd, Timothy M, E. Özarslan, A T Yachnis, M A King, and S J Blackband (2007). "Diffusion tensor microscopy indicates the cytoarchitectural basis for diffusion anisotropy in the human hippocampus". *American Journal of Neuroradiology* 28.5, pp. 958–964.

Shimojo, Hiromi, Toshiyuki Ohtsuka, and Ryoichiro Kageyama (2008). "Oscillations in Notch Signaling Regulate Maintenance of Neural Progenitors". *Neuron*. DOI: 10.1016/j.neuron.2008.02.014.

Shirvalkar, Prasad R., Peter R. Rapp, and Matthew L. Shapiro (2010). "Bidirectional changes to hippocampal theta-gamma comodulation predict memory for recent spatial episodes". *Proceedings of the National Academy of Sciences of the United States of America* 107.15, pp. 7054–7059. DOI: 10.1073/pnas.0911184107.

Siegle, Joshua H and Matthew A Wilson (2014). "Enhancement of encoding and retrieval functions through theta phase-specific manipulation of hippocampus". *eLife* 3, pp. 1–18. DOI: 10.7554/elife.03061.

Siok, C. J., J. A. Rogers, B. Kocsis, and M. Hajós (2006). "Activation of α7 acetylcholine receptors augments stimulation-induced hippocampal theta oscillation". *European Journal of Neuroscience*. DOI: 10.1111/j.1460-9568.2005.04560.x.

Skaggs, William E., Bruce L. McNaughton, Matthew A. Wilson, and Carol A. Barnes (1996). "Theta phase precession in hippocampal neuronal populations and the compression of temporal sequences". *Hippocampus* 6.2, pp. 149–172. DOI: 10.1002/(SICI)1098-1063(1996)6:2<149::AID-HIPO6>3.0.CO;2-K.

Slomianka, L. (1992). "Neurons of origin of zinc-containing pathways and the distribution of zinc-containing boutons in the hippocampal region of the rat". *Neuroscience* 48.2, pp. 325–352. DOI: 10.1016/0306-4522(92)90494-M.

Slomianka, Lutz, Irmgard Amrein, Irene Knuesel, Jens Christian Sørensen, and David P. Wolfer (2011). "Hippocampal pyramidal cells: the reemergence of cortical lamination". en. *Brain Structure and Function* 216.4, pp. 301–317. DOI: 10.1007/s00429-011-0322-0.

Smart, I H (1982). "Radial unit analysis of hippocampal histogenesis in the mouse." *Journal of anatomy* 135.Pt 4, pp. 763–93.

Solstad, Trygve, Charlotte N Boccara, Emilio Kropff, May-Britt Moser, and Edvard I Moser (2008). "Representation of Geometric Borders". *Science* 322.5909, pp. 1865–1868. DOI: 10.1126/science.1166466.

Soltesz, Ivan, Bradley E. Alger, Masanobu Kano, Sang Hun Lee, David M. Lovinger, Takako Ohno-Shosaku, and Masahiko Watanabe (2015). "Weeding out bad waves: Towards selective cannabinoid circuit control in epilepsy". *Nature Reviews Neuroscience* 16.5, pp. 264–277. DOI: 10.1038/nrn3937.

Soltesz, Ivan and Attila Losonczy (2018). "CA1 pyramidal cell diversity enabling parallel information processing in the hippocampus". *Nature Neuroscience* 21.4, pp. 484–493. DOI: 10.1038/s41593-018-0118-0.

Somogyi, Peter, Linda Katona, Thomas Klausberger, Bálint Lasztóczi, and Tim J. Viney (2014). "Temporal redistribution of inhibition over neuronal subcellular domains underlies state-dependent rhythmic change of excitability in the hippocampus". *Philosophical Transactions of the Royal Society B: Biological Sciences* 369.1635. DOI: 10.1098/rstb.2012.0518.

Somogyi, Peter and Thomas Klausberger (2005). "Defined types of cortical interneurone structure space and spike timing in the hippocampus." *The Journal of physiology* 562.Pt 1, pp. 9–26. DOI: 10.1113/jphysiol.2004.078915.

— (2017). "Hippocampus: Intrinsic Organization". In: *Handbook of Brain Microcircuits*. Oxford University Press, pp. 199–216. DOI: 10.1093/med/9780190636111.003.0017.

Spampanato, Jay and F. Edward Dudek (2017). "Targeted interneuron ablation in the mouse hippocampus can cause spontaneous recurrent seizures". *eNeuro* 4.4, pp. 1–17. DOI: 10.1523/ENEURO.0130-17.2017.

Stanfield, Brent B. and W. Maxwell Cowan (1979). "The development of the hippocampus and dentate gyrus in normal and reeler mice". *The Journal of Comparative Neurology* 185.3, pp. 423–459. DOI: 10.1002/cne.901850303.

Strange, Bryan A., Menno P. Witter, Ed S. Lein, and Edvard I. Moser (2014). "Functional organization of the hippocampal longitudinal axis". *Nature Reviews Neuroscience* 15.10, pp. 655–669. DOI: 10.1038/nrn3785.

Subramanian, Lakshmi and Shubha Tole (2009). "Mechanisms underlying the specification, positional regulation, and function of the cortical hem". *Cerebral Cortex* 19.SUPPL. 1, pp. 90–95. DOI: 10.1093/cercor/bhp031.

Sugar, Jørgen and May-Britt Moser (2019). "Episodic memory: Neuronal codes for what, where, and when". *Hippocampus*, hipo.23132. DOI: 10.1002/hipo.23132.

Sun, Qingtao, Xiangning Li, Anan Li, Jianping Zhang, Zhangheng Ding, Hui Gong, and Qingming Luo (2020a). "Ventral Hippocampal-Prefrontal interaction affects social behavior via parvalbumin positive neurons in the medial prefrontal cortex". *iScience* 23.3, p. 100894. DOI: 10.1016/j.isci.2020.100894.

Sun, Xiaochen, Max J Bernstein, Meizhen Meng, Siyuan Rao, Andreas T Sørensen, Li Yao, Xiaohui Zhang, Polina O Anikeeva, and Yingxi Lin (2020b). "Functionally Distinct Neuronal Ensembles within the Memory Engram." *Cell*, pp. 1–14. DOI: 10.1016/j.cell.2020.02.055.

Supèr, Hans and Eduardo Soriano (1994). "The organization of the embronic and early postnatal murine hippocampus. II. Development of entorhinal, commissural, and septal connections studied with the lipophilic tracer DiI". *Journal of Comparative Neurology* 344.1, pp. 101–120. DOI: 10.1002/cne.903440108.

Swann, J. W., R. J. Brady, and D. L. Martin (1989). "Postnatal development of GABA-mediated synaptic inhibition in rat hippocampus". *Neuroscience*. DOI: 10.1016/0306-4522(89)90004-3.

Swanson, L. W., P. E. Sawchenko, and W. M. Cowan (1981). "Evidence for collateral projections by neurons in Ammon's horn, the dentate gyrus, and the subiculum: A multiple retrograde labeling study in the rat". *Journal of Neuroscience* 1.5, pp. 548–559. DOI: 10.1523/jneurosci.01-05-00548.1981.

Swanson, L.W. and W.M. Cowan (1978). "An Autoradiographic Study of the Organization of the Efferent Connections of the Hippocampal Formation in the Rat". *Journal of Comparative Neurology* 172, pp. 49–84.

Sweeney, Patrick and Yunlei Yang (2015). "An excitatory ventral hippocampus to lateral septum circuit that suppresses feeding". *Nature Communications* 6.1, p. 10188. DOI: 10.1038/ncomms10188.

Szőnyi, András, Katalin E. Sos, Rita Nyilas, Dániel Schlingloff, Andor Domonkos, Virág T. Takács, Balázs Pósfai, Panna Hegedüs, James B. Priestley, Andrew L. Gundlach, Attila I. Gulyás, Viktor Varga, Attila Losonczy, Tamás F. Freund, and Gábor Nyiri (2019). "Brainstem nucleus

incertus controls contextual memory formation". *Science (New York, N.Y.)* 364.6442, pp. 0–14. DOI: 10.1126/science.aaw0445.

Takács, Virág T., Tamás F. Freund, and Attila I. Gulyás (2008). "Types and synaptic connections of hippocampal inhibitory neurons reciprocally connected with the medial septum". *European Journal of Neuroscience*. DOI: 10.1111/j.1460-9568.2008.06319.x.

Takeuchi, Tomonori, Adrian J. Duszkiewicz, Alex Sonneborn, Patrick A. Spooner, Miwako Yamasaki, Masahiko Watanabe, Caroline C. Smith, Guillén Fernández, Karl Deisseroth, Robert W. Greene, and Richard G.M. Morris (2016). "Locus coeruleus and dopaminergic consolidation of everyday memory". *Nature* 537.7620, pp. 357–362. DOI: 10.1038/nature19325.

Talbot, Zoe Nicole, Fraser Todd Sparks, Dino Dvorak, Bridget Mary Curran, Juan Marcos Alarcon, and André Antonio Fenton (2018). "Normal CA1 Place Fields but Discoordinated Network Discharge in a Fmr1-Null Mouse Model of Fragile X Syndrome". *Neuron* 97.3, pp. 684–697. DOI: 10.1016/j.neuron.2017.12.043.

Tamamaki, N and Y Nojyo (1995). "Preservation of topography in the connections between the subiculum, field CA1, and the entorhinal cortex in rats." en. *The Journal of comparative neurology* 353.3, pp. 379–90. DOI: 10.1002/cne.903530306.

Tan, Hui Min, Thomas Joseph Wills, and Francesca Cacucci (2017). "The development of spatial and memory circuits in the rat". *Wiley Interdisciplinary Reviews: Cognitive Science* 8.3, e1424. DOI: 10.1002/wcs.1424.

Tanaka, Kazumasa Z., Hongshen He, Anupratap Tomar, Kazue Niisato, Arthur J.Y. Huang, and Thomas J. McHugh (2018). "The hippocampal engram maps experience but not place". *Science* 361.6400, pp. 392–397. DOI: 10.1126/science.aat5397.

Tang, Jonathan C.Y., Stephanie Rudolph, Onkar S. Dhande, Victoria E. Abraira, Seungwon Choi, Sylvain W. Lapan, Iain R. Drew, Eugene Drokhlyansky, Andrew D. Huberman, Wade G. Regehr, and Constance L. Cepko (2015). "Cell type-specific manipulation with GFP-dependent Cre recombinase". *Nature Neuroscience* 18.9, pp. 1334–1341. DOI: 10.1038/nn.4081.

Tannenholz, Lindsay, Jessica C Jimenez, and Mazen A Kheirbek (2014). "Local and regional heterogeneity underlying hippocampal modulation of cognition and mood." *Frontiers in behavioral neuroscience* 8, p. 147. DOI: 10.3389/fnbeh.2014.00147.

Tasic, Bosiljka, Vilas Menon, Thuc Nghi Nguyen, Tae Kyung Kim, Tim Jarsky, Zizhen Yao, Boaz Levi, Lucas T. Gray, Staci A. Sorensen, Tim Dolbeare, Darren Bertagnolli, Jeff Goldy, Nadiya Shapovalova, Sheana Parry, Changkyu Lee, Kimberly Smith, Amy Bernard, Linda Madisen, Susan M. Sunkin, Michael Hawrylycz, Christof Koch, and Hongkui Zeng (2016). "Adult mouse cortical cell taxonomy revealed by single cell transcriptomics". *Nature Neuroscience*. DOI: 10.1038/nn.4216.

Taube, Jeffrey S. (2007). "The Head Direction Signal: Origins and Sensory-Motor Integration". *Annual Review of Neuroscience* 30.1, pp. 181–207. DOI: 10.1146/annurev.neuro.29.051605.112854.

Teixeira, Catia M., Zev B. Rosen, Deepika Suri, Qian Sun, Marc Hersh, Derya Sargin, Iva Dincheva, Ashlea A. Morgan, Stephen Spivack, Anne C. Krok, Tessa Hirschfeld-Stoler, Evelyn K. Lambe, Steven A. Siegelbaum, and Mark S. Ansorge (2018). "Hippocampal 5-HT Input Regulates Memory Formation and Schaffer Collateral Excitation". *Neuron* 98.5, pp. 992–1004. DOI: 10.1016/j.neuron.2018.04.030.

Teles-Grilo Ruivo, Leonor M. and Jack R. Mellor (2013). "Cholinergic modulation of hippocampal network function". *Frontiers in Synaptic Neuroscience* 5.JUL, pp. 1–15. DOI: 10.3389/fnsyn.2013.00002.

Thome, Christian, Tony Kelly, Antonio Yanez, Christian Schultz, Maren Engelhardt, Sidney B Cambridge, Martin Both, Andreas Draguhn, Heinz Beck, and Alexei V Egorov (2014). "Axon-carrying dendrites convey privileged synaptic input in hippocampal neurons." *Neuron* 83.6, pp. 1418–30. DOI: 10.1016/j.neuron.2014.08.013.

Tirko, Natasha N., Katherine W. Eyring, Ioana Carcea, Mariela Mitre, Moses V. Chao, Robert C. Froemke, and Richard W. Tsien (2018). "Oxytocin Transforms Firing Mode of CA2 Hippocampal Neurons". *Neuron* 100.3, pp. 593–608. DOI: 10.1016/j.neuron.2018.09.008.

Tole, Shubha, Caprice Christian, and Elizabeth A. Grove (1997). "Early specification and autonomous development of cortical fields in the mouse hippocampus". *Development* 124.24, pp. 4959–4970.

Tole, Shubha and Elizabeth A. Grove (2001). "Detailed field pattern is intrinsic to the embryonic mouse hippocampus early in neurogenesis". *Journal of Neuroscience* 21.5, pp. 1580–1589. DOI: 10.1523/jneurosci.21-05-01580.2001.

Tort, Adriano B.L., Robert W. Komorowski, Joseph R. Manns, Nancy J. Kopell, and Howard Eichenbaum (2009). "Theta-gamma coupling increases during the learning of item-context associations". *Proceedings of the National Academy of Sciences of the United States of America* 106.49, pp. 20942–20947. DOI: 10.1073/pnas.0911331106.

Tovote, Philip, Jonathan Paul Fadok, and Andreas Lüthi (2015). *Neuronal circuits for fear and anxiety*. DOI: 10.1038/nrn3945.

Towfighi, Javad, Cathy Housman, Robert Brucklacher, and Robert C. Vannucci (2004). "Neuropathology of seizures in the immature rabbit". *Developmental Brain Research* 152.2, pp. 143–152. DOI: 10.1016/j.devbrainres.2004.06.009.

Tricoire, Ludovic, Kenneth A. Pelkey, Michael I. Daw, Vitor H. Sousa, Goichi Miyoshi, Brian Jeffries, Bruno Cauli, Gord Fishell, and Chris J. McBain (2010). "Common origins of hippocampal ivy and nitric oxide synthase expressing neurogliaform cells". *Journal of Neuroscience*. DOI: 10.1523/JNEUROSCI.5123-09.2010.

Tricoire, Ludovic, Kenneth A Pelkey, Brian E Erkkila, Brian W Jeffries, Xiaoqing Yuan, and Chris J McBain (2011). "A blueprint for the spatiotemporal origins of mouse hippocampal interneuron diversity." *The Journal of neuroscience : the official journal of the Society for Neuroscience* 31.30, pp. 10948–70. DOI: 10.1523/JNEUROSCI.0323-11.2011.

Tronson, Natalie C, Christina Schrick, Yomayra F Guzman, Kyu Hwan Huh, Deepak P Srivastava, Peter Penzes, Anita L Guedea, Can Gao, and Jelena Radulovic (2009). "Segregated populations of hippocampal principal CA1 neurons mediating conditioning and extinction of contextual fear." *The Journal of neuroscience : the official journal of the Society for Neuroscience* 29.11, pp. 3387–94. DOI: 10.1523/JNEUROSCI.5619-08.2009.

Trouche, Stéphanie, Vadim Koren, Natalie M. Doig, Tommas J. Ellender, Mohamady El-Gaby, Vítor Lopes-dos-Santos, Hayley M. Reeve, Pavel V. Perestenko, Farid N. Garas, Peter J. Magill, Andrew Sharott, and David Dupret (2019). "A Hippocampus-Accumbens Tripartite Neuronal Motif Guides Appetitive Memory in Space". *Cell* 176.6, pp. 1393–1406. DOI: 10.1016/j.cell.2018.12.037.

Twining, Robert C., Katie Lepak, Adam J. Kirry, and Marieke R. Gilmartin (2020). "Ventral hippocampal input to the prelimbic cortex dissociates the context from the cue association in trace fear memory". *The Journal of Neuroscience*. DOI: 10.1523/jneurosci.1453-19.2020.

Tyssowski, Kelsey M, Nicholas R DeStefino, Jin-Hyung Cho, Carissa J Dunn, Robert G Poston, Crista E Carty, Richard D Jones, Sarah M Chang, Palmyra Romeo, Mary K Wurzelmann, James M Ward, Mark L Andermann, Ramendra N Saha, Serena M Dudek, and Jesse M Gray

(2018). "Different Neuronal Activity Patterns Induce Different Gene Expression Programs." *Neuron* 98.3, pp. 530–546. DOI: 10.1016/j.neuron.2018.04.001.

Tyzio, Roman, Gregory L. Holmes, Yehezkiel Ben-Ari, and Roustem Khazipov (2007). "Timing of the developmental switch in GABAA mediated signaling from excitation to inhibition in CA3 rat hippocampus using gramicidin perforated patch and extracellular recordings". In: *Epilepsia*. DOI: 10.1111/j.1528-1167.2007.01295.x.

Tyzio, Roman, Alfonso Represa, Isabel Jorquera, Yehezkel Ben-Ari, Henri Gozlan, and Laurent Aniksztejn (1999). "The establishment of GABAergic and glutamatergic synapses on CA1 pyramidal neurons is sequential and correlates with the development of the apical dendrite". *Journal of Neuroscience*. DOI: 10.1523/jneurosci.19-23-10372.1999.

Udakis, Matt, Victor Pedrosa, Sophie E. L. Chamberlain, Claudia Clopath, and Jack R. Mellor (2020). "Interneuron-specific plasticity at parvalbumin and somatostatin inhibitory synapses onto CA1 pyramidal neurons shapes hippocampal output". *Nature Communications* 11.1, p. 4395. DOI: 10.1038/s41467-020-18074-8.

Valero, Manuel, Elena Cid, Robert G Averkin, Juan Aguilar, Alberto Sanchez-Aguilera, Tim J Viney, Daniel Gomez-Dominguez, Elisa Bellistri, and Liset Menendez de la Prida (2015). "Determinants of different deep and superficial CA1 pyramidal cell dynamics during sharp-wave ripples." *Nature neuroscience* 18.9, pp. 1281–90. DOI: 10.1038/nn.4074.

Valero, Manuel and Liset Menendez de la Prida (2018). "The hippocampus in depth: a sublayer-specific perspective of entorhinal–hippocampal function". *Current Opinion in Neurobiology* 52, pp. 107–114. DOI: 10.1016/j.conb.2018.04.013.

Vandecasteele, Marie, Viktor Varga, Antal Berényi, Edit Papp, Péter Barthó, Laurent Venance, Tamás F Freund, and György Buzsáki (2014). "Optogenetic activation of septal cholinergic neurons suppresses sharp wave ripples and enhances theta oscillations in the hippocampus." *Proceedings of the National Academy of Sciences of the United States of America* 111.37, pp. 13535–40. DOI: 10.1073/pnas.1411233111.

Vanderwolf, C.H. (1969). "Hippocampam Electrical Activity And Voluntary Movement In The Rat". *Electroencephalography and Clinical Neurophysiology* 26.4, pp. 407–418. DOI: 10.1053/j.semss.2007.06.005.

Varela, C., S. Kumar, J. Y. Yang, and M. A. Wilson (2014). "Anatomical substrates for direct interactions between hippocampus, medial prefrontal cortex, and the thalamic nucleus reuniens". *Brain Structure and Function* 219.3, pp. 911–929. DOI: 10.1007/s00429-013-0543-5.

Vertes, Robert P. (1991). "A PHA-L analysis of ascending projections of the dorsal raphe nucleus in the rat". *Journal of Comparative Neurology*. DOI: 10.1002/cne.903130409.

— (2006). *Interactions among the medial prefrontal cortex, hippocampus and midline thalamus in emotional and cognitive processing in the rat*. DOI: 10.1016/j.neuroscience.2006.06.027.

Vertes, Robert P., William J. Fortin, and Alison M. Crane (1999). "Projections of the median raphe nucleus in the rat". *Journal of Comparative Neurology*. DOI: 10.1002/(SICI)1096-9861(19990517)407:4<555::AID-CNE7>3.0.CO;2-E.

Verwer, Ronald W.H., Ron J. Meijer, Hannie F.M. Van Uum, and Menno P. Witter (1997). "Collateral projections from the rat hippocampal formation to the lateral and medial prefrontal cortex". *Hippocampus* 7.4, pp. 397–402. DOI: 10.1002/(SICI)1098-1063(1997)7:4<397::AID-HIPO5>3.0.CO;2-G.

Villette, Vincent, Philippe Guigue, Michel Aimé Picardo, Vitor Hugo Sousa, Erwan Leprince, Philippe Lachamp, Arnaud Malvache, Thomas Tressard, Rosa Cossart, and Agnès Baude (2016). "Development of early-born γ-Aminobutyric acid hub neurons in mouse hippocampus

from embryogenesis to adulthood". *Journal of Comparative Neurology* 524.12, pp. 2440–2461. DOI: 10.1002/CNE.23961.

Vogel, Jacob W., Renaud La Joie, Michel J. Grothe, Alexandr Diaz-Papkovich, Andrew Doyle, Etienne Vachon-Presseau, Claude Lepage, Reinder Vos de Wael, Rhalena A. Thomas, Yasser Iturria-Medina, Boris Bernhardt, Gil D. Rabinovici, and Alan C. Evans (2020). "A molecular gradient along the longitudinal axis of the human hippocampus informs large-scale behavioral systems". *Nature Communications* 11.1, p. 960. DOI: 10.1038/s41467-020-14518-3.

Wagatsuma, Akiko, Teruhiro Okuyama, Chen Sun, Lillian M. Smith, Kuniya Abe, and Susumu Tonegawa (2017). "Locus coeruleus input to hippocampal CA3 drives single-trial learning of a novel context". *Proceedings of the National Academy of Sciences of the United States of America* 115.2, E310–E316. DOI: 10.1073/pnas.1714082115.

Walker, David L., Donna J. Toufexis, and Michael Davis (2003). "Role of the bed nucleus of the stria terminalis versus the amygdala in fear, stress, and anxiety". *European Journal of Pharmacology* 463.1-3, pp. 199–216. DOI: 10.1016/S0014-2999(03)01282-2.

Wang, Melissa E., Ellen G. Wann, Robin K. Yuan, Manuel M.Ramos Álvarez, Squire M. Stead, and Isabel A. Muzzio (2012). "Long-term stabilization of place cell remapping produced by a fearful experience". *Journal of Neuroscience*. DOI: 10.1523/JNEUROSCI.0480-12.2012.

West, Anne E., Eric C. Griffith, and Michael E. Greenberg (2002). "Regulation of transcription factors by neuronal activity". *Nature Reviews Neuroscience*. DOI: 10.1038/nrn987.

Williams, Philip A., Phillip Larimer, Yuan Gao, and Ben W. Strowbridge (2007). "Semilunar granule cells: Glutamatergic neurons in the rat dentate gyrus with axon collaterals in the inner molecular layer". *Journal of Neuroscience* 27.50, pp. 13756–13761. DOI: 10.1523/JNEUROSCI.4053-07.2007.

Witter, M. P., H. J. Groenewegen, F. H. Lopes da Silva, and A. H.M. Lohman (1989). "Functional organization of the extrinsic and intrinsic circuitry of the parahippocampal region". *Progress in Neurobiology* 33.3, pp. 161–253. DOI: 10.1016/0301-0082(89)90009-9.

Witter, Menno P. (1993). "Organization of the entorhinal—hippocampal system: A review of current anatomical data". *Hippocampus* 3.1 S, pp. 33–44. DOI: 10.1002/hipo.1993.4500030707.

Wood, Emma R, Paul A Dudchenko, R Jonathan Robitsek, and Howard Eichenbaum (2000). "Hippocampal Neurons Encode Information about Different Types of Memory Episodes Occurring in the Same Location". 27, pp. 623–633.

Wouterlood, Floris G., Enrique Saldana, and Menno P. Witter (1990). "Projection from the nucleus reuniens thalami to the hippocampal region: Light and electron microscopic tracing study in the rat with the anterograde tracer Phaseolus vulgaris-leucoagglutinin". *Journal of Comparative Neurology*. DOI: 10.1002/cne.902960202.

Xu, Chun, Sabine Krabbe, Jan Gründemann, Paolo Botta, Jonathan P. Fadok, Fumitaka Osakada, Dieter Saur, Benjamin F. Grewe, Mark J. Schnitzer, Edward M. Callaway, and Andreas Lüthi (2016a). "Distinct Hippocampal Pathways Mediate Dissociable Roles of Context in Memory Retrieval". *Cell* 167.4, pp. 961–972. DOI: 10.1016/j.cell.2016.09.051.

Xu, Hua-Tai, Zhi Han, Peng Gao, Shuijin He, Zhizhong Li, Wei Shi, Oren Kodish, Wei Shao, Keith N Brown, Kun Huang, and Song-Hai Shi (2014). "Distinct lineage-dependent structural and functional organization of the hippocampus." *Cell* 157.7, pp. 1552–64. DOI: 10.1016/j.cell.2014.03.067.

Xu, Xiangmin, Yanjun Sun, Todd C. Holmes, and Alberto J. López (2016b). "Noncanonical connections between the subiculum and hippocampal CA1". *Journal of Comparative Neurology* 524.17, pp. 3666–3673. DOI: 10.1002/cne.24024.

Yoshida, Keitaro, Michael R. Drew, Masaru Mimura, and Kenji F. Tanaka (2019). "Serotonin-mediated inhibition of ventral hippocampus is required for sustained goal-directed behavior". *Nature Neuroscience* 22.5, pp. 770–777. DOI: 10.1038/s41593-019-0376-5.

Young, Brian J., Gregory D. Fox, and Howard Eichenbaum (1994). "Correlates of hippocampal complex-spike cell activity in rats performing a nonspatial radial maze task". *Journal of Neuroscience* 14.11 I, pp. 6553–6563. DOI: 10.1523/jneurosci.14-11-06553.1994.

Zeng, Hongkui (2018). "Mesoscale connectomics". *Current Opinion in Neurobiology* 50, pp. 154–162. DOI: 10.1016/j.conb.2018.03.003.

Zhang, Wei Ning, Tobias Bast, and Joram Feldon (2002). "Effects of hippocampal N-methyl-D-aspartate infusion on locomotor activity and prepulse inhibition: Differences between the dorsal and ventral hippocampus". *Behavioral Neuroscience*. DOI: 10.1037/0735-7044.116.1.72.

Zhang, Zhe, Valentina Ferretti, Ilke Güntan, Alessandro Moro, Eleonora A. Steinberg, Zhiwen Ye, Anna Y. Zecharia, Xiao Yu, Alexei L. Vyssotski, Stephen G. Brickley, Raquel Yustos, Zoe E. Pillidge, Edward C. Harding, William Wisden, and Nicholas P. Franks (2015). "Neuronal ensembles sufficient for recovery sleep and the sedative actions of α 2 adrenergic agonists". *Nature Neuroscience* 18.4, pp. 553–561. DOI: 10.1038/nn.3957.

Zhou, C. F., Y. Li, R. J. Morris, and G. Raisman (1990). "Accurate reconstruction of three complementary laminar afferents to the adult hippocampus by embryonic neural grafts". *Neuroscience Research Supplements*. DOI: 10.1016/0921-8696(90)90030-7.

Zhou, Yiming, Huiwen Zhu, Zhiyuan Liu, Xi Chen, XiuJuan Su, Chaonan Ma, Zhen Tian, Bing Huang, Enhui Yan, Xing Liu, and Lan Ma (2019). "A ventral CA1 to nucleus accumbens core engram circuit mediates conditioned place preference for cocaine". *Nature Neuroscience 2019* 22.December, pp. 1–14. DOI: 10.1038/s41593-019-0524-y.

Zhu, Hu, Kristen E. Pleil, Daniel J. Urban, Sheryl S. Moy, Thomas L. Kash, and Bryan L. Roth (2014). "Chemogenetic inactivation of ventral hippocampal glutamatergic neurons disrupts consolidation of contextual fear memory". *Neuropsychopharmacology*. DOI: 10.1038/npp.2014.35.

Zirlinger, M., L. Lo, J. McMahon, A. P. McMahon, and D. J. Anderson (2002). "Transient expression of the bHLH factor neurogenin-2 marks a subpopulation of neural crest cells biased for a sensory but not a neuronal fate". *Proceedings of the National Academy of Sciences* 99.12, pp. 8084–8089. DOI: 10.1073/pnas.122231199.

Ziv, Yaniv and Kunal K. Ghosh (2015). *Miniature microscopes for large-scale imaging of neuronal activity in freely behaving rodents*. DOI: 10.1016/j.conb.2015.04.001.